

**AIRWAY IMPEDANCE, HETEROGENEITY AND
VARIABILITY IN ADULT ASTHMA**

by

Swati Anil Bhatawadekar

Submitted in partial fulfilment of the requirements
for the degree of Doctor of Philosophy

at

Dalhousie University
Halifax, Nova Scotia
March 2015

© Copyright by Swati Anil Bhatawadekar, 2015

To my parents

TABLE OF CONTENTS

List of Tables	vii
List of Figures	viii
ABSTRACT	xi
List of Abbreviations and Symbols Used	xii
Acknowledgements	xvi
Chapter 1: Introduction	1
1.1 Overview	6
1.2 Manuscripts and Conference Abstracts and Proceedings	7
Chapter 2: Review of Relevant Literature	12
2.1 Structure and function of the lung	12
2.2 Asthma	13
2.3 Asthma severity and control	15
2.4 Diagnosing asthma.....	18
2.5 Spirometry.....	19
2.5.1 Assessment of airway obstruction	19
2.5.2 Assessment of airway hyperresponsiveness	23
2.6 Forced oscillation technique	24
2.7 Measurement and modelling of lung mechanics	36
2.8 Lung function and airway hyperresponsiveness	43
2.9 Variability of airway function in asthma	46
2.9.1 Amplitude structure and short term variation of airway caliber	47
2.9.2 Temporal structure of variation of airway caliber	50
2.10 Heterogeneity in asthma	53
2.11 Research hypotheses and aims.....	57
2.11.1 Elastance as an indicator airway dysfunction	57
2.11.2 Quantifying respiratory mechanics with airway heterogeneity	57
2.11.3 Removal of impedance artifacts in FOT using wavelets	58
2.11.4 Variability of impedance in response to methacholine and bronchodilator	58
2.11.5 Variability of impedance as a function of lung volume.....	59

Chapter 3: Respiratory System Elastance Compared with Resistance in Reversibility Testing in Asthma	61
3.1 Introduction.....	61
3.2 Methods.....	63
3.2.1 Subjects	63
3.2.2 Measurements	64
3.2.3 Protocol	65
3.2.4 Data Analyses	65
3.2.5 Statistical Analyses	66
3.2.6 Modeling.....	67
3.3 Results.....	71
3.4 Discussion.....	79
3.5 Conclusion	85
Chapter 4: Modelling Resistance and Reactance with Heterogeneous Airway Narrowing in Mild to Severe Asthma	86
4.1 Abstract.....	87
4.2 Introduction.....	88
4.3 Methods.....	90
4.3.1 <i>In vivo</i> respiratory mechanics	90
4.3.2 Multi-branch airway tree model.....	91
4.3.3 Simulations	94
4.3.4 Statistical Analyses	94
4.4 Results.....	95
4.5 Discussion.....	100
4.6 Conclusions.....	104
Chapter 5: A Study of Artifacts and Their Removal during Forced Oscillation of the Respiratory System.....	105
5.1 Abstract.....	106
5.2 Introduction.....	107
5.3 Methods.....	108
5.3.1 Subjects	108
5.3.2 Measurements	109

5.3.3 Protocol	110
5.3.4 Data Analyses	111
5.4 Results.....	124
5.5 Discussion.....	132
5.6 Conclusions.....	139
Chapter 6: Variability of Impedance in Response to Methacholine	140
6.1 Introduction.....	140
6.2 Methods.....	141
6.2.1 Subjects	141
6.2.2 Measurements	143
6.2.3 Protocol	144
6.2.4 Data analyses	145
6.2.5 Statistical Analyses	146
6.3 Results.....	147
6.4 Discussion.....	158
6.5 Conclusions.....	165
Chapter 7: Variability of Impedance in Response to Bronchodilator	166
7.1 Introduction.....	166
7.2 Methods.....	167
7.2.1 Subjects	167
7.2.2 Measurements	167
7.2.3 Protocol	167
7.2.4 Data Analyses	168
7.2.5 Statistical Analyses	168
7.3 Results.....	168
7.4 Discussion.....	174
7.5 Conclusion	176
Chapter 8: Variability of Impedance as a Function of Lung Volume	177
8.1 Introduction.....	177
8.2 Methods.....	178
8.2.1 Subjects	178

8.2.2 Measurements	179
8.2.3 Protocol	181
8.2.4 Data Analyses	181
8.2.5 Statistical Analyses	182
8.3 Results.....	183
8.4 Discussion.....	193
8.5 Conclusion	198
Chapter 9: Discussion	199
9.1 Summary.....	199
9.1.1 Small-airway function and Lung mechanics.....	199
9.1.2 Variability of respiratory resistance and reactance.....	203
9.1.3 Removing artifacts using Wavelet Transforms.....	205
9.1.4 Variability of resistance with changes in lung volume.....	205
9.2 Significance and Implications.....	206
9.3 Original Contributions Made	208
9.4 Future Directions	211
REFERENCES.....	216
Appendix A.....	239
Appendix B.....	242

List of Tables

Table 3.1: Medication details of asthma subjects	63
Table 3.2: Subject demographics and lung function for study subjects.....	73
Table 3.2: Comparison between model respiratory impedances evaluated using Poiseuille and Womersley flow	77
Table 4.1: Model R_{rs} and X_{rs} at 5 Hz matched to <i>in vivo</i> R_{rs} at 18 Hz and X_{rs} at 5 Hz from healthy and asthmatic subjects	96
Table 4.2: Central-airway narrowing relative to control and small-airway narrowing required to reproduce <i>in vivo</i> mechanics in asthma	96
Table 5.1: Subject demographics and lung function.....	109
Table 6.1: Medication details of asthmatic subjects	142
Table 6.1: Subject demographics and lung function.....	148
Table 6.3: AHR classification of asthmatic subjects based on their PC20	149
Table 8.1: Subject demographics and lung function	184
Table 8.2: FRC and changes in EELV in controls subjects.....	185
Table 8.4: R_{rs} and R_{rsSD} at FRC and at lung volumes above and below FRC	186
Table 8.5: Comparisons between control (CL1) and asthma (AL1) groups at FRC and at EELVs below FRC.....	190
Table 8.6: Breath-to-breath variation in FRC and EELVs above and below FRC in control and asthmatic subjects	191

List of Figures

Figure 2.1: The single-compartment model of the respiratory system.....	36
Figure 2.2: Schematic presentation of R_{rs}	37
Figure 2.3: The viscoelastic model.....	39
Figure 2.4: Schematic representation of the constant-phase model.....	40
Figure 2.5: The linear two-compartment models.....	41
Figure 3.1: Multi-branch airway tree with small-airway closures and the model respiratory mechanics for controls and asthmatic subjects.....	69
Figure 3.2: Baseline and post-BD values in the control subjects (n=18) and subjects with asthma (n=18).	74
Figure 3.4: Percent decreases in $R_{rs,mod}$ and $E_{rs,mod}$ following simulated..... bronchodilation in the multi-branch tree model.....	78
Figure 3.5: Percent decreases in resistance and elastance <i>in vivo</i> (R_{rs} and E_{rs}) and in the model ($R_{rs,mod}$ and $E_{rs,mod}$) redrawn.	79
Figure 4.1: Mean respiratory resistance (R_{rs}) and reactance (X_{rs}) versus frequency in healthy and asthmatic subjects with mild to severe airway obstruction	90
Figure 4.2: Multi-branch airway-tree model depicting airway heterogeneity in moderate asthma	91
Figure 4.3: The model respiratory resistance ($R_{rs,mod}$) and reactance ($X_{rs,mod}$) over 0.4 to 20 Hz for the control model and the mild, moderate, and severe airway obstruction models of asthma	97
Figure 4.4: The frequency dependence of model respiratory system resistance ($R_{rs,mod}$) for the different frequency ranges	98
Figure 4.5: Model respiratory system elastance ($E_{rs,mod}$) compared with <i>in vivo</i> respiratory system elastance (E_{rs})	99
Figure 4.6: Effect of upper airway shunt impedance (Z_{uaw}) on $R_{rs,mod}$ and $X_{rs,mod}$ in the moderate and severe models of asthma.....	100
Figure 5.1: Flow and pressure and their time-frequency analysis for cough artifacts...	114
Figure 5.2: Removal of cough artifacts by wavelets and sensitivity and specificity of wavelet coefficients	117

Figure 5.3: Removal of flow leak artifacts	123
Figure 5.4: % Sensitivity and % specificity for male vocalizations and swallows	126
Figure 5.5: Glottal images and resistance trace showing for vocalizations.....	129
Figure 5.6: % Sensitivity and % specificity for leak artifact rejected using discrete wavelet decomposition of flow signal	130
Figure 6.1: Baseline R_{rs} and $R_{rs}SD$ in the control subjects (n=19) and subjects with asthma (n=19)	149
Figure 6.2: Percent changes in FEV_1 , R_{rs} , and $R_{rs}SD$ following the PC20 or the last dose of methacholine.....	150
Figure 6.3: Dose-response curves for FEV_1 % predicted, R_{rs} and $R_{rs}SD$ at low frequencies (L).....	151
Figure 6.4: Baseline X_{rs} and changes in X_{rs} following methacholine.....	152
Figure 6.5: Baseline $X_{rs}SD$ and changes in $X_{rs}SD$ following methacholine	152
Figure 6.6: Baseline E_{rs} and percent increases in E_{rs} following the last dose of methacholine).....	153
Figure 6.7: Correlation between $R_{rs}SD$ and AHR by dose-response slope	155
Figure 6.8: Correlations between $R_{rs}SD$ and R_{rs} pre- and post-methacholine challenge	156
Figure 7.1: Baseline R_{rs} and $R_{rs}SD$ in the controls subjects (n=18) and subjects with asthma (n=18).	169
Figure 7.2: Percent changes in R_{rs} and $R_{rs}SD$ post BD.....	170
Figure 7.3: $X_{rs}SD$ and changes in $X_{rs}SD$ post BD.	171
Figure 7.4: Correlations between $R_{rs}SD$ and R_{rs} pre- and post- BD	172
Figure 7.5: Correlation between E_{rs} and ACQ score in the subjects with asthma	173
Figure 8.1: Schematic and 3D model of tremoFlo™ OS-Beta actuator unit.....	179
Figure 8.2: Baseline R_{rs} , X_{rs} , and variations of R_{rs} and X_{rs}	184
Figure 8.3: R_{rs} and $R_{rs}SD$ versus EELV in the control subjects	187
Figure 8.4: R_{rs} and $R_{rs}SD$ versus EELV in the subjects with asthma	188
Figure 8.5: Normalized R_{rs} and $R_{rs}SD$ versus normalized EELVs	189
Figure 8.6: Respitrace output in a representative asthmatic subject.....	192

Figure 8.7: Baseline $R_{rs}SD$ versus R_{rs} in the controls (n=7) and subjects with asthma (n=7). 193

ABSTRACT

While bronchodilator (BD) reversibility is a feature of asthma, the relative contributions of small and large airways to BD is unclear, and the effect of small-airway heterogeneity on respiratory system impedance, Z_{rs} has not been directly quantified. Furthermore while short-term variability in Z_{rs} has been contentiously ascribed to asthma, how it may relate to airway pathology is unclear. This thesis addresses these questions, and contributes a novel method to remove transient artifacts.

I found that while respiratory system resistance R_{rs} decreased due to BD in both health and asthma, elastance, E_{rs} derived from the reactance (X_{rs}) decreased only in asthma. Using a multi-branch airway tree model, the large airway response in R_{rs} to BD was nearly identical in both healthy and asthmatic subjects, while the small airways accounted for nearly all the differences in R_{rs} and X_{rs} in asthma, suggesting that X_{rs} may be a sensitive measure of small-airway function in asthma.

When comparing E_{rs} to the frequency dependence of R_{rs} in graded heterogeneity, I found as expected the frequency dependence of R_{rs} increased with heterogeneity, but depended largely on the frequency range, while E_{rs} also increased with heterogeneity, but independent of frequency. Thus, E_{rs} may be a more useful measure of small-airway dysfunction and asthma.

I also developed an automated technique based on the discrete wavelet transform to eliminate transient artifacts in Z_{rs} which achieved sensitivity and specificity greater than 95%.

While R_{rs} and X_{rs} responded significantly to bronchostriction and BD in both health and asthma, variation in R_{rs} and X_{rs} were altered only in asthma, but the changes in variation did not exceed the changes in R_{rs} and X_{rs} , and variability was not associated with lack of asthma control. Thus, confirming that while variability in R_{rs} and X_{rs} may be distinguishing features of asthma, they may not have much more clinical significance than R_{rs} and X_{rs} .

This thesis has shown that while R_{rs} , its variability, and the frequency dependence of R_{rs} , and its responses to agonists are altered in asthma, E_{rs} may be a better distinguishing measure of asthma because it can be mechanistically related to small-airway dysfunction.

List of Abbreviations and Symbols Used

ACQ	asthma control questionnaire
ACT	asthma control test
AHR	airway hyperresponsiveness
ASM	airway smooth muscle
ATS	American Thoracic Society
BD	bronchodilator
ERS	European Respiratory Society
cmH ₂ O	centimeter of water
CO	cardiogenic oscillations
COPD	chronic obstructive pulmonary disease
CoV	coefficient of variation
CT	computed tomography
C _{rs}	compliance of the respiratory system
DFA	detrended fluctuation analysis
DI	deep inspiration
ECG	electrocardiography
EEG	electroencephalography
EELV	end-expiratory lung volume
E _{L,mod}	model lung elastance
E _{rs}	elastance of the respiratory system
E _{rs,mod,no_shunt}	model respiratory system elastance without inclusion of shunt
E _t	elastance of a terminal airway unit
f	frequency
FEF _{25-75%}	forced expiratory flow between 25 -75% of forced vital capacity
FEV ₁	forced expiratory volume in one second
FFT	fast Fourier transform
FOT	forced oscillation technique
FRC	functional residual capacity
FSIF	Flow Shape Index Filter

FVC	forced vital capacity
G	tissue damping
GINA	Global Initiative for Management of Asthma
H	tissue elastance
^3He	Helium-3
HRCT	high resolution computed tomography
I_{aw}	Lung impedance
ICS	inhaled corticosteroids
I_{rs}	inertance of the respiratory system
Kg	kilogram
l_a	airway length
L	liter
LABA	long acting beta-2 agonist
MRI	magnetic resonance imaging
Mch	methacholine challenge test
OVW	optimal ventilator waveform
P	pressure
Pa	pascal
PC10FEV ₁	provocative concentration causing 10% decline in FEV ₁
PC20FEV ₁	provocative concentration causing 20% decline in FEV ₁
PC35R _{rs}	provocative concentration causing 35% increase in R _{rs}
PC60R _{rs}	provocative concentration causing 60% increase in R _{rs}
PEEP	positive end-expiratory pressure
PEF	peak expiratory flow
PT	pneumotach
r_a	airway radius
R _{aw}	airway resistance
RIP	respiratory inductive plethysmography
R _{L,mod}	model lung impedance
R _{rs}	resistance of the respiratory system
R _{rs,mod}	model respiratory system resistance

R_{rs,mod,no_shunt}	model respiratory system resistance without inclusion of shunt
$R_{rs}SD$	standard deviation of R_{rs}
$R5-R20$	R_{rs} at 5 Hz minus R_{rs} at 20 Hz
R_{ti}	tissue resistance
RV	residual volume
s	second / seconds
SABA	short acting beta-2 agonist
SD	standard deviation
SE	standard error of mean
SNR	signal to noise ratio
SVC	slow vital capacity
TLC	total lung capacity
TV	tidal volume
V'	flow
VC	vital capacity
$X_{L,mod}$	model lung reactance
X_{rs}	reactance of the respiratory system
$X_{rs,mod}$	model respiratory system reactance
X_{rs,mod,no_shunt}	model respiratory system reactance without inclusion of shunt
$X_{rs}SD$	standard deviation of X_{rs}
Z_a	impedance model non-terminal airway branch
Z_c	closed system impedance (FOT)
Z_{in}	input impedance of the respiratory system
Z_L	lung impedance
$Z_{L,mod}$	model lung impedance
Z_{meas}	impedance from the measured signals
Z_o	open system impedance (FOT)
Z_{rs}	impedance of the respiratory system
$Z_{rs,mod}$	model respiratory system impedance
$Z_{rs}SD$	standard deviation of Z_{rs}
Z_{tr}	transfer impedance

Z_{tube}	impedance of intervening tubing and anti-bacterial filter
Z_{uaw}	upper airway impedance
α_a	Womersley number
η	hysteresitivity
μ_{air}	viscosity air
ρ_{air}	density of air
ω	angular frequency

Acknowledgements

The work presented in this dissertation is a reflection of intellectual, moral, and financial support I have received over past few years from a constellation of people. Foremost, I thank Atlantic Canada Opportunities Agency, Lung Association of Nova Scotia, and NSERC for funding this work.

I am deeply indebted to my thesis supervisor, Dr. Geoff Maksym, for his persistent guidance, encouragement, and patience. I would like to thank very warmly Dr. Paul Hernandez and Dr. Colm McParland (Halifax Infirmary) for their support and insightful feedback on my work. I am grateful to Dr. J. H. T. Bates (University of Vermont) and Dr. Peter Gregson (Electrical Engineering, Dalhousie University) for serving on my supervisory committee despite their busy schedules. Your constructive criticism and suggestions were always helpful. Furthermore, I sincerely express my gratitude to my masters' supervisor Dr. C. P Gadgil (Government College of Engineering, Pune, India) who inspired me perusing my doctoral research in the field respiratory mechanics. Your motivation has been an integral part of this journey.

I would like to thank several other people who contributed to my work at different stages. I first thank Victoria Delange for her meticulous work on the forced oscillation device. I also recognize the support from the Division of Respiriology, Halifax Infirmary; special thanks go to Scott Fulton for his help in participant recruitment and lung function measurements. Not to under-emphasize is the cooperation from my study participants; this research was impossible without their participation.

I have been fortunate to have wonderful lab mates and friends. My dear thanks go to Ubong Peters, Del Leary, Hamed Hanafi, Lucas Posada and Rachel Wise. I have always enjoyed our interesting discussions in the student office and during lab meetings. I also much appreciate Darren Cole's help in the cell mechanics lab. My warm thanks to my friends and roommates; Yamuna, Kannan, Rowena, Kristin, Siddhartha, Kamala, Shailesh, and Chaitrali. Sandy Mansfield from the School of Biomedical Engineering deserves a special mention; you have been a loving and caring friend.

Lastly, I would like to say few special words for my family to share my love and appreciation. Mom and Dad, thank you for giving me enormous courage and support to

pursue my dream. And finally my very dear thanks go to my brother Paritosh, and his wife Bhargavi for their love and encouragement, and my nieces Sai and Radha for making me smile every day.

Chapter 1: Introduction

In this chapter, we present the central aims of the thesis with a brief rationale for each aim. An overview of the thesis chapters is presented in Section 1.1. In Section 1.2, we provide a list of manuscripts presented in this thesis and my contribution to them. A more in-depth discussion of the background literature follows in Chapter 2.

Asthma is a chronic inflammatory disorder of the lung characterized by reversible airway obstruction, increased sensitivity of airways to various exogenous and endogenous stimuli, described as airway hyperresponsiveness or AHR, and variable and recurrent breathing symptoms. Although the etiology of asthma is complex and varies among individuals, it ultimately leads to airway narrowing, involving constriction of airway smooth muscle (ASM) and leading to decreased ventilation [1]. Asthma can be diagnosed at any age, but most often it develops in childhood. Risk factors of asthma have been related to gene-environment interactions and exposure of the immune system to allergens in early childhood. Studies in children suggest that interaction between the immune system and exposure to inhaled allergens at an early age likely plays an important role in the development of asthma in subsequent years of life [2].

Global prevalence of asthma ranges from 1-18% of the population in different countries, and there is a concerning increase in the prevalence of asthma across all ages, sex and racial groups in recent decades [3]. Prevalence is highest in the developed countries [4, 5] and continues to rise, likely due to increased urbanization and adoption of the western life style. A 2004 estimate reports that there are 300 million people of all ages and ethnic backgrounds suffering from asthma globally with an estimated increase of 100 million by 2025 [6]. Canada has one of the highest rates of asthma in the world. Indeed, a statistics Canada report from 2012 states that 8.1% of Canadians of age 12 and above, approximately 2.4 million Canadians have been diagnosed with asthma [7]. Due to significant prevalence, asthma imposes a heavy economic burden on patients, their families, and health care system. The economic cost associated with asthma includes the direct cost in terms of medicines and hospital admissions, in addition to the indirect cost such as time lost from work and premature deaths. In the US, the total annual cost of

asthma from 2002 to 2007 was \$56 billion [8] and this amount is likely increased today. In Canada, the total cost of chronic lung diseases, including asthma, was \$12 billion in 2010 and is projected to double by 2030 [9].

Airway dysfunction in asthma

A number of studies have conclusively demonstrated the involvement of small airways in the pathogenesis of asthma [10-13]. There is strong evidence of small-airway narrowing and closures or near closures in asthma as reported by physiological measures using wedged bronchoscope [12, 14], spirometry by measuring maximum flow during helium-oxygen breathing [15], resistance and reactance measured by forced oscillation technique [16], nitrogen gas wash out technique [17-19], and novel imaging techniques [20-23].

The forced oscillation technique (FOT) provides a minimally invasive assessment of respiratory mechanics. FOT applies small amplitude pressure or flow oscillations on a subject's normal breathing, and determines mechanical impedance to airflow from the relationship between pressure and flow recorded at the subjects' airway opening. Resistance (R_{rs}) measured using FOT reflects resistance of the respiratory system including central and small airways, upper airway structures, and chest wall, but is largely dominated by large airways, while reactance (X_{rs}) reflects stiffness of the respiratory system at low frequencies. Low frequency X_{rs} and derived elastance (E_{rs}), have been found to be sensitive to the changes in small airways [24, 25]. Narrowing or closure of small airways obstructs ventilation in the lung leading to the formation of poorly ventilated regions called ventilation defects [20, 26], and decreases in X_{rs} at low frequencies [27]. Furthermore modelling and animal studies have shown that lung elastance is sensitive to heterogeneous peripheral airway constriction [24, 25]. These findings suggest that E_{rs} may be a clinically useful measure of airway dysfunction in asthma at the level of small airways, and may also be used together with R_{rs} to qualitatively distinguish between central- and small-airway narrowing in asthma. However, utility of E_{rs} compared with R_{rs} to assess central versus small-airway narrowing has not been quantified. This gap in the knowledge led to the research described in Chapter 3. In this work, we measured the respiratory mechanics using FOT in healthy and

asthmatic subjects following a bronchodilator (BD). We then reproduced the *in vivo* mechanics in these subjects using a multi-branched airway tree model of the human lung, and compared the model's response to simulated bronchodilation with the BD response of mechanics *in vivo*.

Quantifying respiratory mechanics with heterogeneous airway narrowing in asthma

In obstructive diseases such as asthma, R_{rs} has been found to exhibit frequency-dependent decreases over an intermediate frequency range of 5 to 20 Hz [27-30]. This frequency dependence of R_{rs} has been thought to be a good measure heterogeneous small-airway narrowing in asthma. However just how the frequency dependence R_{rs} may be related to airway heterogeneity is not clear. Furthermore, the frequency dependence is known to be influenced by the impedance of the compliant upper airway structures (upper airway shunt) including the cheeks and soft palate of the mouth [31]. However, the effect of upper airway shunt has not been computationally assessed relative to actual small-airway heterogeneity in asthma.

Another possible index of heterogeneity might be the E_{rs} derived from low frequency X_{rs} . As stated above, E_{rs} is sensitive to small-airway narrowing and closure [24, 32], and thus, could potentially be related heterogeneity, however, this has not been quantitatively assessed. To answer these intriguing questions, we employed the computational model of the lung used in Chapter 3, and reproduced the respiratory mechanics in 3 groups of asthmatic subjects with either mild, moderate, or severe airway obstruction reported by Cavalcanti et al. [27]. In particular, to account for the *in vivo* mechanics in subjects with asthma, we narrowed the central airways, and imposed airway heterogeneity by narrowing the small airways at different airway generations. We then compared the sensitivity of the model E_{rs} and frequency dependence of R_{rs} to the imposed heterogeneity, and also quantified the contribution of upper airway shunt to the model mechanics.

Artifacts in forced oscillation measurements

Even if FOT measurements cause minimal interference to subjects' normal breathing, the measurements are often contaminated by events such as coughs, swallows,

vocalizations, or airflow leaks. These events induce abnormal changes in the recorded pressure and flow signals leading to artifactual estimates of impedance values. While in adult patients, artifacts may be minimized by instructions or training, this is not possible in infants and children. In any case, elimination of artifacts is important to ensure accuracy and quality of the impedance data. Since the artifacts are usually transient in nature, they are dominated by high frequencies. This suggests that they may be detected using wavelet transform, a method that offers high temporal resolution for high frequency events. To explore this, in Chapter 5, we developed a novel automated method based on discrete wavelet transform to remove the transient artifacts from FOT measurements.

Variability of lung function in asthma

In asthma, respiratory symptoms and lung function widely fluctuate over time [33, 34]. Variability of lung function in asthma has been observed over multiple time scales. The peak expiratory flow (PEF) and forced expiratory volume in one second (FEV₁), assessed twice daily over a period of several weeks have been found to be highly variable in asthma [35, 36]. On the time scale of minutes, R_{rs} measured using FOT varies continuously in all individuals [37, 38]. In fact, variation of R_{rs} ($R_{rs}SD$, estimated as the standard deviation of R_{rs}) has been found to be higher in asthmatics than in healthy subjects in both adults and children [37-39]. This measurable difference on a short time scale may have important implications to clinical assessment and diagnosis and monitoring of asthma. Previous studies showed that in healthy subjects, $R_{rs}SD$ increased with activation of ASM by methacholine in the supine position to the level observed in asthmatic subjects [38], though asthmatic subjects were not assessed. Further studies in asthmatic children showed that $R_{rs}SD$ decreased following inhaled bronchodilator (BD). Together these studies suggested that there may be a useful relationship between $R_{rs}SD$ and AHR in asthma. As a part of this thesis, we investigated if $R_{rs}SD$ is related to AHR in adult subjects with asthma, and also examined the changes in $R_{rs}SD$ that occur in response to BD (Chapters 6 and 7).

Respiratory symptoms such as shortness of breath, wheezing, cough, and chest tightness are one of the key indicators for considering a diagnosis of asthma, and also for

assessment of asthma control and severity. However, patient-reported symptoms are highly subjective, and poorly associated with lung function measurements [40-42]. Currently there is no objective measure that relates disease state to asthma symptoms. Previous studies in children found that $R_{rs}SD$ differed according to asthma therapy [39]. Furthermore there is evidence that patients with higher $R_{rs}SD$ have clinically worsened condition [38]. These observations suggest that $R_{rs}SD$ may be related to poor asthma control. However, this requires a systematic investigation as previous studies did not assess patients' asthma control. Furthermore, AHR has been shown to be associated with presence of breathing symptoms and poor quality of life in asthmatic patients. This led us to think; if we find that increased $R_{rs}SD$ in asthma is associated with AHR, $R_{rs}SD$ may also be related to lack of asthma control. And if they are related, this will mean that FOT provides a simple, short, and objective assessment of lack of asthma control. Thus, as a part of this work, we also investigated the relationship between $R_{rs}SD$ and asthma control in patients with asthma.

Lung volume and variation in lung function

FOT measurements are sensitive to changes in lung volume. Indeed the relationship between R_{rs} and lung volume is well known; R_{rs} varies inversely with lung volume. Previous studies investigating the utility of variation in R_{rs} found a strong linear correlation between R_{rs} and $R_{rs}SD$ in both healthy and asthmatic subjects [37-39]. This suggests that $R_{rs}SD$ may also exhibit similar dependence on lung volume. Previously Que et al. measured $R_{rs}SD$ in healthy subjects in the upright and supine position [38], but they did not measure lung volumes. Indeed there is no systematic study examining how changes in lung volume may affect variations in R_{rs} in health and asthma. Thus in Chapter 8 of this thesis, we investigated the relationship between $R_{rs}SD$ and lung volume in a group of healthy and asthmatic subjects. In particular, we assessed $R_{rs}SD$ at functional residual capacity (FRC), and at 4 end-expiratory lung volumes; roughly 1 tidal volume (TV) and 2 TVs above and below the subjects' FRC, and characterized the relationship between $R_{rs}SD$ and lung volume in these subjects.

1.1 Overview

Chapter 2 is intended to provide an overview of the background literature relevant to this dissertation. It begins with a description of the lung structure and function. This is followed by characteristic features of asthma, asthma severity and control classification, and diagnosis and assessment of asthma using spirometry. Following this, it reviews the forced oscillation technique (FOT) and its application in the assessment of lung mechanics in asthma. Lastly, it reviews the literature on airway heterogeneity, variability of lung function, and effects of lung volume on lung function and AHR in asthma. Thesis aims with their rationales and hypotheses are stated at the end.

In Chapter 3, we measured changes in respiratory mechanics following BD in healthy and asthmatic subjects, and modeled the *in vivo* mechanics using a multi-branched airway-tree model of the human lung. We then assessed the degree of airway dilation that would be predicted to occur centrally and peripherally to account for the observed changes in mechanics *in vivo*.

In Chapter 4, using the computational model, we modelled the *in vivo* mechanics in patients with mild, moderate, or severe airway obstruction by narrowing the central airways and occluding the small airways. We then compared the changes in E_{rs} and frequency dependence R_{rs} in relation to the imposed heterogeneity over 0.2-5 Hz and 5-20 Hz. This work resulted in an original manuscript entitled ‘Modelling resistance and reactance with heterogeneous airway narrowing in mild to severe asthma’” authored by Swati Bhatawadekar, and co-authored by Del Leary and Dr. Maksym. The manuscript is published in the Canadian Journal of Physiology and Pharmacology. The chapter presents a modified version of this manuscript.

In Chapter 5, a novel technique based on the discrete wavelet transforms was developed to remove common impedance artifacts in FOT caused by coughs, swallows, vocalizations, and air flow leaks at the mouthpiece. This technique was used to eliminate controlled and spontaneous artifacts generated by healthy and asthmatic subjects. This work resulted in an original manuscript entitled ‘A study of artifacts and their removal

during forced oscillation of the respiratory system' authored by S. A. Bhatawadekar and co-authored by Del Leary, Yuanyuan Chen, Junichi Ohishi, Dr. Hernandez, Dr. Brown, Dr. McParland, and Dr. Maksym, published in the Annals of Biomedical Engineering, Jan 2013. The chapter presents a modified version of this manuscript.

Chapter 6, we present the assessment of variation of R_{rs} (R_{rsSD}) and X_{rs} (X_{rsSD}) as measures of AHR and lack of control in adult subjects with asthma. In this study, we assessed R_{rsSD} and X_{rsSD} in healthy and asthmatic subjects during assessment of AHR to methacholine, and investigated the relationship between R_{rsSD} , X_{rsSD} , and AHR. We also investigated the relationship between R_{rsSD} and lack of asthma control.

In Chapter 7, we present the assessment of BD response of R_{rsSD} in health and asthma. In this study, we measured R_{rsSD} at baseline and following a BD in healthy and asthmatic subjects, and investigated whether R_{rsSD} was useful indicator of patients' response to BD.

In Chapter 8, we present our work on the assessment of R_{rsSD} as function of end-expiratory lung volume in health and asthma. In this work, we assessed R_{rsSD} at FRC and end-expiratory lung volumes increased and decreased from FRC, and investigated the relationship between R_{rsSD} and the lung volumes.

Chapter 9 summarizes this thesis work, discusses key results, and presents original contributions made by this dissertation to the field of lung mechanics. Suggestions for future work are provided at the end.

1.2 Manuscripts and Conference Abstracts and Proceedings

This dissertation work resulted in two original manuscripts; articles 1 and 3 provided in the list of journal articles below. Different individuals assisted with the

participant recruitment, data collection and analysis, and interpretation of results, and have been acknowledged in appropriate sections.

For the thesis objectives, Dr. Maksym and I were responsible for defining hypotheses and methodology. I was responsible for the data collection and analysis, interpretation of results, and writing and submitting manuscripts. I was the first author of the manuscripts 1 (Chapter 4) and 3 (Chapter 5).

Del Leary provided the computational model of the human lung for the studies presented in Chapters 3 and 4. He was also involved in the interpretation of results, and the review of manuscripts for Chapters 3 and 4. Victoria Delange was involved in the development and testing of the FOT device, development of the Matlab code for analysing FOT patient data, and patient measurements for Chapters 3, 5, 6, and 7. Junichi Ohishi assisted in the data analyses for the work presented in Chapter 5. Guy Drapeau (Thorasys Thoracic Medical Equipment Inc., Montreal, Canada) provided the Matlab code for analysing the tremoFlo™ data presented in Chapter 8.

Dr. Hernandez and Dr. McParland were the clinical investigators on all patient studies (Chapters 3, 5, 6, 7, and 8), and responsible for the clinical assessment of study participants. They were involved in the interpretation of results (Chapters 3, 5, 6, 7, and 8) and the review of manuscripts presented in Chapters 3 and 5. Dr. Brown performed the glottal imaging using fiber-optic nasopharyngoscopy for the work in Chapter 5. Scott Fulton (Division of Respiriology, Halifax Infirmery) was the respiratory technician for all patient studies. He performed the measurements in the pulmonary function laboratory.

The forced oscillation system (Chapters 3, 5, 6, 7) was designed and built by Dr. Maksym and his colleagues at Dalhousie University. Thorasys Inc. (Montreal) provided the tremoFlo™ device for the work presented in Chapter 8.

The abstracts based on the research were presented at various national and international conferences. They are listed below following the list of journal articles and manuscripts arising from this dissertation.

Journal Articles and Manuscripts

1. Bhatawadekar S. A, Leary D, Maksym G. N. Modelling resistance and reactance with heterogeneous airway narrowing in mild to severe asthma. *Can J Physiol Pharmacol*. 2015 Mar; 93(3): 207-14
2. Hanafi H., Posada L., Bhatawadekar S. A, Brown J., Maksym G. N. A resonance-mode piezoelectric device for measurement of respiratory mechanics. *JBiSE* 2013 Nov; 6 (11): 1062-1071
3. Bhatawadekar S. A, Leary D., Chen Y., Ohishi J., Hernandez P., Brown T., McParland C., Maksym G. N. A study of artifacts and their removal during forced oscillation of the respiratory system. *Ann of Biomed Eng*. 2013; May; 41(5): 990-1002
4. Leary D, Bhatawadekar S.A., Parraga G., Maksym G. N. Modeling stochastic and spatial heterogeneity in a human airway tree to determine variation in respiratory system resistance. *J Appl Physiol*. 2012 Jan; 112(1): 167-75

** For articles 2 and 4, Bhatawadekar S. A. interpreted the results of experiments.

Conference Abstracts and Proceedings

1. Bhatawadekar S. A, Maksym G.N. Quantifying changes in respiratory mechanics with increasing degrees of small airway heterogeneity in asthma: a computational model study. Accepted for poster presentation, ATS 2015, Denver, CO
2. Marwa Alamer, Peters Ubong, Bhatawadekar S. A, Watson W. T, Maksym G. N. Repeatability of respiratory impedance and bronchodilatory response in asthmatic children. Accepted for post presentation, ATS 2015, Denver, CO

3. Peters Ubong, Bhatawadekar S. A, Dechman G, Ellsmere J, Hernandez P, Henzler D, Maksym G. N. Bariatric surgery improves lung mechanics of severely obese patients in the supine position. Accepted for poster presentation, ATS 2015, Denver, CO
4. Bhatawadekar S. A, Leary D, Maksym G. N. Quantifying effects of upper airway shunt on peripheral heterogeneity: a computational model study. BMES, San Antonio, Texas, P520, 2014
5. Bhatawadekar S. A, Leary D, Hernandez P, McParland P, Maksym G. N. Assessment of heterogeneity in asthma by airwave oscillometry. CSHRF and National CIHR Poster Competition, 2014, Winnipeg, Manitoba
6. Bhatawadekar S. A, Leary D, Fulton S, Hernandez P, McParland P, Maksym G. N. Frequency dependence of resistance compared with reactance as a measure of small airway heterogeneity. Am J Respir Crit Care Med 269: A3549, 2014
7. Bhatawadekar S. A, Leary D, Hernandez P, McParland P, Fulton S, Maksym G. N. Elastance bronchodilator response reflects asthma pathology. ERJ, Vol. 42, no. Suppl 57, P4695, 2013
8. Peters Ubong, Bhatawadekar S. A, Dechman G, Ellsmere J, Hernandez P, Henzler D, Maksym G. N. Lung mechanics in obesity and changes with bariatric surgery: the role of airway smooth muscle tone and airway unloading. ERJ, Vol. 42, no. Suppl 57, P4708, 2013
9. Bhatawadekar S. A, Leary D, Hernandez P, McParland C, Fulton S, Maksym G. N. Elastance derived from airway reactance is a better indicator of peripheral airway constriction in asthma. BMES, Atlanta, GA, P-A-167, 2012

10. Bhatawadekar S. A., Hernandez P, McParland C, Fulton S, Maksym G. N. Elastance derived from airway reactance can discriminate asthma from healthy controls. Am J Respir Crit Care Med 185: A2054, 2012
11. Bhatawadekar S. A., Hernandez P, McParland C, Fulton S, Maksym G. N. Bronchodilatory induced changes in airway reactance and its variation. BMES, Hartford, CT, P-B-171, 2011
12. Bhatawadekar S. A., Fulton S, Hernandez P, McParland C, Maksym G. N. Short term variation of airway resistance and response to bronchodilator in adults with asthma. Am J Respir Crit Care Med 183: A5563, 2011
13. Bhatawadekar S. A., Chen Y, Ohishi J, Hernandez P, Brown T, McParland C, Maksym G. N. A study of artifacts and their removal during forced oscillation. Biomedical Engineering Society (BMES), Austin, TX, PS-8A-15-194, 2010
14. Chen Y., Brown T, Bhatawadekar S. A, Leary D, Peters U, Deng L, Maksym G. N. A Method of assessing glottis aperture variation on airway resistance by forced oscillation. BMES, Austin, TX, PS-8B-15-181, 2010
15. Bhatawadekar S. A., Watson W. T, Maksym G. N. Variation of airway resistance in children with well-controlled asthma has similar response to bronchodilator as occurs in healthy children. Am J Respir Crit Care Med 181: A5024, 2010
16. Bhatawadekar S. A., Maksym G. N. Removal of artifacts in Forced Oscillation measurements in asthma using wavelets. Am J Respir Crit Care Med 179: A4433, 2009

** For abstracts 2, 3, 8, and 14, Bhatawadekar S. A. assisted in the data collection, and interpreted the results.

Chapter 2: Review of Relevant Literature

This chapter provides an overview of the literature relevant to this dissertation. Topics reviewed include structure and function of the lung, asthma characteristics and asthma severity and control classification, lung function tests used in diagnosis of asthma, forced oscillation technique (FOT) and measurement of lung mechanic using FOT. This is followed by a review of the literature on airway variability and heterogeneity in asthma, and the role of lung volume in lung function and airway hyperresponsiveness. The research hypotheses with aims and approaches are presented at the end.

2.1 Structure and function of the lung

The respiratory system is our body's link to the external environment to get fresh supply of oxygen for life. Its primary function is to supply oxygen to the venous blood and to remove carbon dioxide from it as per body's metabolic requirements. This is achieved by a unique design of the human lung, which brings blood and air into close contact over a large surface area, nearly the size of a tennis court ($\sim 130 \text{ m}^2$) [43]. For this to happen in an orderly manner, a branched airway network connects to the ~ 300 million alveoli, which constitute the gas exchange region.

The respiratory system can be divided into three major parts: the upper airway, the lower airway, and the chest wall (rib cage and abdomen). The chest wall houses the lungs and other structures, and assists during breathing. The upper airway which includes the nose and nasal passage, pharynx, and larynx conducts inhaled air from the nose and mouth down to the trachea. The major structures of the lower airway include the trachea, the bronchial tree and the lungs.

The function of gas exchange is achieved by the asymmetric, dichotomously branching tree-like structure that starts with the trachea, and bifurcates successively into the various level bronchi; main, lobar, segmental and then subsegmental. This bifurcation process continues down to the terminal bronchioles, which are the final

‘conducting airways’ and the smallest airways without alveoli [44]. The terminal bronchi branch into the respiratory bronchioles (with bubble-like alveoli occasionally budding from their walls), the alveolar ducts (completely lined with alveoli) and the alveoli, which make up the lung parenchyma comprising 80-90% of the lung. The alveoli are highly compliant largely due to the decreased surface tension at the air-liquid interface provided by the pulmonary surfactant. The airway smooth muscle (ASM) encircles the airways in a helical manner throughout the lung, and its contraction promotes airway narrowing.

A human airway tree constitutes approximately 23 generations [45] organized in a fractal pattern; each daughter airway replicates its parent airway in terms of structure and function. The airways become progressively narrower as they populate exponentially. However, their cross sectional area also increases markedly as they penetrate deeper into the lung, thus resistance contributed by the peripheral airways (lumen < 2mm) to the total airway resistance is remarkably small in a healthy lung [46]. Recently computational models have reproduced this structure using a combination of high resolution computed tomography (HRCT) and volume filling algorithms that approximate natural lung structure [47].

The pulmonary airways are much less compliant compared to the alveoli, but they are not completely rigid. During vigorous forced exhalation, they are prone to collapse even in a healthy individual. In fact a healthy person cannot exceed expiratory flow rate during forced exhalation in spite of increases in expiratory muscle efforts. This phenomenon, known as expiratory flow limitation is the basis of the most common pulmonary function test, spirometry, used in the diagnosis and monitoring of asthma. More details on spirometry are provided in Section 2.5.

2.2 Asthma

Asthma is chronic disease of the airways characterized by multiple features. One of its principle features is the reversibility of airway obstruction demonstrated as improvement in lung function either spontaneously or by treatment with medications. Subjects with asthma often report typical breathing symptoms such as chest tightness, cough, wheeze or episodic breathlessness particularly at night and/or early morning [48].

These symptoms vary in frequency and severity. Asthma is also characterized by chronic inflammation of the airways which leads to airway wall remodeling. The airway inflammation is heterogeneous in terms of intensity, cellular and mediator pattern and response to therapy, and characterized by a number of inflammatory cells including mast cells, eosinophils, T lymphocytes and macrophages, and airway structural cells including epithelial cells and airway smooth muscle. The inflammatory cells release a variety of key mediators such as chemokines, cytokines, histamines, and others which amplify the inflammatory response by promoting recruitment, activation and trafficking of other inflammatory cells to the inflammation sites, thus enhancing ASM contraction and mucus production. Previously, inflammation in asthma was believed to be present in large airways, however, it has been recognized that small airways are the major sites of inflammation and airway obstruction [10, 11]. Indeed, studies assessing peripheral airways with wedged bronchoscope technique showed that peripheral airway resistance was nearly 10-fold higher in mild asthma although their spirometry results were within normal limits [49]. Chronic inflammation results in irreversible changes in the structure of the airway wall. This phenomenon which does not appear to be fully responsive to treatment is called remodeling [50]. The remodeling and repair process increase airway wall thickness, and reduce airway lumen thereby restricting normal dilation of airways with lung inflation. Increased thickness of the airway wall may result in irreversible airway narrowing [51] and could possibly exaggerate airway narrowing with ASM contraction despite no changes in the mechanical properties of the airways and ASM [52].

Another characteristic physiological feature of asthma is increased airway hyperresponsiveness (AHR). AHR is defined as exaggerated airway narrowing upon exposure to a variety of endogenous and exogenous stimuli which underpins the periodic bronchoconstriction and resulting breathing symptoms typical in asthma, and characterized by two key attributes: increased sensitivity i.e. airways narrow too easily and at lower concentrations of non-specific contractile agonists than in normal subjects, and greater maximal airway narrowing i.e. at the highest dose of agonist, the extent airway narrowing can be greater than that can be induced in normal airways. It is the second component that is more dangerous and may induce life threatening attacks of

airway narrowing [53]. The severity of AHR generally correlates with severity of asthma [52, 54, 55]. However, AHR is a dynamic process [56] ; it appears or becomes worse after exposure to various triggers, and may decrease spontaneously or in response to anti-inflammatory therapy[57].

It is not yet known how the development of asthma can be prevented or how asthma can be cured. However it may be controlled by avoiding triggers provoking asthma episodes and by using appropriate medications. Poor management of the disease can lead to clinical complications resulting in poor health and impaired quality of life, hospitalizations, and even deaths.

2.3 Asthma severity and control

Prior to the 2008 GINA guidelines [48], asthma was classified by severity into four categories as: intermittent, mild persistent, moderate persistent and severe persistent where severity was defined as the intensity of the disease. This classification was primarily based on the level of symptoms, airflow limitation, and variability of lung function before commencement of treatment, and thus important for determining the initial level or step of asthma therapy. But once a patient is treated, its value is less clear. Many of the asthma features observed before the initiation of therapy change or disappear with proper medication, education, and environmental control, therefore assessing severity over time becomes challenging. The principle limitation of severity classification was its poor value in predicting the required treatment and patient's response to the treatment. Also, reassessment of severity requires patients' medications to be withdrawn for 2-4 weeks which is unethical and also impractical in some patients. Furthermore, there was little research evidence that a patient's untreated state could consistently inform future management decisions, or could predict the ease or difficulty of attaining good disease control once treatment was started [58]. In fact for a heterogeneous disease like asthma, continuous assessment and adjustment of therapy is necessary. Considering these factors, it was suggested that the severity classification is useful during a patient's initial presentation when the patient is not taking any medications, but it is not appropriate for effective prediction of the patient's treatment and responsiveness to the treatment. Thus it

is recommended that ongoing treatment decisions for a patient should be based on the patient's level of asthma control which is described further below.

Nevertheless in view of the limitations of above classification, severity is now defined in terms of intensity of treatment required to control asthma symptoms and exacerbations [59, 60]. That is, once the diagnosis of asthma is confirmed after excluding comorbidities, smoking, and poor adherence to treatment, severity reflects the lowest level of treatment required to achieve good control. Accordingly, the recommended classification of severity for clinical practice is [60] : mild asthma (with as-needed reliever medication alone or with low intensity controller treatment), moderate asthma (with low doses of ICS /long acting β 2 agonist (LABA)), and severe asthma (with high intensity dose of ICS/ LABA to prevent it from becoming uncontrolled, or asthma that remains uncontrolled despite this treatment). Severity is not a static feature of asthma, but varies over months or years. It can be assessed once the patient has been on controller medications for several months, and if treatment has been stepped down to find the patient's effective level of treatment.

Asthma control describes the degree to which clinical manifestations of the disease (symptoms, functional impairments and risk of exacerbations) are observed in the patient, or have been minimized or removed by treatment, and the goals of therapy are met [48, 58, 61, 62]. The level of asthma control results from the interaction between asthma phenotype, genetic and environmental factors, and response to treatment. Asthma control is classified as [58]: 1) controlled: patients with symptoms and reliever use twice per week or less, no night waking, no activity limitation or airway obstruction, or an exacerbation 2) partly controlled: symptoms or reliever use are present twice per week, any night waking, activity limitation or airway obstruction, or an exacerbation in any week 3) uncontrolled: the presence of any three or more of these individual features within any week. This classification is consensus based, and has not been formally validated [48, 58]. However it correlates well with asthma control test (ACT) [63] and with an assessment of asthma control as per the 3rd Expert Panel report guidelines [62]. Asthma control can change over time [64], therefore it needs to be assessed periodically, and medications may be adjusted accordingly. For example, therapy should be stepped up

when asthma is uncontrolled or considered if it is partly controlled in order to achieve or maintain control. But once good control is achieved, treatment should be stepped down.

The goal of asthma treatment is not just to control patient's symptoms, but also to prevent future adverse outcomes including exacerbations, a rapid decline in lung function, and side effects of the treatment. Thus assessing asthma control constitutes of two domains: symptom control (previously current clinical control) and risk factors for future adverse outcomes, and treatment issues such as inhaler technique and adherence, side effects, and comorbidities. Symptom control can be assessed from frequency of day-time and night-time symptoms, and reliever use to get relief from symptoms, work or school days missed, and ability to perform daily normal activities and functional limitation. Indeed a number of tools are available to assess symptom control which include questionnaires providing scores and cut off points to distinguish levels of symptom control for adults [65-67] and children [68, 69]. However, patients' perception of symptoms or exacerbations is subjective, and varies among patients. Thus objective measures such forced expiratory volume in one second (FEV_1), forced vital capacity (FVC) and FEV_1/FVC ratio are used to assess functional limitation. These measures are reviewed in Section 2.5.

Since lung function and symptoms vary over time, future risk of asthma exacerbations cannot be easily predicted. Moreover, asthma severity is poorly associated with risk of exacerbations [70]. For example, a patient with few symptoms and minimal day-to-day impairment may still be at serious risk of severe asthma attack [70, 71]. It has been suggested that factors such as frequent use of reliever medications, frequent asthma symptoms, frequent hospitalizations or emergency room visits, present use or recent withdrawal of systemic steroids are risk factors for future asthma exacerbation, hospitalization or death [72]. It has been recommended that future risk of exacerbations, fixed flow limitation, and medication side effects should be assessed despite good symptom control [60].

In summary, asthma severity and control are related but still distinct concepts. Asthma severity describes the intensity of treatment required to manage patient's asthma and achieve adequate control. Asthma control is the extent to which clinical manifestations of asthma are seen, and have been reduced or removed by treatment.

Control-based management of asthma involves adjusting patient's treatment in a continuous cycle of assessment, treatment and review of his /her response to symptom control and assessment of future risk [60]. Furthermore, the primary goal of asthma treatment is identical for all patients regardless of disease severity which is to achieve optimal disease control.

2.4 Diagnosing asthma

The heterogeneous nature of asthma makes its diagnosis challenging. However a correct diagnosis is a first step to effective management of asthma [73]. For this reason guidelines have been released [62] which identify key points essential to help establish a diagnosis of asthma.

The diagnosis of asthma is based on a combination of subjective and objective measures such as patient's detailed medical history, physical examination of upper respiratory tract, presence of symptoms of airflow obstruction or AHR, and evidence of reversible obstruction from pre and post bronchodilator (BD) lung function. Sometimes a family history of asthma, seasonal variability of symptoms, and/or the occurrence of symptoms after incidental exposure to allergens may all be used to guide the diagnosis.

In primary care where asthma is managed, diagnosis is based on a history of breathing symptoms like wheeze, shortness of breath, and cough [58]. However, as stated above, breathing symptoms are variable in severity over time [74]. Furthermore they are non-specific, and overlap with other respiratory diseases such as COPD or non-respiratory diseases such as cardiac failure or obesity thus necessitating an objective assessment to validate a diagnosis of asthma.

In symptomatic subjects, diagnosis is based on objective assessment of airflow obstruction by spirometry [48, 58, 75, 76]. Baseline spirometry is a good measure of asthma severity and airway obstruction. Furthermore, improvement in spirometric measures following a BD is an index of reversible airway obstruction, and confirms the diagnosis of asthma. Response to inhaled BD differs significantly between health and asthma, but it has been found to be poorly sensitive in diagnosing mild asthma in some studies [77]. This might have been because in mild asthma the airways are largely well

dilated at baseline and are thus less likely to exhibit a minimal significant response demonstrated as greater than 12% and 200 ml increase in FEV₁ from its baseline value (in children, > 12% of the predicted value) [60] after inhaling a BD.

Another test which is not a part of the diagnostic routine but helps rule out the possibility of asthma is the bronchial-challenge test. Bronchial-challenge is used to assess AHR to inhaled contractile agonists [48, 75, 78]. During the test, AHR is manifested as decline in FEV₁ which occurs at smaller doses of contractile agonist and which is greater in amplitude in asthma compared to healthy subjects. Bronchial-challenge is suggested when asthma is a serious possibility, and bronchodilator reversibility has not established or eliminated the diagnosis of asthma. However, bronchial-challenge test is more useful to exclude a diagnosis than to establish one because of its higher negative predictive power than its positive predictive power [78].

2.5 Spirometry

Spirometry measures flow and volume during a forced vital capacity maneuver, and the position and shape of the flow-volume curve during expiratory effort is useful diagnostically. Spirometry has been used to assess baseline lung function and severity of airway obstruction, monitor disease progression and result of therapeutic interventions in many pulmonary conditions. This section reviews the assessment of airflow obstruction and AHR using spirometry.

2.5.1 Assessment of airway obstruction

Spirometry is a classic objective test to assess presence and severity of airflow obstruction in a variety of settings including clinical trials [79], epidemiologic studies [80], primary care clinical setting [81] and assessment of asthma attacks in emergency rooms [82]. Currently it is the gold standard to assess pulmonary function, and performed in patients in whom asthma is suspected. It is a non-invasive and easy to implement testing in both clinics and outpatient departments. The instruments mostly are portable, easy to use, and widely available at a reasonable cost. Furthermore the test procedures

and results interpretation are comprehensively standardized which makes it an important tool in assessment of lung function.

Spirometry uses a simple instrument called a spirometer that typically measures flow as a primary signal and calculates volume by integration of flow. Among several parameters measured by spirometry, two important ones are forced expiratory volume in one second (FEV_1) and forced vital capacity (FVC), both requiring a maximal forceful effort to exhale air out of the lungs. FVC is the total quantity of air exhaled after a full inspiration while FEV_1 is the volume of air exhaled during the first second of FVC.

Both FEV_1 and FVC are reduced in asthma, however, FEV_1 reduces much more resulting in reduced FEV_1/FVC ratio. A ratio of greater than 80% is usually obtained in normal adult lungs [83] and possibly greater than 90% in children [48]. Lowered FEV_1 values predicts the presence of airflow obstruction. Measured values of FEV_1 are compared with the predicted values based on age, height, gender, and ethnic origin allowing patients to be categorized according to severity of airway obstruction. Standards require that forced expiratory maneuvers be repeated three times for reliable and reproducible test results, and the largest of the three values be recorded [84].

The forced expiratory volume in one second is the most repeatable measure derived from spirometry having a short-term within subject reproducibility of ≤ 200 ml and 5% in both healthy and asthma subjects of all age [85, 86]. It is inversely and linearly related to the severity of airway obstruction [86]. However as mentioned before, it is highly nonspecific and is influenced by a number of factors including total lung capacity, muscle effort during expiration, airway caliber, airway wall stiffness and lung elastic recoil [87]. Furthermore the FEV_1 maneuver requires taking a deep inspiration before the forced exhalation, which is now established to have pronounced effects on airway smooth muscle tone [88, 89]. In health and mild asthma, deep inspiration causes transient airway dilation which may last up to a few minutes [90-92]. However in severe asthma, these effects may be null or blunt, or the deep inspiration may even result in airway constriction [92, 93]. These effects may actually be important in determining difference in AHR between asthma and health, but they are not well understood.

Spirometry has a few significant shortcomings. The principal among these is the requirement of learned maneuvers requiring patient training, coordinated patient efforts,

and trained technicians for reliable and reproducible results. Due to the challenges of the maneuver, spirometry cannot be accomplished in patients such as infants, young children, elderly or paralyzed patients, mechanically ventilated patients, or patients with neuromuscular, and cognitive defects. Furthermore, acceptable test results are highly variable in children under age 8, and spirometry is not recommended in children of age below 6 years [94]. Lastly, while FEV₁ remains fundamental to the current clinical diagnosis of asthma, it is a single integrative measure of airflow measured at the mouth. The complex branching structure of the human airway tree indicates potential for complex flows with regional heterogeneities in airway segments, particularly towards the lung periphery. In a normal airway tree, the maximum resistance to air flow is provided by 4th to 8th airway generations, and change in the resistance of this region of the airway tree is reflected as changes in the FEV₁. Thus FEV₁ largely reflects resistance of large and medium airways, and is insensitive to events in small airways, which contribute to airway dysfunction in asthma.

Apart from FEV₁ and FVC, other commonly used spirometric measures are average expiratory flow rate measured over the mid half of the expiration (FEF_{25-75%}) and peak expiratory flow (PEF), which are briefly discussed below.

PEF is measured during routine spirometry or by a handheld device known as PEF meter. PEF is the highest instantaneous expiratory flow achieved during a forceful expiratory effort started from the position of maximal lung inflation. It usually occurs within the first 150 ms of forced expiration, and is affected by the first few hundred milliliters of exhaled air [95]. PEF reflects large airway caliber while FEV₁ reflects caliber of both large and medium size airways [95], although changes in PEF often parallel those in FEV₁ with increasing airway obstruction. However, PEF is less sensitive in detecting bronchial obstruction, and is poorly correlated with FEV₁ [96].

Circadian variations in airway caliber are often assessed by measuring variations in PEF twice or thrice a day or by measuring PEF over several days. In healthy subjects, variation in PEF is minimal, but it is increased in patients with poorly controlled asthma. However the association between PEF and asthma symptoms is poor [40, 97]. Furthermore temporal variations in PEF are found to correlate with asthma severity, and higher variability in diurnal variations in PEF is considered to be a predictor of high risk

of asthma exacerbations [35, 98]. Nevertheless the fact that increased variability manifested from the diurnal measurements is observed in other lung disorders as well makes PEF less specific in clinical practice [76].

Since PEF is reached early during the forced exhalation, it is relatively easier to perform than the sustained expiratory maneuver required for FVC. However like FEV₁, PEF also requires instructions and demonstration to patients for accurate test results. Also, there is variability in both published predicted reference values and values obtained by different peak flow meters [62]. Therefore, if PEF is to be used for monitoring purposes, the same brand of PEF meter should be used. PEF measurement is a simple and inexpensive method to determine airflow obstruction, and is widely accepted in the management and education of asthma. However it has been recommended only for monitoring and not for diagnostic purposes [62].

During forced maximal expiration, central airways largely contribute to the measurements during the early phase of expiration while peripheral airways contribute mostly at the end of expiration [99]. Therefore, FEF_{25-75%}, the flow averaged over mid-quartile range of the FVC, has been thought to better reflect small-airway obstruction in subjects with normal FEV₁ values [100]. However this has not been established, and the measurement itself has some challenges. The main problem with FEF_{25-75%} is its high measurement variability [100]. Furthermore, compared with successive FEV₁ measurements, FEF_{25-75%} has lower reproducibility [101]. Furthermore, FEF_{25-75%} partly depends on FVC; if FVC changes due to variable efforts, so does FEF_{25-75%}. It also gets altered by the changes in FVC that occur by air trapping and bronchodilation due to a shift in the range over which it is determined. Thus, FEF_{25-75%} cannot be used to assess reversibility of obstruction following BD when FVC has increased significantly, and there are no established cut off values for its reversibility [102]. Moreover, the normal values of FEF_{25-75%} vary greatly, and can be interpreted only when FVC is normal, therefore FEF_{25-75%} has limited reliability [102]. The National Heart, Lung, and Blood Institute Severe Asthma Research Program reports a poor correlation between FEF_{25-75%} and other measures of airway trapping such as FVC and RV/TLC [103]. Furthermore FEF_{25-75%} correlates poorly with resistance in the small airways in subjects with normal spirometry. In fact only one investigation reports a reduction in

FEF_{25-75%} and an increase in small-airway resistance measured by a wedged bronchoscope in subjects with mild asthma [49]. Although FEF_{25-75%} is widely used in pediatrics practice, it is difficult to interpret because of its dependence on lung volume, and is unlikely to contribute any information in addition to that provided by FEV₁ and its ratio to FVC [104].

2.5.2 Assessment of airway hyperresponsiveness

As discussed above, airway hyperresponsiveness (AHR) is not a unique feature of asthma. Nevertheless, its assessment helps establish the diagnosis of asthma in individuals presenting symptoms consistent with asthma but having normal lung function. AHR is often demonstrated in symptomatic individuals [105], and is most often absent in healthy subjects, although there may be some overlap. In asymptomatic individuals, AHR may be the only lung function abnormality [106] in which case AHR assessment may be useful to find out if the individuals are at increased risk of developing asthma [57, 106]

AHR is generally assessed by challenging the airways with progressively increasing doses of inhaled contractile agonists until a measure of lung function changes by a predetermined amount. Test results are presented on a dose-response curve in which dose represents the amount or concentration of the contractile agonist while response is the decrease in a lung function measure, often FEV₁. AHR is quantified in terms of the provocative concentration, PC₂₀ (or dose, PD₂₀) of the agonist causing 20% decrease in FEV₁ [105, 107]. However, other indices such as reactivity or slope of the dose-response curve have also been proposed [108]. A PC₂₀ value < 8 mg/ml confirms the presence of AHR in an individual [78]. Subjects with asthma may have PC₂₀ of less than 8 mg/ml whereas in most non-asthmatic subjects, PC₂₀ exceeds 16mg/ml. The airway response to contractile agonists often plateaus in normal subjects [54, 109] whereas it is elevated, or abolished in asthmatics which is thought to account for the morbidity and mortality associated with asthma [110].

Methacholine challenge is a highly diagnostic test giving positive results in symptomatic individuals [111], however it has a limited specificity [112]. This is because AHR can be found in healthy subjects and in patients with other lung diseases [113]

including allergic rhinitis [114], cystic fibrosis [115], bronchiectasis [116], and COPD [117]. It is a safe test, but requires more technical skills than spirometry, and an access to special equipment. Moreover it is time consuming, however, test-shortening procedures have been suggested [118]. AHR can also be assessed using other provocative stimuli such as mannitol, hypertonic saline or adenosine monophosphate challenge test, eucapnic voluntary hyperpnoea, or exercise which do not directly stimulate airway smooth muscle, but provoke bronchoconstriction indirectly by inducing release of bronchoconstricting mediators from mast cells, nerve endings or other cells resident in the airways [78, 106]. In general direct challenge using methacholine or histamine is more sensitive for demonstrating AHR while indirect challenges are more specific but insensitive for clinical asthma [119].

FEV₁ is the most commonly used endpoint in provocative challenge testing but other end points such as respiratory system resistance measured by the forced oscillation technique (FOT) may also be used. FOT needs minimal patient efforts and cooperation, and is therefore useful in non-cooperative patients or in those who cannot perform spirometry. However, FOT is not used currently in clinical practice, and its use is mainly reserved for patients unable to perform spirometry [78]. The forced oscillation technique is reviewed in Section 2.6.

In summary, spirometry is the current gold standard to assess disease severity and monitor disease progression in obstructive diseases such as asthma. It is a simple and highly standardized test for assessing respiratory function. Spirometry may not provide definitive diagnosis of asthma due to overlap between various diseased states and variation in lung function between various diseases; nevertheless it is an imperative tool that aids diagnosis and monitoring of asthma.

2.6 Forced oscillation technique

In patients who are unable to perform spirometry, an alternative method that requires minimal patient cooperation is the Forced Oscillation Technique (FOT). Lung function is assessed by FOT during normal tidal breathing. Therefore FOT has special importance in pediatric lung function assessment. FOT has a strong theoretical basis, and

its utility in the assessment of lung function has been demonstrated in multitude of investigations. A fairly comprehensive literature is now available on the use of FOT in humans, and guidelines have been developed on the methodological details of application of FOT in humans [89].

FOT was introduced by Dubois et al. more than 60 years ago as a non-invasive tool for characterizing the mechanics of the respiratory system [120], but it has only recently gained clinical recognition. The basic principle of FOT is to evaluate the response of the respiratory system to small amplitude, predefined oscillatory pressure or flow oscillations (also referred to as perturbation or forcing oscillations) in terms of mechanical impedance. The perturbation is applied in the absence of, or superimposed on, spontaneous breathing, and is limited in magnitude to avoid invoking non-linearities of the respiratory system, and causing discomfort to the patient. FOT can be set up in a number of approaches depending on where the forced oscillations are applied, and where the oscillatory flow and pressure changes are measured. When pressure and flow are measured at different sites e.g. pressure oscillations are generated around the body surface and the resulting flow is measured at the mouth (or vice versa), the impedance obtained is the transfer impedance, Z_{tr} . However, in the vast majority of clinical studies [121-124], flow (pressure) oscillations have been applied at mouth and resulting pressure (flow) changes have been recorded at the same site, in which case the relationship between pressure and flow is called the input impedance, Z_{in} (referred as Z_{rs} , impedance of the respiratory system in this document). Z_{tr} is the same as Z_{rs} when there is no parallel impedance between the sites of pressure and flow measurements.

The most conventional FOT set up utilizes a loud speaker encased in a closed chamber. The loud speaker produces low amplitude pressure oscillations that are applied at the subject's mouth during spontaneous breathing. To allow spontaneous breathing, the system is open to the atmosphere. This can be a resistive path, or often it is via a wide bore bias tube placed in parallel to the loud speaker. The bias tube offers low impedance to the atmosphere for breathing frequencies, but high impedance to the forcing frequencies [125]. The oscillatory changes in the pressure (P) and the flow (V') are recorded using pressure and flow transducers located near the airway opening. While sitting upright and wearing a nose clip, the subjects breathe on the device through an

antibacterial / antiviral filter. They supports their cheeks and mouth floor firmly with both hands to reduce errors caused by the shunt effect of upper airway impedance [31]. A continuous draft of fresh air is provided via the bias tubing to avoid carbon dioxide build up in the equipment dead space. The mechanical impedance of the respiratory system (Z_{rs}) is a complex mathematical quantity derived from the relationship between pressure and flow in the frequency domain, and is given by,

$$Z_{rs}(\omega) = \frac{P(\omega)}{\dot{V}(\omega)} \quad (2.1)$$

where $P(\omega)$ and $\dot{V}(\omega)$ are the Fourier transforms of the pressure and flow signals respectively, $\omega=2\pi f$, where ω is angular frequency in rad/sec and f is the oscillation frequency in Hz. Instead of the direct calculation from Fourier components, Z_{rs} is usually calculated by windowed spectral averaging but other approaches for accurate estimation of Z_{rs} exist. Z_{rs} is most often expressed in terms of Cartesian coordinates in the complex plane with real (resistance, R_{rs}) and imaginary (reactance, X_{rs}) components representing processes in the lung associated with energy dissipation and energy storage respectively,

$$Z_{rs}(\omega) = R_{rs}(\omega) + jX_{rs}(\omega) \quad (2.2)$$

where ‘j’ is an imaginary number defined as $\sqrt{-1}$. Z_{rs} represents the mechanical load presented by resistive, elastic and inertial components of respiratory system to the oscillatory flow. Reference values of R_{rs} and X_{rs} , as a function of sex, age, and anthropometric characteristics have been reported for both children [126] and adults [127, 128].

The real component of Z_{rs} , R_{rs} , is a measure of airway obstruction, and includes resistance of intrathoracic and extrathoracic airways, lung tissue and chest wall. R_{rs} and X_{rs} are functions of frequency, and their behavior is often characterized by fitting parametric models to the measured data described in Section 2.7. The most common model is the single-compartment model, where $R_{rs}(\omega)$ is described by a constant resistance taken as the average of R_{rs} over all frequencies, and $X_{rs}(\omega)$ can be well described by the equation,

$$X_{rs}(\omega) = \omega I_{rs} - j \frac{E_{rs}}{\omega} \quad (2.3)$$

where, I_{rs} and E_{rs} are the inertance and elastance of the respiratory system respectively, which are constant over the studied frequency range. E_{rs} is dominant at low frequencies, and reflects tissue and chest wall stiffness but is also inversely proportional to the amount of ventilated alveolar units and size of the lung. I_{rs} , on the other hand, is dominant at high frequencies, and accounts for the energy required to move primarily the gases within the respiratory system in response to the forced oscillations. At a specific frequency known as the resonant frequency, the elastic forces balance the inertial forces in the lung, and Z_{rs} is determined entirely by R_{rs} . At this point X_{rs} becomes zero, thus solving equation (2.3) for $X_{rs}(\omega) = 0$ gives,

$$\omega_{res} = \sqrt{\frac{E_{rs}}{I_{rs}}} \quad (2.4)$$

where ω_{res} is the resonant frequency from the model fit. In healthy adults, resonant frequency lies between 6-11 Hz [120, 123]. It increases with decreases in lung compliance due to stiffening of the lung tissue. Resonant frequency may be lowered in diseases which are associated with an increase in lung compliance, for example, emphysema.

Z_{rs} is sensitive to changes in lung volume [124, 129]. R_{rs} increases, and X_{rs} decreases at all frequencies in sitting subjects by reducing the lung volumes from their resting lung volume (FRC). These changes are accompanied by an increase in the resonant frequency. The increase in R_{rs} is accounted for by increases in lung resistance with decreases in the lung volume, while the increase in resonant frequency is accounted for by increased stiffness of the respiratory system at lower lung volumes as stated above. Significant alterations in R_{rs} and X_{rs} have been reported when assuming the supine position from the sitting position in both health and asthma [130, 131], which can be explained by a decrease in FRC with the postural change. Since FRC is reduced in obesity, and this is associated with narrower airways, R_{rs} is increased in obese individuals

[131]. Indeed lung volume has a profound effect on airway function. This is reviewed in Section 2.8.

FOT can be performed at a single sinusoidal frequency or over a range of frequencies [124, 132]. Single frequency FOT is technically easy to implement, and since all signal energy is concentrated at one frequency, a high signal to noise ratio (SNR) can be obtained. However modern FOT systems utilize a more complex perturbation containing multiple frequencies of interest allowing the characterization of the mechanical behavior of the respiratory system over a range of frequencies in a single measurement. This also shortens the data collection period, and reduces the risk of test results being affected by temporal changes in the mechanical properties of the lung. A multi-frequency signal may be a random noise signal [124], recurring impulses [123], or pseudorandom noise signal [129] containing optimized frequencies. In the multi-frequency signals, the oscillatory power of the signal is distributed among all frequencies contained in the signal, usually in a manner with higher amplitudes at the lower frequencies to help increase SNR above the noise due to breathing frequencies described as follows. The breathing frequencies range from 0.1 to 0.3 Hz, but may contain harmonics that extend an order of magnitude above 0.3 Hz. Breathing noise introduces systematic errors in Z_{rs} estimates, and lowers the reliability of Z_{rs} at low frequencies, especially in children and obstructed patients where breathing frequencies are high and rich in harmonics. Therefore the multi-frequency signal is designed in a way to enhance signal power at low oscillation frequencies, allowing higher SNR at low frequencies which are most affected by breathing harmonics. Special procedures have been developed to generate optimum pseudorandom signals that help minimize breathing noise related error [133].

Most of the FOT studies in humans have been performed during spontaneous breathing because it requires no special cooperation of the patient, and glottal closure is better prevented when awake. However when performed during spontaneous breathing, the lowest frequency in the oscillation signal should be roughly 10 times above spontaneous breathing frequency to avoid overlap with the higher breathing harmonics [121, 122, 134]. Therefore, the intermediate frequency range starts from 2 to 4 Hz in adults [89] and 4 to 8 Hz in children [135], and extends up to 30 to 40 Hz. In healthy

adults, R_{rs} normally varies from 2 to 3.5 cmH₂O. s. L⁻¹ at low frequencies (4-5Hz), and either remains constant thereafter or decreases slightly between 5 and 20 Hz [120, 123, 136]. Some studies also report a slight positive frequency dependence of R_{rs} beyond 10 Hz [123], which has been attributed to the influence of airway gas inertia on resistance [137]. Children have higher values of low frequency resistance, due to smaller airways than in adults, which markedly decreases over 4 to 20 Hz with decreasing age and size [138, 139].

The intermediate range of frequencies allow measurement of impedance during spontaneous breathing, however, low frequencies provide information more relevant to mechanical properties over physiological breathing range than that obtained at high frequencies. The low frequency range (< 10 Hz) is particularly sensitive to normal physical processes as well as pathologic structural changes. For example phenomena such as parallel time-constant heterogeneity [140], airway wall distensibility [141], tissue viscoelasticity [142], expiratory flow limitation [143], and collateral ventilation [144] more greatly influence Z_{rs} over frequencies between 0.1-10Hz, and thus are of interest to researchers. Generally, assessment of lung mechanics at frequencies near spontaneous breathing are performed in the absence of voluntary breathing. A few previous studies have obtained low frequency data by voluntary apnea [145] or muscle paralysis [146]. However, they required their subjects to remain apneic for approximately 30 sec at FRC with open glottis when oscillations were imposed [145], which is certainly impractical in the majority of patients. Lutchen et al. developed a technique for characterizing low frequency mechanics using a broadband signal called the optimal ventilator waveform (OVW) that combines mechanical ventilation with impedance estimation [147]. The OVW has been employed to partition airways and tissue properties in normal subjects following methacholine [148], in asthma following BD [149] and to assess inspiratory impedance in flow-limited patients [150]. It can be used to assess mechanical properties and mechanisms that affect breathing in subjects with healthy and diseased lungs which was not possible previously using the alveolar capsule technique [151, 152]. However, it is difficult to perform and less practical and viable in clinical settings.

FOT has demonstrated its clinical utility in the assessment of lung function. It has been shown to distinguish between healthy subjects and subjects with respiratory

complaints [153]. Recently it has been shown to be able to discriminate between asthma [27] and COPD patients [154] based on severity of baseline airway obstruction. Several studies have confirmed FOT to be an alternative tool to assess degree of bronchodilation in asthma and COPD [29, 94, 155-157]. However the results on sensitivity of FOT to BD response are contradictory. For example van Noord et al. reported that R_{rs} at 6 Hz was less sensitive than FEV_1 or resistance by plethysmography in patients with severe airway obstruction [29]. On the contrary, Zerah et al. reported comparable sensitivity and specificity for changes in FEV_1 and respiratory system conductance (inverse of zero intercept R_{rs}) in response to BD [156]. Similarly, a recent study found that FOT parameters and FEV_1 had comparable sensitivities to detect bronchodilation in mildly obstructed subjects [158] while another study found that FOT parameters including R_{rs} at 5 Hz were more sensitive than FEV_1 [159]. These differences may partly be due to differences in subjects or differences in devices or differences in end point FOT measures. On the whole, this may mean that any difference in sensitivities that may exist between techniques may not be clinically meaningful. Also, there are not many studies on bronchodilator response in healthy adult subjects, except two recent studies [128, 160]. Recently Oostveen et al. assessed BD response of FOT outcomes in a wide population of healthy Caucasian subjects over 4-26 Hz [128]. They reported an average decrease of 11% in R_{rs} across all frequencies following BD, and a 95th percentile equal to a 32% decrease in R_{rs} at 4Hz. Their average cut off value was close to the 15% decrease in R_{rs} reported previously by Nair et al.[160]. These values could serve as a reference in future studies, nevertheless, a prospective evaluation of these values is required to establish their utility in diagnosis and management of asthma in clinics.

FOT studies are also focusing on the reactance (X_{rs}) component of Z_{rs} which yields information on elastic properties of the respiratory system at low frequencies. It has been shown that low frequency X_{rs} is decreased (becomes more negative) when there is heterogeneous airway narrowing and closure or near closure in the peripheral lung regions [24, 161, 162] suggesting that low frequency X_{rs} may be a measure of heterogeneous airway narrowing. Indeed Walker et al. found that in moderate to severe COPD, the decreases in FEV_1 following methacholine were closely related to the decreases in X_{rs} , and these changes occurred in association with an increase in residual

volume and inspiratory capacity. These findings suggested narrowing and /or closure or near closure of small airways in response to methacholine [163]. Furthermore, using animal models of lung conditions that commonly occur in intensive care unit patients, Dellaca et al. showed that an increase in the respiratory system compliance derived from X_{rs} at 5 Hz is an index of the amount of open and ventilated lung [25]. Thus, they suggested that X_{rs} may be used to indicate lung recruitment / de-recruitment irrespective of how it is distributed in the lung, and the changes in low frequency X_{rs} could also be used to indicate the amount of recruited or de-recruited lung volume. The authors also developed a method using within-breath variation in X_{rs} in humans, and found this to be a sensitive measure of tidal expiratory flow limitation in COPD patients [143]. Furthermore, a recent study of asthmatic children found that area under the reactance curve demonstrated continued improvement after initial 12 weeks of inhaled corticosteroid (fluticasone) therapy during a total 48 week period of the study [164]. The authors speculated that this might be reflective of ongoing improvement in small-airway function in these children. More recently Kelly et al. demonstrated that X_{rs} is sensitive to changes in lung volume, and this lung volume dependence is substantially altered following BD in asthma [165]. These data suggest that low frequency X_{rs} and derived measures may also be used to assess changes in lung mechanics following therapy.

FOT has been successfully employed to assess AHR to methacholine [166] and histamine [167], exercise [168, 169], and cold air provocation [170] in both adults and children. Since FOT does not require deep inspirations which are known to influence the test results [88], it has been thought to be more sensitive to detect AHR than FEV_1 [171]. Furthermore, the post-bronchoconstrictor changes in R_{rs} and FEV_1 have been found to be well correlated [172-174]. In addition, previous studies found that assessment of AHR by FOT required three-fold lower concentrations of a contractile agonist than determined using forced expiratory maneuvers [174], which suggests that the use of FOT may shorten the bronchial-challenge duration. However, there is no agreement yet on increases in R_{rs} that would correspond best to 20% decrease in FEV_1 , although since these are different measures, a close correspondence is unlikely to exist. Nevertheless a consensus is needed for FOT to be more widely adopted as a clinical tool for assessment of airway hyperresponsiveness. Thus far, threshold values ranging from 30% to 90%

increase in R_{rs} have been used [89]. In any case, FOT outcomes have been found to be more sensitive to symptoms than FEV_1 . Indeed, a significant correlation has been observed between methacholine induced asthma symptoms and changes in R_{rs} and X_{rs} at 5 Hz, but not with FEV_1 [175]. Together these observations suggest that FOT may be a reliable and sensitive method to assess AHR in adult asthma.

Assessing lung function by FOT is rapid, thus FOT is preferred in young children. It is also well tolerated in the children. Indeed children unable to perform spirometry have been found to produce acceptable FOT results [94]. Furthermore, FOT has been shown to be able to distinguish between children with and without normal spirometry. FOT has also been shown to reliably evaluate airflow obstruction and its reversibility in young children [94]. For defining reversibility in young children, a 12% decrease from the baseline R_{rs} has been suggested as a normal physiological response to BD, and the optimum definition of significant bronchodilation has been defined as a decrease in R_{rs} of ≥ 2 SD score [89]. However further studies involving different age group children are required to confirm appropriateness of this cut off level. FOT has also been employed during bronchial-challenges in children, and found to have sensitivity comparable to that of spirometry and body plethysmography. During bronchial-challenge, the dose of the bronchoconstrictor that produces a 50% increase in R_{rs} ($PD50R_{rs}$) has been reported to be closely related to $PC20FEV_1$ [89].

There are some advantages to using FOT over spirometry. The principal advantage is that unlike FEV_1 , FOT does not require strenuous breathing maneuvers which are often difficult to accomplish in younger, old age, or sick patients. Therefore it is a valuable alternative in situations where spirometry is difficult or unfeasible. FOT has been used to track changes in respiratory mechanics in infants [176, 177], in sleep studies [178, 179] and in mechanically ventilated patients [180, 181]. Another advantage of FOT is that on account of the little cooperation required from patients, measurements can be repeated frequently without patient discomfort. This makes FOT useful in assessing efficacy of treatments.

FOT has some key limitations which must also be acknowledged. As describe above, a subject's breathing is an important source of error in FOT measurements. Breathing noise can be reduced by using signal frequencies at least 10 times higher than

the spontaneous breathing frequencies [89], although there is trade-off between using single and multiple frequencies as discussed earlier. Filtering techniques have been developed to reduce breathing noise errors [182]. Secondly, FOT measurements are sensitive to changes in lung volume, therefore test results must be interpreted carefully. Thirdly, FOT results are strongly influenced by upper airway shunt mechanics particularly in children and in obstructive patients when input impedance is measured. The upper airway shunt tends to underestimate impedance of the respiratory system, and the error is more pronounced at higher frequencies. A number of approaches have been proposed to minimize the upper airway shunt effect which are reviewed in the next section. Surprisingly, FOT does not provide the distinction between restrictive and obstructive lung diseases [89]. The changes in Z_{rs} in restrictive diseases have been found to be similar to those in moderate obstructive lung disease. This has been thought to be due to the upper airway shunt impedance which may mask differences in changes in lung mechanics resulting from various lung diseases.

FOT measurements considerations

When impedance is measured by forcing oscillations at the mouth and measuring flow also at the mouth, the upper airway wall (mouth, pharynx, and larynx) which is mechanically in parallel with the respiratory system, is exposed to the same pressure variation as the mouth. Some part of the excitation signal does not enter the trachea, but is lost in the movement of the compliant upper airway wall, mainly the cheeks, soft palate of mouth and pharynx [120]. This leads to an error in the estimates of impedance (Z_{rs}) [124], and the error becomes progressively larger as Z_{rs} increases because less and less flow is able to enter into the lungs with increasing pulmonary resistance. Moreover, the shunt impedance falls steeply with increasing frequencies; consequently Z_{rs} is underestimated at high frequencies. This effect varies among individuals according to the ratio of Z_{uaw} to Z_{rs} . Previous studies have shown that the effect of shunt is minimal in healthy subjects, but it leads to an artifactual frequency dependence of R_{rs} over the intermediate frequency range, an underestimation of X_{rs} , and an overestimation of resonant frequency in children and patients with moderate obstruction [31, 183]. However the effect of shunt impedance has not been directly quantified in relation to

airway obstruction in patients with asthma. The upper airway shunt is important particularly in children and infants in whom the shunt impedance is disproportionately smaller relative to Z_{rs} causing alterations in magnitude as well as frequency dependence of R_{rs} .

Different approaches have been proposed to minimize the effect of upper airway shunt. FOT guidelines recommend that the cheeks and the floor of the mouth be firmly supported with both palms [89]. This has been shown to increase R_{rs} at higher frequency (20 Hz) in healthy subjects by reducing the oscillatory flow shunted to the compliant upper airways [184, 185]. However, cheek support does not remove the effect of shunt perfectly [31, 184]. It only doubles Z_{uaw} , but the upper airways are not completely stiffened, still acting as compliant structures [124, 183, 186]. Thus, the higher the impedance of the structures distal to the larynx, the more the upper airway compliance shunts the oscillations applied at mouth into the upper airway structures. Another approach proposed by Michelson et al. is to obtain Z_{uaw} separately from the pressure-flow relationship at the mouth during expiratory efforts against a closed glottis (Valsalva maneuver) to correct Z_{rs} [124]. However, Z_{uaw} obtained during a closed glottis is larger than that obtained during quiet breathing, perhaps due to contraction of facial muscles, thus Z_{rs} is somewhat under-corrected [187]. Furthermore, the maneuver requires a large degree of training and cooperation from the subject to obtain reproducible data, and cannot be accomplished in all individuals. A more elegant approach is to use the head generator technique suggested by Peslin et al. [184]. In the head generator technique, the oscillations are generated around the subject's head rather than at his mouth. This considerably minimizes transmural pressure across the upper airway walls and suppress the upper airway wall motion. Measurements in healthy children and patients with moderate airway obstruction have found that the negative frequency dependence of R_{rs} observed with conventional FOT over intermediate range frequency tends to disappear with the head generator [183, 184] suggesting elimination of the shunt effect. In severely obstructed patients, however, the frequency dependence persists even with the use of head generator [183], indicating that the frequency dependence in these patients is due to the severe obstruction in distal lung regions. Thus, it has been suggested that negative frequency dependence of R_{rs} may be an artifact due to the upper airway shunt, but only in

patients with moderate airway obstruction [183]. In healthy adults, impedance measured using the head generator is not different than conventional FOT as Z_{rs} is smaller than the extrathoracic airway impedance, and therefore the effect of upper airway wall motion is negligible. The head generator technique is more cumbersome and less comfortable than conventional FOT. It may cause claustrophobic reactions in subjects, and stiffening of the soft tissues along the neck because of neck collar. Moreover the clinical utility of the head generator technique is not yet established [89]. Therefore further investigations are required to determine its sensitivity and specificity in clinical practice.

Cardiac activity may also be a source of error in FOT measurements. The close juxtaposition between the heart and lungs produces mechanical deformation of the lungs with each heartbeat, resulting in fluctuations in airway flow or pressure, called cardiogenic oscillations (CO). Cardiogenic interference in the flow can be measured at the airway opening during open glottis condition, and in the pressure can be measured just near the site of occlusion when the airway opening is occluded. The CO are found to be an uncorrelated source of noise in the FOT flow signal [124]. They mainly occur in the frequency range of 1-4Hz, and thus are an important source of noise below 4Hz. When any of the FOT frequencies coincide with the frequency of the heart beat or its harmonics, the FOT signal is corrupted resulting in less reliable estimates of impedance. One solution to reduce CO induced error is to increase the power of low frequency components which helps minimize the effect of CO interference commensurately [124]. Also CO in flow are absent or get diminished with increase in airway resistance [188]. Therefore CO artifacts are less likely to affect impedance estimates in patients with high airway resistance. Furthermore, filtering pressure and flow prior to impedance estimation helps eliminate cardiac interference, and increase the reliability of impedance in the low frequency range [189]. It is challenging to quantify the effects of cardiogenic interference on Z_{rs} . Poor coherence between the low-frequency pressure and flow signals has been used to indicate cardiogenic interference [189]. However this approach has been reported for experiments performed in the absence of breathing. Adaptive filtering has also been shown to be effective at eliminating interference at 1Hz [189]. The filtering technique however, was tested on apneic subjects; and its performance on signals containing breathing has not been studied.

2.7 Measurement and modelling of lung mechanics

In diseased conditions, mechanical properties of the respiratory system are significantly altered. Under these circumstances, measurement of lung mechanics by FOT allows for sophisticated interpretation of the mechanics using mechanistically based mathematical models of lung mechanics. In this section, we review some of these models.

Single-compartment model

Z_{rs} over the common frequency range of 4-32Hz has been reasonably well predicted using a simple model with two lumped elements comprising a balloon (representing homogeneously ventilated alveoli) sealed to a rigid cylindrical conduit (representing conducting airways from mouth to the alveolar regions. This arrangement, called the linear single-compartment model of the respiratory system is the simplest model (Fig. 2.1A). The model features R as a linear resistance to gas flow in the conduit and E as a linear elastance. At high frequencies, it becomes necessary to include an inertive element (I) to the model to account for the acceleration and deceleration of the gas and tissue in the lung.

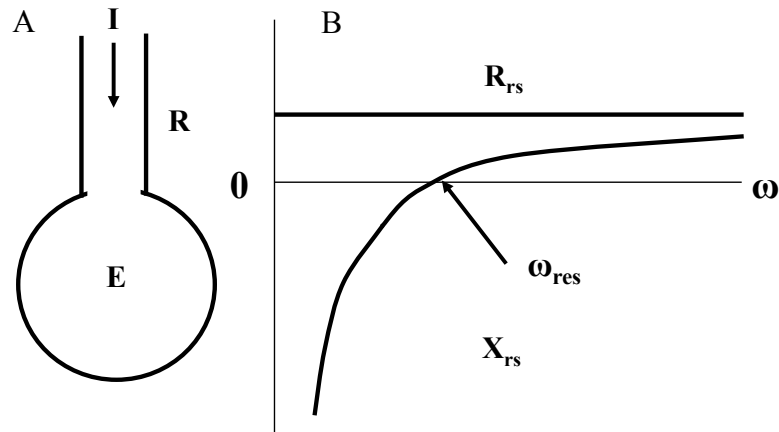


Figure 2.1: The single-compartment model of the respiratory system. A) The model schematic. R represents resistance, E, elastance and I, inertance B) R_{rs} and X_{rs} predicted by the single-compartment model in (A) as a function of frequency ω . Arrow indicates resonant frequency.

The single-compartment model predicts that R_{rs} remains virtually constant over the entire frequency range, and X_{rs} is a negative hyperbolic function of frequency, initially negative, and increasing monotonically with frequency after crossing zero at the resonant frequency (Fig. 2.1B).

Frequency dependence of R_{rs} and C_{rs}

Of course, the single-compartment model is not a complete representation of the lung, but it seems to mimic lung function reasonably well, at least in health. However it is too simple to characterize dynamic mechanical behavior of the lung in diseases or even under normal condition at very low frequencies. In health, frequency dependence in humans is exhibited at very low frequencies below 0.04 Hz [190]. In healthy children [191] or in animals [161, 192], frequency dependence in R_{rs} extends to higher frequencies. In obstructive disease particularly in asthma, frequency dependence is a common feature often measured between 5 and 20 Hz [18, 27-30, 124, 153, 193, 194].

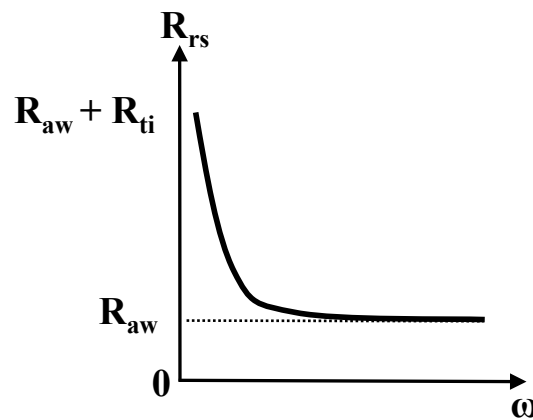


Figure 2.2: Schematic presentation of R_{rs} versus frequency behavior in a healthy lung. R_{rs} is comprised of two components, the tissue resistance R_{ti} which is dominant at very low frequencies and decreases quasi-hyperbolically with increasing frequency, the airway resistance R_{aw} .

A number of studies particularly in the 1990's attributed the frequency-dependent R_{rs} in a healthy lung to the viscoelastic properties of the lung tissue (tissue resistance R_{ti}), and the constant R_{rs} above the transition to plateau behavior to the viscous losses in the

airways (Newtonian resistance R_{aw}) (Fig 2.2) [195]. However it was recognized that the tissue viscoelasticity may not be the only mechanism of the frequency dependence of R_{rs} . Other seminal and recent studies showed that the frequency dependence can also arise because of regional differences in the mechanical time constants of the lung [24, 32, 140, 141, 148, 149, 196, 197]. Thus the frequency dependence of R_{rs} suggests that describing Z_{rs} features in healthy and diseased lung requires models with multiple compartments with different time constants.

Interpretation of frequency dependence of R_{rs}

Tissue viscoelasticity

The frequency dependence of R_{rs} and C_{rs} observed over low frequencies intrigued Mount [142] to introduce a model of tissue viscoelasticity (Fig. 2.3) which was later reintroduced and substantiated by Bates et al.[198-200]. Mount's model consists a dashpot connected in parallel with a Kelvin body. The dashpot R_{aw} accounts for resistance of the entire conducting airway tree, in open chest animals [201], but will also include the contribution from the chest wall in intact animals [202]. The Kelvin body comprises three elements, E_{sti} , R_{ti} and E_{ti} . The stiffness of the spring E_{sti} accounts for the static elastic properties of the lung tissue, while the series combination of R_{ti} and E_{ti} (a Maxwell Body) accounts for its viscoelastic behavior. Other models of lung mechanics with two-compartments were also proposed such as two balloons and conduits connected in parallel [140] or in series [141], and indeed these models and Mount's model are mathematically equivalent [203]. Subsequent studies with the alveolar capsule technique [204] and the flow interrupter technique [199, 200] suggested that the two-compartment tissue viscoelasticity model was the most appropriate to describe low-frequency mechanical behavior a normal lung ventilated at normal breathing frequencies. It is important to note that Mount's model accounts for only some of the frequency dependence of R_{rs} , however it does not well describe the '1/f' behavior of R_{rs} as it has only two time constants.

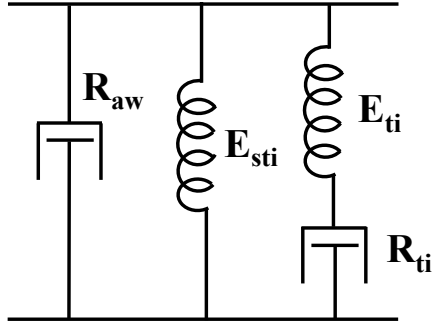


Figure 2.3: The viscoelastic model of the lung. The dashpot denoted by R_{aw} accounts for the resistance of the conducting airways. The mechanical properties of the lung tissue are described by a Kelvin body consisting three elements, E_{sti} , E_{ti} , and R_{ti} .

The Constant-phase Model

Rather than limiting the mechanical impedance to idealized lumped elements of a single or two time constants, a different approach introduced in the 1990s was to use the constant-phase model [205]. The constant-phase model constitutes a single homogenous airway compartment in series with a homogenous frequency-dependent tissue compartment (Fig. 2.4). The airway compartment is described by a Newtonian (i.e. frequency independent) resistance R_{aw} , and inertance, I_{aw} . I_{aw} reflects the inertance due to the gas in the conducting airways. The tissue compartment has two parameters, G for dissipative energy losses in lung tissues (damping) and H for elastic energy storage (stiffness). The model predicts the lung impedance Z_L as a function of frequency given by the equation,

$$Z_L(\omega) = R_{aw} + j\omega I_{aw} + \frac{G-jH}{\omega^\alpha} \quad (2.5)$$

The real (G) and imaginary (H) components of the tissue impedance decrease with ‘ ω ’ raised to the power α , and are related via a relation $\alpha = 2/\pi \tan^{-1}(H/G)$. The term constant-phase arises from the observation that the phase angle between pressure and flow across the lung tissue component ($\tan^{-1}(H/G)$) is independent of frequency, and therefore constant. Of note, the tissue component model is consistent with the structural damping hypothesis which has broad application in the dynamic mechanics of many materials, and

which in lung states that dissipative and elastic processes in lung tissue are closely coupled at a fundamental level [206]. The ratio $\eta = G/H$ is known as hysteresitivity or the structural damping coefficient. The constant-phase model accurately predicts the frequency dependence of R_{ti} described above.

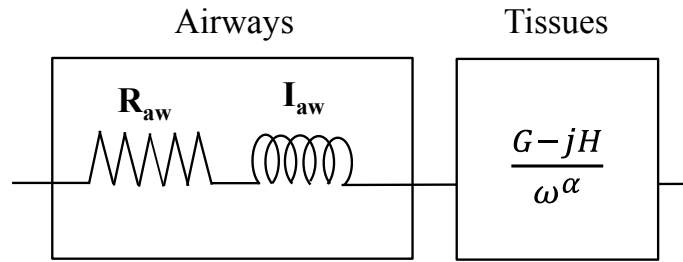


Figure 2.4: Schematic representation of the constant-phase model

It is remarkable that the constant-phase model allows partitioning the total lung impedance into airway and tissue components using only four parameters. Also, the model has provided extremely good fits to Z_{rs} data below 20Hz in humans [91, 207] and animals [202, 205, 208-210]. Moreover, it been also shown to fit Z_{rs} data in pathological conditions such as acute lung injury [211] and emphysema [212], and during bronchoconstriction [201, 210] with a remarkable precision, suggesting that even an extremely inhomogeneous, diseased lung structure may virtually behave like a homogenous lung structure.

Heterogeneous Models

While earlier studies attributed the frequency dependence of R_{rs} to the material properties of lung tissue, two early studies pointed out that the frequency dependence may also arise due to regional heterogeneity in time constants. Otis et al. [140] analytically described the impedance behavior with simple heterogeneity using a parallel two-compartment system (two parallel alveolar compartments (connected by two separate pathways) (Fig. 2.5A). The parallel two-compartment model predicts that if the two pathways have equal time constants, then their impedances change proportionately

with frequency, and the effective resistance and compliance of the system will remain unaltered at all frequencies. That is, the system will behave as if there is only one compartment with a single time constant. However, time constants inequalities due to non-uniform airway constriction and/or non-uniform tissue compliances will result in an unequal distribution of flows and volumes between the two compartments and cause frequency dependent decreases in R_{rs} and C_{rs} that occur typically in healthy adults between 0.2 and 1 Hz.

Another structural model that can also provide two time constants is the series two-compartment model proposed by Mead [141] (Fig. 2.5B). Mead's model comprises a compartment proximal to the airway opening (representing distensible central airways) connected in series with a distal compartment (representing homogenous lung periphery) as depicted in Fig. 2.5B. Mead suggested that the negative frequency dependence of C_{rs} observed in obstructed patients results from the shunting of airflow in the compliant central-airway wall when distal airways are severely constricted.

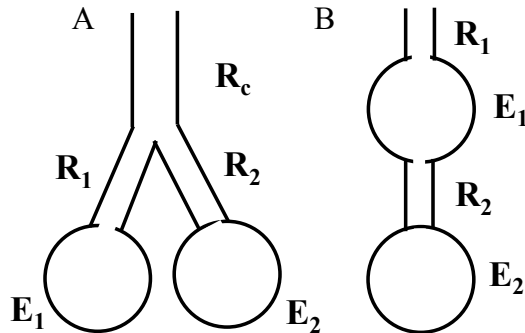


Figure 2.5: The linear two-compartment models. A) The parallel two-compartment model B) The series two-compartment model

While the Otis and Mead models partially predict the frequency dependent behavior of R_{rs} and C_{rs} by either parallel or serial heterogeneities, it is possible that in a diseased lung, serial heterogeneity of mechanical time constants and parallel pathway heterogeneities can coexist. Models with multiple parallel branches, and thus multiple

time constants can better account for the frequency dependence of R_{rs} over a broad frequency range.

Combined Models

Of course it is possible to use the constant-phase model together in a model which includes parallel heterogeneity such as with two parallel constant-phase models. This can be further extended by connecting multiple constant-phase models in parallel resulting in an arrangement called the distributed parallel compartment model. This type of distributed model may well describe the heterogeneous lung behavior in many different pathologies more accurately [213-215]. Indeed Kaczka et al. used the distributed model to describe the behavior of challenged lungs in 4 dogs [215]. They found that at the highest dose of methacholine, the model provided a superior fit in half of the dogs suggesting that the model accounted for the heterogeneities better than the single-compartment constant-phase model. The distributed approach can also be used to account for the serial heterogeneity. In this case, the homogenous airway compartment is divided into two equal halves by a shunt airway wall compliance to account for the compliant airway walls [148]. This model has been found to fit impedance data fairly well in patients with severe asthma [149] and COPD [216]. The distributed models do not provide specific information on anatomy or structural alterations that occur in chronic disease conditions or acute physiological perturbations [217]. Nevertheless they are able to quantify mechanical heterogeneity and characterize global lung function using a minimal number of free parameters [218].

In summary, the above approaches describe two principle mechanisms to describe the frequency dependence of R_{rs} . In health, the frequency dependence is most likely due to the viscoelastic behavior of the lung tissue, as heterogeneity is unlikely to be significant. In asthma, heterogeneities contribute substantially, and indeed, this appears to be the most common interpretation for the origin of the frequency dependence of R_{rs} , resulting in the substantial shift in the frequency dependence from below 0.2 Hz in health to the forced oscillation frequency range between 5 and 20 Hz. However, some portion of the frequency-dependence change in disease could be attributable to changes in tissue viscoelasticity, but this has not been clearly examined.

Since most of the frequency dependence in diseases such as asthma are thought to be due to heterogeneity, currently the frequency dependence of R_{rs} has been promoted as a useful index of heterogeneity in asthma. However, it is not known just how the frequency dependence of R_{rs} is quantitatively linked to heterogeneity. Another possible index might be the elastance. Elastance, E_{rs} derived from X_{rs} is thought to represent lung volume de-recruitment caused by small-airway narrowing, and thus could potentially be used to quantify this closure, but this has not been explored specifically. In Chapter 3 of this thesis, we used computational modeling of FOT data to quantify the relative contribution of small-airway heterogeneity and central-airway narrowing in mild asthma. In Chapter 4, we extended this work one step further to moderate and severe asthma. In particular, using a computational model of the human lung, we explored ways to quantify heterogeneity and relate it to E_{rs} , and compared the sensitivity of E_{rs} and frequency dependence of R_{rs} to airway heterogeneity in moderate and severe asthma.

2.8 Lung function and airway hyperresponsiveness

Lung volume and lung volume history have important effects on airway function. Lung volume affects airway diameters by dilating airways during inspiration and permitting re-narrowing of the airways during expiration. Indeed lung volume is a key determinant of airway resistance stretching the airway wall via airway-parenchymal interdependence [219, 220]. The parenchymal attachments on the external walls of intrapulmonary airways exert outward pulling forces on airways which are directly related to lung volume; greater forces are exerted at higher lung volumes leading to airway dilation. Conversely, reduction in the lung volume reduces parenchymal tethering. The decreased forces of interdependence favor airway narrowing and closure requiring greater pressure to re-inflate the lungs [221]. The extent to which increases in lung volume decrease airway resistance is also determined by elastic recoil of the lung [222], ASM tone [223], and stiffness of the airways. ASM constricts airways to some extent at baseline due to intrinsic tone, and can constrict airways to closure during activation, while parenchymal tethering dilates airways. Thus, at any instant in time, airway caliber is determined by a dynamic process rather than solely a static balance of forces, and this

is dependent on lung volume as well as lung volume history. A characteristic example of this is the bronchodilatory and bronchoprotective effects of DIs. In healthy subjects, DIs taken prior or during induced bronchoconstriction act to prevent or reduce subsequent airway narrowing whereas these effects are either diminished or lost in asthma [91, 207, 224]. When ASM constricts, the principal opposition to its shortening is provided by the elastic properties of airways and the forces of interdependence between airways and surrounding lung parenchyma. In fact the parenchymal attachments transmit transpulmonary pressure across the airway wall that opposes the ASM shortening. Thus when ASM shortens, it narrows the airway lumen only if it can generate enough force to overcome the load that opposes its shortening. When this load is reduced, the ASM can shorten more. The critical role of this load in determining the degree of airway constriction is evident from observations that AHR exhibits marked inverse dependence on both tidal volume [225] and mean lung volume [226, 227].

The effect of changes in lung volume on the ASM function in humans was first demonstrated by Ding et al. [227]. In this seminal study, the authors investigated the effect of changes in end-expiratory lung volume (EELV) on the degree of methacholine induced bronchoconstriction in healthy subjects. The most striking finding of this study was that decreasing or increasing EELV from FRC only by 500 mL profoundly enhanced or blunted the subjects' maximal airway response to methacholine respectively. This showed that in healthy subjects, at FRC, elastic load opposing airway constriction is significant, and maximal airway narrowing is highly sensitive to small changes in this load. Successive studies in humans performed under reduced lung volume condition achieved by supine position [228] or chest wall strapping [229, 230] have found large increases in the respiratory or lung resistance with the reduction in lung volume following methacholine. Indeed the role of lung volume in the pathogenesis of AHR was also noted by Skloot et al. [93]. They showed that prohibiting DIs during methacholine challenge produced similar airway response to methacholine in healthy and asthmatic subjects. However, the DIs had a striking effect in preventing methacholine induced constriction in healthy subjects, whereas this effect was absent in asthmatics.

A number of animal studies have clearly demonstrated how acute changes in lung volume significantly alter the response of lung mechanics to constricting stimuli. Higher

lung volume has been shown to decrease the onset rates and response of airway resistance to histamine and methacholine in animals. Nagase et al. elevated lung volume of rats above FRC by increasing positive end-expiratory pressure (PEEP) [231], and found that airway resistance to inhaled histamine was reduced by 12% for every unit increase in PEEP. Similarly Bates et al. measured airway response to injected methacholine in rats, and showed that an increase in PEEP reduced the rate of increase of airway resistance by an order of magnitude [226]. Another group studying the effect of reducing PEEP on the time course of lung resistance following histamine in dogs [232] reported that reducing PEEP of 0.5kPa by half caused a dramatic increase in the rate of increase of lung resistance and airway narrowing. The authors concluded that this was likely the result of reduced parenchymal tethering forces on airways caused by reduction in lung volume with reduction in PEEP. Collectively these observations are in agreement with findings of Ding et al. study described above [227], and demonstrate the profound influence of lung volume on the ASM contractile function and airway diameter.

The load opposing ASM constriction may be reduced for several reasons. The most efficient opposing force to ASM shortening is provided by lung elastic recoil. When lung elastic recoil is reduced such as it occurs in emphysema, ASM can shorten more easily for a given level of stimulus, causing excessive airway narrowing [233]. Even though there is no conclusive evidence that elastic recoil is reduced or lost in asthma [234-239], it has been found that even small changes in the transpulmonary pressure near FRC have significant impact on the contraction of ASM. As shown by Ding et al., breathing at lung volumes just 0.5L below FRC, which corresponds to only a slight reduction in the transpulmonary pressure, can enhance methacholine induced airway narrowing in healthy subjects [227]. Another and perhaps most likely reason for ASM unloading in asthma is the decoupling of airways and parenchyma, presumably by peribronchial edema or inflammatory exudate. Another load that can limit ASM shortening is the elastic load provided by cartilage stiffness. Previous studies in rabbits have shown that softening of tracheal cartilage caused by papain increased the airway resistance and maximal airway response to acetylcholine [240, 241].

In summary, the above discussed studies demonstrate that lung volume is the principle determinant of lung function and the effect of ASM function. Acute and chronic

changes in lung volume alter the degree of airway narrowing, and airway response during provocation challenges, and these effects are indeed important in asthma. Previous studies suggest that increased variability of the respiratory system resistance, R_{rs} , might be associated with ASM dysfunction in asthma [38, 39]. However the effect of lung volume changes on variability of R_{rs} has not been systematically investigated. Indeed Que et al. found that reducing the resting lung volume (FRC) by lying down in supine position significantly increased the variation in R_{rs} from healthy subjects, however the authors did not measure the subjects' lung volumes. Subsequent investigations in this area found a strong correlation between mean R_{rs} and temporal variation in R_{rs} [37]. This strong linear association, and the well-known inverse lung volume dependence of R_{rs} together suggest that variation in R_{rs} may also be related to lung volume. In Chapter 8 of this thesis, we investigated the lung volume dependence of the variation of R_{rs} in healthy and asthmatic subjects. In particular, we measured R_{rs} and its variation at FRC and lung volumes above and below FRC in these subjects, and assessed their relationship.

2.9 Variability of airway function in asthma

The respiratory system is continuously exposed to different fluctuating and heterogeneous stimuli, and non-linear interaction between these stimuli and the components of the respiratory system gives rise to highly complex and erratic fluctuations of many of its physiological variables [34]. Often these fluctuations in variables are indicative of a healthy condition [242], while lack of fluctuations or excessive fluctuations is abnormal, and associated with illness. For example, in health heart rate displays a high degree of variability with long-range correlations, whereas decreased heart rate variability is associated with severe heart conditions, aging and diabetic neuropathy, and is a predictor of mortality following myocardial infarction [243]. This suggests that variations in physiologic data may encode important information about underlying structure or a process in a condition of health, and analysis of changes in the variations may indicate abnormality, and provide prognostic information. This section reviews the literature on the assessment of variability of lung function in asthma.

2.9.1 Amplitude structure and short term variation of airway caliber

FOT outcome measures have been found to be more variable than FEV_1 in terms of day-to-day and week-to-week variation in diseased subjects. For example, Gimeno et al. compared R_{rs} with FEV_1 and slow inspiratory VC in healthy and COPD subjects over 10 successive days [244], and found that within subject variability in R_{rs} was larger than in FEV_1 and VC in COPD subjects. They attributed this to changes in airway mechanics caused by the underlying disease process. Recently Timmins et al. also reported that day-to-day to variation in R_{rs} was higher in COPD than in health and asthma [245]. Similar observations have been reported in children [246, 247]. Indeed Timonen et al. found that in children with asthma, day-to-day and week-to-week variation in R_{rs} measured at 8 Hz was higher than in spirometric indices [246]. Moreover the authors found that R_{rs} was the most sensitive measure among all measures during exercise challenge indicating that R_{rs} was sensitive to short-term functional changes in the respiratory system. More recently Trubel et al. compared variability of R_{rs} measured at 10 Hz in healthy and asymptomatic asthmatic children over 40 consecutive respiratory cycles [248]. While there was no difference in the mean resistance values between the two groups, variability in R_{rs} was significantly higher in asthmatics than in healthy children. Together these reports suggest that long term variation in R_{rs} may be a characteristic feature of asthma, and may have some clinical value.

In addition to tracking the variability in lung function over periods of days to weeks, recent studies have assessed the variation in lung function over time scale of minutes. Que et al. first reported that variation in Z_{rs} (quantified by standard deviation of natural logarithm of Z_{rs} , $\ln Z_{rs}SD$) was significantly higher in asthmatics than in healthy subjects [38]. The most intriguing finding of this study was that in healthy subjects, activating the ASM by methacholine in the upright position increased mean Z_{rs} , whereas activating it in supine position increased $\ln Z_{rs}SD$, and more interestingly brought both Z_{rs} and $\ln Z_{rs}SD$ to the level in asthmatic subjects. Thus combining activation and unloading of the ASM induced in healthy lungs the same degree of airway obstruction and variability of airway caliber that was present in asthmatic lungs. Similar observations have been reported recently by Gobbi et al. [230]. They also found that combining muscle activation and lung volume reduction (achieved by chest wall strapping)

increased variability in R_{rs} in subjects with asthma. Together, these findings suggest that increased variability of airway caliber in asthma might be associated with increased activity of ASM in asthma, and might be useful to predict subsequent asthma attacks. Lall et al. assessed $R_{rs}SD$ in asthmatic children [39], and showed that $R_{rs}SD$ decreased in response to BD more than the improvement in R_{rs} and FEV_1 . This suggested that $R_{rs}SD$ could potentially be used to assess effectiveness of BD, and patients' response to BD. It is important to point out that while variability in R_{rs} may arise from the increased contractile function of the airway smooth muscle, variability may also be influenced by other factors including variations in glottal aperture [249, 250], tidal breathing-associated changes in flow and lung volume [223], nonlinear flow dependence of R_{rs} , and transducer noise due to breathing.

It is important to note that subsequent reports do not support the usefulness of short-term variation in impedance. Diba et al. determined the clinical utility of variability of R_{rs} in asthma [37], however, they were unable to confirm Que et al.'s findings. In contrast to Que et al. and Lall et al. [38, 39], while Diba et al. found $Z_{rs}SD$ to be increased in asthmatics compared to healthy subjects, they found no differences in the variation of Z_{rs} (standard deviation of $\log Z_{rs}$, $\ln Z_{rs}SD$) between healthy and asthmatic subjects, and unlike in the study of Que et al., simultaneous activation and unloading of the ASM did not cause an increase in $\ln Z_{rs}SD$ in healthy subjects [37]. Moreover, the authors did not find any association between $\ln Z_{rs}SD$ and AHR or variations in PEF in their asthmatics. Recently, Muskulus et al. also did not find any difference in the variability of Z_{rs} between healthy and asthmatic subjects [251]. The exact reasons for these differences in findings are unclear, but possible explanations include differences in subjects or differences in magnitude of Z_{rs} between healthy and asthmatic subjects. In the study of Que et al. [38], Z_{rs} in asthmatic subjects was almost $3 \text{ cmH}_2\text{O}\cdot\text{s}\cdot\text{L}^{-1}$ higher than in healthy subjects, and the standard deviation of Z_{rs} and log transformed Z_{rs} were also higher in asthma than in healthy subjects. On the contrary, in the study of Diba et al. [37], Z_{rs} in asthmatic subjects was nearly $1.5 \text{ cmH}_2\text{O}\cdot\text{s}\cdot\text{L}^{-1}$ higher than in healthy subjects, and while the standard deviation of Z_{rs} was also higher in asthmatics than in healthy subjects, the latter difference disappeared when Z_{rs} was log transformed [37]. Collectively, these

observations suggest that differences in variability in R_{rs} between health and asthma may be related to differences in airway caliber between the two populations.

While increased variability in R_{rs} in asthma has been thought to be associated with the increased activity of ASM, previous observations suggest that it might also be related to lack of asthma control. The Diba et al. study patients were well controlled and clinically stable [37], whereas, the Que et al. patients had worsened clinical stability [38], and had been admitted to hospital for respiratory complications (personal communication between Geoff Maksym and Peter Macklem, Meakins-Christie Laboratories). This was similar in the study of Lall et al. where variability was increased in children with asthma. In that study, the attending clinician modified several of the children's asthma therapies based on their asthma symptoms following measurements (personal communication between Geoff Maksym and Paul Pianosi, Mayo Clinic), and many of these children required a step up in their therapy [39]. This suggests that perhaps increased variability of R_{rs} reported by Lall et al. and Que et al. in their patients may have been associated with poor asthma control. Unfortunately these studies did not assess their patients' level of asthma control, thus a systematic investigation of a relationship between $R_{rs}SD$ and asthma control is required.

Previous and recent studies have reported a strong linear correlation between $R_{rs}SD$ and mean R_{rs} [37, 38, 230]. This linear dependence arises from the nonlinear transformation between airway diameter and airway resistance [39, 252]. Due to the inverse 4th power relationship between resistance and diameter ($R \propto 1/d^4$), even a small change in airway diameter leads to a much larger change in airway resistance, and $R_{rs}SD$ is linearly related to R_{rs} for purely geometric reasons. Interestingly, some studies have reported deviations from this strong linear association. Indeed Lall et al. found that $R_{rs}SD$ was mildly correlated to R_{rs} ($r^2=0.4$) in children with asthma [39]. Moreover, the authors found that amongst asthma classification, a greater proportion of mild persistent and moderate persistent asthmatics decreased $R_{rs}SD$ more than R_{rs} following BD. This may mean that in these subjects, additional variation in R_{rs} at baseline was perhaps due to the variations in airway diameters caused by the activity of ASM, which decreased following BD. Furthermore Que et al. [38] found that the correlation between Z_{rs} and its variability largely disappeared when Z_{rs} was log transformed, and moreover, variability of $\ln Z_{rs}$

could be dissociated from airway narrowing during the high dose of methacholine (32 mg/ml) in healthy adults. Thus, while Diba et al. [37] concluded that correlation between Z_{rs} and its variability weakens the clinical utility of variability of Z_{rs} , the lack of perfect correlation found in Que et al. [38] and Lall et al. [39] studies suggest that variability of R_{rs} (Z_{rs}) may provide additional information that is not contained in the magnitude of R_{rs} (Z_{rs}). On another interesting note, the slopes of $R_{rs}SD$ versus R_{rs} relationship from the studies of Que et al., Diba et al., and Gobi et al. have been found to be similar [37, 38, 230], meaning that likely the factors influencing the slopes do not vary much across individuals. In addition, the proportionality between $R_{rs}SD$ and R_{rs} is likely maintained under different conditions including airway narrowing and heterogeneous ventilation as shown by recent modeling studies [252]. Overall, these findings suggest that the slope of the $R_{rs}SD$ versus R_{rs} relationship may be useful to distinguish between health and asthma.

In summary, while there is some evidence against the clinical utility $R_{rs}SD$ in asthma, other studies suggest that $R_{rs}SD$ may be useful, and associated with the ASM function. If increased $R_{rs}SD$ in asthma is reflective of increased contractile activity of ASM, it may be associated with AHR. Moreover, if $R_{rs}SD$ decreases with BD, it may be clinically useful to monitor a patient's response to asthma therapy. Furthermore, it has been shown that AHR relates to asthma symptoms. Thus if $R_{rs}SD$ is related to AHR, it would be interesting to explore if $R_{rs}SD$ also relates to lack of asthma control. If true, this may mean that a simple, short, and minimally invasive measurement of lung function could provide an objective measure of lack of asthma control. These interesting questions motivated us to investigate variability of R_{rs} in subjects with asthma (Chapters 6 and 7). In particular, we investigated $R_{rs}SD$ in asthmatics during methacholine challenge and airway reversibility test, and assessed the response of $R_{rs}SD$ to methacholine and BD respectively. Furthermore, we also assessed the relationship between $R_{rs}SD$ and asthma control in these patients.

2.9.2 Temporal structure of variation of airway caliber

It is well known that peak expiratory flow (PEF) exhibits a circadian rhythm in both health and asthma. The amplitude of this circadian rhythm is significantly greater in asthma than in healthy subjects [253-255], and has been associated with early morning

and nocturnal asthma [255]. Furthermore, the coefficient of variation (CoV) of PEF recorded over 2 weeks in asthmatic subjects in remission has been found to be related to worsening of the clinical status of asthma in the subsequent three months. This suggests that higher CoV of PEF may predict risk of future exacerbations, and be a useful prognostic index [35].

Another measure used to assess the variation of airway function in asthma is the diurnal variation in PEF which has been related to the variations in airway diameters. As stated before, variation of airflow assessed from twice daily recordings of PEF is increased in asthma, and used as an important tool in the diagnosis and monitoring of asthma [48, 62]. Variability of PEF correlates with AHR, asthma symptoms and impaired lung function in the general population [96, 256]. Frey et al. characterized the time series of the twice daily PEF values from asthmatic subjects, and investigated their utility as possible predictors of future asthma exacerbations. They found that the long term variation in PEF exhibits long-range correlations, and these correlations might be useful to predict the risk for asthma exacerbations [98]. Frey et al. also found that the long-range correlations of PEF were related to the bronchodilator used by the patients. In patients using short-acting β_2 agonist (SABA), PEF was more variable, and the long-range correlations of PEF were random and uncorrelated as compared to in patients using long-acting β_2 agonist (LABA). These findings have important consequences for the future risk prediction of asthma episodes. For any system, decreases in or loss of long-range correlations are associated with instability and unpredictable function. Thus random and uncorrelated long-range correlations of PEF variation in patients on SABA implied that these patients were likely at an increased risk of severe asthma episodes. Furthermore these findings also highlight the importance of long-term effects of SABA on airway function, which may be important clinically. SABAs are still used as the first-line rescue medications for asthma patients. Increased randomness of temporal correlations following SABA found by Frey et al. suggests that regular use of SABA may make airway function less stable, and enhance the risk of asthma attacks. By contrast, LABAs may help stabilize the lung function over extended period and reduce the risk of asthma episodes. Subsequently Thamrin et al. showed that long-range correlations of PEF could be used to predict patients's response to a treatment before initiation of the treatment

[257]. They showed that patients with medium to high long-range correlations of PEF during the placebo period were likely to experience more symptom-free days during 150 days with a LABA treatment, but not with a SABA treatment.

Interestingly the long-term variation of airway caliber does not correlate with its short term variation. Previously Diba et al. reported that there was no association between diurnal variability of PEF assessed over two weeks and variability of Z_{rs} over 15 minutes [37]. This suggests that mechanisms responsible for variations in lung function on short and on long time scales are perhaps different. It may be that the ASM tone contributes to the variability observed over shorter time scale [258] whereas additional factors such as circadian rhythm or day-to-day variations in heterogeneous external stimuli that the respiratory system is exposed to influence the lung function over longer time scales [72].

More recent studies have looked at the time-series data of the impedance of the respiratory system Z_{rs} for its utility to distinguish between health and disease. Muskulus et al. quantified the long-range correlations in variation in Z_{rs} in healthy, asthmatic, and COPD subjects using detrended fluctuation analysis [251], but did not obtain any significant differences in DFA scaling exponents. Furthermore, the exponents were close to 0.5 indicating characteristics of a random process, and the exponents in COPD appeared to be somewhat closer to the value of 0.5 than in healthy and asthmatic subjects indicating increased randomness of lung function in these subjects. However, the long range correlations could not distinguish between health and asthma or between asthma and COPD suggesting that the long-range correlations of Z_{rs} may not any have clinical value. However the authors also found that the DFA exponents for the scales above breathing period were more reliable than for the scales lower than the average breathing period. In fact exponents greater than 0.5 have been found in time series of tidal breathing parameters at larger time scales [259]. This may mean that perhaps Z_{rs} also exhibits similar behavior, but this conclusion will require much longer Z_{rs} recordings than used by Muskulus et al.

2.10 Heterogeneity in asthma

Heterogeneous airway constriction is a fundamental feature in humans. It is well known that anatomic asymmetry and structural heterogeneity in the branching of the human airway tree leads to regional differences in the degree of narrowing in the provoked lungs, referred to as airway heterogeneity. Detailed studies using HRCT have confirmed heterogeneity in human subjects [21, 260, 261] with the degree of heterogeneity being greater in patients with asthma [21]. Indeed, earlier studies using multiple-inert-gas elimination technique [262] and positron-emission tomography (PET) [263] showed heterogeneous airway closure and ventilation-perfusion mismatch following bronchoconstricting stimuli in asthmatic subjects suggesting heterogeneity in airway narrowing. Moreover HRCT studies have established heterogeneity of individual airway response to constricting stimuli in both humans [261] and animals [264]. Heterogeneity has important physiological consequences in asthma. Heterogeneous airway constriction leads to inhomogeneous alveolar ventilation causing inefficient gas exchange and impaired mechanical function, and contributes to airway hyperresponsiveness in both younger and older patients [265, 266].

In the last decade, inhaled-gas magnetic-resonance imaging (MRI) has been developed to non-invasively and regionally evaluate distal-airway function in COPD and asthma. In particular, studies with hyperpolarized MRI have identified large and contiguous regions of poor or no ventilation called ventilation defects [26, 267]. The large and contiguous nature of defects led to an initial speculation that defects are perhaps caused by severe narrowing of large airways feeding the constricted regions. However measurements of luminal area by computed tomography in rabbits showed paradoxical constrictor response in the central airways characterized by constriction or dilation in individual airways in different generations [268], which fails to explain the hypoventilation in large ventilation defects. The paradoxical dilation has also been observed in other species. In healthy human subjects, Brown et al. reported paradoxical dilation of some airways following inhaled methacholine, however the authors did not report if this was frequent in large conducting airways [261]. Furthermore, animal imaging studies have found moderate constriction in central airways despite the occurrence of large ventilation defects following methacholine [269]. Together, these

data and predictions from other modeling studies suggest that ventilation defects arise largely due to heterogeneous constriction of small airways [23, 24].

As described in Section 2.7, Otis et al. [140] and Mead [141] were the first to systematically examine the mechanical behavior of inhomogeneous lungs from a theoretical point of view. Using simple parallel and series linear two compartment models, the authors showed that regional differences in time constants among airways in parallel or series could arise from regional differences in airway narrowing or airway compliances leading to heterogeneous alveolar ventilation. Subsequently more complex computational models of the lung have been developed to gain deeper and more specific insight into the structural origins of low-frequency mechanical behavior of the lungs in asthma [24, 32, 196, 270]. These models incorporate anatomically explicit and morphological data obtained from living animals/ humans and their cadavers which include airway-wall thicknesses, the amount of airway smooth muscle for each airway generation, and assigned lung-tissue properties. These models predict that lung resistance and elastance from 0.1 to 5 Hz are extremely sensitive to peripheral airway constriction. In particular, mild peripheral airway constriction (~10%) with a few severely constricted or closed or nearly closed airways randomly dispersed throughout the lung periphery would result in dramatic increases in the levels and frequency dependence of both lung resistance and elastance predominantly near breathing frequencies. Such a constriction pattern would cause difficulty in breathing [270] and ventilation distribution [196]. These predictions have been found to be consistent with experimental data from provoked asthmatic subjects [271] and from ventilation-imaging studies [267]. Thus, these computational models provide conceptual understanding of different mechanisms that may or may not occur in asthma, and their effect on the mechanical properties of the respiratory system.

While ventilation imaging shows those regions that are well ventilated to those that are not, advancing our understanding of pathophysiological changes in asthma, the imaging data alone provide a limited understanding of how dynamic functional changes are related to alterations in structure in the disease. For example, imaging data does not fully answer a number of important questions. One question is which airways (locations and size) are responsible for impaired ventilation function in asthma. Another question is

whether the same airways are responsible for impaired mechanical function, whether airway constriction is random or clustered. A further question is whether the random or clustered constriction affects the level of mechanical impedance, and how much constriction is required to produce changes in mechanics that are observed *in vivo*. For example, as stated above, modeling studies suggest that airway response in asthma is dominated by peripheral airways (< 2 mm in diameter), however current imaging methods are unable to resolve airways less than 2 mm in diameter due to their limited spatial resolution [272]. These questions have led to the development of a novel approach known as image functional modeling or IFM.

Tgavalekos et al. have used IFM which combines ventilation imaging and lung impedance data with an anatomically explicit 3D airway-tree model to probe detailed structure-function relationship in asthma [16, 23, 273]. IFM was originally developed for lung images obtained from PET, but has been more recently advanced using hyperpolarized helium 3 magnetic resonance imaging (HP ³He MRI) [274]. Briefly and in general, in IFM, the 3D model is first scaled to a lung volume defined by a subject's PET or MRI image, and locations of ventilation defects are spatially mapped into the airway tree model to determine the terminal airways that are not ventilated due to constriction. Next, the largest sized airways of the model are identified that, if selectively constricted, could recreate ventilation defects in the model that best match the size and anatomic locations of defects imaged by PET/MRI without creating any new defects inconsistent with the image. Lastly, the best constriction pattern is identified for the airways outside the ventilation defects to match the model's respiratory mechanics to the subject's measured mechanics. The end result is a subject specific airway tree model that accounts for both ventilation defects and mechanical impedance data. The model can be used to predict specific airway constriction conditions that would be consistent with both imaging and mechanical data on personalized basis. Using IFM Tgavalekos et al. quantified the relative contribution of small and large airways in simultaneous deterioration of mechanical function and ventilation in asthma [23]. They found that severe ventilation defects in provoked mild to moderate asthma resulted from closures or near closures of the airways confined to the lung periphery, and these closures had to be in diameters < 2.4mm and mostly 0.44 mm. More importantly, the authors found that

constriction in the large airways could match only the impedance data in their patients, however matching both the impedance data and size and location of ventilation defects required constriction either in the small airways alone (< 2.4 mm), or in both the small and large airways, but not in the large airways alone. These findings suggested that in asthmatic subjects at least in this study, while large airway constriction contributed to mechanical dysfunction, degradation in ventilation function required heterogeneous narrowing and/or closures of small airways. Subsequently Campana et al. [274] advanced these findings [23] and showed that recreating the imaged ventilation defects in the model does not require full closure or collapse of airways leading to the defects, but needs only a mean constriction of $\sim 70\%$. This interesting finding suggests that although ventilation defects are observed as clusters of very poorly ventilated lung regions, and often perceived as nearly or completely closed regions, they may in fact be receiving some ventilation, but likely with time constants that make them functionally closed for gas exchange.

The patchiness of ventilation defects has been thought to be related to the integrative behavior of the lung [20]. Venegas et al. used an integrative model of the lung which incorporated the local behavior of a single terminal airway [275] and the global behavior of whole lung during breathing, including airway smooth-muscle forces, interaction among airways, and interaction between airways and surrounding lung parenchyma. In this model, low-level airway smooth-muscle activation led to virtually uniform constriction of the airway tree, and thus uniform distribution of ventilation. However, with increasing the muscle stimulation, clusters of poorly ventilated terminal airways emerged when the stimulation reached a critical level, and they were very similar to those observed in PET images of asthmatic lungs. The authors suggested that likely the serial and parallel interactions among airways led to a self-organized patchiness of ventilation with severe narrowing of airways within ventilation defects, and analogous mechanisms are involved in asthmatic lungs. This may mean that interdependence among airways is likely the key essential mechanism for emergence of ventilation defects.

2.11 Research hypotheses and aims

2.11.1 Elastance as an indicator airway dysfunction

The first objective of this thesis was to model the changes in *in vivo* mechanics in health and asthma following BD, and quantify the relative contributions of central and peripheral airways in airway narrowing in asthma. The following null hypothesis was tested.

- Respiratory system elastance (E_{rs}) estimated from respiratory reactance, X_{rs} , reflects small-airway dysfunction in asthma better than R_{rs} .

The aim of this hypothesis was to probe changes in R_{rs} and E_{rs} with BD in health and asthma, and compare the BD response to the simulated BD response of a multi-branch airway-tree model with central-airway narrowing and heterogeneous airway closure.

Approach: Lung mechanics were assessed using FOT at baseline and following inhaled BD (Salbutamol 200 mcg) in healthy and asthmatic subjects. We developed an anatomically-correct three-dimensional multi-branch airway tree model [252], and reproduced the baseline *in vivo* mechanics in asthmatics by occluding small airways and constricting central airways. We then opened the occluded airways and dilated the central airways to match the model's response to the *in vivo* BD response. We compared the relative changes in magnitude of the model's R_{rs} and E_{rs} following bronchodilation to the *in vivo* changes in R_{rs} and E_{rs} .

2.11.2 Quantifying respiratory mechanics with airway heterogeneity

The second objective of this thesis was to a) model and quantify the degree of heterogeneity required to produce respiratory mechanics in 3 groups of patients, those with either mild, moderate, or severe airway obstruction reported by Cavalcanti et al. [27] b) compare sensitivities of E_{rs} derived from X_{rs} and frequency dependence of R_{rs} to the imposed heterogeneity, and c) quantify the contribution due to upper airway shunt

Approach: We used the multi-branched airway tree model used in 2.9.2. We induced small-airway heterogeneity in the model by narrowing randomly chosen airways in the 10th airway generation to 10% of their initial diameters to account for E_{rs} at 5 Hz in asthma, and narrowed remaining airways to account for R_{rs} at 18 Hz. We also included the upper airway shunt impedance values from [276] to the model, and evaluated the model's respiratory mechanics over two frequency ranges: 0.2 to 5 Hz and 5 to 20 Hz.

2.11.3 Removal of impedance artifacts in FOT using wavelets

The third objective of this thesis was to develop an automated technique to remove artifacts such as coughs, swallows, vocalizations, short glottal closures and airflow leaks during FOT measurements.

Approach: Healthy subjects produced the above said artifacts at defined time intervals in a controlled manner while breathing spontaneously on FOT. A novel algorithm based on discrete wavelet transforms was developed, and impedance estimates were analysed using a novel wavelet-based algorithm. The algorithm was also tested on spontaneous artifacts produced by participants enrolled in studies presented in Chapters 6 and 7.

2.11.4 Variability of impedance in response to methacholine and bronchodilator

The fourth objective was to a) probe relationships between R_{rsSD} and AHR and lack of asthma control b) evaluate bronchodilator response of R_{rsSD} . The following null hypotheses were tested.

- Variation of respiratory resistance (R_{rsSD}) increases with ASM activation, and correlates to AHR in subjects with asthma.
- R_{rsSD} decreases following BD in asthmatics and more than in healthy subjects.
- R_{rsSD} correlates with asthma symptoms reflecting lack of asthma control.

Approach: To determine if R_{rs} relates to AHR, we measured R_{rs} over one minute during methacholine challenge following each dose of methacholine in healthy and asthmatic subjects, and studied the correlations between $R_{rs}SD$ and AHR. To determine if $R_{rs}SD$ is a measure of BD response in asthma, we assessed $R_{rs}SD$ before and after BD in subjects from the objective stated in Section 2.10.2. We assessed patients' level of asthma control using the Asthma Control Questionnaire [65].

The aims specific to these hypotheses were as follows.

- To generate a methacholine dose-response curve of $R_{rs}SD$ and compare it to the FEV_1 (forced expiratory volume in one second) dose-response curve, and determine if all subjects exhibit similar increases in $R_{rs}SD$ at the concentration of methacholine causing 20% decline in FEV_1 .
- To compare the increases in $R_{rs}SD$ with the decreases in FEV_1 following methacholine challenge.
- To compare the decreases in $R_{rs}SD$ with increases in FEV_1 following BD.
- To examine the changes in $R_{rs}SD$ with methacholine and BD for correlations with patients' level of asthma control.

2.11.5 Variability of impedance as a function of lung volume

The last objective was to assess the lung volume dependence of $R_{rs}SD$ in health and asthma. The following null hypothesis was tested.

- $R_{rs}SD$ correlates to R_{rs} with changes in lung volume and exhibits a functional dependence on lung volume similar to R_{rs} .

The aim for this hypothesis was to examine how changes in end-expiratory lung volume modify $R_{rs}SD$ in healthy and asthmatic subjects.

Approach: Lung mechanics were assessed by FOT at 6 Hz at FRC and at two end-expiratory lung volumes, approximately 1 tidal volume (TV) and 2 TVs above and below

FRC. Measurement at each lung volume was performed for 60 sec. Tidal volume was measured by respiratory inductive plethysmography, and changes in FRC were estimated from the differences in end-expiratory changes in TV. FRC was measured in the body plethysmograph following FOT.

Chapter 3: Respiratory System

Elastance Compared with Resistance

in Reversibility Testing in Asthma

3.1 Introduction

In asthma, airway obstruction primarily lies in small airways (diameter < 2-3 mm) [10, 12, 144]. However, assessing small airways is challenging using spirometry in mild or moderate asthma as the small airways contribute a very small component to total resistance, although this is increased in severe asthma [10]. While mean forced expiratory flow, FEF_{25-75%} is thought to better reflect small-airway obstruction compared with FEV₁, it is highly variable, and dependent on the forced vital capacity, FVC. FVC is also reduced in asthma due to small-airway closure and gas trapping, but using predicted FVC to detect small-airway obstruction is not very sensitive [277].

A number of methods have been used to assess small-airway function in asthma including nitrogen washout [17, 18], forced oscillation technique (FOT) [23], and functional imaging such as hyperpolarized noble-gas imaging, high resolution computed tomography, and positron-emission tomography [20, 21, 26]. FOT has been used to detect small-airway dysfunction through the frequency dependence of respiratory system resistance, R_{rs} , and altered respiratory system reactance, X_{rs} [136, 153]. Frequency dependence of R_{rs} , commonly taken to be the decrease in R_{rs} over the range from 5 Hz to 20 Hz has been thought to be a good measure of heterogeneous small-airway narrowing in asthma [278]. However, frequency dependence of R_{rs} may also be an artifact resulting from the shunting of flow oscillations into compliant upper-airway structures when the peripheral airways are severely obstructed [31]. Furthermore reports indicate that frequency dependence of R_{rs} may be device dependent suggesting that frequency dependence may not be a reliable index of heterogeneity [128].

Increasingly there is interest in using respiratory system reactance, X_{rs} , as a measure of lung pathology [25, 143, 165]. X_{rs} arises from the pressure-volume relation

during oscillations, and reflects the stiffness of the lungs at low frequencies, and inertive properties of the oscillating air at higher frequencies. The low frequency behavior of X_{rs} is of most interest in asthma as it is thought to reflect when peripheral airways close or narrow sufficiently leading to loss of communicating airspaces during breathing and forced oscillation [279]. Indeed X_{rs} has been shown to be substantially altered in asthma [27, 149, 271]. Previous studies have shown that X_{rs} decreases with increasing degree of airway obstruction [27] and airway heterogeneity [148, 271], and increases following bronchodilator (BD) [28, 29]. Cavalcanti et al. reported that respiratory compliance (C_{rs}) derived from the low-frequency X_{rs} was smaller in asthmatics than in healthy subjects, and increased significantly only in asthmatics following BD [28]. Furthermore Kaczka et al. found that in asthmatics, unlike in healthy subjects, lung elastance (inverse of compliance) increased sharply over 2-8Hz, and decreased following BD [149]. They attributed the decreases in lung elastance to increases in the accessible lung volume by opening and/or dilation of small airways by BD. Moreover animal studies have indicated that low-frequency X_{rs} is related to open and ventilated lung regions [25]. While the above studies have shown that X_{rs} and the derived quantity E_{rs} may be useful measures of small-airway narrowing in asthma, the utility and degree of E_{rs} compared with R_{rs} and spirometry has not been directly quantitatively assessed.

In this study, we used FOT and a computational model of the human lung to quantify the relative contributions of large and small airways in BD response in asthma. We measured spirometry and respiratory system mechanics by FOT in healthy subjects, and in subjects with mild-to-moderate asthma pre- and post- inhaled BD. We modeled the *in vivo* mechanics using a multi-branch airway-tree model, simulating central- and small-airway narrowing. We then assessed the degree of airway dilation that would be predicted to occur centrally and peripherally to account for the observed changes in mechanics *in vivo*.

3.2 Methods

3.2.1 Subjects

Eighteen healthy subjects (11 females) and 18 subjects with asthma (10 females) were enrolled in the study (Table 3.1). All subjects provided written informed consent approved by the Capital Health Research Ethics Board. Inclusion criteria for subjects with asthma included a physician diagnosis of asthma for at least for 12 months (based on symptoms and/or airflow reversibility), no changes or worsening of respiratory symptoms in past 6 weeks, and no changes in asthma medications in past 4 weeks before measurements. Control subjects had no history of asthma or any other respiratory condition. Current or ex-smokers with more than 10 pack years of smoking history were excluded. The asthma subjects' medications details are provided in Table 3.1

Table 3.1: Medication details of asthma subjects

Medications	No. of subjects
Short-acting beta-2 agonist (SABA)	4
SABA and inhaled corticosteroid (ICS)	2
SABA, ICS, and leukotriene receptor antagonist (LTRA)	1
SABA and a combination of long-acting beta-2 agonist (LABA) and ICS	3
Combination of LABA and ICS	3
LTRA and a combination of LABA and ICS	1
ICS	1
No medication	3

3.2.2 Measurements

Impedance of the respiratory system (Z_{rs}) was measured using an in-house built FOT device described previously [280]. Briefly, small-amplitude pressure oscillations (approximately ± 1 cmH₂O) generated using a loud speaker were applied at the subject's mouth via a disposable antibacterial / antiviral filter (MicroGard, Viasys Respiratory Care, Palm Springs, CA). The subjects wore a nose clip, and sat upright with their cheeks and chin firmly supported with their palms while breathing on the FOT device. The pressure and flow changes at the subject's mouth were recorded using a pressure transducer (TD-05-AS, SCIREQ) and Pneumotach (Fleisch No. 2, Lausanne, Switzerland) connected to a differential-pressure transducer (TD-05-AS, SCIREQ) respectively. The pressure and flow were amplified, and filtered using a Bessel filter (SC24, SCIREQ, Cut off 100 Hz), and sampled at 240 Hz with 16-bit resolution (DAQ 6036E, National Instruments, Austin, TX). The loud speaker was driven by a multi-frequency sinusoidal signal containing 3 frequencies at 5, 15, and 20 Hz which allowed for more rapid tracking of changes in R_{rs} since the fundamental period was 0.2 sec, or 4, 10, and 22 Hz, which were non-integer multiples to avoid effects of harmonic interference between frequencies. Twelve subjects (6 asthma and 6 controls) were measured at 5-15-20 Hz while 24 subjects (12 asthma and 12 controls) were measured at 4-10-22 Hz. The signal frequencies were grouped for analysis as: low, L: 4 and 5 Hz, mid, M: 10 and 15 Hz and high, H: 20 and 22 Hz.

The pressure transducer was calibrated using a U-tube fluid manometer, and the Fleisch pneumotach was calibrated by flow-integral method using a calibrated 3L syringe. While the pressure and flow transducers were calibrated first at DC, we also did open and closed compensation using a method described by Davey and Bates [281] Schuessler et al. [282]. This ensured that the impedance of the device was compensated for over the entire frequency range. The device was validated using a standard test load of 5 cmH₂O.s.L⁻¹ (Hans Rudolph, Inc., KS, USA) over the full frequency range ensuring that the DC calibration was accurate over the full frequency range. The open and closed compensation is described in detail in the following section.

Spirometry was measured by a constant-volume type body plethysmograph (VE20-VE62J, SensorMedics, USA) in accordance with ERS/ATS guidelines [283] and expressed using the Global Lung Initiative reference values [284].

3.2.3 Protocol

Three one minute FOT measurements separated by 15-20 s and spirometry were measured in the same order. Bronchodilator (salbutamol, 200 mcg) was administered, and the measurements were again performed 12-15 min thereafter.

3.2.4 Data Analyses

Data were analyzed using Matlab (The Mathworks Inc., Natick, MA). The three FOT recordings were concatenated, and Z_{rs} was estimated as follows. The concatenated pressure and flow signals were digitally filtered by using a Fast Fourier Transform, removing components up to 1 Hz, which removed most of the breathing signal, and inverse transforming to the time domain. They were divided into 1 s data blocks with 50% overlap, and each block was multiplied by a Hamming window function to minimize the effects of non-stationarity and remaining edge artifacts. Impedance at each excitation frequency (Z_{meas}) was estimated from the ratio of Fourier transforms of the pressure to the flow.

Conventionally impedance of the respiratory system Z_{rs} is described as being computed from the pressure and flow recordings obtained near the subject's airway opening. However in our set up, the pressure and flow transducers were located at some distance from the subject's airway opening and separated from the airway opening by a small piece of intervening tubing and the bacterial filter. Therefore to obtain impedance of the respiratory system, Z_{rs} , we compensated for the impedances of the bias tubes, bacterial filter, and tubing between the subject and the bacterial filter, Z_{tube} using a method described by Davey and Bates [281] and Schuessler et al. [282]. Briefly, we measured two complex system impedances: Z_c , closed system impedance (bacterial filter blocked by a rubber stopper) and Z_o , open system impedance (bacterial filter open to atmosphere). Z_c was the shunt impedance to the ground that primarily represented the

compressibility of gas within the tubing. It was assumed that the mechanical properties of the intervening tubing components are linear and do not change with time [282]. Z_{tube} was identified from Z_c and Z_o as,

$$Z_{tube}(\omega) = \frac{Z_c Z_o}{Z_c - Z_o} \quad (3.1)$$

and Z_{rs} was estimated as

$$Z_{rs}(\omega) = \frac{Z_{meas} Z_c}{Z_c - Z_{meas}} - Z_{tube} \quad (3.2)$$

where, Z_c , Z_o , Z_{tube} were defined as the ratio of pressure to the flow in frequency domain.

Resistance (R_{rs}) and reactance (X_{rs}) of the respiratory system were real and imaginary parts of Z_{rs} respectively. We estimated E_{rs} by least squares fitting of X_{rs} versus frequencies to the single-compartment model [136] $X_{rs} = 2\pi f I_{rs} - E_{rs}/2\pi f$, where I_{rs} was the inertance of the respiratory system. The quality of the model fits was assessed from r^2 values, and E_{rs} was discarded if r^2 was < 0.90 .

Outlying Z_{rs} values resulting from coughs, swallows, and glottal closures were discarded. Z_{rs} estimates were retained only if coherence was > 0.95 and /or signal to noise ratio (SNR) of the pressure and flow signals was > 20 dB [39].

3.2.5 Statistical Analyses

Data are presented as mean \pm standard error of mean (SE) unless otherwise specified. Normality and equal variance of the data were determined using Shapiro-Wilk and Levene's test respectively. For normally distributed data, changes in measures within subjects from baseline to post BD were compared using either a one tailed or a two tailed paired Student t-test wherever appropriate, and differences in measures between controls and asthmatics were compared using a two-tailed unpaired Student t-test. For non-normally distributed data, we used Wilcoxon signed rank test to compare changes in measures within a group, and Mann Whitney Rank sum test to compare differences in

measures between controls and asthmatics. For all tests, statistical significance was accepted at $p < 0.05$. Statistical tests were performed with SigmaPlot 12 version 12.3 (Systat Software, Inc. Chicago, Illinois, USA).

3.2.6 Modeling

Multi-branch airway tree

To help interpret the mechanics *in vivo*, we developed a multi-branch airway tree model [252]. The model was based on an anatomically correct three-dimensional human-airway geometry provided by Merryn Tawhai (The University of Auckland, New Zealand) [47] (Fig. 3.1A, airway tree shown with airway closures), and consisted of 26 generations and 64896 airways. The airway-tree model, up to the first 8 airway generations, was generated using a host-specific volume derived from x-ray multi-detector computed-tomography imaging. The remaining generations were created using a volume-filling algorithm maintaining daughter diameter ratios consistent with the established morphometry [285]. Since the Tawhai model is at total lung capacity (TLC), we reduced airway diameters and lengths to 80% of their original values, assuming a homogeneous isotropic volume change, and maintaining the plethysmographically measured functional residual capacity (FRC) to TLC ratio of 0.5 in our control and asthmatic subjects. This ratio was also approximately equal to the upright FRC to TLC ratio of the Tawhai model lung [47].

Because of the turbulent flow profile in some of the larger airways, we described the flow using Womersley flow rather than Poiseuille flow. For the model simulating the baseline condition in our control subjects (described in Simulations), we computed the Womersley number, α_a , for each airway branch given by,

$$\alpha_a = r_a \sqrt{\frac{2\pi\rho_{air}f}{\mu_{air}}} \quad (3.3)$$

where, r_a is the radius of the airway, ρ_{air} is the density of air (1.11 kg/m^3), μ_{air} is the dynamic viscosity of humid air at 37 C ($1.85 \times 10^{-5} \text{ Pa.s}$), and f , the oscillation frequency in Hz. We found that α_a was > 1 for 99 airways at 4 Hz (diameters $> 1.57\text{mm}$), for 688

airways at 10 Hz (diameters > 1mm), and for 2882 airways at 22 Hz (diameters > 0.68mm). Since a significant number of large airways had the Womersley number greater than 1, we decided to use the Womersley flow for our simulations. Accordingly, the complex impedance of a non-terminal airway was determined assuming Womersley flow [218] as

$$Z_a(f) = \frac{j2f\rho_{air}l_a}{r_a^2} \left[1 - \frac{2J_1(\alpha_a\sqrt{-j})}{\alpha_a\sqrt{-j}J_0(\alpha_a\sqrt{-j})} \right]^{-1} \quad (3.4)$$

where l_a is the length of the airway, and, J_0 and J_1 are the complex Bessels functions of order 0 and 1 respectively, α_a is the Womersley number of the airway, and j is the unit imaginary number.

Because of the very small volume of gas in the airways compared to the airspaces, we distributed the model lung elastance evenly among the terminal airways, with each terminal airway functionally serving as an alveolar compartment accounting for parenchymal stretch, surface tension and any gas compression [273]. This approach neglects any contribution from airway wall compliance or any gas compression within the airways, but this effect is much smaller than the effect of alveolar compartment [141, 286]. The impedance of a terminal airway was defined as

$$Z_t = Z_a - j\frac{E_t}{\omega} \quad (3.5)$$

where E_t is the elastance of the terminal airway unit. The impedance of the airway tree was calculated using a lumped element approach from the series and parallel network relations of airway impedances, and separated into its real ($R_{L,mod}$) and imaginary ($X_{L,mod}$) components. We then estimated $E_{L,mod}$ by fitting the single-compartment model to the $X_{L,mod}$ versus frequency data.

We also accounted for the trachea, glottis, and chest-wall mechanics which was not originally included in the Tawhai tree. The tracheal and glottic resistance, and the

chest-wall resistance of $0.5 \text{ cmH}_2\text{O}\cdot\text{s}\cdot\text{L}^{-1}$ each [129, 287, 288] were added to $R_{L,\text{mod}}$ to obtain the model respiratory system resistance $R_{\text{rs},\text{mod},\text{no shunt}}$. Furthermore, we added the chest-wall elastance of $9.3 \text{ cmH}_2\text{O}\cdot\text{L}^{-1}$ [288] to $E_{L,\text{mod}}$ to obtain the model respiratory system elastance, $E_{\text{rs},\text{mod},\text{no_shunt}}$.

We included the upper-airway shunt impedance (Z_{uaw}) to the model to account for the mechanics of compliant upper airway structures including cheeks and soft palate from the study of Cauberghs and Woestijne [276]. $Z_{\text{rs},\text{mod}}$ including the shunt impedance was computed from the parallel sum of Z_{uaw} , and $Z_{L,\text{mod},\text{no shunt}}$ that included the airway-tree impedance in series with tracheal and glottal resistances, and chest-wall impedance. $Z_{\text{rs},\text{mod}}$ was separated into resistance, $R_{\text{rs},\text{mod}}$ and reactance $X_{\text{rs},\text{mod}}$.

We evaluated the model performance at 4, 10, and 22 Hz, however here we report the mechanics at 4 Hz as this is one of the most commonly reported low frequencies.

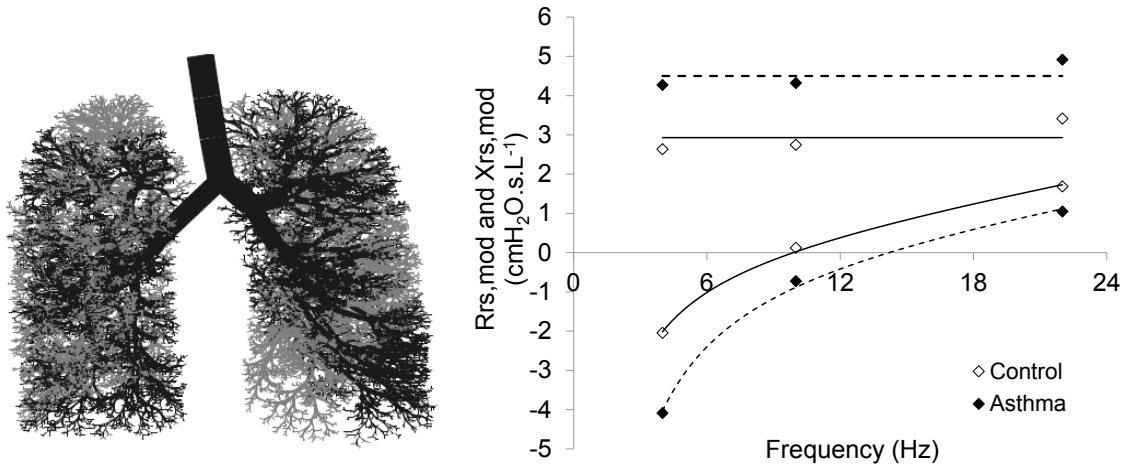


Figure 3.1: Multi-branch airway tree with small-airway closures and the model respiratory mechanics for controls and asthmatic subjects A) Multi-branch airway tree model with multiple ventilation defects created by occluding 475 of 1002 airways in the 10th airway generation. B) $R_{\text{rs},\text{mod}}$ and $X_{\text{rs},\text{mod}}$ estimated for the control and asthma models with their single-compartment model fits shown by solid and dotted lines. $R_{\text{rs},\text{mod}}$ at low frequencies and $E_{\text{rs},\text{mod}}$ were matched to the *in vivo* values in controls and asthmatics. Open symbols represent the model data mimicking our healthy subjects while closed symbols represent the model data mimicking our asthmatic subjects. Solid (controls) and dotted (asthma) lines indicate the single-compartment model fits to $R_{\text{rs},\text{mod}}$ and $X_{\text{rs},\text{mod}}$. r^2 values for the X_{rs} model fits were 0.99.

Simulations

For baseline simulations, we assumed that all airways were open. Because the Tawhai lung model is derived from a single individual, and the computed resistance does not match the mean resistance of the subjects, we scaled the Tawhai model relative to the model baseline FRC by 30.7% narrowing of the Tawhai diameters. This matched $R_{rs,mod}$ to the mean low-frequency R_{rs} at baseline in the controls (2.64 cmH₂O.s.L⁻¹). The elastance $E_{rs,mod}$ derived from $X_{rs,mod}$ was matched to the average E_{rs} in the controls (60.7 cmH₂O.s.L⁻¹) by distributing an elastance of 53 cmH₂O.L⁻¹ equally to all terminal units.

To reproduce the mechanics in the subjects with asthma, we first simulated random occlusions of the small airways at specific points within the airway tree by narrowing selected branches to 10% of their initial diameters. We limited our model to be as simple as we thought, to account for *in vivo* E_{rs} by a single variable parameter, the number of narrowed airways, where narrowing was chosen to be by 90%. This limited ventilation to less than a few percent of baseline, modelling defects in ventilation to airspaces peripheral to the sites of closure. We performed 10 repeated simulations of the random occlusions of 10th generation airways for a range of defect volumes, and averaged $R_{rs,mod}$ and $E_{rs,mod}$ estimates of these simulations. We then chose the defect volume for which the average $E_{rs,mod}$ was close to E_{rs} in the asthmatic subjects. Airway occlusion would lead to some increase in $R_{rs,mod}$, thus we accounted for any remaining $R_{rs,mod}$ by homogenous narrowing of central airways to match $R_{rs,mod}$ to low frequency R_{rs} in the asthmatic subjects.

We reproduced the BD-induced changes in respiratory mechanics via dilation of the central airways and opening of the occluded airways. For this, we performed 10 simulations of random opening of the airways from 475 occluded airways ranging from 25 to 200, and computed $R_{rs,mod}$ and $E_{rs,mod}$ for each simulation. We then computed percent decreases in $R_{rs,mod}$ and $E_{rs,mod}$ for each simulation with respect to the baseline condition, and averaged these decreases.

We also estimated the control- and asthma-model impedances using Poiseuille flow using the equations for resistance and inertance described by Leary et al. [252], and compared the impedances with those estimated using the Womersley flow described above.

3.3 Results

Demographics

Controls and asthmatics were matched for sex, age, and height although asthmatics were slightly heavier than controls ($p=0.043$, Table 3.2).

Pre and post BD lung function and mechanics

There was no difference in FEV₁ and FVC between controls and asthmatics at baseline (Table 3.2), however asthmatics had smaller FEV₁/FVC than in controls. Following BD, FEV₁ increased in both groups with a significantly larger increase in asthmatics than in controls. Furthermore FEV₁/FVC increased in both groups, but with no significant group differences, while FVC remained unaltered in both groups.

Baseline R_{rs} was higher in asthmatics at low and mid frequencies compared to in controls (Mann Whitney rank sum test, $p < 0.05$, Fig. 3.2A). Following BD, R_{rs} decreased significantly in asthmatics at all frequencies (Wilcoxon signed rank test, $p < 0.001$ for low and mid frequencies, and $p=0.001$ for high frequencies), and in controls, at low and mid frequencies (one tailed paired t-test, $p < 0.05$). The percent decreases in R_{rs} were higher in asthmatics (26.6 ± 4.9 SE %) than in controls ($11.7 \pm 3.1\%$) at low frequencies only (two tailed, unpaired t-test, $p=0.038$). We did not observe any frequency dependence R_{rs} in the asthmatics. In the asthmatics, while R_{rs} at low frequencies was slightly higher than at higher frequencies (Fig. 3.2A, $R_L-R_H = 0.44 \pm 1.9$ SD cmH₂O.s.L⁻¹), the difference between low and high frequency R_{rs} was not statistically significant (Wilcoxon signed rank test, $p=0.9$). Following BD, R_{rs} at high frequencies was larger than R_{rs} at low frequencies ($R_L-R_H = -0.55 \pm 0.5$ cmH₂O.s.L⁻¹, $p < 0.001$).

There was no difference in X_{rs} values between controls and asthmatics at baseline (Mann Whitney rank sum test, Fig. 3.2B). Following BD, X_{rs} increased only in asthmatics (Wilcoxon signed rank test, $p < 0.001$) but not in controls. When we compared the differences pre- and post-BD, the increases in X_{rs} were significantly larger in asthmatics than in controls (Mann Whitney rank sum test, $p < 0.05$).

As described above, E_{rs} was estimated by fitting the single-compartment model to the X_{rs} values at 3 oscillation frequencies. In 4 subjects (1 control and 3 with asthma), r^2 values for X_{rs} model fits were < 0.90 . Excluding these 4 subjects, there was no difference

in baseline E_{rs} values between the control (n=17) and asthma subjects (n=16) (Fig. 3.3). However, following BD, E_{rs} decreased only in asthmatics (Wilcoxon signed rank test, $p < 0.001$) but not in controls, and the decreases were higher in asthmatics (23.2 ± 5.3 SE %) than in controls ($3.9 \pm 4.2\%$, two tailed unpaired t-test, $p=0.007$). Comparing the decreases in R_{rs} between controls and asthmatics, we found that the decreases in R_{rs} in asthmatics ($23 \pm 4.7\%$) were not different than in controls ($13.5 \pm 4.7\%$, two tailed unpaired t-test, $p=0.17$).

Table 3.2: Subject demographics and lung function for study subjects

	Groups		p value
	Controls (n=18)	Asthma (n=18)	
Sex, male / female	8 / 10	7 / 11	
Age, years	35.2 ± 3.2	35.9 ± 3.2	0.84
Height, cm	169.2 ± 2.7	168.8 ± 2.2	0.92
Weight, kg	70 ± 3.8	83.1 ± 4.9	0.043*
BMI, kg/m ²	24.4 ± 1.12	29 ± 1.6	0.01
FEV₁, % predicted			
baseline	96.8 ± 2.1	83 ± 6	0.21
post BD	$100.4 \pm 2.4^{##}$	$91.7 \pm 4.5^{##}$	
% change	3.7 ± 0.7	16.3 ± 5.9	0.022**
FEV₁ Z-score			
baseline	-0.3 ± 0.2	-1.2 ± 0.4	0.2
post BD	$0.04 \pm 0.2^{##}$	$-0.6 \pm 0.3^{##}$	
change	0.3 ± 0.06	0.7 ± 0.2	0.025**
FVC, % predicted			
baseline	100.2 ± 3.2	97 ± 4.8	0.92
post BD	100.1 ± 3.2	102.2 ± 3.4	
% change	-0.2 ± 0.37	8.4 ± 4.78	0.21
FVC Z-score			
baseline	-0.02 ± 0.3	-0.2 ± 0.4	0.71
post BD	-0.03 ± 0.3	0.2 ± 0.3	
change	-0.01 ± 0.03	0.4 ± 0.2	0.27
FEV₁/FVC %			
baseline	80.8 ± 1.7	69.9 ± 3.4	0.007**
post BD	$83.8 \pm 1.4^{\#}$	$74.2 \pm 2.9^{##}$	
% change	3.8 ± 0.6	7.2 ± 2.2	0.06
FEV₁/FVC Z-score			
baseline	-0.33 ± 0.3	-1.7 ± 0.4	0.002
post BD	$0.13 \pm 0.2^{\#}$	$-1.2 \pm 0.3^{##}$	
change	0.5 ± 0.1	0.5 ± 0.1	0.7

Data are presented as mean \pm SE. n, number of subjects, BMI, body mass index, FEV₁, forced expiratory volume in one second as percent of predicted [289]; FVC, force vital capacity as percent of predicted [290]; # or ## indicates significant difference between baseline and post-BD values within individual groups using the paired t-test or Wilcoxon signed rank test respectively. p <0.05 indicate significant difference between controls and asthmatics using *unpaired t-test or **Mann-Whitney rank sum test

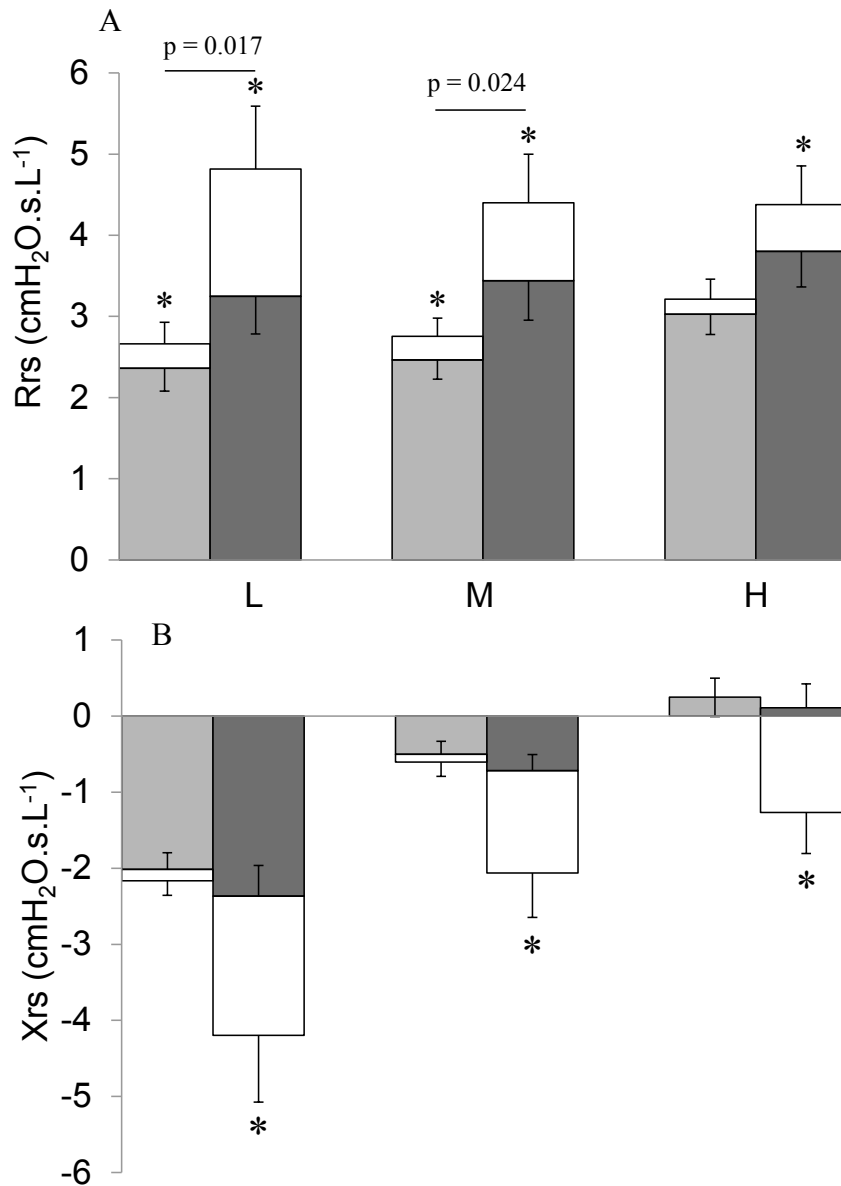


Figure 3.2: Baseline and post-BD values in the control subjects (n=18) and subjects with asthma (n=18). A) R_{rs} B) X_{rs} at low (L, 4 & 5 Hz), mid (M, 10 & 15 Hz) and high (H, 20 & 22 Hz) frequencies. Post-BD response bars (filled bars) are superimposed on the baseline data bars (empty bars). Light grey represents the BD response in the control subjects, and dark grey represents the BD response in the asthmatics. Error bars indicate standard error of mean. * denotes significant change comparing pre- and post-BD values using the one tailed paired t-test or Wilcoxon signed rank test, $p < 0.05$. p values indicate significant difference between controls and asthmatics at baseline using the two tailed t-test or Mann-Whitney rank sum test. FOT frequencies: 4-10-22 Hz for n=24 (12 controls, 12 subjects with asthma) and 5-15-20 Hz for n=12 (6 controls, 6 subjects with asthma)

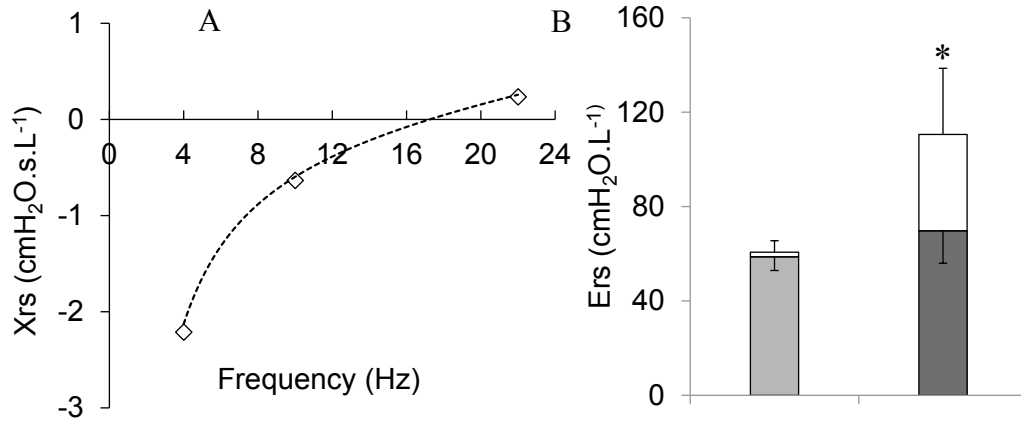


Figure 3.3: E_{rs} model fit, and E_{rs} pre- and post-BD in controls and asthmatics. A) Experimental X_{rs} (diamonds) and the single-compartment model fit (dotted line) to X_{rs} in subjects with asthma measured at 4-10-22 Hz (n=11). r^2 value for the model fit=0.99. B) Baseline and post-BD E_{rs} in controls and asthmatics * denotes significantly different from baseline; $p < 0.05$

Correlations between E_{rs} and Spirometric indices of small-airway obstruction

FVC is considered to be an indirect measure of airway closure, and could be related to E_{rs} . We found that E_{rs} was modestly correlated to FVC %predicted ($r^2=0.42$, $p=0.003$), and that decreases in E_{rs} following BD were poorly correlated to increases in FVC ($r^2=0.36$, $p=0.007$). Furthermore, E_{rs} was found to be modestly correlated to predicted values of FEF25-75% ($r^2=0.40$, $p=0.004$).

Simulations

Control

For the control model, baseline $R_{rs,mod}$ was 2.63, 2.75, 3.41 cmH₂O.s.L⁻¹ and $X_{L,mod}$ was -2.05, 0.12, 1.69 cmH₂O.s.L⁻¹ at 4, 10, and 22 Hz respectively and, $E_{rs,mod}$ was 60.5 cmH₂O.L⁻¹. We began simulations with no ventilation defects present, and dilated the central airways from 1 to 10%. As expected, E_{rs} changed insignificantly, while R_{rs} decreased with increasing airway dilation. A 7.5% dilation of the central airways resulted in a 13.6% decrease in $R_{rs,mod}$ and a 1.43% decrease in $E_{rs,mod}$ (pointed bars Fig. 3.4A). This approximated the *in vivo* changes in mechanics in controls.

Asthma

For the asthma model, occluding 475 of 1002 airways in the 10th airway generation from the control model increased $R_{rs,mod}$ at 4 Hz from 2.63 to 3.17 ± 0.07 SD $\text{cmH}_2\text{O}\cdot\text{s}\cdot\text{L}^{-1}$, but R_{rs} *in vivo* was $4.3 \text{ cmH}_2\text{O}\cdot\text{s}\cdot\text{L}^{-1}$. Thus we narrowed the central-airway diameters by 11.5% relative to the control diameters reproducing the baseline R_{rs} at 4 Hz (4.27 ± 0.07 SD $\text{cmH}_2\text{O}\cdot\text{s}\cdot\text{L}^{-1}$) and E_{rs} ($110.1 \pm 4.1 \text{ cmH}_2\text{O}\cdot\text{L}^{-1}$) from the asthmatics. To account for the BD induced change in E_{rs} , opening 150 of the occluded airways provided a percent decrease in $E_{rs,mod}$ of $20.5 \pm 2.8\%$. Thus keeping 325 of 475 airways occluded and varying the central-airway dilation (not shown), we found that a 6.8% dilation of the central airways produced nearly similar decreases in $R_{rs,mod}$ ($22.2 \pm 1.3\%$) and $E_{rs,mod}$ ($21.8 \pm 2.8\%$), reproducing the *in vivo* response in asthmatics (Fig. 3.4B, pointed bars). We also found that in the asthma model, there was a only small positive frequency dependence of $R_{rs,mod}$ of $-0.65 \pm 0.06 \text{ cmH}_2\text{O}\cdot\text{s}\cdot\text{L}^{-1}$ at baseline, which increased to $-0.76 \pm 0.04 \text{ cmH}_2\text{O}\cdot\text{s}\cdot\text{L}^{-1}$ following simulated bronchodilation ($p < 0.05$).

Effect of Poiseuille flow on the model mechanics

The respiratory impedances estimated using Poiseuille and Womersley flow are presented in Table 3.2. Poiseuille flow had a negligible effect on the model lung resistance $R_{L,mod}$ at 4 Hz, but it underestimated $R_{L,mod}$ at 10 and 22 Hz in both control and asthma models. Furthermore, in both the models, the model reactance $X_{rs,mod}$ was slightly overestimated at 4 Hz, and underestimated at 10 and 22 Hz.

Table 3.2: Comparison between model respiratory impedances evaluated using Poiseuille and Womersley flow

	Model Respiratory Impedance (cmH ₂ O.s.L ⁻¹)					
	R _{rs,mod}			X _{rs,mod}		
	4 Hz	10 Hz	22 Hz	4 Hz	10 Hz	22 Hz
Control Model						
Poiseuille Flow	2.6	2.6	3.01	-2.2	-0.07	1.45
Womersley Flow	2.63	2.75	3.41	-2.05	0.12	1.69
Asthma Model						
Poiseuille Flow	4.25	4.15	4.4	-4.3	-0.98	0.82
Womersley Flow	4.27	4.32	4.92	-4.03	-0.73	1.05

Effect of Z_{uaw} on the model mechanics

As expected, Z_{uaw} underestimated the R_{rs,mod} at 4 Hz and E_{rs,mod}; by 7.8% and 8% respectively in the control model, and by 14.5 ± 0.44 SD % and 11.6 ± 0.27% respectively in the asthma model.

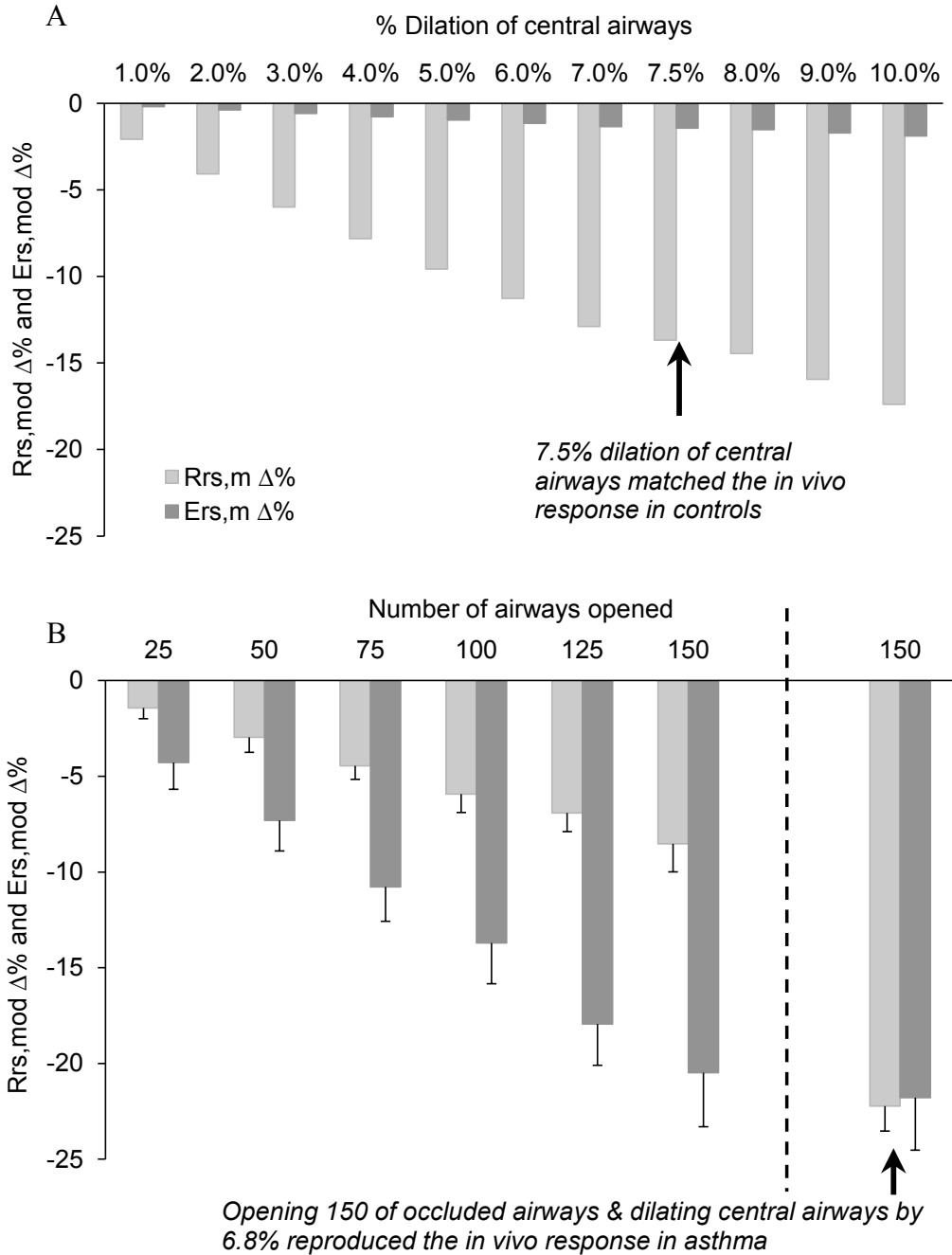


Figure 3.4: Percent decreases in $R_{rs,mod}$ and $E_{rs,mod}$ following simulated bronchodilation in the multi-branch tree model. A) Imposing central-airway dilation from 1% to 10% with no airways closures. The bars pointed indicate the model response that mimicked the *in vivo* BD response in the controls B) Effect of opening from 25 to 150 of the occluded airways. Opening 150 airways and dilating the central airways by 6.8% reproduced the *in vivo* BD response in the asthmatics. Error bars indicate standard deviation for 10 random simulations of airways opening.

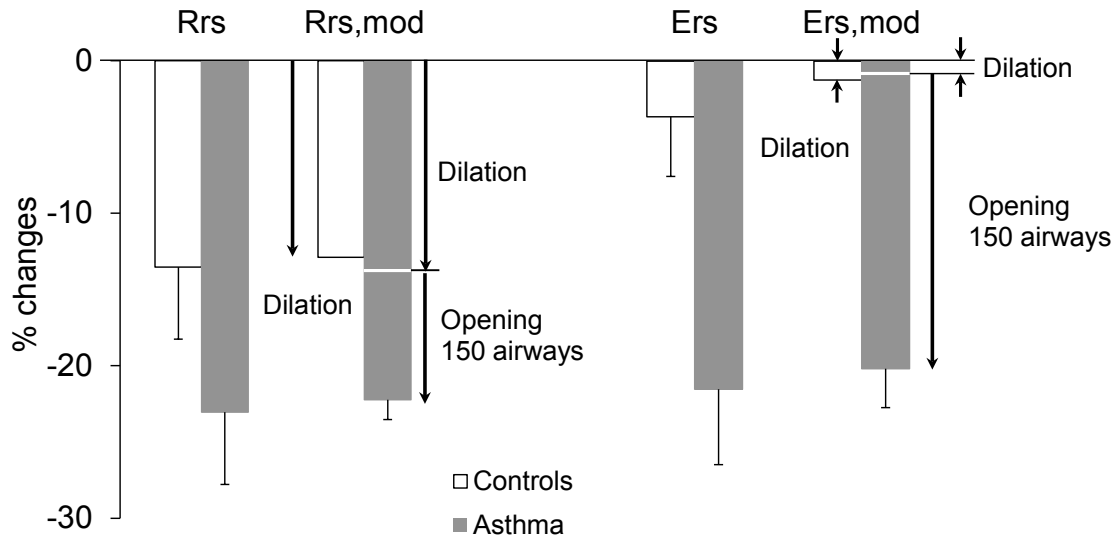


Figure 3.5: Percent decreases in resistance and elastance *in vivo* (R_{rs} and E_{rs}) and in the model ($R_{rs,mod}$ and $E_{rs,mod}$) redrawn. The model response showed that in asthmatics, nearly half of decreases in R_{rs} resulted from large airway dilation while the remaining half resulted from small-airway dilation; however, decreases in E_{rs} were almost entirely due to small-airway opening. Error bars indicate SE for the *in vivo* data, and standard deviation for 10 random simulations for the model data.

3.4 Discussion

This study evaluated respiratory system elastance (E_{rs}) and its BD response as a measure of small-airway obstruction in asthma. We found that with BD, while R_{rs} decreased in both groups, E_{rs} decreased only in asthmatics, and the decreases in R_{rs} and E_{rs} were similar in magnitude. Using a multi-branch airway-tree model, this behaviour could be accounted for as follows. In asthma, the BD caused a change in R_{rs} of approximately similar magnitude arising from both dilation of central airways and opening of small airways, while the larger change in E_{rs} arose almost entirely due to opening of small airways. In controls, there was no significant change in E_{rs} , implying no measureable airway closure. Controls did show airway dilation with BD, but it was largely central, and of nearly the same magnitude to the central-airway dilation indicated in asthma using the model. Together, these findings suggest that central-airway response to BD was similar in control and asthmatic subjects, however what distinguished asthma from control subjects was the BD response of small airways. Thus, E_{rs} assessed by FOT

may be a clinically useful measure to assess small-airway narrowing or closure, and response to BD therapy in asthma.

Consistent with previous reports [28, 29, 153, 156], we found that R_{rs} was higher in asthmatics than in controls, and decreased in both groups in response to BD. Furthermore, in controls, R_{rs} remained nearly constant over the oscillation frequencies [28, 136] suggesting a homogeneous behaviour of the respiratory system. We did not observe any frequency dependence of R_{rs} in the asthmatics. Frequency dependence of R_{rs} has been previously observed in asthma, but dependent on asthma severity [27, 291], and has been ascribed to the time-constant heterogeneities in ventilation [140] or airway wall shunting [141] or both [226]. In asthma, at very low frequencies (0.2 to 1 Hz), heterogeneity will manifest itself as a pronounced frequency dependence of R_{rs} . However, frequency dependence of R_{rs} does not seem to be prevalent in mild asthma over 5-20 Hz, yet it has been used as a marker of heterogeneity in this frequency range. Here we explicitly induced ventilation heterogeneity in the model via heterogeneous small-airway narrowing, which accurately reproduced the *in vivo* reactance data at low frequencies. However, despite this marked heterogeneity, we did not observe frequency dependence of R_{rs} in either our model or in our subjects. Yet we did find that E_{rs} increased significantly with heterogeneity. Together our results suggested that frequency dependence of R_{rs} was not a sensitive measure of heterogeneity in asthma

While X_{rs} was more negative in asthmatics than in controls, the difference in X_{rs} between the two groups was not statistically significant, likely due to large variability in X_{rs} among asthmatics, and an overlap in X_{rs} values between controls and asthmatics. Nevertheless, in agreement with previous reports, in asthma, X_{rs} increased following BD reflecting decreases in the stiffness of the respiratory system by airway opening and dilation [28, 29]. Furthermore, with BD, E_{rs} decreased only in asthmatics, but not in controls, the latter implying no measurable airway closure in controls as anticipated. We interpret that the decrease in E_{rs} in the asthma was indicative of an increase in lung volume due to opening of previously occluded or closed airways and/or an increase in the existing airspace by dilation of small airways. These findings are in agreement with previous reports [27]. Previously Cavalcanti et al. [27] found that C_{rs} increased significantly following BD in asthmatics. However, they attributed the increases in C_{rs} to

decreases in airway wall stiffness following BD [292]. However, the airway wall is stiffer than lung parenchymal tissue, and represents a very small fraction of the available compliant tissue surface that contributes to the total compliance of the respiratory system. Thus, we believe that because of the highly parallel nature of the lung structure, changes in E_{rs} mostly reflect events in the small airways. Mounting evidence now supports that increases in E_{rs} result from small-airway narrowing or near-closures or closures. Studies using morphometric models of dog lungs have shown that lung elastance is sensitive to peripheral airway constriction, and increases with increasing heterogeneity of peripheral airway constriction [24]. Furthermore studies using animal models of acute lung injury and acute respiratory distress syndrome also have shown that C_{rs} derived from low frequency X_{rs} is related to the number of open airway spaces. Dellaca et al. [25] demonstrated that C_{rs} varied inversely in proportion to the area of nonaerated lung regions due to atelectasis.

The *in vivo* behaviour in asthmatics was well accounted for by our model. Our simulations demonstrated that, in asthmatics, nearly half of the decrease in R_{rs} arose from dilation of central airways while the remaining half arose from the dilation of small airways (Fig. 3.5). However, the decreases in E_{rs} in asthmatics arose almost entirely from the opening and dilation of peripheral airways. The latter results are similar to those of Lutchen et al. [24] and Kaczka et al. [149]. We too found that the model elastance was sensitive to heterogeneous small-airway constriction. However, while Lutchen et al. focused on locations and patterns of airway narrowing to account for changes in lung mechanics [24]; we showed that amongst lung mechanical measures it is not R_{rs} that is the most sensitive to small-airway narrowing, but E_{rs} , and indeed changes in R_{rs} due to dilation or opening of small airways are dwarfed by changes in the central airways that are seen in both health and asthma. We used a model to indicate that E_{rs} , more than R_{rs} and its frequency dependence, is a more direct, and likely a more useful measure of small-airway obstruction. In addition, we extended the findings by Kaczka et al. [149] over the common frequency range (4-22 Hz) used in FOT.

In this study, we used Womersley flow rather than Poiseuille flow because the Womersley flow affects the large airways, and this effect is even larger at higher oscillation frequencies. When comparing with Poiseuille flow, we found that there was

no difference in the model impedance at 4 Hz, although a significant number of large airways had the Womersley number > 1 . However there was a modest difference in the impedance at high frequencies. Thus at our low frequency (4 Hz), comparing the changes in resistance or elastance due to BD in asthma was not affected by choice of either Womersley or Poiseuille flow.

We also quantified the effect of upper airway shunt impedance on the model mechanics at baseline conditions. Our results indicated that shunt had a small effect on lung mechanics in the control model while it moderately underestimated the resistance at 4 Hz and elastance in the asthma model.

We estimated E_{rs} by fitting the single-compartment model to reactance data, largely to take into account the contribution of inertive properties, while past studies have derived E_{rs} or C_{rs} from reactance at a single low frequency. The latter is a good approach when inertive effects can be neglected, as is the case generally with airway obstruction, and when a simpler index that approximates lung stiffness is desired. We found that the r^2 values for the model fits were > 0.9 for all but 4 subjects. It is well known that the single-compartment model may describe well healthy lungs, but fails to describe diseased lungs. Thus, in moderate to severe asthma, it would be appropriate to estimate elastance from the low frequency reactance as reported in other studies [28].

We found a modest association between E_{rs} and the spirometric indices of small-airway narrowing and closure, FEF25-75% and FVC. While a higher E_{rs} can be ascribed to nearly closed or closed airways during normal breathing, a reduced FEF25-75% and FVC likely reflect airway closures or collapses that may occur during forced expiration.

This study has some limitations which we acknowledge here. We assigned all lung compliance to lung parenchyma assuming non-compliant airway walls. However, airways do have some finite wall compliance, although much smaller than that of lung parenchyma due to small volume of air in airways. Nevertheless this leads to some shunting of airflow decreasing E_{rs} and R_{rs} , particularly with severe peripheral airway obstruction, and like upper airway shunt may contribute to frequency dependence of R_{rs} [141]. The lack of including airway wall compliance may underestimate the number of airways required to be occluded and reopened in our asthma model. However, because airway compliance is much smaller than the parenchyma, this effect is small, and indeed

we did not observe any frequency dependence of R_{rs} . We did include the more significant effect of upper airway shunt which did not have much effect on our findings. Another limitation is that we did not include the possible effects of airway-parenchyma interdependence which arise from the tethering of the parenchyma to the airway wall. With increased airway wall stiffness due to smooth muscle tone in asthma, the nearby parenchyma stiffens as well, albeit decreasing inversely with distance from the airway wall. This could contribute to increased E_{rs} in asthma and the decrease in E_{rs} with BD, and thus would oppose any effects of shunt. However, since airway-parenchymal interdependence extends into the lung from the airways, this affects a larger volume of the lung, and thus may have a larger effect than airway wall shunt. Again, since the volume of parenchyma affected would be small with diminishing effects away from the airway, the elastance would still be dominated by the unaffected parenchyma and the effects of functional airway closure.

Using the model, we examined the degree to which central and small-airway narrowing affect the lung mechanics via simulated ventilation defects and homogenous central-airway narrowing. Similar to Tgavalekos et al.[23], we simplified the airway narrowing in our model using a simple bimodal distribution in which some airways were narrowed by 90% while the remaining airways were unchanged. This was done on purpose to limit the number of variables, and to most clearly indicate the effect of very narrowed or closed airways sufficient to impair ventilation to a region of the lung, separate from the effect of a more generalized moderate airway narrowing throughout the lung. However, the bimodal distribution allows limited time-constant heterogeneity because of limited time-constant distribution. Indeed, *in vivo* airway diameters would be narrowed over a broad distribution leading to larger heterogeneity. A more distributed approach to airway narrowing would permit greater flexibility in modelling giving a frequency distribution of R_{rs} and E_{rs} , and may be more representative of the *in vivo* pattern. However, to a great extent this is not required, and there is insufficient information in the impedance data to easily recover a more graded distribution, even though more complex models are possible [215].

Also, it required occluding 475 airways at generation 10 in the model to account for E_{rs} in our asthmatic subjects. While this produced a given volume of ventilation defect

that can account for the *in vivo* data, the same volume of defect could have been produced by narrowing airways at different generations or combinations of generations. It is likely that *in vivo* defects involve several generations, but we do not anticipate this to greatly affect our results, as the defect size determining E_{RS} and the change in E_{RS} is the important effect, and moving the defect to a lower generation using two daughter airways is equivalent to a parent airway closing. For example, we could achieve the same result by closing nearly half of the airways in the 9th airway generation. Nevertheless, it is possible that the volume of defect we chose is an underestimate for the volume of defect required for the mean response, since in the presence of collateral ventilation, some regions may receive ventilation from neighbouring units in which case one may be required to close more airways to reproduce the *in vivo* data.

Another interesting finding from this study is that in the model, the percentage of airway closure to account for the baseline data in asthma was much larger (~ 47%) than predicted by imaging studies. Recent hyperpolarized helium imaging studies showed that ventilation defects volume in asthmatics varied from 6% (mean) to 13% (median) of the total lung volume [293, 294], but depending on the disease severity (mild to severe), signal acquisition, and threshold setting. We think that the difference in defect volumes between our study and the imaging studies is likely due to the difference in the lung time constant. In ^3He imaging, gas mixture is inhaled, and images are acquired 8-15 sec after during a breath-hold maneuver. This relatively longer time frame may be sufficient for redistribution of gas from well ventilated units to poorly ventilated units through collateral channels or via pedelluft, resulting in a relatively smaller defect volume at the time of image acquisition. Moreover, ^3He gas is highly diffusive, and may penetrate even narrowed airways, thus some ^3He ventilation is possible resulting in a smaller defect volume [293]. On the other hand, at forced oscillation frequencies well above breathing frequencies, perhaps redistribution of inhaled air within the lung does not occur due to the smaller lung time constant. This may result in a larger defect volume.

Lastly, we simulated airway narrowing and dilation in the model by homogeneous narrowing and dilation of the entire airway tree, and assumed it to be equivalent to central-airway narrowing and dilation. This is a valid assumption since majority of airway resistance is contributed by airways up to the seventh generations [295]. Thus

narrowing or dilating just the larger airways instead would not have significantly changed our results.

3.5 Conclusion

In conclusion, using a multi-branch airway impedance tree model we demonstrated that in asthma E_{rs} is more sensitive to peripheral airway obstruction and heterogeneity than R_{rs} . Our results suggest that E_{rs} could potentially be a clinically useful measure to assess small-airway dysfunction and response to bronchodilator therapy in asthma.

Chapter 4: Modelling Resistance and Reactance with Heterogeneous Airway Narrowing in Mild to Severe Asthma

Authors

Swati A. Bhatwadekar
Del Leary
Geoff N. Maksym

Published in Canadian Journal of Physiology and Pharmacology, 2015 March;
93(3): 207-14

This manuscript has been modified from its original format to conform to the structure of this dissertation

4.1 Abstract

Ventilation heterogeneity is an important marker of small-airway dysfunction in asthma. Frequency dependence of respiratory system resistance (R_{rs}) from oscillometry is used as a measure of this heterogeneity. However, this has not been quantitatively assessed or compared with other outcomes of oscillometry including respiratory system reactance (X_{rs}) and associated elastance (E_{rs}). Here, we used a multi-branch model of the human lung including upper airway shunt to match previously reported respiratory mechanics in mild to severe asthma. We imposed heterogeneity by narrowing a proportion of peripheral airways to account for patient E_{rs} at 5 Hz, and then narrowed central airways to account for remaining R_{rs} at 18 Hz. It required $> 75\%$ of the small-airway narrowing to account for severe asthma. While the model produced frequency dependence in R_{rs} , it was upward shifted below 5 Hz relative with *in vivo* indicating that other factors including more distributed airway narrowing or central-airway wall compliance are required. However, E_{rs} quantitatively reflected the imposed heterogeneity better than the frequency dependence of R_{rs} , independent of the frequency range for estimation, and thus was a more robust measure of small-airway function. Thus E_{rs} appears to have greater potential as a clinical measure of small-airway disease in asthma.

4.2 Introduction

Heterogeneous airway narrowing is a hallmark feature of asthma. This is also supported by the occurrence of patchy ventilation characterized by ventilation defects in asthmatic subjects as seen in ventilation imaging studies [20]. Modeling studies suggest that ventilation defects are largely caused by the heterogeneous pattern of constriction of small airways which includes randomly distributed closures or near closures [23, 24]. A number of methods have been applied to assess small airways which include nitrogen gas washout [18, 296], frequency dependence of dynamic compliance [297], and imaging techniques such as magnetic resonance imaging using hyperpolarized helium and xenon [267, 293], and high resolution computed tomography [21]. While these methods provide insight to our understanding of the pathophysiology of asthma, at present they are largely limited to research applications.

The forced oscillation technique, also referred to as oscillometry, can also be used to assess small-airway dysfunction using the resistance (R_{rs}) and reactance (X_{rs}) of the respiratory system. Studies using morphometric models of animal lungs have shown that R_{rs} and X_{rs} are sensitive to constriction in the small airways at low frequencies [24, 25, 32]. R_{rs} has been shown to exhibit frequency-dependent decreases over 3 to 22 Hz in asthmatic subjects at baseline [27, 28, 132] and with methacholine [193], and this was related to the severity of airway obstruction [27]. Human data demonstrating frequency dependence, and studies using computational models of animal lungs has led to the suggestion that R_{rs} at low frequencies reflects resistance from both large and small airways, whereas R_{rs} at high frequencies reflects resistance in the large airways. Thus, for example, R_{rs} at 5 Hz minus the R_{rs} at 20 Hz (R_5-R_{20}) is often taken as a measure of heterogeneous small-airway constriction [298-300]. Because the oscillometry is simple to perform, this interpretation is becoming widespread, and is beginning to be used clinically, although the relationship between frequency dependence and heterogeneity has not been directly assessed quantitatively. Moreover, frequency dependence of R_{rs} may also arise from the shunting of flow oscillations to the motion of the upper airway structures including the cheeks and soft palate. This occurs especially when a patient has high lung impedance [31]. Moreover recent reports have indicated that frequency

dependence of R_{rs} may be dependent on the oscillometry device [128] which questions the utility of frequency dependence of R_{rs} as an indicator of small-airway heterogeneity.

Previous studies have reported that X_{rs} at frequencies ≤ 5 Hz, a measure of respiratory system stiffness, is decreased (becomes more negative) in asthma at baseline [30] in association with the severity of airway obstruction [27] and following methacholine [163], and is increased with a bronchodilator [28, 29]. Since X_{rs} is sensitive to small airways, and its effects are predominantly associated with small-airway closures or near closures [23], the changes in low frequency X_{rs} reflect heterogeneous small-airway constriction in asthma, however, this has not been directly quantitatively assessed.

While E_{rs} should be related to peripheral airway heterogeneity, the degree to which it is related has not been clearly established, and although frequency dependence of R_{rs} is used as an indicator of peripheral airway heterogeneity, the degree to which frequency dependence reflects heterogeneity due to peripheral defects is relatively less clear. Our aim was to quantify the frequency dependence of R_{rs} , and compare it with the elastance (E_{rs}) derived from the low-frequency X_{rs} in a simulation with varying degrees of small-airway heterogeneity in asthma. We used a computational model of the human lung to impose small-airway heterogeneity directly, and simulated respiratory mechanics in 3 groups of asthmatic subjects with either mild, moderate, or severe airway obstruction reported previously by Cavalcanti et al. [27]. In particular, we implemented central-airway narrowing, and small-airway near-closures induced by 90% airway narrowing [23, 252, 274] at different airway generations to account for the *in vivo* mechanics in asthma. We then quantified and compared the effects of small-airway heterogeneity on the model E_{rs} and frequency dependence of model R_{rs} at 0.2 to 5 Hz and 5 to 20 Hz. We also included the upper airway impedance reported by Cauberghs & Van de Woestijne [276], and quantified its effect on the model mechanics.

4.3 Methods

4.3.1 *In vivo* respiratory mechanics

We modeled the *in vivo* R_{rs} at 18 Hz and X_{rs} at 5 Hz obtained using oscillometry from healthy ($n=25$) and asthmatic subjects ($n=65$) reported previously [27] (Fig. 4.1). The healthy subjects had no history of pulmonary or cardiac disease, or of tobacco use, and the asthmatic subjects had clinical diagnosis of asthma based on the presence of respiratory symptoms and the reversibility of airway obstruction following a bronchodilator. The asthmatic subjects had been classified as patients with mild ($n=25$), moderate ($n=25$) and severe ($n=15$) airway obstruction based on their pre-bronchodilator FEF_{25-75}/FVC and FEV_1/FVC relationships [27].

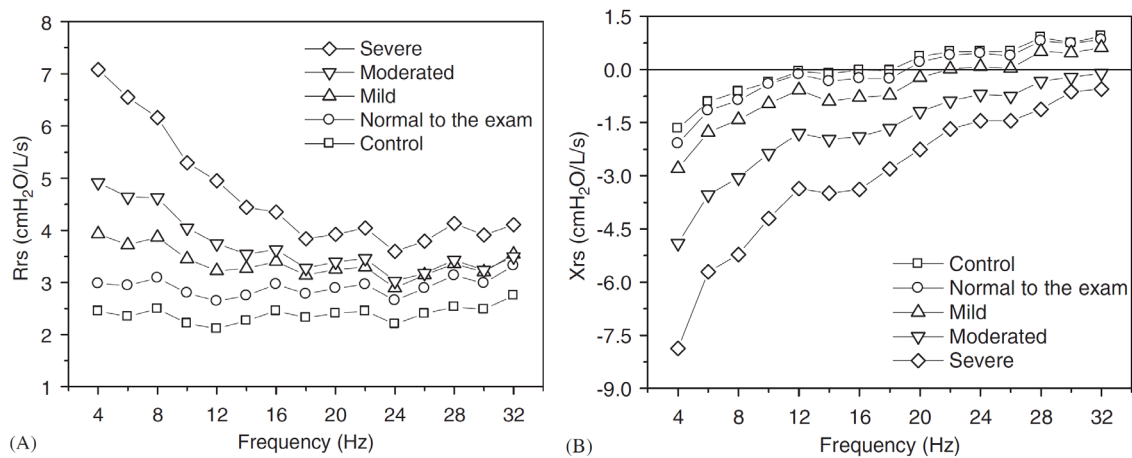


Figure 4.1: Mean respiratory resistance (R_{rs}) and reactance (X_{rs}) versus frequency in healthy and asthmatic subjects with mild to severe airway obstruction; reproduced with permission from [27]. In healthy subjects, R_{rs} was nearly constant over the entire frequency range while in asthma, R_{rs} and its frequency dependence both increased with increasing levels of airway obstruction. Furthermore, X_{rs} was frequency dependent, and became more negative with severity of airway obstruction.

The oscillometry measurements [27] were performed on the same device, and all subjects held their cheeks and mouth floor with their hands in order to minimize the effect of upper airway shunt. The measurements were provided at the harmonics of 2 Hz

from 4-32 Hz. We obtained R_{rs} and X_{rs} at 5 and 15 Hz by linear interpolation of data from 4 and 6 Hz, and 14 and 16 Hz respectively (Table 4.1), and computed the frequency dependence of R_{rs} over 5 to 20 Hz as R_{rs} (5 Hz) minus R_{rs} (20 Hz).

4.3.2 Multi-branch airway tree model

We devised a 26-generation airway-tree model based on an anatomically correct 3-dimensional human airway geometry provided by Merryn Tawhai (The University of Auckland, New Zealand) [47] (Fig. 4.2). The airway tree model, up to the first 8 airway generations, was generated using a host-specific volume derived from x-ray multi-detector computed-tomography imaging. The remaining generations were created using a volume-filling algorithm maintaining daughter diameter ratios consistent with the established morphometry [285].

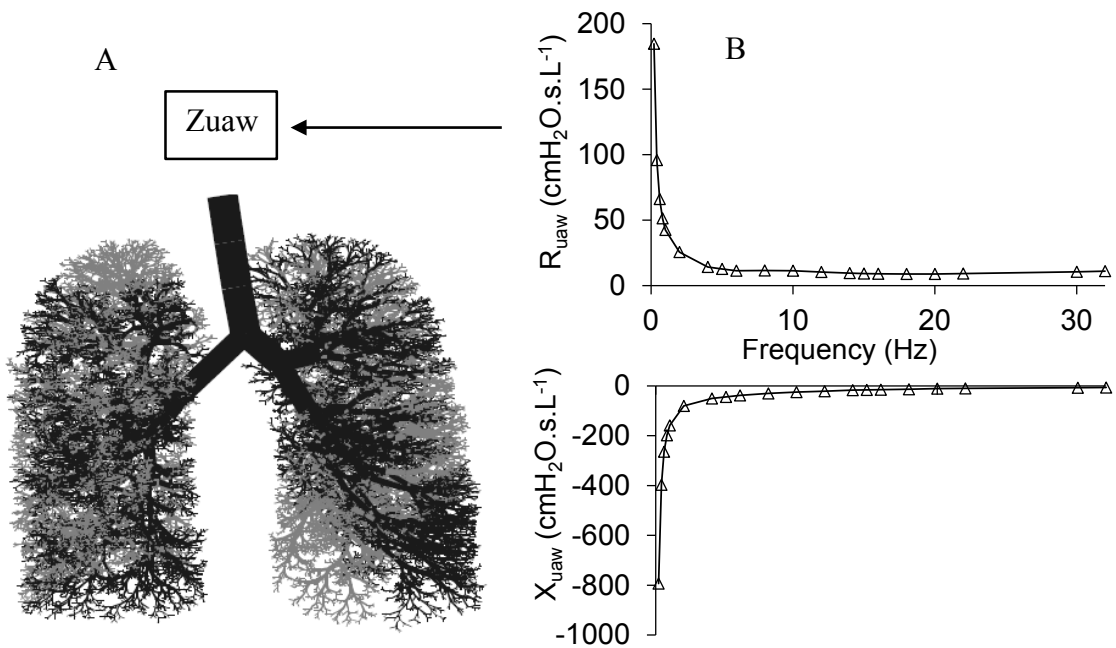


Figure 4.2: Multi-branch airway-tree model depicting airway heterogeneity in moderate asthma A) The model was based on *in vivo* R_{rs} at 18 Hz and X_{rs} at 5 Hz in moderate asthma [27]. The *in vivo* mechanics in moderate asthma could be reproduced by 3.6% narrowing of the central-airway diameters relative to control, and 90% narrowing of 670 of 1002 airways in the 10th airway generation. B) Upper airway shunt resistance (R_{uaw}) and reactance (X_{uaw}) adapted with permission from Cauberghe & Van de Woestijne [276]. The shunt impedance Z_{uaw} was included in parallel with the model lung impedance $Z_{L,mod}$. See Methods for details.

The Tawhai model was imaged at total lung capacity (TLC), thus we reduced the airway diameters and lengths to 80% of their original to achieve an FRC reference lung assuming a homogeneous isotropic volume change, and an arbitrarily chosen model FRC to TLC ratio of 0.5 which is approximately the upright FRC to TLC ratio of the Tawhai model lung [47]. Since flow is more plug-like in some of the larger airways and better described by Womersley flow than only Poiseuille flow, the complex impedance of each non-terminal airway branch was calculated assuming Womersley flow [218] as follows.

$$Z_a(f) = \frac{j2f\rho_{air}l_a}{r_a^2} \left[1 - \frac{2J_1(\alpha_a\sqrt{-j})}{\alpha_a\sqrt{-j}J_0(\alpha_a\sqrt{-j})} \right]^{-1} \quad (4.1)$$

where r_a is the radius and l_a is the length of the airway, f is the oscillation frequency in Hz, ρ_{air} is the density of air (1.11 kg/m^3), J_0 and J_1 are the complex Bessels functions of order 0 and 1 respectively, j is the unit imaginary number, and α_a is the Womersley number for the airway branch given by

$$\alpha_a = r_a \sqrt{\frac{2\pi\rho_{air}f}{\mu_{air}}} \quad (4.2)$$

where, μ_{air} is the dynamic viscosity of humid air at $37 \text{ }^\circ\text{C}$ ($1.85 \times 10^{-5} \text{ Pa.s}$). Since the compliance of the lung is dominated by the compliance of the parenchyma due to its large volume relative to the airways, we distributed the model lung elastance evenly among the terminal airways. Thus each terminal airway served as an alveolar compartment accounting for parenchymal stretch, surface tension and gas compression [273]. We recognize that our approach neglects any contribution from airway-wall compliance or gas compression within airways, however, this effect is much smaller than the effect of alveolar compartment [141, 301]. The impedance of each terminal airway was defined as

$$Z_t = Z_a - j \frac{Et}{\omega} \quad (4.3)$$

where E_t is the elastance of the terminal airway unit. The model lung impedance ($Z_{L,mod}$) was evaluated from series and parallel summations of all airway impedances assuming a lumped element approach, and separated into resistance ($R_{L,mod}$) and reactance ($X_{L,mod}$). The model respiratory mechanics was evaluated at 0.2-32 Hz.

We accounted for the trachea and glottis, as well as chest wall mechanics since the Tawhai model did not include them. The trachea and glottis resistance, and chest wall resistance were assigned the values of $0.5 \text{ cmH}_2\text{O}\cdot\text{s}\cdot\text{L}^{-1}$ each [129, 287, 288], and added to $R_{L,mod}$ to obtain the model respiratory system resistance R_{rs,mod,no_shunt} . Furthermore, we added the chest wall elastance ($10.6 \text{ cmH}_2\text{O}\cdot\text{L}^{-1}$) [302] to the model lung elastance ($E_{L,mod}$) to obtain the model respiratory system elastance (E_{rs,mod,no_shunt}), where $E_{L,mod}$ at an oscillation frequency, f was obtained as $-2\pi f X_{L,mod}$.

We included upper airway shunt impedance (Z_{uaw}) which accounts for cheeks and soft palate mechanics in the model using the Z_{uaw} values from Cauberghe & Woestijne [276] (Fig. 5.2B). Z_{uaw} values were at the harmonics of 2 Hz from 2-32 Hz. Because we were missing the shunt values at frequencies 0.2-1 Hz, we extrapolated Z_{uaw} over these frequencies as follows. The shunt resistance (real component of Z_{uaw}) for the range 0.2-1 Hz was extrapolated by fitting a model $R=A(1/f) + B$ to the real part of Z_{uaw} at 2-20 Hz assuming $1/f$ dependence of the shunt resistance where, R was resistance, f frequency, and A and B were constants. The shunt reactance values (imaginary component of Z_{uaw}) for the range 0.2-1 Hz were evaluated by fitting the linear single-compartment model to the shunt reactance at 2-8 Hz, and again extrapolating to lower frequencies. $Z_{rs,mod}$ including upper-airway shunt was computed from the parallel sum of Z_{L,mod,no_shunt} that included airway-tree impedance in series with tracheal and glottal resistances and chest wall impedances and Z_{uaw} . $R_{rs,mod}$ is the real part of $Z_{rs,mod}$ and $X_{rs,mod}$ is the imaginary part of $Z_{rs,mod}$, and $E_{rs,mod}$ at an oscillation frequency, f was obtained as $-2\pi f X_{rs,mod}$, here.

The frequency dependence of $R_{rs,mod}$ was evaluated over two ranges, the “low frequency range” of 0.2-5 Hz ($R_{rs,mod}0.2$ - $R_{rs,mod}5$) which is normally not accessible by common forced oscillation methods but where frequency dependence of R_{rs} is more easily observed, and the “oscillometry frequency range” of 5-20 Hz ($R_{rs,mod}5$ - $R_{rs,mod}20$). We use these terms to define these two frequency ranges.

4.3.3 Simulations

For our baseline control simulation, we assumed that all airways were open (unoccluded), and thus matched resistance via airway narrowing, and reactance by distributing lung elastance among the terminal airspaces as described above. We matched $R_{rs,mod}$ to the *in vivo* R_{rs} in the plateau region, choosing R_{rs} at 18 Hz. In healthy subjects, airway diameters were narrowed by 21.2% relative to the baseline model at FRC. This scaled the R_{rs} computed from the Tawhai airway tree model to the mean R_{rs} at 18 Hz ($R_{rs}=2.47 \text{ cmH}_2\text{O}\cdot\text{s}\cdot\text{L}^{-1}$) in healthy subjects from Cavalcanti et al. [27]. The reactance, $X_{rs,mod}$ ($E_{rs,mod}$) was matched to the control X_{rs} (E_{rs}) at 5 Hz ($X_{rs}=-1.28 \text{ cmH}_2\text{O}\cdot\text{s}\cdot\text{L}^{-1}$ and $E_{rs}=40.1 \text{ cmH}_2\text{O}\cdot\text{L}^{-1}$), which could be achieved by distributing an elastance of 45 $\text{cmH}_2\text{O}\cdot\text{L}^{-1}$ equally to all terminal units.

Having reproduced the data in the controls, we reproduced the data in the asthmatics from Cavalcanti et al. [27] as follows. We first matched elastance assuming only small-airway heterogeneity in a very well-defined quantifiable approach. A defined proportion of airways were occluded in the 10th generation only. Airway occlusion was achieved by narrowing airways down to 10% of their control diameters (90% narrowing) which was more than sufficient to prevent oscillatory airflow in these airways. We performed 10 repeated simulations of airway narrowing induced by 90% occlusion of randomly selected airways to match the model respiratory elastance $E_{rs,mod}$ to E_{rs} in the subjects mild to severe obstruction. While this matched the low frequency reactance of the subjects' data, the airway narrowing also increased $R_{rs,mod}$, but insufficiently to account for the reported increases in R_{rs} *in vivo*. Thus we then narrowed all of the remaining airways relative to their FRC diameters to match the model respiratory resistance $R_{rs,mod}$ to R_{rs} *in vivo*.

4.3.4 Statistical Analyses

Data are presented as mean \pm standard deviation (SD). Normality and equal variance of the data were determined using Shapiro-Wilk and Levene's test respectively. For normally distributed data, model R_{rs} at 5 Hz and 20 Hz were compared using a two tailed paired Student t-test, with values $p < 0.05$ considered statistically significant.

Statistical tests were performed with SigmaPlot 12 version 12.3 (Systat Software, Inc. Chicago, IL).

4.4 Results

The *in vivo* and the model R_{rs} values at 18 Hz and X_{rs} values at 5 Hz for healthy and asthmatic subjects are given in Table 4.1, and the central-airway narrowing and small-airway occlusions required to reproduce the mechanics *in vivo* are given in Table 4.2. The central-airway narrowing relative to the control was required to account for the additional increases in $R_{rs,mod}$ not provided by the peripheral airway narrowing (which was provided by matching to E_{rs} at 5 Hz). In the mild case, $R_{rs,mod}$ at 18 Hz arising from the peripheral airway narrowing increased from 2.42 to 2.63 ± 0.03 SD $\text{cmH}_2\text{O}\cdot\text{s}\cdot\text{L}^{-1}$ but the *in vivo* data was $3.22 \text{ cmH}_2\text{O}\cdot\text{s}\cdot\text{L}^{-1}$. Thus, the central-airway diameters were required to be narrowed by 9.3% relative to control diameters. However, for the moderate case, $R_{rs,mod}$ at 18 Hz due to peripheral airway narrowing was larger; $2.99 \pm 0.05 \text{ cmH}_2\text{O}\cdot\text{s}\cdot\text{L}^{-1}$; which was fairly close to the *in vivo* data of $3.33 \text{ cmH}_2\text{O}\cdot\text{s}\cdot\text{L}^{-1}$, thus required less central-airway narrowing. This was similar in the severe asthma; the $R_{rs,mod}$ at 18 Hz was $3.48 \pm 0.11 \text{ cmH}_2\text{O}\cdot\text{s}\cdot\text{L}^{-1}$ close to the value of *in vivo* data ($3.92 \text{ cmH}_2\text{O}\cdot\text{s}\cdot\text{L}^{-1}$). Thus, the small amount of central-airway narrowing was due to the small increase in R_{rs} for the mild asthma case, and for the moderate and severe cases, due to the increasing contribution from peripheral airway narrowing. Reproducing X_{rs} at 5 Hz in the asthmatic subjects required substantial numbers of airways to be narrowed; in the severe case more than 75% of the airways had to be nearly closed to account for the large difference in X_{rs} .

Table 4.1: Model R_{rs} and X_{rs} at 5 Hz matched to *in vivo* R_{rs} at 18 Hz and X_{rs} at 5 Hz from healthy and asthmatic subjects

Group	$R_{rs}, \text{cmH}_2\text{O.s.L}^{-1}$		$X_{rs}, \text{cmH}_2\text{O.s.L}^{-1}$	
	<i>In vivo</i>	Model	<i>In vivo</i>	Model
Control	2.47	2.42	-1.28	-1.28
Mild	3.22	3.24	-2.32	-2.27
Moderate	3.33	3.23	-4.24	-4.1
Severe	3.92	4.04	-6.82	-6.88

Table 4.2: Central-airway narrowing relative to control and small-airway narrowing required to reproduce *in vivo* mechanics in asthma

Group	Central-airway narrowing	Number of 10 th generation airway occluded (%)
Mild	9.3 %	405 (40.4%)
Moderate	3.6 %	670 (66.8%)
Severe	6.7 %	810 (80.8%)

Fig. 4.3 shows the model lung resistance ($R_{rs,mod}$) and reactance ($X_{rs,mod}$) versus frequencies for the control and asthmatic subjects at 0.4-32 Hz. The models exhibited behavior similar to the *in vivo* data, with constant resistance over the entire frequency range in the controls, and a marked frequency dependence that increased with the severity of airway obstruction in the asthmatics. $X_{rs,mod}$ was frequency dependent as observed in the *in vivo* data, and also became more negative with severity of airway obstruction.

When we quantified the frequency dependence of $R_{rs,mod}$ in the two frequency ranges, we found that there was marked frequency dependence of the model in the low frequency range, increasing from 0.51 $\text{cmH}_2\text{O.s.L}^{-1}$ to 37.61 (SD, 7) $\text{cmH}_2\text{O.s.L}^{-1}$ in the mild to severe asthma models respectively but there was slight positive frequency dependence in the oscillometry frequency range in control, and mild and moderate asthma and a negligible frequency dependence in severe asthma (Fig. 4.4). However, the

in vivo data shows a marked frequency dependence in the oscillometry range, unlike the model. Thus it appears the model frequency dependence has been upward shifted to lower frequencies.

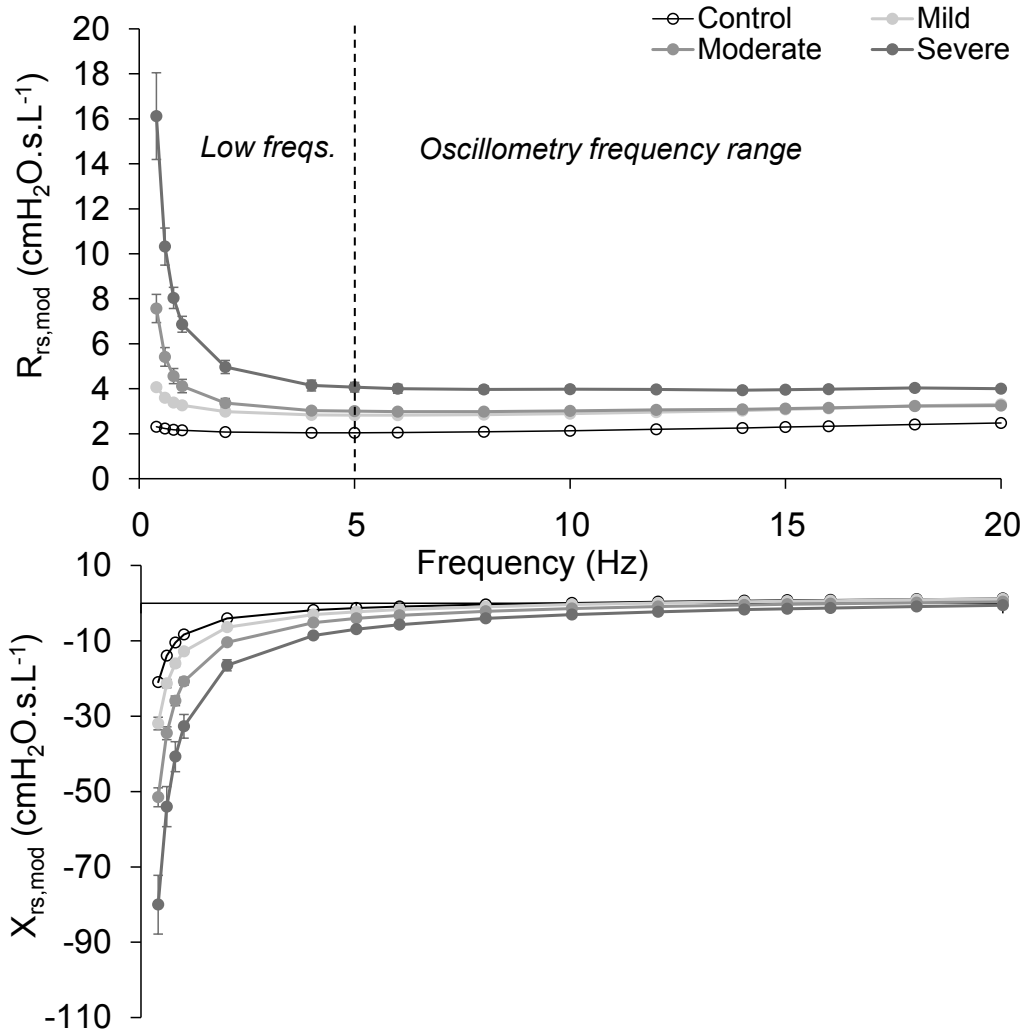


Figure 4.3: The model respiratory resistance ($R_{rs,mod}$) and reactance ($X_{rs,mod}$) over 0.4 to 20 Hz for the control model and the mild, moderate, and severe airway obstruction models of asthma. For the asthma models, data represent mean obtained from 10 random simulations, and error bars indicate standard deviation (SD). As more airways were narrowed from baseline (control case) to mild to severe heterogeneity, $R_{rs,mod}$ and frequency dependence of $R_{rs,mod}$ both increased but largely confined to the low frequency range. $X_{rs,mod}$ was frequency dependent as observed in the published data, and also became more negative with severity of airway obstruction.

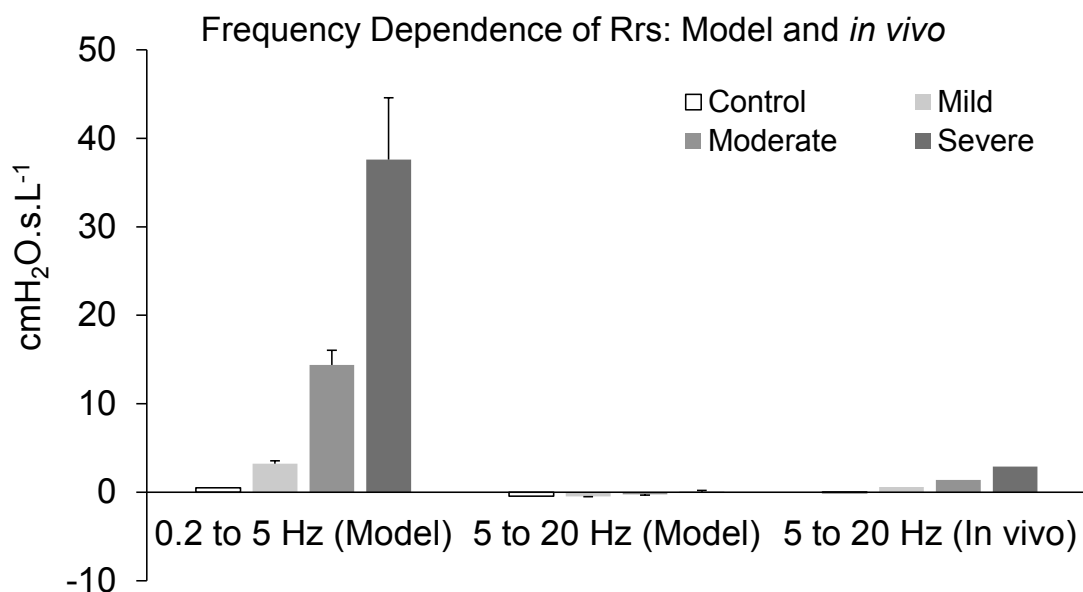


Figure 4.4: The frequency dependence of model respiratory system resistance ($R_{rs,mod}$) for the different frequency ranges tested by the model and *in vivo*: the low (0.2 to 5 Hz) and oscillometry frequency range (5 to 20 Hz), and frequency dependence of *in vivo* R_{rs} over 5 to 20 Hz adapted from Cavalcanti et al.[27] in health and mild to severe asthma over 5 to 20 Hz. Each group of bars indicates the frequency dependence over the frequency range specified on x-axis for control, and mild, moderate, and severe asthma. For example, the frequency dependence of $R_{rs,mod}$ for moderate asthma was 14.4 $\text{cmH}_2\text{O}\cdot\text{s}\cdot\text{L}^{-1}$ over 0.2 to 5 Hz and $-0.24 \text{ cmH}_2\text{O}\cdot\text{s}\cdot\text{L}^{-1}$ over 5 to 20 Hz, while the frequency dependence of *in vivo* R_{rs} in moderate asthma was 1.4 $\text{cmH}_2\text{O}\cdot\text{s}\cdot\text{L}^{-1}$ over 5 to 20 Hz. $R_{rs,mod}$ was computed including the upper airways and chest wall mechanics to the model lung resistance as described in the text.

When we computed elastance from the model at 0.2 Hz and at 5 Hz, we found that as expected, $E_{rs,mod}$ increased as airways were closed from mild to severe heterogeneity, and the increases were consistent at these two frequencies (Fig. 4.5), unlike the increases in $R_{rs,mod}$ which were frequency dependent (Fig. 4.4).

When we removed the upper airway shunt, this had a negligible effect on $R_{rs,mod}$ and $X_{rs,mod}$ in controls and mild asthma (not shown here). However, there was sizeable effect in moderate and severe asthma in both the low and high frequency ranges (Figs. 4.6A and 4.6C). In moderate asthma, removing the shunt increased $R_{rs,mod}$ by 17.7%, 13.8%, 10.2%, and 6.3% at 5, 10, 15 and 20 Hz respectively. The effect was much larger

in severe asthma with $R_{rs,mod}$ being increased by 30.3%, 26.6%, 25.4% and 23.8% at 5, 10, 15 and 20 Hz respectively when the shunt was removed from the model.

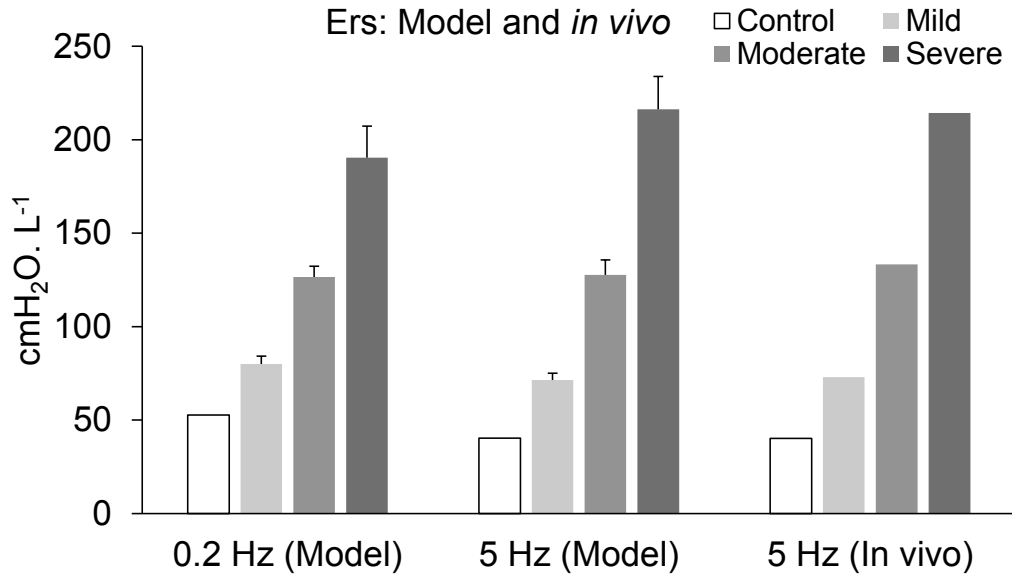


Figure 4.5: Model respiratory system elastance ($E_{rs,mod}$) compared with *in vivo* respiratory system elastance (E_{rs}) adapted from Cavalcanti et al. [27] $E_{rs,mod}$ and E_{rs} were derived from $X_{rs,mod}$ and X_{rs} respectively as described in the text. $E_{rs,mod}$ increased similarly in the low and oscillometry frequency ranges in mild, moderate, and severe heterogeneity.

Interestingly, as can be observed in Fig. 4.6, when we removed the upper airway shunt impedance, we found that this did not have a major effect on the frequency dependence on $R_{rs,mod}$. The shunt underestimated $R_{rs,mod}$ in the moderate and severe case at all frequencies, by approximately 3.1 and 4.6 $\text{cmH}_2\text{O} \cdot \text{s} \cdot \text{L}^{-1}$ at 0.4 Hz, by 1.2 and 2.3 $\text{cmH}_2\text{O} \cdot \text{s} \cdot \text{L}^{-1}$ at 5 Hz, and by 1.0 and 2.1 $\text{cmH}_2\text{O} \cdot \text{s} \cdot \text{L}^{-1}$ at 20 Hz in the moderate and severe cases respectively. The effect of shunt was greater at low frequencies, even comparing 5 Hz to 20 Hz ($p < 0.001$). Nevertheless, the shunt did not contribute to an increase in the frequency dependence. This was true either in the low frequency range (Fig. 4.6A) where heterogeneity of airway narrowing provided the observed frequency dependence of R_{rs} , and in the high frequency range, where there was very little frequency dependence of R_{rs} (Fig. 4.6C). $X_{rs,mod}$ was affected at the lowest frequency 0.2 Hz and also at the highest

frequency of 20 Hz, but not substantially at 5 Hz, which was the low end of the FOT range (Figs. 4.6B and 4.6D).

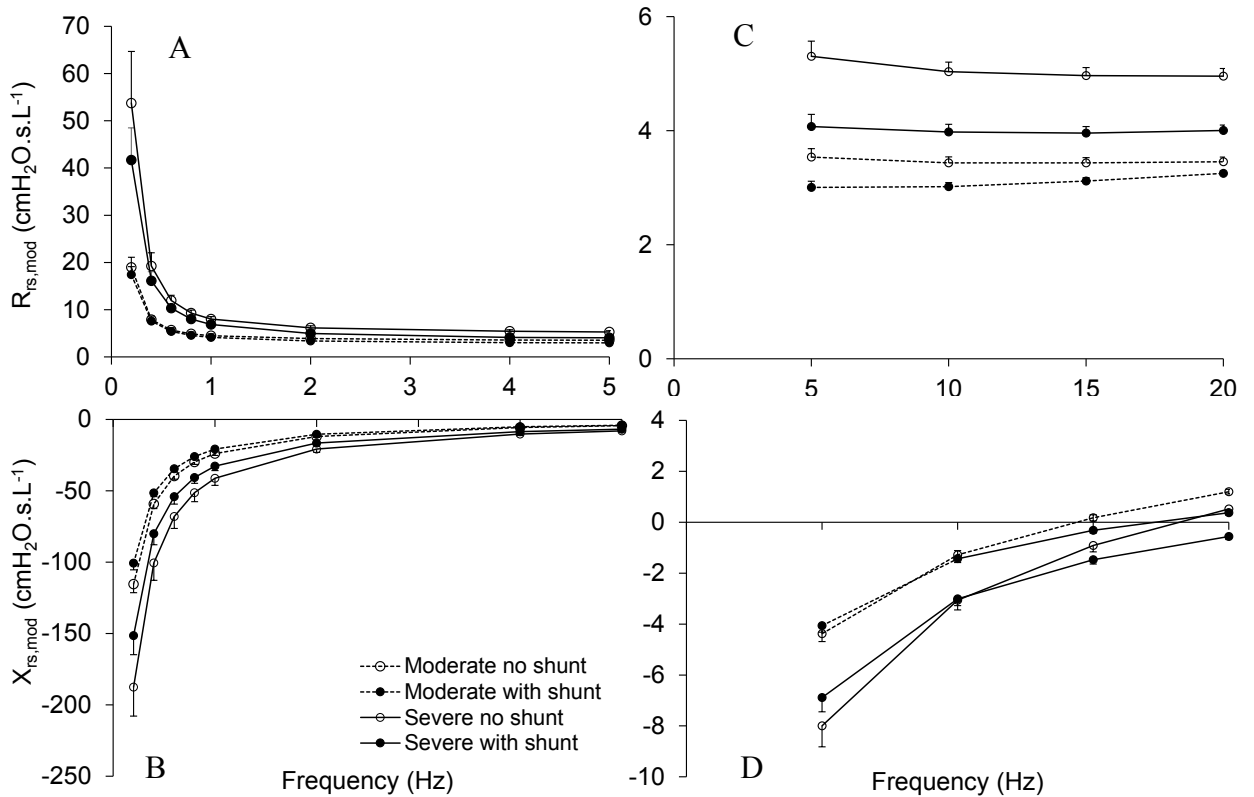


Figure 4.6: Effect of upper airway shunt impedance (Z_{uaw}) on $R_{RS,mod}$ and $X_{RS,mod}$ in the moderate and severe models of asthma shown over 0.2-5 Hz (A and B) and 5-20 Hz (C and D). Data are represented as mean \pm SD for 10 repeated simulations as described in the text.

4.5 Discussion

In this study, we, using a computational model of the human lung, reproduced the respiratory mechanics in asthmatic subjects with mild to severe airway obstruction published previously [27], and quantified the E_{RS} derived from low frequency X_{RS} , and the frequency dependence of the model R_{RS} in the low and oscillometry frequency ranges. Our principle findings are as follows. 1) E_{RS} derived from the *in vivo* data, and computed from our simple model of small-airway heterogeneity was a more strongly differentiating parameter of differences between healthy and asthmatic subjects compared with the

frequency dependence of R_{rs} in the oscillometry frequency range with measured and simulated increasing severity of asthma. 2) The model E_{rs} was also largely independent of the frequencies with consistent values at 0.2 Hz and 5 Hz. These findings are not without some limitations as described below.

We found that E_{rs} derived from reactance at 5 Hz was sensitive to asthma severity *in vivo*, and was sensitive in our model of small-airway heterogeneity to the number of obstructed airways. That E_{rs} is reflective of small-airway narrowing and closure due to de-recruitment of alveolar units is not new, as this finding is in agreement with previous modeling studies that showed that low frequency X_{rs} is sensitive to parallel airway heterogeneity and airway closure [24, 32]. Additionally, studies using morphometric models of animal lungs have shown that E_{rs} is highly sensitive to the pattern of airway construction in the lung periphery. Using a dog lung model, Lutchen et al. showed that airway constriction that includes a few highly constricted or closed peripheral airways can produce a large increase in the level of lung elastance at all frequencies [24]. Furthermore, studies in an allergic mouse model of AHR [162], and a pig model of acute lung injury [25] have also shown that low frequency X_{rs} is sensitive to the number of alveolar units blocked from receiving ventilation by airway closure and atelectasis. While our results are in agreement with these results, the purpose of this study was to compare the sensitivity of the E_{rs} derived from X_{rs} and the frequency dependence of R_{rs} .

A number of studies have reported frequency-dependent decreases in R_{rs} in asthmatic subjects at baseline and with methacholine over 3 to 22 Hz [27, 28, 132, 158, 193]. Theoretical models predict that the frequency dependence of R_{rs} can arise due to serial [141] or parallel time-constant heterogeneity [140] in the lung. For our study, we chose a very simplified model of parallel heterogeneity in the periphery by occlusion of different number of selected airways in a given generation. This was able to account for the great majority of the behavior provided by the *in vivo* data [27], but left a few important parameter discrepancies. While we observed a large frequency dependence in $R_{rs,mod}$, it was upward shifted to low frequencies by approximately 4 Hz, with a lesser frequency dependence in the oscillometry frequency range than observed *in vivo* [27]. The differences are likely due to the factors not included in our simplified model, such as

more complex patterns of airway narrowing and finite airway-wall compliance. We discuss each of these factors below.

We modeled the small-airway heterogeneity in patients with mild to severe airway obstruction [27] purposely choosing a bimodal distribution of narrowing, so that in as much as was possible given the data, E_{rs} would be accounted for by the number of occluded airways. By bimodal distribution, some of the airways are narrowed by 90%, while the remaining airways are unchanged. Of course a more distributed approach is more realistic. Kaczka et al. found that to model constriction in dogs, they required a continuous distribution of viscoelastic time constants to describe Z_{rs} data [215]. Tgavalekos et al. [23] and Campana et al. [274] similarly applied distributed airway narrowing over multiple generations including both central and small airways, and were able to match the R_{rs} frequency dependence they observed *in vivo* over the range from 0.1 to 8 Hz. As the frequency dependence arises from the heterogeneity of airway narrowing, and thus heterogeneity in ventilation time constants [140, 303], it is likely that the distribution of airway narrowing over more airways could shift the frequency dependence rightward. Nevertheless, from our study, it is remarkable how many of the principle features exhibited by the lung mechanics in asthma can be reproduced with a bimodal distribution of airway narrowing.

Another simplification of our model was that we restricted the lung compliance to the lung parenchyma, and assumed rigid airway walls rather than compliant airway walls. While airway wall compliance is much smaller than the parenchyma owing to the small volume of air in the airways, it is known that with peripheral airway obstruction, there would be increased shunting of the flow into the airways although more at high frequencies greater than 5 Hz [197]. This would alter the time constants of ventilation, and thus could alter the frequency dependence of R_{rs} [141]. Thus, compliant airway walls may also introduce greater time-constant heterogeneity, and shift the frequency dependence rightward. However, this would not likely affect our conclusions regarding the role of peripheral airways causing heterogeneity accounted for in our model by E_{rs} . Indeed airway wall compliance would lead to some shunting and would require an increase, albeit small, in the number of occluded airways required to account for the data.

In this study, we distributed the airway narrowing randomly which produced patchy areas of airflow obstruction not dissimilar to that observed from imaging (Fig. 4.2) and computed impedance. When repeated, this led to small variation in the impedance values, as indicated by the standard deviation in R_{rs} and X_{rs} (Fig. 4.3). It is possible that defects might occur that are more clustered than those produced by random selection, and this would likely affect the impedance. Indeed, recently Amin and Suki showed in a bifurcating tree that if airways are more clustered, involving narrowing of neighboring pathways, this can increase R_{rs} compared with more random distributed narrowing (Personal communication between Geoff Maksym and S. Amin, at BMES 2014 Annual meeting, San Antonio, Texas, USA and [304]). While the effect on X_{rs} was not examined, since X_{rs} largely reflects the lung compliance determined from the recruitment of terminal airspaces, X_{rs} would be less susceptible to the spatial correlation of airway narrowing.

Previous studies have put forth the idea that the frequency dependence of R_{rs} can also arise because of the effect of upper airway impedance (Z_{uaw}) [31, 183]. The compliant upper airway structures including the cheeks and the soft palate of the mouth shunt the flow oscillations, particularly during severe airway constriction. This results in an underestimation of R_{rs} assumed to occur predominantly at high frequencies [31, 89, 183]. Furthermore, as the resistance of the upper airways has a strong frequency dependence, it is reasonable to think that with increased impedance of the periphery, R_{rs} would increasingly reflect this frequency dependence. Here as expected, we found that the shunt led to a decrease in R_{rs} , but only substantially in moderate and severe asthma, and the effect was largely insensitive to frequency (Fig. 4.6). This is likely due to the shunt being a substantially stiffer compartment, and with frequency dependence in the same frequency range, leading to a nearly parallel shift in R_{rs} .

In our simple model, we chose to narrow airways in one particular generation, the 10th. When we narrowed airways a generation above or below the 10th instead, there was a little overall difference in behavior (not shown). This is likely since the effect of narrowing the two daughter airways beyond a bifurcation on impedance is very similar to occluding the parent. However, when we narrowed airways further up the tree in the 6th generation, we found that it provided a poorer match with the measured data. This is

because there are only few airways in this generation, and the impedance depends on which airways are narrowed.

One of the interesting findings from our study is that the percentage of airway narrowing that accounted for the *in vivo* E_{rs} in asthmatic subjects was much larger than would be required to produce the ventilation defects observed in recent imaging studies [293, 294]. Ventilation defects are regions with negligible or very poor inhalation of observable gas, presumably due to closure of the airways supplying these regions. These studies found that ventilation defect volumes varied from 6% (mean) to 13.5% (median) of the total lung volume, whereas our models required airway narrowing in excess of 60% for even moderate asthma, which would correspond to comparable defect volume percentage. This may be due to differences in the characteristic time of each measurement. In hyperpolarized helium imaging, images are acquired during a breath hold maneuver 8 to 15 sec after the gas mixture is inhaled. The inhaled gas can thus penetrate regions with long time constants. Oscillometry probes from 4 to 32 Hz, and thus probes the lung at much shorter time constants and can thus be more sensitive to small-airway narrowing.

4.6 Conclusions

In conclusion, we have shown that elastance derived from the low frequency reactance was a robust and consistent measure of small-airway constriction and heterogeneity compared to frequency dependence of R_{rs} , and was not sensitive to upper airway wall shunting. Thus, low frequency reactance and associated elastance may be clinically more useful measures of small-airway disease in asthma. While frequency dependence of R_{rs} was related to heterogeneity, it was surprisingly insensitive to upper airway shunting, unlike R_{rs} itself, but may depend on other factors associated with airway narrowing.

Chapter 5: A Study of Artifacts and Their Removal during Forced Oscillation of the Respiratory System

Authors

Swati A. Bhatawadekar
Del Leary
Y. Chen
Junichi Ohishi
Paul Hernandez
Tim Brown
Colm McParland
Geoff N. Maksym

Published in Annals of Biomedical Engineering, 2013 May; 41(5):990-1002

This manuscript has been modified from its original format to conform to the structure of this dissertation.

5.1 Abstract

Respiratory impedance measured by the forced oscillation technique (FOT) can be contaminated by artifacts such as coughing, vocalization, swallowing or leaks at the mouthpiece. We present a novel technique to detect these artifacts using multilevel discrete wavelet transforms.

FOT was performed with artifacts introduced during separate 60 second recordings at known times in 10 healthy subjects. Brief glottal closures were generated phonetically and confirmed by nasopharyngoscopic imaging of the glottis. Artifacts were detected using Daubechies wavelets by applying a threshold to squared detail coefficients from the wavelet transforms of both pressure and flow signals. Sensitivity and specificity were compared over a range of thresholds for different level squared detail coefficients.

Coughs could be identified using 1st level detail (cd1) coefficients of pressure achieving 96% sensitivity and 100% specificity while swallowing could be identified using cd2 thresholds of pressure with 95% sensitivity and 97% specificity. Male vocalizations could be identified using cd1 coefficients with 88% sensitivity and 100% specificity. For leaks at the mouthpiece, cd3 thresholds of flow could identify these events with 98% sensitivity and 99% specificity. Thus, this method provided an accurate, easy and automated technique for detecting and removing artifacts from measurements of respiratory impedance using FOT.

5.2 Introduction

The forced oscillation technique (FOT) is an established tool to assess the oscillatory mechanical properties of the respiratory system, which is increasingly being used in the clinical assessment of lung disease. FOT determines the respiratory mechanical impedance (Z_{rs}) to airflow from pressure oscillations at the mouth. Most commonly the method is used to measure respiratory system resistance (R_{rs}) which is closely related to airway diameter and reflects airflow limitation, but the method can also provide the respiratory system reactance (X_{rs}). X_{rs} can be used to determine the respiratory system elastance, which reflects lung stiffness and which is also altered in a variety of lung diseases [89]. FOT is comfortable for subjects and is usually performed during normal breathing; thus, FOT can be used in situations when standard measurement of lung function by spirometry is difficult, impractical or not feasible [89]. Z_{rs} measured by FOT is useful in the assessment of lung function for a variety of diseases including asthma, COPD, and cystic fibrosis [30, 156]. During FOT measurements, the respiratory signals of pressure and flow can be contaminated by transient artifacts such as coughing, swallowing, vocalizations, and leaks at the mouthpiece. When these are obvious and the operator well-trained, the recordings can either be discarded and the measurement repeated, or the offending portion of the recording removed manually before estimation of the impedance. However, some artifacts may be difficult to detect, and manual post processing to remove artifacts may not be reliable. Thus, efficient methods to improve data quality are useful, and are sought in the measurement of respiratory impedance.

A number of simple techniques are currently used to remove artifacts, but their effectiveness has been rarely assessed. FOT guidelines recommend that data quality be minimally maintained by verifying that the signal coherence is greater than 0.95 [89] to ensure that contamination by noise is minimal [123, 124, 305]. Less commonly, signal-to-noise ratio (SNR) is used to assess data quality [39], or specialized techniques that remove values at suspected glottal closures at low flow points during breathing [37, 306]. The most commonly employed technique is to remove extreme values of Z_{rs} or R_{rs} , such as values greater than 3-5 standard deviations from the mean Z_{rs} or R_{rs} from multiple measurements at a specific frequency [39, 307]. However, the effectiveness of these methods has not been compared.

Artifacts are usually transient events that occur very briefly during recordings and thus tend to be dominated by high frequency content. This suggests that their presence and localization in time may be detected using methods that have high temporal resolution for high frequency events, a feature of wavelet transform analysis. Wavelet transforms are commonly applied to monitor signals in which frequency content changes temporally, and have found broad application in biomedical signals such as electrocardiography (ECG), electroencephalography (EEG) and electromyography (EMG) [308-310].

To attempt to provide an automated technique for artifact removal from FOT signals and to explore the high temporal resolution of wavelet-based approaches to detect high-frequency events, in this study we evaluated the ability of a wavelet transform-based method to identify and remove artifacts automatically from pressure and flow signals during forced oscillation.

5.3 Methods

5.3.1 Subjects

Ten healthy subjects (4 males and 6 females) were enrolled following obtaining informed consent (Table 5.1). The study was approved by the Capital Health Research Ethics Board.

Table 5.1: Subject demographics and lung function

Sex, male / female	4 / 6
Age, years	34 ± 2.5
Height, cm	154.5 ± 12.7
Weight, kg	66.2 ± 1.6
FEV ₁ , % predicted	104 ± 3.7
FVC, % predicted	102 ± 4.7

Data are presented as mean ± standard error of mean. FEV₁, forced expiratory volume in 1s as percent of predicted [289], ; FVC, forced vital capacity as percent of predicted [290]

5.3.2 Measurements

Impedance of the respiratory system (Z_{rs}) was measured using the FOT device [39] developed by Dr. Maksym and colleagues at Dalhousie University. The device comprised a loud speaker enclosed in a wooden box to generate small-amplitude pressure oscillations (approximately ±1 cmH₂O). The loud speaker was driven by a multi-frequency sinusoidal signal containing frequencies 4, 10, and 22 Hz.

The sinusoidal pressure oscillations generated by the loud speaker were applied at the subject's airway opening via disposable antibacterial / antiviral filter (MicroGard, Viasys Sensormedics, USA). A fan provided a bias flow of approximately 12 L/min of fresh air to avoid buildup of exhaled air in the dead space, and a long, high-inertance, stiff-walled bias tube (1.9cm diameter×176.5cm length) shunted the subject's breathing to the atmosphere. Subjects sat upright with their heads in a neutral position, wore a nose clip, and supported their cheeks and soft tissue below the chins firmly with both palms to minimize errors due to upper airway shunt [89]. Pressure at the airway opening was measured by a differential pressure transducer (TD-05-AS, SCIREQ Inc., Montreal, Canada) with respect to the atmospheric pressure, while oscillatory changes in flow at the airway opening were recorded by a Fleisch type pneumotach (Fleisch No. 2, Lausanne,

Switzerland) connected to a similar pressure transducer. The pneumotach was heated at 38 °C to avoid condensation and clogging of internal parts by the subject's breathing. The pressure transducer was calibrated using a U-tube fluid manometer, and the pneumotach was calibrated by flow-integral method using a calibrated 3L syringe. The device impedance was compensated for over the entire frequency range using the method described in Section 3.2.2. The device was validated using a standard test load of 5 cmH₂O.s.L⁻¹ (Hans Rudolph, Inc., KS, USA) over the full frequency range ensuring that the DC calibration was accurate over the full frequency range.

Forced expiratory volume in one second (FEV₁) and forced vital capacity (FVC) were recorded (Vmax Encore 20, Viasys Respiratory Inc., Palm Springs, CA) according to American Thoracic Society (ATS) criteria [283]. Predicted values of Morris et al.[289, 290] were used to report values.

5.3.3 Protocol

The subjects were trained to introduce artifacts such as light coughs, swallowing, mouthpiece leaks and vocalizations at predetermined times (10, 20, 30, and 40 sec) during 1 minute FOT measurement. The protocol was repeated at least once for each artifact type giving a minimum 4 repeated measures for each artifact from each subject. Artifacts were easily confirmed by operator observation or confirmation by the subjects that they had produced the 4 artifacts per trial or both observation and confirmation.

To investigate the effect of glottal narrowing, we purposely mimicked glottal narrowing using phonetically generated artifacts produced by subjects by vocalizing short, quiet, but audible 'hee' sounds in separate recordings. We also requested in a few subjects that they repeat the test with decreasing sound intensity to zero in an attempt to reduce the glottic gap without producing audible sound. Momentary glottal narrowing was confirmed in all subjects by transient changes in pressure, flow or resistance or audibly but also in one subject by imaging the glottis using a pediatric nasopharyngoscope inserted via the nose while glottal images were obtained from videos recorded during quiet breathing and during vocalization.

5.3.4 Data Analyses

The respiratory pressure and flow signals were amplified and low-pass filtered using a 6 pole Bessel filter, cut off 100Hz (SC24, SCIREQ), and sampled at 240 Hz (National Instruments DAQ 6036E). Data was analyzed using a custom code written in Matlab (The Mathworks Inc., Natick, MA) as described below.

The pressure and flow signals were high-pass filtered by Fast Fourier transforming in the frequency domain, removing all components less than 1 Hz, which removed most of the breathing signals, and inverse transforming the signal to the time domain. They were then divided into 1 sec data blocks with 50% overlap and each block was multiplied by the Hamming window function to reduce effects of any non-stationarity and edge artifacts. Finally impedance from the measured signals (Z_{meas}) at each excitation frequency was estimated from the ratio of Fourier transforms of the pressure to the flow. We estimated Z_{rs} after compensating Z_{meas} for impedances of the bias tubes, bacterial filter and tubing between the subject and the bacterial filter as described in Section 3.2.4.

Artifact Detection

Following artifact detection we calculated sensitivity (ratio of true positives to sum of true positives and false negatives) and specificity (ratio of true negatives to sum of true negatives and false positives) to compare algorithm performance and compared the wavelet-based approach to other automated currently accepted approaches, including coherence, SNR estimates, and extreme values of impedance based on standard deviations. For the detection of leak artifacts, we also developed a method based on low absolute impedance. These methods are described below.

Time-frequency analysis of pressure and flow

An initial examination of the time-frequency content of the FOT signals was done using the Short Time Fourier Transform (STFT), which is repeated application of the Fourier transform in sequential time windows (Fig. 5.2C). For STFT, the pressure and the flow signals were divided into segments of 256 samples with 50% overlap and each

segment was multiplied by the Hanning window function of the same width. Time and frequency resolutions were 1.06 sec and 0.93Hz respectively.

Wavelet Transforms and rejection of artifacts using wavelets

Unlike the STFT which uses fixed-size windows for each frequency, the wavelet transform employs windows with scaled length in time and frequency according to a prescribed wavelet basis function as described elsewhere [308]. Here, we used discrete wavelet analysis for non-redundant time-frequency mapping of the signal information and performed a wavelet analysis of the pressure and the flow signals using a variety of wavelets such as Daubechies 4 (db4), Daubechies 5 (db5), Daubechies 6 (db6) and Symlet 5 (sym5).

The choice of the wavelet function for a particular application depends on the properties of the wavelet suitable for the application as well as the shape of the signal under analysis [311]. For instance, the Harr wavelet which has a square shaped function is most suitable for signals with sudden transitions or discontinuities while other more continuous or smooth wavelets can be used for smoothly changing signals. Here we selected db5 wavelet because of its resemblance to pressure and flow signals contaminated by artifacts and its effective filter implementation, and because it is fairly commonly employed. Furthermore in preliminary measurements, there was not any appreciable difference in db4, db5 and db6 in terms of identifying artifacts, therefore we chose db5.

Locations of possible artifacts were identified by a threshold algorithm as follows. The pressure and the flow signals were subjected to multi-level (resolutions) DWT decomposition, which provided detail coefficients with increasing, finer levels of detail (Fig. 5.1D). Bursts or spikes in a particular detail coefficient plotted verse time revealed the presence of a possible artifact. To detect the artifacts, the detail coefficients were squared and defects identified if the coefficients exceeded a prescribed threshold. Squaring the coefficients provided a positive only signal and nonlinearly amplified the detail coefficient signals to provide better detection (Fig. 5.2A). Once an artifact was identified, two additional data values (one on either side of the artifact value) were eliminated to ensure complete elimination of corrupted values. The sensitivity and

specificity were calculated using a range of threshold values applied across all subjects and averaged.

Since cd1 coefficients largely represent the high-frequency content above a cut-off of 50% of the Nyquist frequency (120 Hz here), we also evaluated the performance examining high-frequency information by digitally high-pass filtering the data with a 60 Hz cut-off in the frequency domain and then inverse Fourier transforming the filtered signal. The filter output was similarly squared and subjected to a range of thresholds.

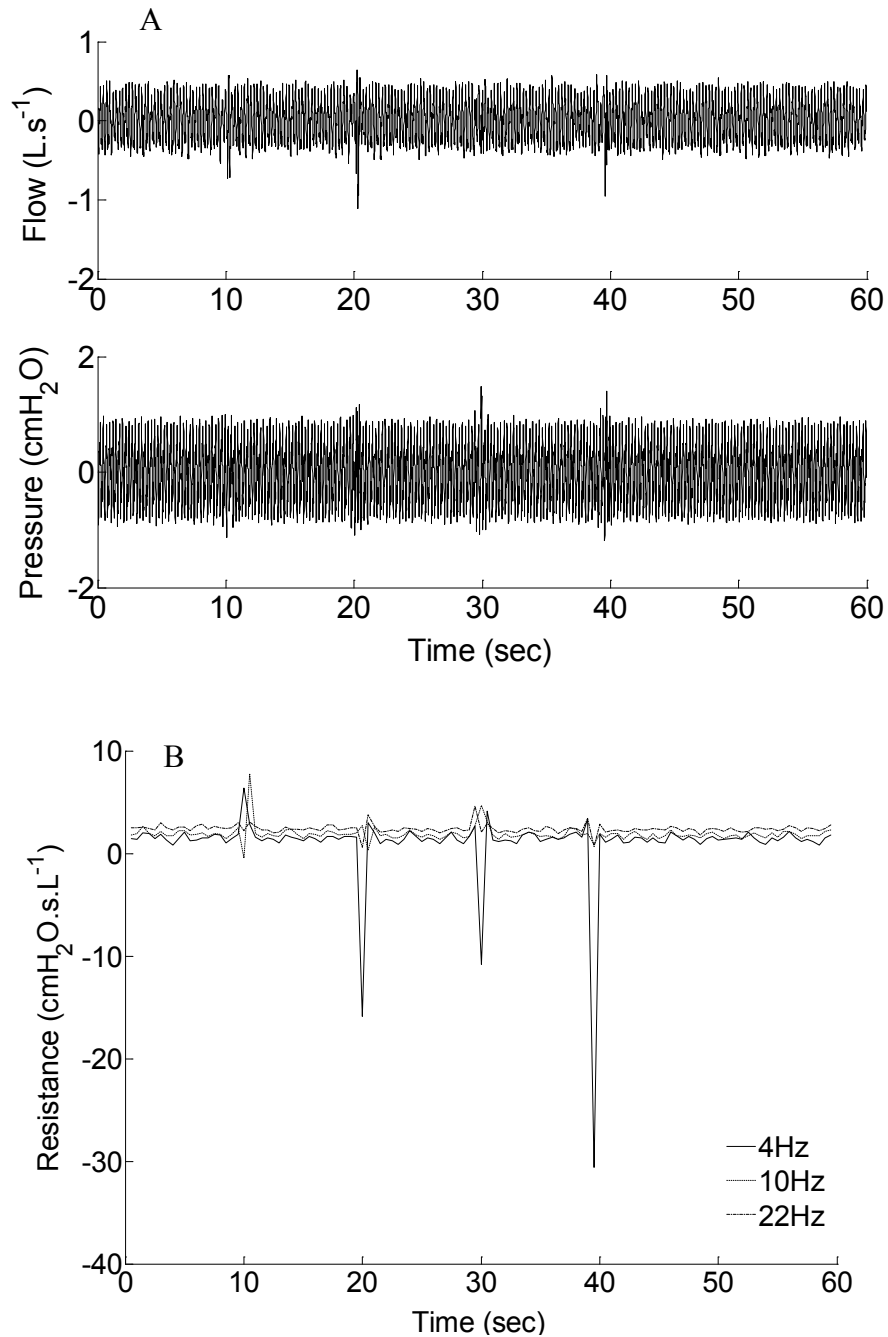


Figure 5.1: Flow and pressure and their time-frequency analysis for cough artifacts A) Flow and pressure measured in a study subject after high-pass filtering to remove breathing artifact. The subject was instructed to cough at times 10, 20, 30 and 40 s B) Resistance estimate showing transients at the times of coughs

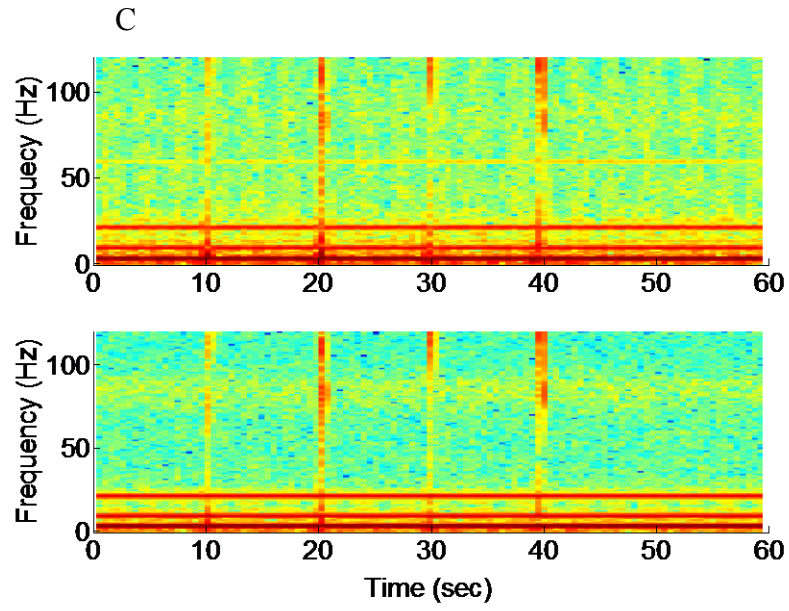


Figure 5.1: C) Spectrogram by STFT of the flow and the pressure in the presence of an example of cough artifacts. The three signal frequencies (4, 10, and 22 Hz) are seen as dark colour horizontal lines at the bottom, and the cough artifacts are seen as dark colour vertical bands at the times of cough, indicating their very short time and broad frequency spectral content.

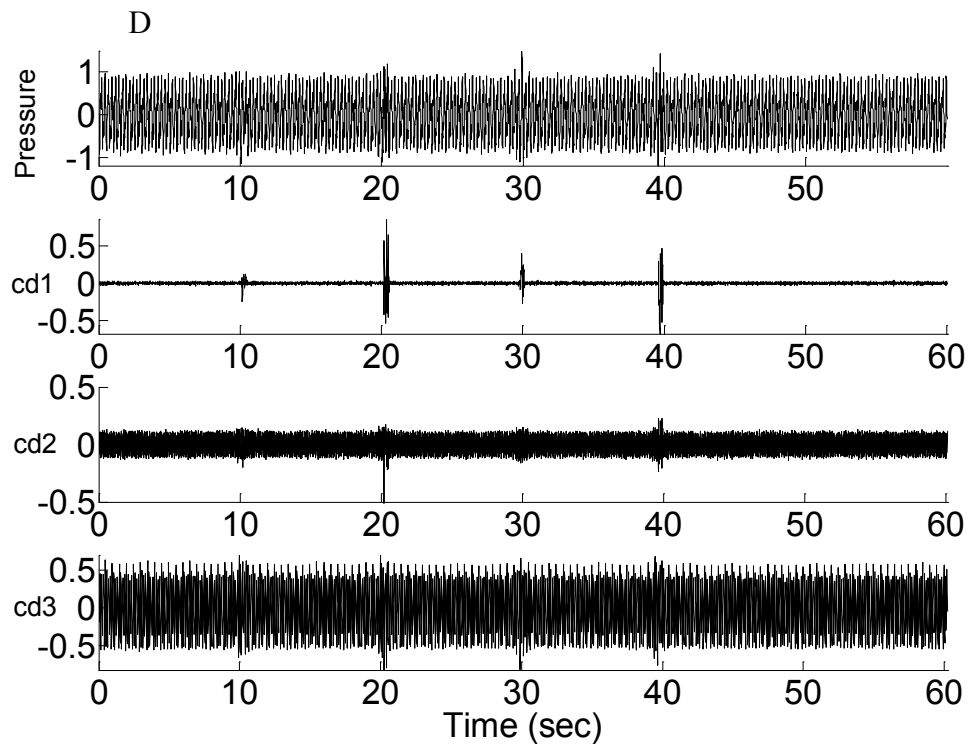


Figure 5.1: D) Pressure signal and its 3 level discrete wavelet decomposition using Daubechies (db5) showing detail wavelet coefficients cd1, cd2 and cd3. Cough artifacts could be seen as spikes in all level wavelet coefficients, more prominently in cd1.

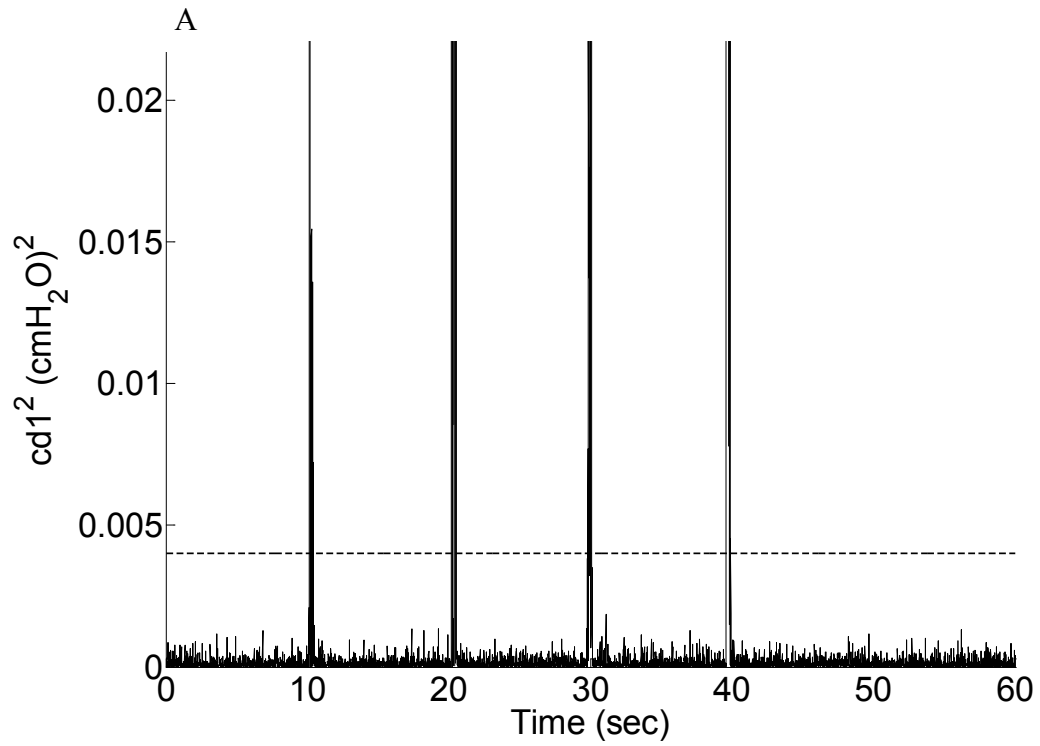


Figure 5.2: Removal of cough artifacts by wavelets and sensitivity and specificity of wavelet coefficients A) Squared first level detail wavelet coefficients $cd1$ versus time and a sample threshold (dashed line) of $0.004 (\text{cmH}_2\text{O})^2$

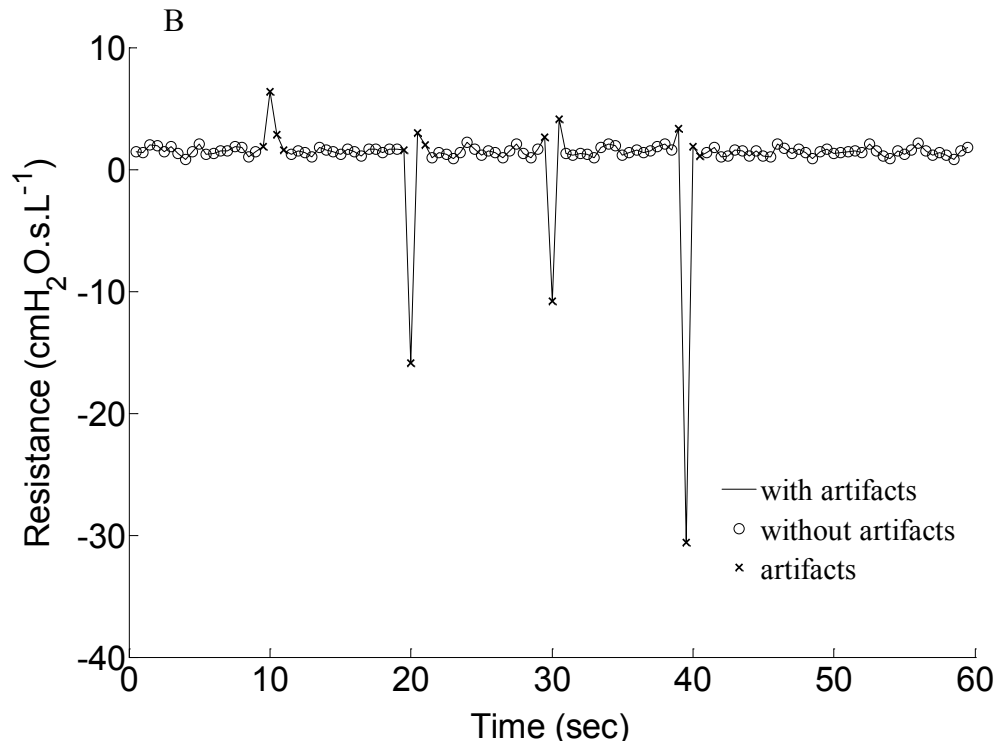


Figure 5.2: B) The artifactual R_{rs} values resulting from coughs detected by discrete wavelet transform technique are shown by crosses.

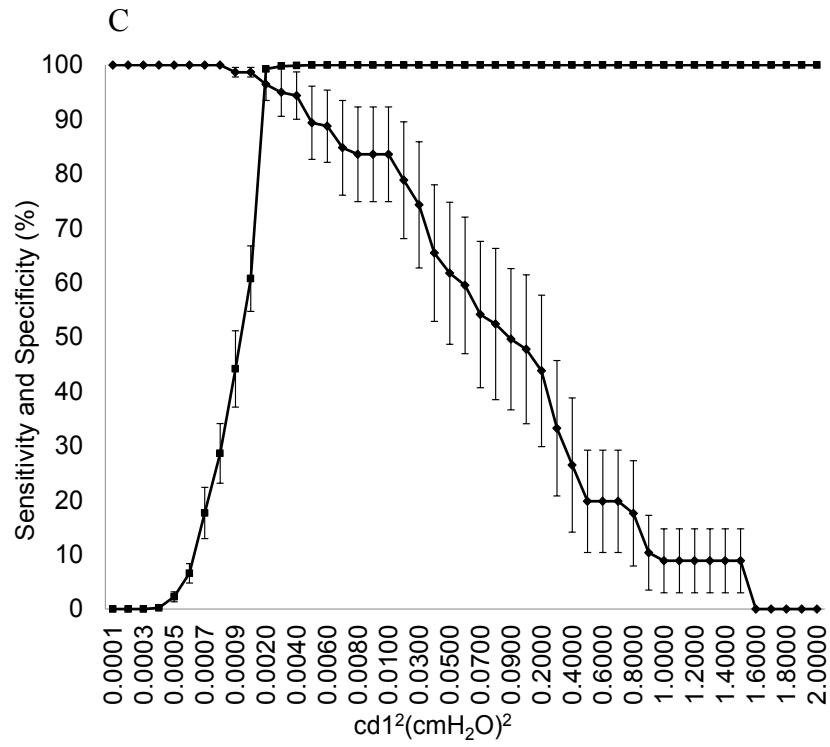


Figure 5.2: C) Cough artifacts: Sensitivity and specificity for the pressure determined over a range of thresholds for 9 subjects. The threshold is expressed as squared first level detail wavelet coefficients $cd1^2$. Error bars indicate standard error of mean.

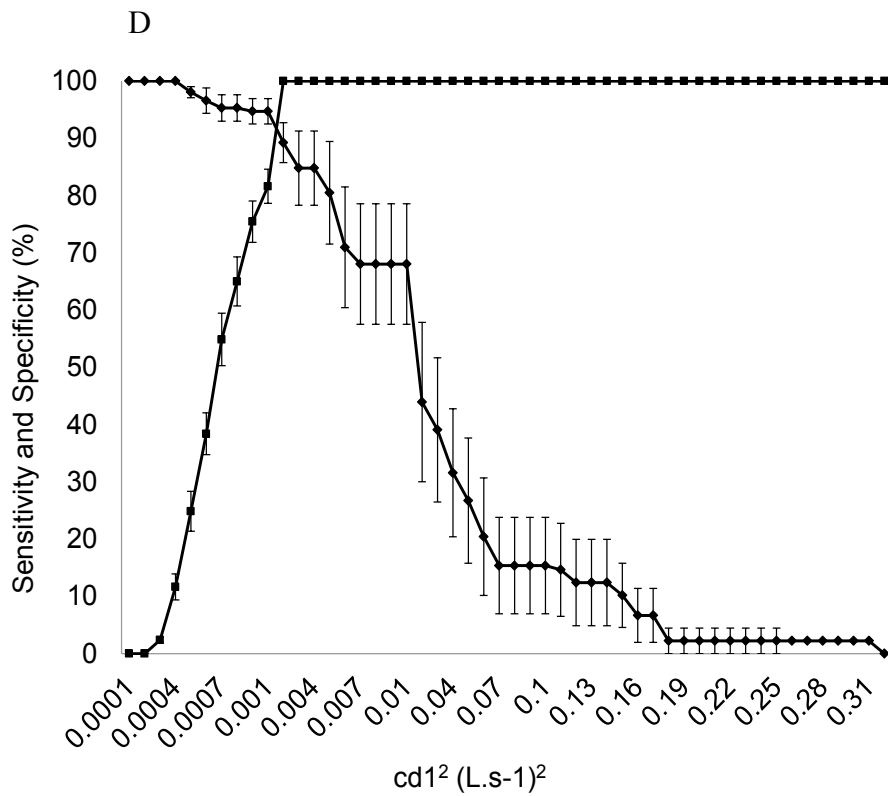


Figure 5.2: D) Cough artifacts: Sensitivity and specificity for the flow determined over a range of thresholds for 9 subjects. The threshold is expressed as squared first level detail wavelet coefficients $cd1^2$. Error bars indicate standard error of mean.

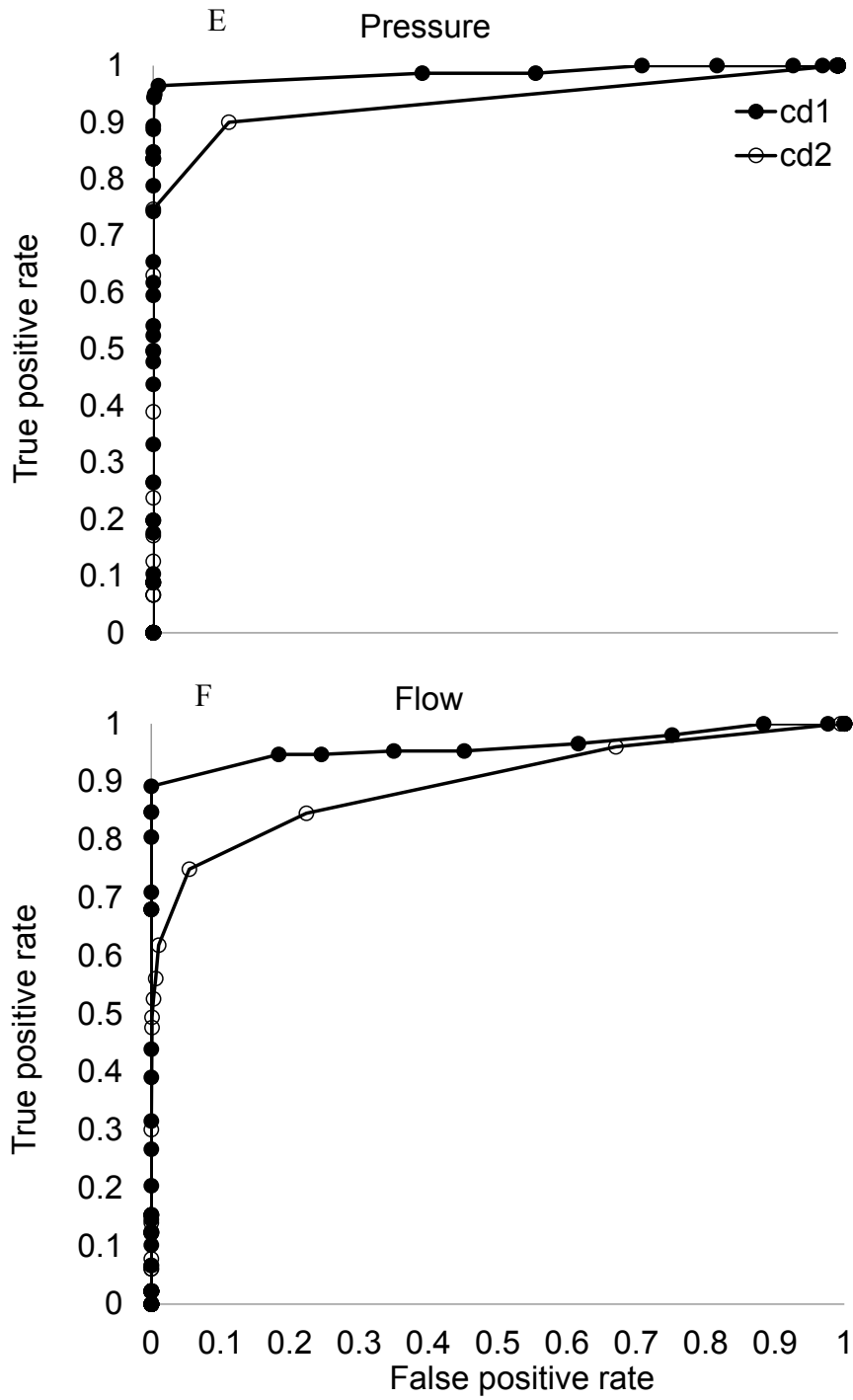


Figure 5.2: (E) & (F) Receiver Operating Characteristic curve for pressure and flow cd1 and cd2 coefficients of cough artifacts. See text for details.

Rejection of artifacts based on coherence between pressure and flow and on SNR

The quality of the impedance estimates were also assessed using the coherence function γ^2 between the pressure and the flow signals calculated as recommended by FOT guidelines and evaluated at each excitation frequency [89]. To detect artifacts that may be contaminating a window within the 16 seconds, γ^2 was obtained from 16 second windows shifted along the signals one second at a time. If $\gamma^2 < 0.95$ then this indicated an artifact was contaminating this particular 16 second block. The block was appended by 1 second, and coherence recalculated with each individual second removed in an attempt to recover $\gamma^2 > 0.95$ for the block. If this failed, two seconds would be removed.

Respiratory pressure and flow signals are low-frequency signals with energy concentrated at the breathing frequency, typically near 0.3 Hz, but including small amplitude components extending much higher than this, and which can contaminate the FOT signal frequencies. The noise contaminating a particular oscillation frequency can be estimated by root mean square averaging neighboring frequency bands. For 4 Hz, the neighboring frequency components used for this estimate were 3 Hz and 5-7 Hz, while for 10 Hz the frequency components were from 7-9 and 11-13 Hz, and for 22 Hz the frequency components used to estimate the noise were 16-21 and 23-28 Hz. At each signal frequency, the noise was estimated for all 1 sec data blocks. SNR was then determined as the ratio of the magnitude of the input signal frequency and the respective noise estimate. R_{rs} estimate for a block was rejected when SNR was less than 20dB for the data block.

Removing leak artifacts by thresholding absolute values of impedance

In addition to the wavelet approach, we also developed an algorithm to detect leak artifacts based on very low or near-zero impedance magnitude indicative of a mouthpiece leak. Fig. 5.3A shows Z_{rs} , R_{rs} , and X_{rs} recordings in a study subject during which purposeful small leaks at the mouthpiece were introduced. The Z_{rs} , R_{rs} , and X_{rs} values can each be seen near zero at the times of artifacts.

A

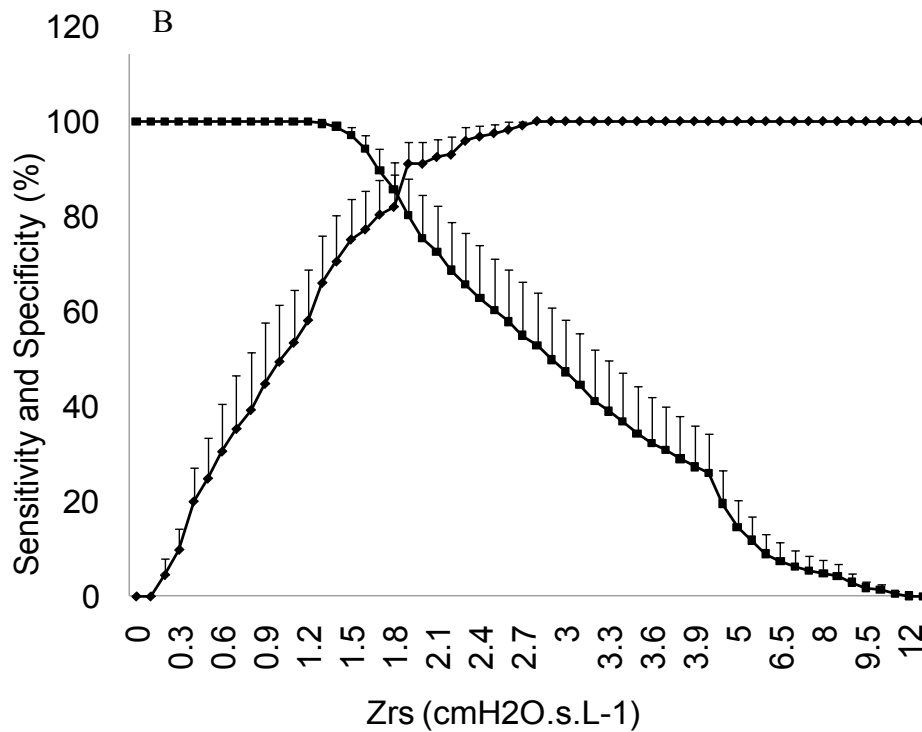
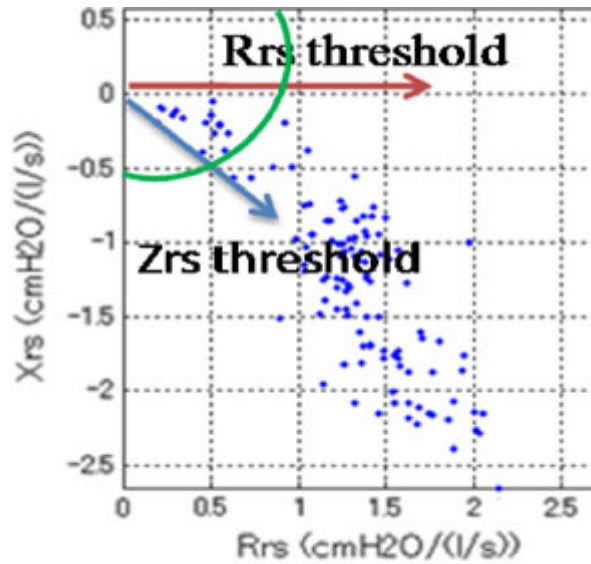


Figure 5.3: Removal of flow leak artifacts A) Method to reject low impedance values due to leaks illustrated for one subject by thresholding $|Z_{rs}|$. B) % sensitivity and specificity for leaks detected by $|Z_{rs}|$ method indicate optimal Z_{rs} threshold across adult subjects of $1.8 \text{ cmH}_2\text{O.s.L}^{-1}$.

Rejection of artifacts based on statistical properties of R_{rs}

Artifacts were also rejected based on the statistical properties of R_{rs} and X_{rs} using two methods. In the first method, R_{rs} and X_{rs} values corresponding to negative R_{rs} values were first eliminated. Then R_{rs} and X_{rs} values 3 standard deviation above and below the means of R_{rs} and X_{rs} were rejected in 3 iterations (3SD method). In the second method, R_{rs} and X_{rs} values 5 standard deviation above and below the means of R_{rs} and X_{rs} were rejected in a single iteration (5SD method). In both the methods, if an artifact was detected in R_{rs} , the corresponding X_{rs} value was eliminated and vice-versa.

Application to patient data

We also applied the wavelet-based algorithm and other basic methods to pressure and flow data with only spontaneously occurring artifacts from 22 subjects with asthma and 16 control subjects enrolled in another research study approved by the REB. In these subjects, some artifacts, like swallowing, were self-reported by patients during recordings, and obvious artifacts were operator-reported during recordings.

5.4 Results

Examining the coefficients, the artifacts typically presented as short-duration spikes, and were most prominent for coughs and male vocalizations in cd1, for swallowing in cd2, for female vocalizations and mouth leaks in cd3. Our principal finding is that in general the wavelet-based method performed better than coherence- and SNR-based methods for all artifacts that we studied, usually achieving sensitivity and specificity greater than 90%. The coherence- and SNR-based methods detected less than 15% of artifacts.

Light Coughs by DWT detection method

The effects of the imposed artifacts can be seen as slight transients on the pressure and flow signals (Fig. 5.1A). Notice that while cough artifacts affected R_{rs} at all three frequencies, the effect was more pronounced at 4 Hz most of the time as seen in the last 3 transients in Fig 5.2B, but could affect R_{rs} similarly at the three frequencies as occurred

upon close examination of the first transient of Fig. 5.1B. Fig. 5.1C shows a spectrogram of the pressure and the flow and Fig. 5.1D shows a pressure signal measured in a study subject and its three-level wavelet decomposition using Daubechies wavelet db5. The cough artifact appeared as spikes in all three order detail coefficients, being most prominent in cd1 which was found to have higher sensitivity and specificity than other coefficients. Fig. 5.2A shows $cd1^2$ for cough artifacts and a sample threshold $0.004 \text{ cmH}_2\text{O}^2$ while the identified artifacts are indicated on R_{rs} as crosses in Fig. 5.2B.

We provide the sensitivity and specificity over a useful range in thresholds where sensitivity and specificity were both greatest. Applying wavelet analysis on the pressure signal using db5 wavelet, cough artifacts could be identified for squared cd1 thresholds ranging from 0.002 to $0.006 \text{ cmH}_2\text{O}^2$, with corresponding sensitivities of $88 \pm 3\%$ to $96 \pm 6.7\%$ for the range (standard error of mean). The specificity for this threshold range was $99 \pm 3\%$ to 100% (Fig. 5.2C). We also conducted the Receiver Operating Characteristic (ROC) analysis as it allowed examination of both true positive rate detection of actual artifacts, and false positive rate detection of false artifacts in a single curve as we varied the wavelet coefficients. This permitted us to robustly compare performance of the wavelet coefficients independent of their values, illustrated for pressure cd1 and cd2 coefficients (Fig. 5.2E). The area under the curve (AUC) for pressure cd1 (0.98) was better than for cd2 (0.93), therefore we chose cd1 coefficients for coughs.

Applying DWT analysis in a similar fashion for the flow signal was slightly less sensitive and provided $70 \pm 3.5\%$ to $89 \pm 10.5\%$ sensitivity and 100% specificity for squared cd1 thresholds ranging from 0.002 to $0.006 \text{ (L}\cdot\text{s}^{-1})^2$ respectively and the AUCs for flow cd1 and cd2 were 0.96 and 0.89 respectively (ROC curves not shown). Very little difference in performance was obtained using other wavelet basis functions.

Light coughs by high-pass filtering respiratory signals

Cough artifacts could also be identified by using only a high pass filter on the pressure and flow signals. For a range of thresholds ranging from 0.0008 to $0.002 \text{ cmH}_2\text{O}^2$ applied to squared filtered pressure signal, 97% (2.2) to 91% (4.8) sensitivity and 93% (2.5) to 99% (0.11) specificity (area under the ROC curve, 0.98) were obtained

and analysis of the flow signal gave $90 \pm 3.2\%$ to $83 \pm 6.6\%$ sensitivity and $97 \pm 1\%$ to $99 \pm 0.3\%$ specificity (area under the ROC curve, 0.96).

Brief glottal closures caused by swallowing and vocalizations by DWT detection method

Three volunteers were asked to perform swallowing that was as light as possible during the measurements. These events could be identified with the wavelet analysis of the pressure signal, but using the second-level wavelet coefficients (cd2). Over a range of cd2² thresholds from 0.022 to 0.025 cmH₂O², swallows could be rejected with $83 \pm 3\%$ to $95 \pm 11\%$ sensitivity and $79 \pm 17\%$ to $97 \pm 1.3\%$ specificity (Fig. 5.4B).

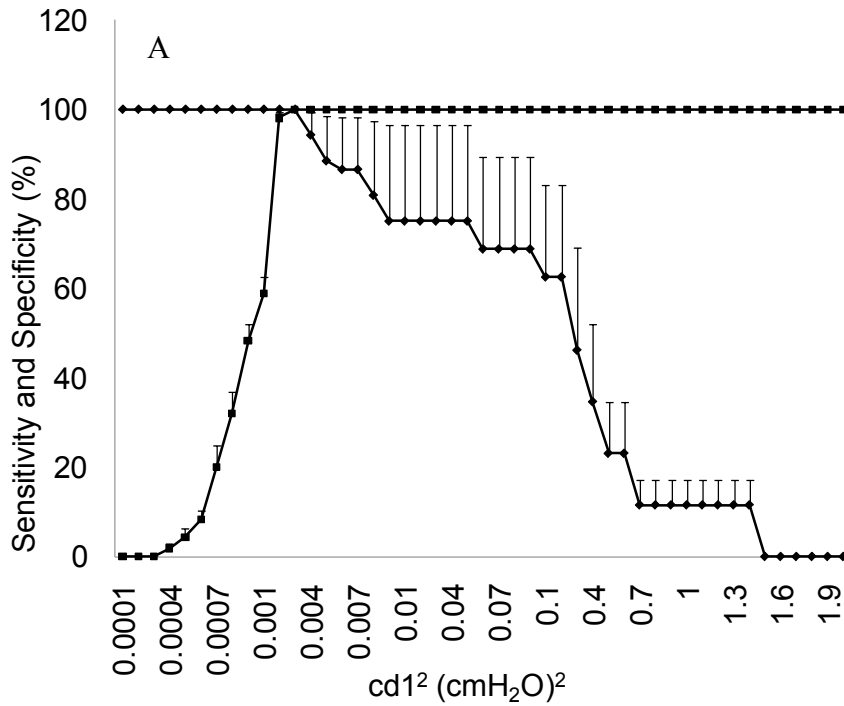


Figure 5.4: % Sensitivity and % specificity for male vocalizations and swallows A) for male vocalizations

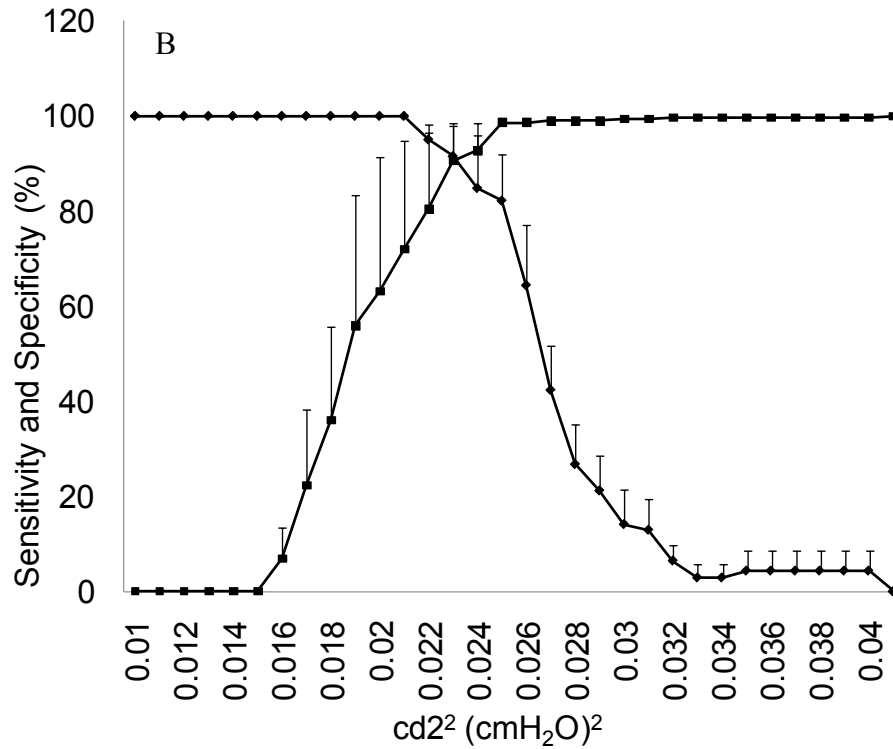


Figure 5.4: B) % Sensitivity and % specificity for male swallows

When we asked study subjects to vocalize a ‘hee’ sound to investigate the effect on R_{rs} of the glottis closure as involuntary glottis narrowing would be hard to capture, vocalizations affected respiratory resistance (Fig. 5.5C) as expected during glottal narrowing, confirmed by direct imaging (Figs. 5.5A and 5.5B). These events appeared as high-amplitude spikes in all detail coefficients, but appeared more prominently in cd1 in male subjects and in cd3 in female subjects. For cd1² threshold for pressure signal ranging from 0.002 to 0.005 cmH₂O², male vocalizations could be identified with $88 \pm 1.5\%$ to 100% sensitivity and $98 \pm 1.5\%$ to 100% specificity (Fig. 5.4A). Out of 6 female subjects, 4 subjects’ artifacts prominently presented as spikes in cd3 squared coefficients which could be identified with $52 \pm 26\%$ to $55 \pm 24\%$ sensitivity and 95 ± 4 to $99 \pm 0.25\%$ specificity for thresholds ranging from 0.42 to 0.45 cmH₂O². In 2 female subjects 50% of the artifacts appeared as spikes in cd3 with a few artifacts appearing in cd2 coefficients. Because it was uncertain if these subjects in fact produced ‘hee’ type

artifacts correctly, they were excluded from all analysis. In order to determine if identifying glottic narrowing resulting from vocalizations was independent of sound quality of vocalizations, we asked one subject to produce short and long inaudible vocalizations. As with the quiet but audible ‘hee’ artifacts, the inaudible ‘hee’ artifacts could be identified prominently in cd3 coefficients with both $> 95\%$ sensitivity and specificity.

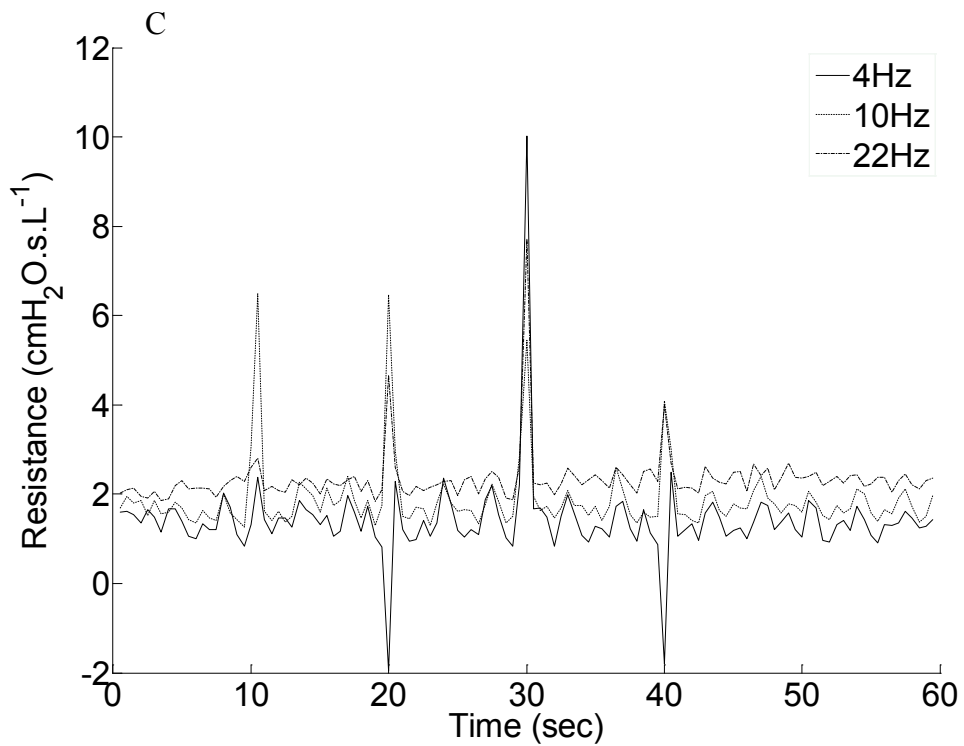
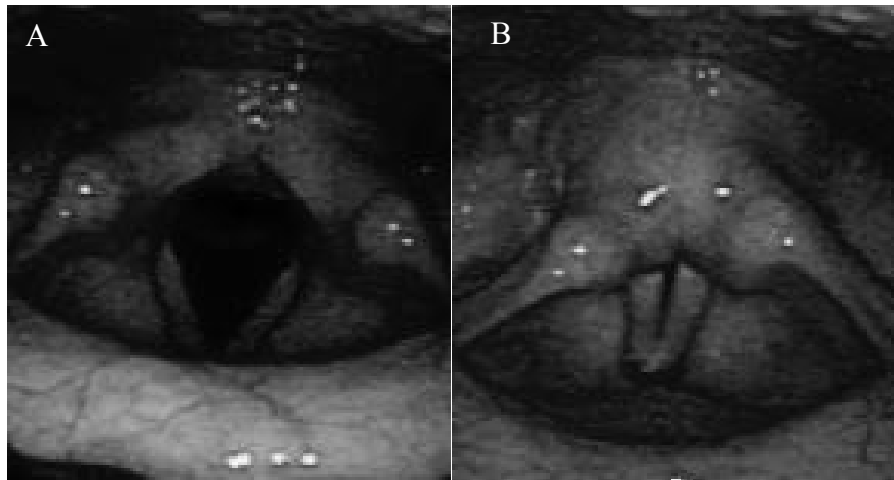


Figure 5.5: Glottal images and resistance trace showing for vocalizations Images of glottis opening in a study subject A) during quiet breathing B) during vocalization (‘hee’ sound). The glottis aperture seems to close momentarily during the vocalization C) Changes in R_{rs} resulting from vocalizations.

Leaks by DWT detection method and by thresholding absolute Z_{rs} values

We found that using cd3 wavelet coefficients had the highest sensitivity and specificity for detecting leaks with cd3 thresholds ranging from 0.07 to 0.09 $(L.s^{-1})^2$ for flow analysis identifying leaks with $90 \pm 1.5\%$ to $98 \pm 6\%$ sensitivity and $94 \pm 9.6\%$ to $99 \pm 0.2\%$ specificity, respectively (Fig. 5.6). The other wavelet basis functions including db4, db6 and sym5 performed similarly (not shown). Using low-value thresholds on R_{rs} , X_{rs} , and $|Z_{rs}|$, we found that $|Z_{rs}|$ performed slightly better than R_{rs} or X_{rs} alone (not shown). For $|Z_{rs}|$ thresholds ranging from 1.8 to 2.3 $cmH_2O.s.L^{-1}$, leaks could be identified with $91 \pm 4.6\%$ to $96 \pm 2.9\%$ sensitivity and $65 \pm 7.7\%$ to $80 \pm 11\%$ specificity (Figs. 5.3A and 5.3B). The threshold where the sensitivity and specificity cross could be considered optimal although, other choices could be made, for example, if greater sensitivity is desired at the expense of specificity.

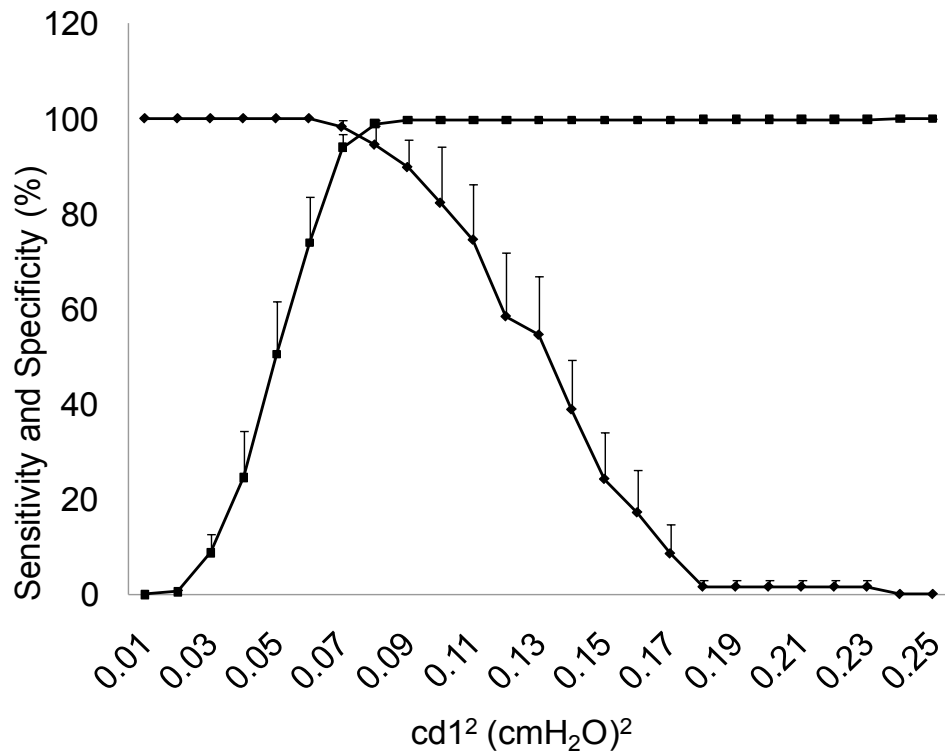


Figure 5.6: % Sensitivity and % specificity for leak artifact rejected using discrete wavelet decomposition of flow signal

Artifacts removal by methods based on statistical distribution

Using the 3SD method, in 9 subjects, coughs could be detected with $53 \pm 21\%$ sensitivity and $98 \pm 1.6\%$ specificity while vocalizations could be identified with $40 \pm 11\%$ sensitivity and $99 \pm 1.4\%$ specificity. In 3 subjects, swallowing could be identified with $50 \pm 4\%$ sensitivity and 100% specificity. Using 5SD method, all artifacts could be identified with $< 50\%$ sensitivity and 95% specificity. Flow leak artifacts could not be identified using either method.

Identifying artifacts introduced under spontaneous conditions

In the recordings that contained spontaneous artifacts, we identified 161 artifacts in the 38 subjects by the wavelet method with thresholds in the mid-range of those provided in the results above. In the 16 subjects with asthma, there were 71 artifacts while in the 22 controls there were 90 artifacts. On careful inspection of those artifacts, most could be discerned to be either coughing, swallowing or glottal closure. Seven out of 161 artifacts were patient-reported swallows, 6 of these could be rejected with $cd2^2$ chosen to be in the middle of the useful range determined from the induced artifact analysis of $cd^2=0.024 \text{ cmH}_2\text{O}^2$ while one could not be identified with any detail coefficient threshold. Six other artifacts were likely leaks or noise leading to very small R_{rs} values which were not detected by the wavelet technique. In remaining 148 detected artifacts in which we could not differentiate between coughs, swallows, or vocalizations, 6 were rejected with pressure $cd1^2=0.004 \text{ cmH}_2\text{O}^2$ and 27 were rejected with pressure $cd2^2=0.024 \text{ cmH}_2\text{O}^2$. If the thresholds were reduced to increase sensitivity, 21 could be rejected with pressure $cd1^2$ thresholds= $0.001 \text{ cmH}_2\text{O}^2$, and 54 could be rejected with pressure $cd2^2$ thresholds= $0.012 \text{ cmH}_2\text{O}^2$ however with reduced specificity. A further four artifacts were identified with $cd2^2$ thresholds= $0.028 \text{ cmH}_2\text{O}^2$, seven artifacts were identified with pressure $cd3$ thresholds ranging from 0.31 to $0.43 \text{ cmH}_2\text{O}^2$, one with flow $cd2$ threshold= $0.004 (\text{L}\cdot\text{s}^{-1})^2$ and one with flow $cd3$ detail thresholds= $0.05 (\text{L}\cdot\text{s}^{-1})^2$ leaving 60 putative artifacts identified by hand that were not detected with the wavelet technique. There were also total 292 negative R_{rs} values which were easily identified as artifactual, but were not detected using the wavelet based approach.

5.5 Discussion

This study presented a novel technique of identifying artifacts in forced oscillation measurements. A fairly simple algorithm that takes advantage of the time-frequency compartmentalization properties of multilevel DWT was developed which could identify with high sensitivity and specificity the most common artifacts in FOT such as coughs, swallows, vocalizations, and airflow leaks at the mouthpiece.

Spirometry, the most common method of lung-function assessment, is a learned maneuver requiring repeated and significant patient effort for reliable and reproducible results, and is thus not feasible in very young children or non-cooperative or paralyzed adult subjects. FOT requires very little cooperation since forced oscillations are superimposed on normal tidal breathing. Thus, it is well suited in patients who are unable to perform spirometry. As a tool for research the FOT technique has found wide application, and is currently gaining clinical use aided by recent publication of guidelines for its use in clinical practice [89]. However, it has been reported that FOT measurements are less repeatable than spirometry measurements. Studies in children and adults have reported more than 9% intra subject coefficient of variation (COV) of R_{rs} while values for spirometry may be lower at less than 5% COV in FEV_1 and FVC [244, 246, 312]. The variability in FOT measurements may be due to underlying physiological variability in R_{rs} that has been reported over durations from minutes to hours to days. However, it is also possible that some of the variability may be due to lower quality assurance [89] or little attention paid to detecting and removing artifacts from undetected glottal narrowing or closures, or from contamination from undetected or ignored coughing, swallowing and mouthpiece leaks.

Although FOT measurements are performed during quiet breathing, events described above are not uncommon, especially in children [313]. These events cause irregular changes in pressure and flow signals causing artifactual values in impedance. While the frequency of artifact occurrence may be low with less than one artifact per 15 second recording, artifacts may occur more frequently in subjects with lung dysfunction. In the latter case, the impact of artifacts may be sufficient to lead to errors in estimating impedance. While the average R_{rs} is only slightly affected by artifacts, unless there are

numerous artifacts, the variation or standard deviation can be more strongly affected, potentially biasing results and peak or minimum values can be erroneous. This is important in studies that examine the variation or spread in reported impedance values [37, 314]. For example in the current study in one subject, removing the four artifacts only changed his calculated mean resistance from $0.95 \text{ cmH}_2\text{O}\cdot\text{s}\cdot\text{L}^{-1}$ to $0.93 \text{ cmH}_2\text{O}\cdot\text{s}\cdot\text{L}^{-1}$ while the coefficient of variation changed from 0.6 to 0.25. Similarly if Z_{rs} is being examined with short time resolution, such as when tracking inspiratory versus expiratory impedance, finer temporal resolution will lead to greater influence of noise and greater frequency of artifacts. Similarly, coefficients of variation can be affected, and as a data quality indicator may lead to rejected data and repeated testing. Recently, it was shown that repeatability of FOT measurements could be improved by optimizing artifact filtering, described further below [314].

The methods to date that are used to reject artifacts are restricted to only a few strategies. When practical, a contaminated measurement is repeated, or if 2 measures are acceptable out of 3 recordings for example, the contaminated recording can either be repeated or discarded as recommended by European Respiratory Society guidelines [89]. Another widely used approach is to remove individual breaths that have been contaminated using evidence such as the obvious occurrence of a cough, or visual inspection of the recording for extreme events either in the flow tracings or in the computed impedance values themselves [306, 313, 315]. This relies on accurate monitoring of these events and data post-processing which is subject to human error. Flow occlusions such as swallows, glottal closure, or tongue occlusion can sometimes be identified as significant decreases in the breathing flow signal and removed manually. Glottal closures occur most often at end expiration or possibly at end inspiration such as during breath holds, and can be detected by examining plots of R_{rs} or Z_{rs} versus breathing flow, and irregular high values outside of the envelope of the majority of the data at or near zero flow can be identified and removed [39, 306, 314]. In the case of mouth-piece leaks, one reported method of detection relies on distinct increases in flow or inverse of impedance, admittance [314].

However, there has been little specific investigation to improve artifact detection and develop tools for their automated detection and removal. Further, it can be

challenging to discriminate between a true artifact and real data that correspond to actual physiological variation [314]. While most common artifacts from coughing or swallowing may be obvious in the pressure or flow signal, some artifacts like light coughs, involuntary glottis narrowing or voluntary or involuntary near vocalizations may not be easily recognizable and thus may go undetected. We purposely asked study participants to make voluntary but small artifacts, at predetermined times. The artifacts were not obvious by inspection of the raw data, but were obvious and easily detected by the wavelet techniques that we have described here, supporting their use in automated signal processing.

Coherence is a commonly reported measure that indicates signal quality, and thus could potentially be used as an automated method to detect artifacts. Poor coherence is indicative of interference from other signals such as breathing or cardiogenic oscillations [279] and noise contamination including artifacts [123, 124, 136, 316, 317]. It is recommended that coherence should be equal to or greater than 0.95 [89], which is associated with impedance with less than 10% coefficient of variation [123]. However, we found that coherence performed poorly; indeed coherence only dropped below 0.95 less than 10% of the time despite the presence of artifacts, which explained the poor sensitivity. Since the artifacts were transient, there was little effect on coherence; thus, coherence is only useful for detecting problems such as continuous transducer noise and is not a suitable tool for detection of artifacts.

Using SNR to detect artifacts also performed poorly. In general, a high SNR exceeding 100 (40 dB) is desirable; however, even when we lowered the threshold to detect SNR below 10 (20 dB), this resulted in less than 20% sensitivity.

Another current broadly applied technique to remove artifacts is based on outliers and the statistical distribution of impedance. In this technique data points exceeding some multiple of the standard deviation from the mean or median value are excluded, e.g. removing impedance values 3 or 5 standard deviations above mean or median of R_{rs} and X_{rs} [39, 314]. Unlike the wavelet approach which assesses pressure or flow signals, using outliers has the disadvantage that it relies on judging the outcome variable directly for the presence of artifactual values which can lead to bias. Additionally, using statistics for this kind of filtering is susceptible to poorer repeatability for short-duration measurements

because estimates of the standard deviation are more susceptible to small sample number than estimates of the mean [314]. Regardless, this method failed to detect many artifacts and had poor sensitivity of less than 55%.

Marchal et al. suggested an artifact-filtering method called the flow shape index filter in which they computed an index expressing the departure of the oscillatory flow from the ideal sinusoid computed per oscillation cycle [313]. However, since this approach is based on the deviation of the flow signal from an ideal sine wave, an artifact may remain undetected if the flow signal is not distorted significantly. This also may reject signals contaminated by non-artifactual noise that occurred in frequency bands other than the oscillation frequency, possibly leading to greater false positive rejection. Nevertheless this technique of artifact detection is also independent of R_{rs} . However, for a 10% threshold, Marchal et al. reported 70% sensitivity and 85% specificity which are less than we report for the wavelet-based approach.

The wavelet transform is a valuable tool in signal analysis due to its ability to elucidate both temporal and spectral information within the signal simultaneously. The transient nature of most artifacts makes wavelets particularly suited for their detection in FOT recordings. The choice of wavelet basis function for a particular application is usually made based on the desired properties of a wavelet and also on the nature of the signal under analysis, but may also be a matter of trial and error. For smoothly varying signals, wavelets that are curved tend to be more appropriate, while for signals with transient steps or impulses, more cornered wavelet basis functions are sometimes recommended. In general, when choosing amongst the many wavelet basis functions, tests are performed with a number of wavelet functions and the one giving satisfactory or optimum performance is selected. In this study, we used a number of Daubechies wavelets mainly because of their resemblance to the contaminated pressure and the flow signals, and found that they were each able to detect artifacts with high sensitivity and specificity over a similar range of thresholds. We settled on db5 which has 5 points in duration and thus is very efficient compared with larger wavelet lengths.

Because the first level wavelet coefficient $cd1$ captures high-frequency information, we reasoned that a high-pass filter could perform equivalently, and under some cases, could work better if tailored to better match the frequency range of

anticipated artifacts. We found that while the high-pass filter performed well, with sensitivity and specificity comparable to wavelet-based technique, we had slightly higher sensitivity using the wavelet-based technique, perhaps due to the ability of the wavelet basis function to better match the time-domain artifact pattern. Additionally, use of the wavelet-based function simplified the approach to determine which detail coefficient to use.

Swallowing and glottal closures are more likely to occur during long-duration impedance measurements [313]. The fact that male vocalizations, which narrowed the glottis, were best detected in second-level wavelet decomposition of the pressure signal while female vocalizations could be better identified using second and third decomposition may be due in part to differences in the auditory component which, although we attempted to minimize this, would nevertheless appear in the pressure signal. Although we anti-aliased the data to remove sounds above 100 Hz, there would still have been differences in the frequency ranges for remaining sounds affecting these detail coefficients. To examine if this was a factor, male subjects were asked to repeat the ‘hee’ artifacts and decreasing the audible sounds to below a whisper and inaudible, if possible. The narrowing of the glottis was confirmed using laryngoscopy in one subject, and interestingly narrowing of the glottis caused by inaudible ‘hee’ sounds could also be detected with good specificity and sensitivity. This indicates that detection of these artifacts may not be based on the audible component, and thus may be due to pressure oscillations that nevertheless occur with glottal narrowing, but in this case the reason for the difference in best coefficients for female and male glottal results is unclear.

Neither vocalizations nor swallowing substantially altered the coherence between the pressure and the flow signals or the SNR of the flow signals indicating these techniques rely on much more substantial noise and cannot be used to detect transient mild cough or swallow artifacts.

Interestingly in our study with spontaneous artifacts, we found more artifacts detected by the wavelet technique in controls compared to asthma. We did not assess for statistical significance; these results may be a training effect in that the subjects with asthma were more familiar with respiratory measurements than control subjects. In general, artifact detection corresponds to extreme values of impedance and/or disruptions

in the pressure and flow trace, but not always. We were also limited by not knowing fully in the data with spontaneous artifacts which detected events were true artifacts, and which may be false positives - unlike in the case with induced artifacts. However, in the controlled study specificity exceeded 90% thus we expect a similar performance in the spontaneous artifact data.

In choosing the threshold values for artifact detection we believe that it is better to have a few more false positives than false negatives, unless maximum magnitude values of R_{rs} or X_{rs} are being reported. Thus, we generally recommend choosing the low end of our useful range for the squared wavelet coefficients thresholds. However, recently investigators have examined time series of respiratory recordings such as peak flows or impedances and found evidence of long-range correlations in the fluctuations using methods including detrended fluctuation analysis [98], and Wasserstein distances and in some cases enabling discrimination between asthma and chronic obstructive disease [251]. For these types of analysis applied to impedance data, preservation of the intact time-series is important, and thus we recommend using higher thresholds in the ranges following to best preserve as many data values as possible at the possible expense of some artifact corruption. Alternatively approaches may be developed which attempt to correct data corrupted by artifacts, such as using time-frequency identification of artifacts and replacement by interpolation rather than data removal to preserve the time-series as best as possible.

In any case, for general application of the method, the following ranges for thresholds are recommended: for coughs, $cd1^2=0.004-0.006 \text{ cmH}_2\text{O}^2$, for swallows, $cd2^2=0.023-0.025 \text{ cmH}_2\text{O}^2$, for male vocalizations, $cd1^2=0.004-0.005 \text{ cmH}_2\text{O}^2$, and flow leaks, $cd3^2=0.07-0.09 (\text{L}\cdot\text{s}^{-1})^2$. These can be used simultaneously to detect all artifacts.

While we detected artifacts with greater than 90% sensitivity and specificity, we also noted that in some cases where there were negative R_{rs} values occurring, likely due to noise when flow was small, these were not always detected as artifacts. Thus, it is still important to reject negative R_{rs} values as these are artifactual.

We further found that the 3 standard deviation approach was better than the 5 standard deviation approach to identify controlled artifacts in this study. Since we also found that iterations improved the performance of the SD methods, if employed, we

recommend the use of the 3 standard deviation approach with 3 iterations. However, it may have low sensitivity as we report, particularly when the standard deviation is high such as occurs in asthma and children [37, 39, 306]. In this case the threshold for rejection will be abnormally high with lower sensitivity.

Another point to be noted is that while we assessed the performance of our technique for a multi-frequency FOT excitation containing only 3 frequencies (4, 10 and 22Hz), we believe that our choice of thresholds of wavelet coefficients will still be valid for FOT excitation signals in the range 0.1-8Hz which are used to assess airway and tissue properties since these coefficients detect noise above this range of frequencies. Similarly our approach should also work for many other commonly used broad-band FOT waveforms (4-32Hz) except possibly where cd2 is used for swallows which used the frequency range 30-60 Hz and cd3 for leaks which used the frequency range 15-30Hz. The method could be easily modified for swallows by limiting the FOT frequency range to below 30 Hz, or prefiltering the signal for swallow detection to above 32 Hz. In the case of short term leaks such as we tested here, broad-band waveforms that include frequencies > 15 Hz would be susceptible to contamination by these artifacts, however if waveforms that used discrete frequencies in that range were employed other wavelet functions that combined ranges in between oscillation frequencies could be used. We do not recommend the wavelet based approach for broadband FOT excitation signals including higher frequencies, such as 4-64 Hz, but the method could work for discrete frequencies if the excitation frequencies were removed by digital frequency domain filtering prior to application of the wavelet approach although this has not been tested.

Limitations

Our study has some limitations. Firstly, we have found a range of wavelet coefficient thresholds that provide high sensitivity and specificity in adult subjects. However, we did not test our technique in children nor in other respiratory diseases. While the range of R_{rs} in our study subjects was from 1 to 3.5 cmH₂O.s.L⁻¹, R_{rs} found in children or severely obstructed patients is larger. It is possible that the thresholds may need to be increased to avoid decreasing specificity. This may occur if the increased pressure signal with higher impedance increased the noise in the frequency range

employed by the wavelet analyses. While we are uncertain that this would occur to any substantial degree, if it did, maintaining the forced oscillation device to operate within a limited pressure range such as within the guidelines of a maximum pressure of 5 cmH₂O [89] might mitigate this possibility. While we are uncertain if subjects with higher R_{rs} would have sufficiently higher noise in the pressure or flow signals in the higher frequency range requiring higher thresholds, this could be examined in a larger study including subjects with a wide range of resistances. If noise were markedly increased in the higher frequency range, or an increase in false positives were found using the recommended ranges given above this would necessitate developing thresholds that adjusted based on patients' mean resistance.

Secondly for the wavelet approach to work, the artifact must be transient. This is satisfactory for coughs, swallows, and even usually vocalizations and transient leaks. However, a constant leak such as may occur with a poor mouthpiece match would not be detected by our technique, and would have to be noted by operator observation or lower than possible impedance. Furthermore, artifacts induced by patient movements during walking and exercise and by changes in upper airway geometry due to changes in head orientation may also be important which we did not explore in this study. The wavelet functions used here may not apply to these low-frequency artifacts, and further investigation is required. Another limitation of this study is that we did not consider the effect of cardiogenic pressure and flow artifacts which occur in the range 1-4Hz [189], but these are small and tend to be reduced in subjects with higher airway resistance [318]

5.6 Conclusions

In conclusion, this study introduced a new technique for eliminating artifacts in forced oscillation measurement that has high sensitivity and specificity using a wide range of thresholds. The technique is automated and is recommended for improved quality assurance of assessment of respiratory impedance.

Chapter 6: Variability of Impedance in Response to Methacholine

6.1 Introduction

As described in the introduction (Chapter 2), excessive variation in lung function is a characteristic feature of asthma. This is observed as an increase in diurnal variation of peak expiratory flow rate (PEF) and FEV₁ when measured over days to weeks [35, 36, 255]. Indeed, the increased variation in PEF is correlated to airway hyperresponsiveness (AHR) [96] and importantly to the risk of asthma exacerbations [35]. Furthermore, on the time scale of minutes, impedance of the respiratory system (Z_{rs}) is found to be more variable in asthma than in health [37-39, 248], suggesting that increased variation may be associated with increased activation of the airway smooth muscle (ASM). Indeed, Que et al. showed that activation of the ASM with inhaled methacholine increased Z_{rs} in healthy subjects [38]. Furthermore they showed that moving the healthy subjects to a supine position was sufficient to increase their variation of Z_{rs} to the level of that found in a group of asthmatic subjects [38]. In a subsequent study, Lall et al. showed that variation of respiratory system resistance R_{rs} ($R_{rs}SD$) was higher in children with asthma than in healthy children, and relaxing the ASM by bronchodilator (BD) reduced $R_{rs}SD$ in asthma more than in healthy children [39]. However, while the effect of methacholine on $R_{rs}SD$ has been investigated, this effect has not yet been examined in asthma.

In asthma, clinical diagnosis, and assessment of control and severity is largely based on patient-reported respiratory symptoms, especially in children. However the patient-reported symptoms are highly subjective, and currently there is no objective measure of lung function which relates to symptoms. Indeed, the association between symptoms and spirometric measures is poor [40, 319]. Previously, the Lall et al. study reported that in asthmatic children, $R_{rs}SD$ and decreases in $R_{rs}SD$ with BD differed among children when they were grouped based on their daily asthma therapy [39]. They found that in children with mild asthma, $R_{rs}SD$ was higher and decreased more following BD than in children with moderate asthma. Furthermore in the Que et al. study [38], the

subjects with asthma were subjects that had been admitted based on asthma symptoms, and measured. It is possible that these subjects had poorer asthma control, but unfortunately these data was not collected at that time. It is possible that while $R_{rs}SD$ has been reported to be highly correlated with R_{rs} in asthma, if increased variability is also associated with lack of asthma control, then $R_{rs}SD$ may be increased beyond the level predicted by its correlation with R_{rs} . That is, if a patient experiences breathing symptoms, this may correspond to over-activity of the ASM, increased variability in airway diameters and higher $R_{rs}SD$. Moreover, the severity of AHR is strongly associated with the presence of asthma symptoms with lower PC20 values being found in patients experiencing breathing symptoms [320], and AHR to methacholine is associated with poor quality of life [321, 322]. Thus while AHR is related to poor asthma control, the relation between $R_{rs}SD$ and asthma control has not been yet studied.

In this study, we evaluated if $R_{rs}SD$ relates to AHR investigating the hypothesis that $R_{rs}SD$ increases in asthma correlating to AHR. Asthma is known to be a disease characterized by marked heterogeneity in the airway tree. While it is not established if spatial heterogeneity in the airway tree varies temporally, it is possible that changes in R_{rs} during breathing and changes in local airway narrowing and dilation brought about by parenchymal tethering lead to an airway impedance signal that varies temporally, and is reflective of the state of activation of the ASM. We also probed the relationship between $R_{rs}SD$ and patients' level of asthma control assessed by their asthma symptom score. We hypothesized that in asthma $R_{rs}SD$ correlates with respiratory symptoms, and increased $R_{rs}SD$ reflects a lack of disease control.

6.2 Methods

6.2.1 Subjects

Nineteen healthy subjects (9 females) and 19 subjects with asthma (13 females) between 16-70 years of age were enrolled from Halifax Infirmary and the local community. The subjects signed a written informed consent, and the experimental

protocol was approved by the Capital Health Research Ethics Board, Halifax, Nova Scotia.

Inclusion criteria for asthma included diagnosis of asthma by a physician at least 12 months before the study measurements (based on symptoms and/ or airflow reversibility), no changes or worsening of breathing symptoms in the past 6 weeks and no changes in asthma medications in past 4 weeks, no recent respiratory tract infection (within 6 weeks) before study measurements, and less than 10 pack-years smoking history. Healthy controls had no history of asthma or any other chronic respiratory conditions, no recent respiratory tract infection (within 6 weeks) and less than 10 pack-years of smoking history. Current smokers or ex-smokers with a smoking history of 10 pack years or more, subjects with a recent heart attack or stroke, and expectant females were excluded from the study. The asthmatic subjects' medication details are provided in Table 6.1

Table 6.1: Medication details of asthmatic subjects

Medications	No. of subjects
Short-acting beta-2 agonist (SABA)	4
SABA and inhaled corticosteroid (ICS)	2
SABA, ICS, and Leukotriene Receptor Antagonist (LTRA)	1
SABA and a combination of long-acting beta-2 agonist (LABA) and ICS	2
SABA, LTRA, and a combination of LABA and ICS	1
Combination of LABA and ICS	3
LTRA and a combination of LABA and ICS	1
No medication	5

6.2.2 Measurements

Impedance of the respiratory system (Z_{rs}) was measured using the FOT device [39] described in Section 3.2.2. Briefly, small-amplitude pressure oscillations (approximately ± 1 cmH₂O) generated by a loud speaker were applied at the subject's mouth while the subject breathed normally through a disposable bacterial / viral filter (MicroGard, Viasys Sensormedics, USA). The loud speaker was driven by a multi-frequency sinusoidal signal containing 3 frequencies of either 5, 15 and 20 Hz or 4, 10 and 22 Hz. The 5-15-20 Hz signal was being tested for the potential to allow for more rapid tracking of changes in R_{rs} since the fundamental period was 0.2 sec, while the 4-10-22 Hz signal was used to minimize any possible effects of nonlinearities due to harmonics, as these frequencies are non-integer multiples and harmonic interference is avoided. The signal frequencies were grouped for analysis as: low, L: 4 and 5 Hz; mid, M: 10 and 15 Hz; and high, H: 20 and 22 Hz.

Subjects sat upright with head in a neutral position, wore a nose clip and, supported their cheeks and soft tissue below the chin firmly with both palms to minimize errors due to upper airway shunt [89]. A fan provided a bias flow of approximately 12 L/min of fresh air to avoid buildup of exhaled air in the dead space, and a long, high inertance, stiff walled bias tube (1.9cm diameter \times 176.5cm length) shunted the subject's breathing to the atmosphere. The resulting pressure and flow changes were recorded by a pressure transducer (TD-05-AS, SCIREQ) and a Fleisch type pneumotach (Fleisch No. 2, Lausanne, Switzerland) connected to a differential pressure transducer (TD-05-AS, SCIREQ). The pressure and flow transducers were calibrated, and the device impedance was compensated for over the entire frequency range as described in Section 3.2.2. The device calibration was verified using a standard test load of 5 cmH₂O.s.L⁻¹ (Hans Rudolph, Inc., KS, USA).

Lung function was assessed by spirometry in accordance with published guidelines [323]. Dynamic air flows and lung volumes were assessed by a constant-volume type body plethysmograph (VE20-VE62J, Sensormedics, USA). Results were accepted according to the American Thoracic Society (ATS) criteria for adults, and were

expressed as a percentage of predicted values according to reference values [289, 290, 324]. The body plethysmograph was calibrated before each patient assessment.

6.2.3 Protocol

Prior to the study measurements, patients abstained from using SABA for 8-12 hours, LTRA for 2 days, LABA and ICS combinations for 3 days and antihistamines for 1-6 weeks. The subjects' height and weight were recorded, and their level of asthma control was assessed as described below. AHR was assessed by standard methacholine challenge [78] during which FOT was also assessed.

Methacholine doses doubling in concentration (from 0.03 mg/ml to 16 mg/ml for asthma and from 1 mg/ml to 16 mg/ml for controls) and diluted with isotonic sodium chloride (saline) were prepared as per ATS guidelines [78]. The methacholine-saline aerosols were generated using a Wright type Nebulizer (Roxon, Montreal, Canada, output, 8.5 ml/min) and administered using the standard 2-min tidal breathing protocol [325, 326]. Increasing concentrations of methacholine were administered and one minute FOT and FEV₁ were measured in the same order following each concentration. The test was terminated when FEV₁ decreased by 20% or more from its baseline or when the highest concentration of methacholine (16 mg/ml) had been administered. The test results were expressed in terms of the concentration of methacholine at 20% decrease in FEV₁ (PC20). AHR was defined according to the ATS guidelines [78]; subjects were hyperresponsive for PC20 ≤ 8 mg/ml and non-responsive for PC20 > 8 mg/ml. Following the final FEV₁ measurement, Salbutamol (200 mcg) was administered to reverse bronchoconstriction, and FEV₁ was measured.

We also measured the level of dyspnea in all subjects at baseline and following the last dose of methacholine using the modified Borg scale [327] and a 7-item pictorial scale. Additionally in subjects with asthma, we assessed their level of asthma control using the 6-item asthma control questionnaire (ACQ-6) [65, 66]. The 6-item questionnaire includes 5 questions on asthma symptoms, and one question on use of a rescue inhaler (SABA). Subjects' responses are based on their recall of symptoms they experienced in the past week, and are evaluated on a 7 point scale (see Appendix A). All

six questions are equally weighted, and the ACQ score is the average of the responses ranging from 0 to 6 (higher is worse). Based on the ACQ scores, the asthmatics were pooled into two groups: controlled (ACQ score ≤ 1.0 , n=9) and uncontrolled (ACQ score > 1.0 , n=9). One patient did not answer the ACQ, and was excluded from asthma control related comparisons.

6.2.4 Data analyses

This section is provided here for the thesis and is the protocol common to Chapters 3, 5, 6 and 7.

The respiratory pressure and flow signals were recorded and filtered as described in Section 3.2.4. They were compensated for the impedance of the intervening tubing and the bacterial / viral filter to obtain the resistance (R_{rs}) and reactance (X_{rs}) of the respiratory system. Elastance of the respiratory system (E_{rs}) was estimated by least squares fitting X_{rs} to the single-compartment model given by the equation, $X_{rs} = \omega I_{rs} - \omega/E_{rs}$ where I_{rs} was the inertance, $\omega = 2\pi f$ was angular frequency, and f , the oscillation frequencies.

As described in Section 5.2.4, we assessed the quality of Z_{rs} estimates from the coherence between the pressure and the flow signals evaluated at each oscillation frequency. The coherence function was defined over a 16 s window shifted along the signals one second at a time. If coherence was less than 0.95, then this indicated that an artifact contaminated the particular 16 s data block. The block was appended by 1 s, and coherence was recalculated with each individual second removed in an attempt to recover $\gamma^2 > 0.95$ for the block. If this failed, two seconds would be removed in a like manner.

Signal to noise ratio (SNR) was calculated as described in Section 5.2.4. Briefly, noise contaminating oscillation frequencies was estimated by root mean square averaging neighboring frequency bands for each frequency. For the oscillating signal containing frequencies 4, 10 and 22 Hz, the neighboring frequencies used for noise estimates were 3 Hz and 5-7 Hz for 4 Hz, 7-9 Hz and 11-13 Hz for 10 Hz, and 21-26 Hz and 23-26 Hz for 22 Hz. For the signal containing 5, 15 and 20 Hz, the frequencies used for noise estimates were 4 Hz and 6-10 Hz for 5 Hz, 12-14 Hz and 16-18 Hz for 15 Hz, and 17-19 Hz and

21-23 Hz for 20 Hz. At each signal frequency, the noise was estimated for all 1 s data blocks, and SNR was defined as the ratio of magnitude of the input signal frequency and the respective noise estimate. Impedance values resulting from coughs, swallows, and brief glottal closures were eliminated based on SNR at each signal frequency. An impedance estimate for a data block was rejected when SNR was less than 20 dB for that data block.

Artifactual impedance values were also eliminated using standard deviation of the impedance values. Briefly, R_{rs} and X_{rs} data corresponding to negative R_{rs} value were first eliminated. Then R_{rs} and X_{rs} values lying 3 standard deviations on either side of means of R_{rs} and X_{rs} were eliminated in 3 iterations.

Changes in FEV_1 , R_{rs} and $R_{rs}SD$ with increasing methacholine concentrations were presented using the dose-response curves. The slope of a dose-response curve was calculated as a percent decrease in FEV_1 per unit concentration of methacholine (mg/ml) [328, 329].

We estimated PC10 for FEV_1 (concentration of methacholine causing a 10% decrease in FEV_1) from a straight line fit between the baseline FEV_1 value and the FEV_1 value corresponding to a 10% or next to 10% decrease on the FEV_1 dose-response curve. Then we estimated $R_{rs}SD$ at PC10 FEV_1 from a linear model fit to the $R_{rs}SD$ versus logarithm of methacholine concentration data, and evaluated changes in $R_{rs}SD$ at PC10 FEV_1 from the baseline FEV_1 . The quality of $R_{rs}SD$ versus methacholine linear fits was determined from r^2 values. An arbitrary cut off of 0.5 was chosen for the r^2 value, and the linear fits with r^2 less than 0.5 were rejected.

6.2.5 Statistical Analyses

Results are presented as mean \pm standard error of mean (SE) unless otherwise specified. Normality and equal variance of the data were determined using Shapiro-Wilk and Levene's test respectively. For normally distributed data, comparisons between two groups were performed using two tailed unpaired Student t-tests while comparisons within two groups were performed using one tailed paired Student t-tests. For non-normally distributed data, comparisons between two groups were performed using Mann

Whitney rank sum test and within-group comparisons were performed using Wilcoxon signed rank test. Relationships between different variables were analyzed using linear regression. For all tests, statistical significance was accepted at $p < 0.05$. All analyses were performed with SigmaPlot 12 version 12.3 (Systat Software, Inc. Chicago, Illinois, USA). The goodness of E_{rs} model fits was evaluated using r^2 statistics. The slopes of regression lines for $R_{rs}D$ versus R_{rs} values were compared using the analysis of covariance (ANCOVA) tool in Matlab.

6.3 Results

Demographics

Subject demographics and lung function are presented in Table 6.2. Healthy subjects and subjects with asthma were matched for age, height, and weight.

Pre and post methacholine lung function and mechanics

There was no difference in $FEV_1\%$ predicted between asthmatics and controls at baseline (Table 6.2). However $FEV_1/FVC\%$ predicted was significantly smaller in asthma than in control. R_{rs} and $R_{rs}SD$ were both higher in asthmatics than in controls at all frequencies (Fig. 6.1).

Following the methacholine challenge, 13 subjects with asthma were hyperresponsive with $PC_{20} < 8\text{mg/ml}$ (PC_{20} : 1.46 ± 0.98 SD), 1 subject had PC_{20} between 8 to 16 mg/ml while 5 subjects were non-responsive. All healthy subjects were non-responsive ($PC_{20} > 16$ mg/ml (Table 6.3).

Table 6.1: Subject demographics and lung function

	Groups		p value
	Controls (n=19)	Asthma (n=19)	
Sex, male / female	10 / 9	6 / 13	
Age, years	30 ± 2	36.6 ± 3	0.12
Height, cm	169.1 ± 1.8	164.5 ± 1.8	0.07
Weight, kg	69.7 ± 3.4	78.5 ± 3.7	0.08
BMI, kg/m ²	24.3 ± 1.13	29.07 ± 1.37	0.012*
FEV ₁ , % predicted			
baseline	98.6 ± 3.1	91.6 ± 3.5	0.16
% change	-8.3 ± 1.1 [#]	-21 ± 1.5 [#]	<0.001*
FVC, % predicted			
baseline	97.7 ± 3.6	102.7 ± 2.6	0.27
% change	-1.8 ± 0.6 [#]	0.05 ± 1.5	0.6
FEV ₁ /FVC %			
baseline	101.7 ± 1.4	90.35 ± 3.5	0.01**
% change	0.9 ± 0.77	1 ± 1.1	0.94
R _{rs} , cmH ₂ O.s.L ⁻¹			
L	2.2 ± 0.16	4.2 ± 0.65	0.025**
M	2.3 ± 0.15	3.5 ± 0.46	0.007**
H	2.6 ± 0.2	3.6 ± 0.31	0.015**
R _{rs} SD, cmH ₂ O.s.L ⁻¹			
L	0.46 ± 0.046	0.99 ± 0.018	0.001**
M	0.38 ± 0.041	0.56 ± 0.067	0.018**
H	0.22 ± 0.032	0.38 ± 0.063	0.009**

Data are presented as mean ± SE. n, number of subjects, BMI, body mass index; FEV₁, forced expiratory volume in one second as percent of predicted [289]; FVC, force vital capacity as percent of predicted [290]; R_{rs}, respiratory resistance, R_{rs}SD, variation of R_{rs}. # or ## indicate significant difference between baseline and post methacholine values within individual groups using paired t-test or Wilcoxon signed rank test respectively. p < 0.05 values indicates significant difference between asthmatics and controls using *unpaired t-test or **Mann-Whitney rank sum test, L: 4 & 5 Hz, M: 10 & 15 Hz, H: 20 & 22 Hz.

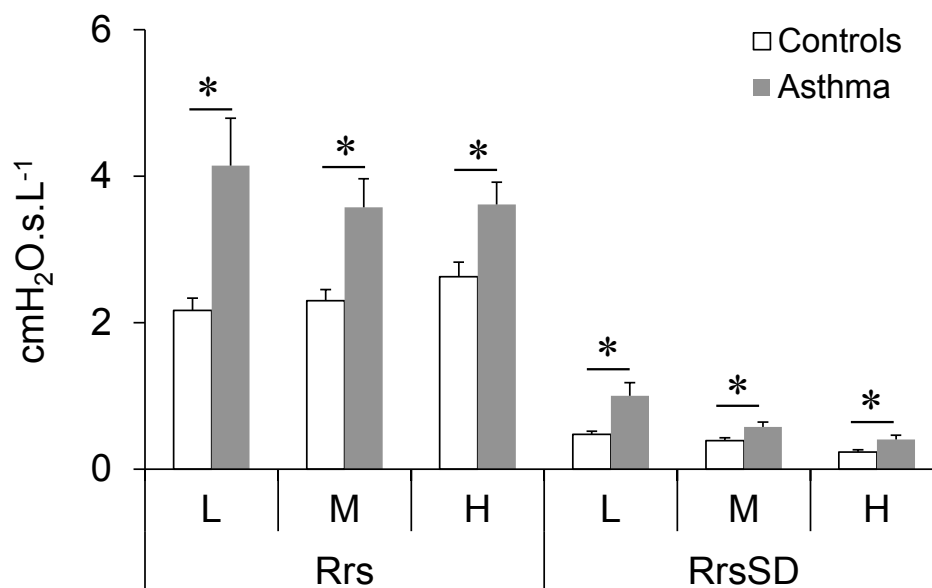


Figure 6.1: Baseline R_{rs} and $R_{rs}SD$ in the control subjects ($n=19$) and subjects with asthma ($n=19$) * denotes significantly different than controls, $p < 0.05$, L: 4 & 5 Hz, M: 10 & 15 Hz, H: 20 & 22 Hz.

Table 6.3: AHR classification of asthmatic subjects based on their PC20

AHR Classification	PC20 dose	No. of subjects
Hyperresponsive	< 1mg/ml	7
	1 to 4 mg/ml	5
	between 4 to 8 mg/ml	1
Non-hyperresponsive	between 8 to 16 mg/ml	1
	>16 mg/ml	5

Fig. 6.2 shows percentage changes in $FEV_1\%$ predicted, R_{rs} and $R_{rs}SD$ evaluated at the final dose of methacholine (PC20 or 16 mg/ml). FEV_1 decreased by $21 \pm 1.5\%$ in asthmatics and by $8.4 \pm 1\%$ in controls, and the decreases in FEV_1 in asthmatics were significantly larger than in controls.

In both control and asthmatic subjects, R_{rs} increased at low and mid frequencies but there were no significant differences in the increases between the two groups. Furthermore increases in R_{rs} at low frequencies were significantly larger than those at high frequencies in both groups (Wilcoxon signed rank test, $p < 0.001$).

Following methacholine, $R_{rs}SD$ did not change in controls, but increased in asthmatics at low and mid frequencies (Wilcoxon signed rank test, $p < 0.001$ and $p=0.001$) respectively), with the increases being significantly higher in asthma than in control subjects (Mann-Whitney rank sum test, $p=0.02$ and 0.03 respectively). However in both groups, changes in $R_{rs}SD$ were not different than those in R_{rs} .

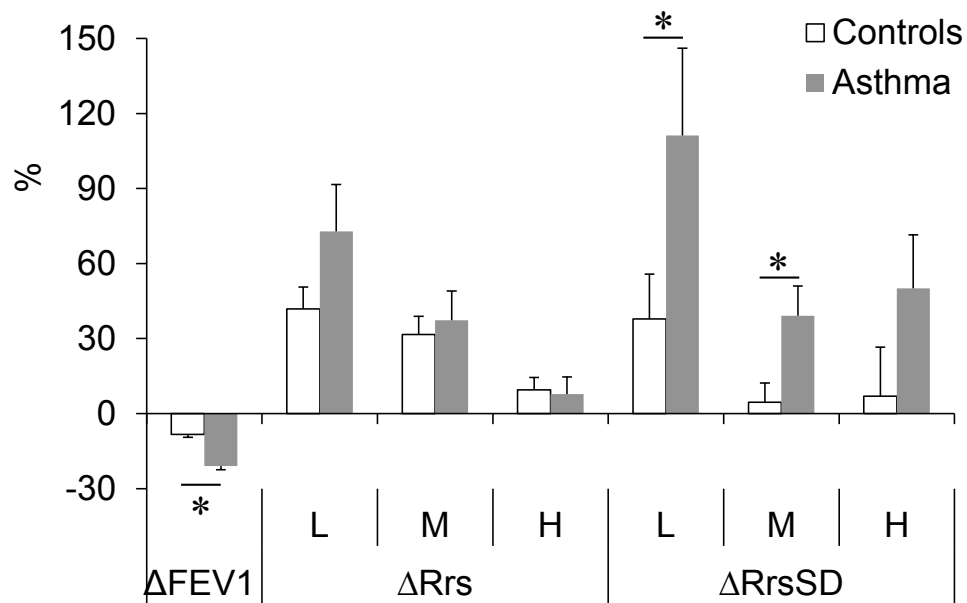


Figure 6.2: Percent changes in FEV_1 , R_{rs} , and $R_{rs}SD$ following the PC20 or the last dose of methacholine.

Fig. 6.3 shows dose-response curves for FEV_1 , R_{rs} and $R_{rs}SD$ with methacholine concentrations on a logarithmic scale (base 2). In asthmatics, R_{rs} response to methacholine was variable. Only a few subjects demonstrated concordant changes in FEV_1 and R_{rs} with increasing doses of methacholine. In some individuals R_{rs} increased at low doses of methacholine, decreased at intermediate doses, and increased again. In a few individuals, R_{rs} decreased following the last concentration of methacholine.

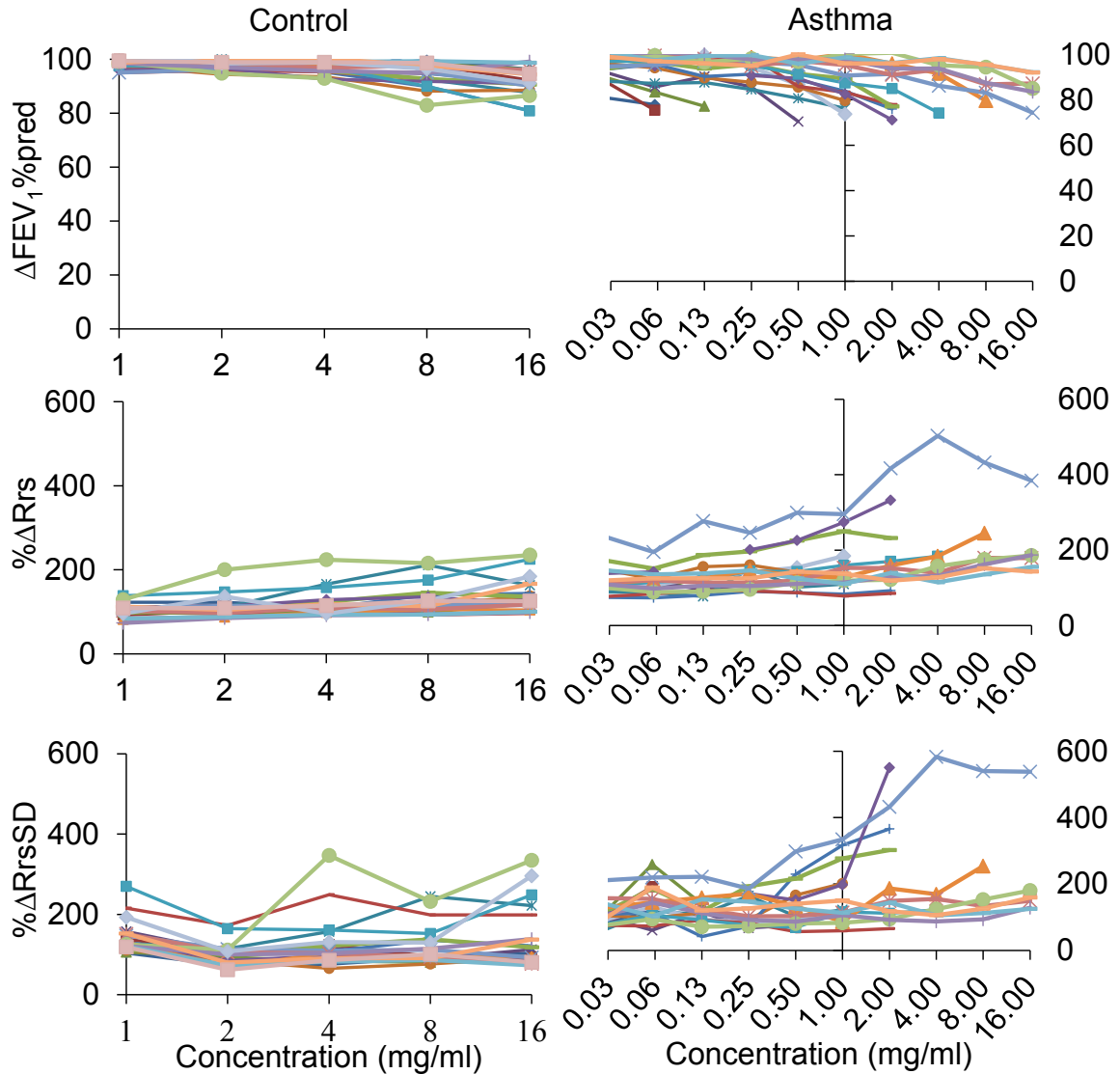


Figure 6.3: Dose-response curves for FEV_1 % predicted, R_{rs} and $R_{rs}SD$ at low frequencies (L). Percent changes in FEV_1 , R_{rs} , and $R_{rs}SD$ versus gradually increasing concentrations of methacholine plotted on a \log_2 scale. Left panel: controls, right panel: asthma subjects

Fig. 6.4 shows X_{rs} and changes in X_{rs} following last dose of methacholine. X_{rs} was lower in asthmatic than in control subjects at baseline (Mann-Whitney rank sum test). Following methacholine, it decreased in both groups at all frequencies (asthma: paired t-test, $p < 0.05$ and controls: Wilcoxon signed rank test, $p < 0.05$) but with significantly larger decreases in asthmatic than in controls at low and mid frequencies

(Mann-Whitney rank sum test). The results for $X_{rs}SD$ were similar to those for X_{rs} . We found that $X_{rs}SD$ was higher in asthmatic than in control subjects at low and mid frequencies (Mann-Whitney rank sum test, $p < 0.05$), and increased following the last dose of methacholine in both groups at low and mid frequencies (Wilcoxon signed rank test, $p < 0.05$) but not differently (Fig. 6.5).

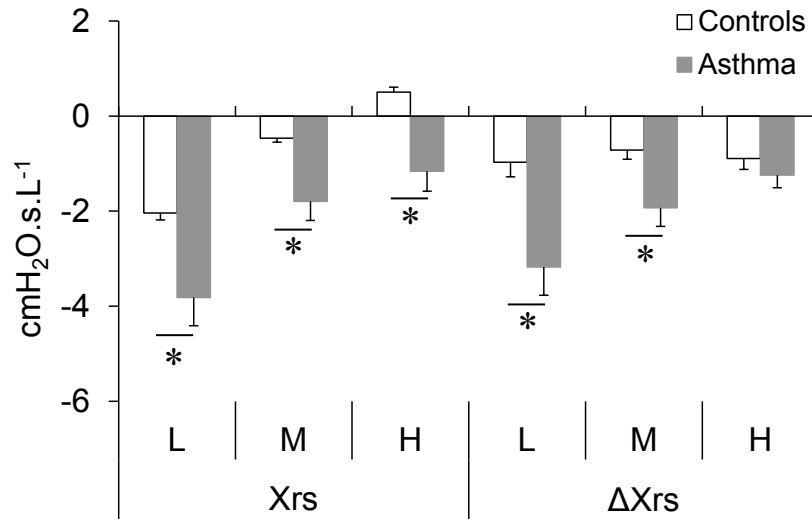


Figure 6.4: Baseline X_{rs} and changes in X_{rs} following methacholine

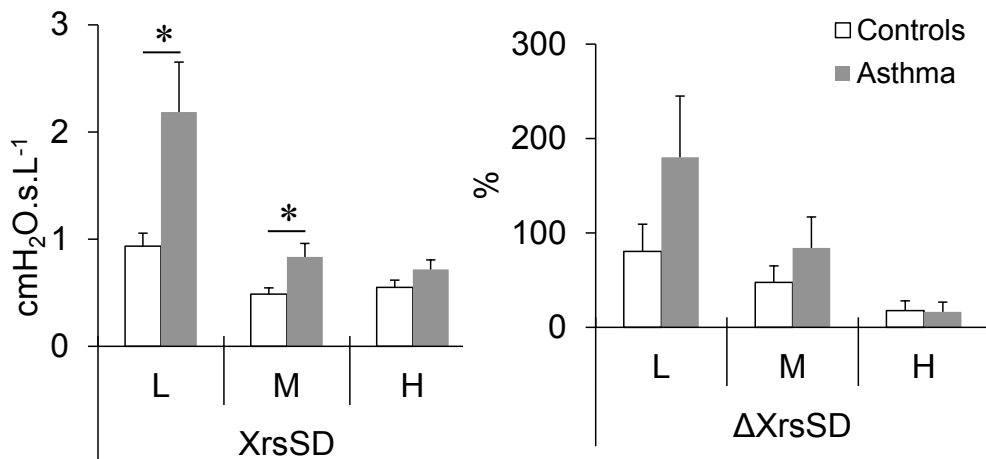


Figure 6.5: Baseline $X_{rs}SD$ and changes in $X_{rs}SD$ following methacholine

As described above, E_{rs} was obtained from X_{rs} by fitting a single-compartment model to X_{rs} values, and the quality of fit was assured by r^2 values. In four asthmatics and in one control subject, r^2 was less than 0.90, thus their data were excluded from E_{rs} related comparisons. Comparing E_{rs} in remaining 15 subjects with asthma and 18 control subjects, we found that there was no difference in baseline E_{rs} values between controls and asthmatics (Mann-Whitney rank sum test, $p=0.09$). Methacholine caused increases in E_{rs} in both groups (asthma: paired t-test, $p < 0.05$, and control, Wilcoxon signed rank test, $p < 0.05$), however the increases in E_{rs} were significantly larger in asthmatics than in control subjects (Mann-Whitney rank sum test, $p=0.014$, Fig. 6.6).

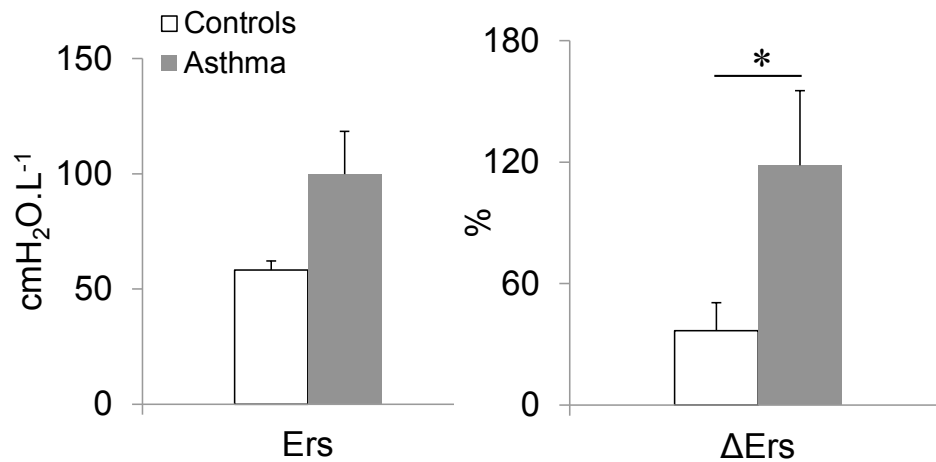


Figure 6.6: Baseline E_{rs} and percent increases in E_{rs} following the last dose of methacholine in the control ($n=18$) and asthmatic subjects ($n=15$)

Correlations between FEV_1 and FOT

We assessed the relationship between FEV_1 and FOT outcomes, and found that in control subjects, there was no correlation between FEV_1 and R_{rs} , X_{rs} and $R_{rs}SD$. However in asthmatic subjects, R_{rs} weakly correlated to FEV_1 (r^2 values, L: 0.47, M: 0.44, H: 0.33, $p < 0.05$), while X_{rs} moderately correlated to FEV_1 at all frequencies (r^2 values, L: 0.55, M: 0.58, H: 0.58, $p < 0.001$). Also, in asthmatics, $R_{rs}SD$, weakly correlated to FEV_1 at low and mid frequencies (r^2 values, L: 0.35, M: 0.28, $p < 0.05$), but did not correlate at high frequencies.

Furthermore, in control subjects, decreases in FEV₁ weakly correlated to increases in R_{rs} at low and mid frequencies (L: r²=0.42, M: r²=0.27, p < 0.05), but did not correlate to increases in R_{rs} at high frequencies (r²=0.01, p > 0.05). In contrast, in asthmatics, decreases in FEV₁ did not correlate with increases in R_{rs} at any frequency (r² values, L: 0.024, M: 0.006, H: 0.012, p > 0.05). Furthermore, there was no association between decreases in FEV₁ and increases in R_{rs}SD and X_{rs}SD in either control or asthmatic subjects.

Relationship between AHR and functional measures

We looked for a correlation between AHR, and spirometry and FOT measures by examining the relationship between the results of the methacholine challenge test; the dose-response slope and PC20 dose of methacholine, and FEV₁, and R_{rs} and R_{rs}SD.

Dose-Response Slope: Examining the relationship between the dose-response slope and functional measures, we found that baseline FEV₁ moderately correlated to the dose-response slope (r²=0.63, p=0.001). Furthermore, we also found that there was a moderate correlation between R_{rs} and the dose-response slope at all frequencies (r² values, L: 0.65, M: 0.66, H: 0.62, p < 0.05) (Figures are not shown here).

While there was a moderate correlation between the dose-response slope and R_{rs}, the relationship between the slope and R_{rs}SD was weak at low frequencies (r²=0.48, p=0.008, Fig. 6.7), and there was no correlation at mid and high frequencies. Also, the changes in R_{rs} and R_{rs}SD following methacholine were not related to the dose-response slope.

PC20 dose of methacholine: When we assessed the relationship between PC20 and functional measures, we found that baseline FEV₁% predicted was moderately correlated to PC20 (r² =0.55, p=0.004). Similar but slightly stronger correlations were found for R_{rs} to PC20 at all frequencies (r² values, L: 0.64, M: 0.68, H: 0.68, p=0.001 for all frequencies) while R_{rs}SD was only moderately correlated to PC20 at low frequencies (r²=0.54, p=0.004), but was not correlated at mid and high frequencies (figures not shown).

here). Furthermore, there was no association between PC20 and changes in R_{rs} , R_{rsSD} and FEV_1 following methacholine.

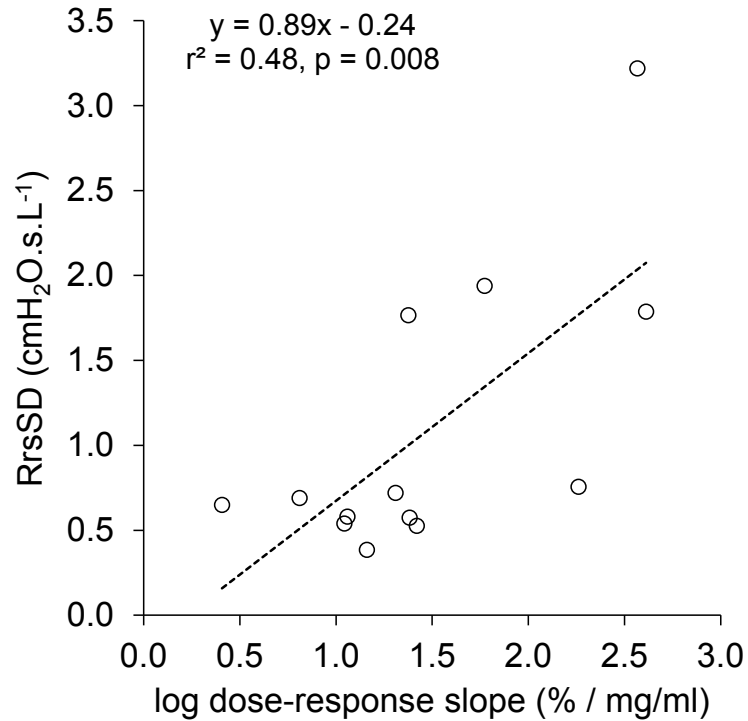


Figure 6.7: Correlation between R_{rsSD} and AHR by dose-response slope in the asthmatic subjects ($n=13$) demonstrating AHR

Correlations between R_{rs} and R_{rsSD}

The correlations between low frequency (4 and 5 Hz) R_{rs} and R_{rsSD} at baseline and following methacholine challenge are shown in Fig 6.8.

Control: We found that in controls, R_{rsSD} was moderately correlated to R_{rs} at baseline (slopes, 0.15, 0.13, 0.13, and $r^2=0.72$, 0.61, 0.37 at low, mid and high frequencies respectively), but was strongly correlated following methacholine at low and mid frequencies (slopes, 0.26, 0.18, and $r^2=0.78$, 0.7 respectively). However there was no correlation of R_{rsSD} to R_{rs} at high frequencies. Also, the slopes of R_{rs} versus R_{rsSD} regression lines were not altered by methacholine.

Asthma: There was a strong correlation between R_{rs} and $R_{rs}SD$ in asthmatic subjects at baseline and following methacholine at low frequencies (baseline: slope, 0.26, $r^2=0.82$, post: slope, 0.34, $r^2=0.73$, Fig. 6.8). At mid frequencies, R_{rs} and $R_{rs}SD$ were weakly correlated at baseline (slope, 0.12, $r^2=0.46$) but strongly correlated following methacholine (slope, 0.22, $r^2=0.7$). Lastly, at high frequencies, there was no correlation between R_{rs} and $R_{rs}SD$ at baseline, but these were weakly correlated post methacholine (slope, 0.2, $r^2=0.39$). Furthermore like in controls, the slopes of regression lines were not altered by methacholine except at mid frequencies where the slope changed only slightly ($p=0.02$).

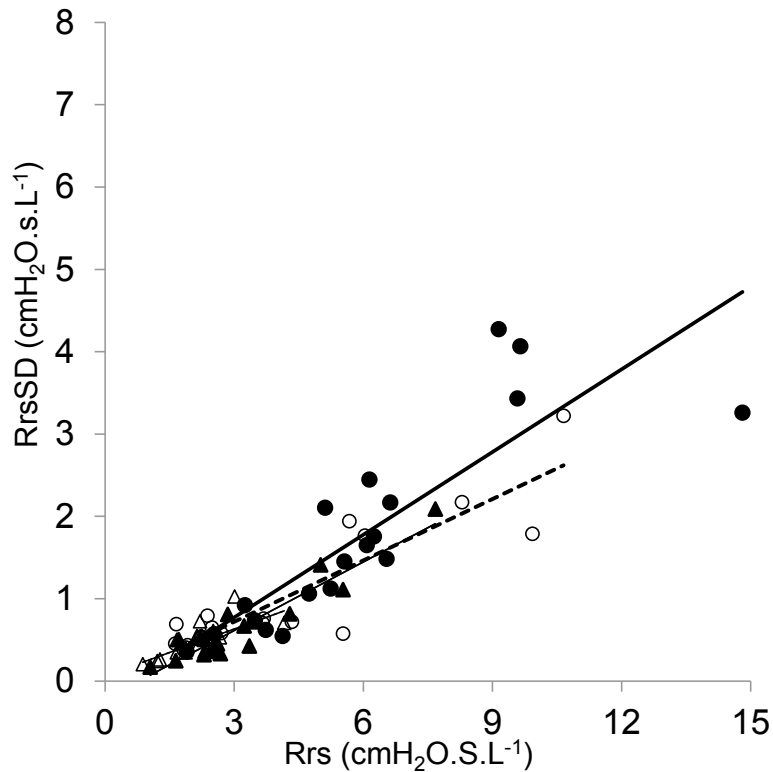


Figure 6.8: Correlations between $R_{rs}SD$ and R_{rs} pre- and post-methacholine challenge in the control and asthmatics subjects at low frequencies. Circles indicate data in the asthmatics, and triangles indicate data in the controls. Open symbols represent baseline data and closed symbols represent post methacholine data. See text for details.

Comparisons between controlled and uncontrolled asthma

We did not find any association between asthma control and our functional measures. Asthma control assessed from asthma symptoms score (ACQ score) and FEV₁, R_{rs}, R_{rs}SD were not related (controlled, n=9 and uncontrolled, n=9).

Comparison of R_{rs}SD at PC10FEV₁ between asthmatics and controls

We could not obtain PC20 in healthy subjects, since it was larger than the highest concentration of methacholine (16 mg/ml) administered in this study. Therefore we attempted to calculate PC10FEV₁, and hoped to compare this to the changes in R_{rs}SD between controls and asthmatics. As explained in Methods, in order to calculate R_{rs}SD at PC10FEV₁, we needed to fit a line to R_{rs}SD versus logarithm of methacholine concentration data with the quality of fits being determined from r² values.

In controls (n=19), PC10 FEV₁ was obtained in only 5 subjects while the remaining 14 subjects had PC10FEV₁ > 16 mg/ml. Furthermore, R_{rs}SD at PC10FEV₁ was obtained in only 2 of 5 controls; in remaining subjects r² values for R_{rs}SD versus methacholine linear fits were smaller than our arbitrarily chosen cut off of 0.5. In asthmatics (n=19), more subjects obtained PC10 FEV₁ (n=17) while 2 subjects had PC10FEV₁ > 16 mg/ml. Among these 17 asthmatics, unfortunately in 10 subjects, R_{rs}SD versus methacholine linear fits r² values were less than 0.5, hence their data could not be used.

The number of subjects with reliable R_{rs}SD response at PC10FEV₁ were too few to compare the behavior between controls and asthmatics, thus we did not perform further comparisons.

Correlation between E_{rs} and spirometric measures in asthma

Comparing E_{rs} to FEV₁ and other spirometry measures in asthmatics, we found that E_{rs} moderately correlated to FEV₁% predicted (r²=0.53, p < 0.001) while the increases in E_{rs} following methacholine were poorly associated with the decreases in FEV₁.

Furthermore, we found that E_{rs} moderately correlated to PC20 ($r^2=0.5$, $p=0.01$), whereas the increases in E_{rs} did not correlate. Also, there was no correlation between E_{rs} and FVC, and between their changes following methacholine.

6.4 Discussion

This study investigated short term temporal variation of R_{rs} ($R_{rs}SD$) during a methacholine challenge to determine if $R_{rs}SD$ relates to AHR, and assessed the relationship between $R_{rs}SD$ and level of asthma control in adult subjects with asthma. We found that 1) $R_{rs}SD$ was higher in asthmatics than in healthy subjects at low oscillation frequencies, and unlike R_{rs} which increased with methacholine in both healthy and asthmatic subjects, $R_{rs}SD$ increased only in asthmatics though not differently than R_{rs} . Furthermore, $R_{rs}SD$ was moderately correlated with AHR assessed by a PC20 dose of methacholine. 2) Mean R_{rs} and $R_{rs}SD$ were strongly linearly related in asthmatics. 3) There was no association between $R_{rs}SD$ and lack of asthma control. 4) E_{rs} derived from X_{rs} increased more in asthmatics than in controls following methacholine, and showed moderate association to AHR. Together our results suggested that $R_{rs}SD$ may be a distinguishing feature of methacholine response of asthma. On the other hand, X_{rs} and related E_{rs} may be useful to assess small airways in asthma. The implications of these results are described below.

Variation of R_{rs}

Consistent with previous studies [37, 39, 306], we found that $R_{rs}SD$ was higher in asthmatic than in healthy subjects at baseline, and was strongly linearly correlated to mean R_{rs} . Previously Diba et al. suggested that the strong linear correlation between R_{rs} and $R_{rs}SD$ weakens the clinical utility of variability of R_{rs} [37] Yet in the present study, we also found that following methacholine, $R_{rs}SD$ increased only asthmatics, but not in controls, whereas R_{rs} increased in both asthmatics and controls. Together these suggests two things: Methacholine response of variability of R_{rs} may help distinguish asthma from health since $R_{rs}SD$ increased only in asthmatics whereas R_{rs} increased in both controls and asthmatics. Alternatively, $R_{rs}SD$ may increase in controls in a larger sample, although

the changes may be still smaller than in asthmatics. Thus, the physiological significance rests on whether the percent change in $R_{rs}SD$ with methacholine in asthma increases more than it does in controls with a larger population. However, the clinical importance may be muted if the difference is not large, even though significant.

In agreement with previous findings [37, 252, 306], we found that $R_{rs}SD$ strongly correlated to R_{rs} across all individuals at baseline and following methacholine which was perhaps indicative of constant CoV. Previously Diba et al. [37] reported a similar correlation between Z_{rs} and its variability in healthy ($n=38$, $r=0.81$) and asthmatic subjects ($n=102$, $r=0.91$). More recently Leary et al. [252] analyzed correlations in studies by Que et al. [38] and Diba et al. [37], and reported that the slopes of regression lines of R_{rs} versus $R_{rs}SD$ relationship in these studies were similar (0.31 and 0.35 respectively) implying a very consistent relationship between R_{rs} and $R_{rs}SD$. In our study, the slope in asthma was slightly smaller (0.26) than found in previous studies, but the slope following methacholine matched those in previous studies [37, 306]. Also despite there being a difference in slopes in asthmatics between baseline and post methacholine, it was only at mid frequencies, and was modest. Nevertheless there was a strong similarity in slopes between the controls and asthmatics, and thus the greatest difference between the two groups is a shift from lower of R_{rs} and $R_{rs}SD$ values to higher values along the regression line. Also, it is truly remarkable that these three studies (two previous studies [37, 306] and our study) performed in two different continents had comparable slopes in healthy and asthmatic subjects despite the differences in subjects and baseline R_{rs} . While it is not clear why the slopes are similar among individuals in different studies, it suggests that perhaps factors that strongly influence the relationship between R_{rs} and its variation do not vary substantially across individuals [252]. Furthermore, the tight correlation between changes in R_{rs} and $R_{rs}SD$ found in our study suggests that these factors are not likely to be altered with airway constriction, and is also in agreement with the theoretical predictions by modeling studies [252].

The strong linear association between R_{rs} and $R_{rs}SD$ suggests that the dominant mechanism responsible for the magnitude of $R_{rs}SD$ in asthma likely was related to the geometric dependence of R_{rs} on airway diameter as suggested by previous studies [39, 252]. If the correlations are associated with breathing-induced changes in airway

diameter, it would be interesting to investigate if variations in R_{rs} are correlated with breathing frequency, however we did not investigate this in our study. Furthermore, it is also not known if the correlations are periodic or random, and this needs further investigation. It is possible that some of the variation in R_{rs} in the asthmatics was due to the variation in airway diameter arising from the activity of the ASM. However, it is also likely that the variation was much smaller than that due to breathing-induced changes in diameter.

Spirometry and R_{rs}

We found that in asthmatics, baseline FEV_1 measurements were in close agreement with previous reports [37] while those in control subjects were within the normal range. As anticipated, decreases in FEV_1 following methacholine were larger in asthmatics than in controls, and were according to the study design.

Consistent with previous findings [27, 29, 153, 156, 330], we found that R_{rs} was higher in asthmatic than in healthy subjects, and this reflected airway obstruction. As expected, R_{rs} increased following administration of methacholine in both groups [331], however the increases in R_{rs} were not different between the two groups. However in both groups, low-frequency R_{rs} increased more than high frequency R_{rs} , and this effect was much stronger in asthmatic subjects (Fig. 6.2). Also, in agreement with previous studies [331], increases in low frequency R_{rs} were accompanied by decreases in low frequency X_{rs} (increases in E_{rs}). Together, this is likely suggestive of airway narrowing and ventilation heterogeneity in the peripheral lung regions following methacholine in both groups. This is consistent with imaging studies showing that airway constriction following bronchial provocation largely involves severe narrowing of small airways leading to heterogeneity in ventilation [20, 274, 332].

We found that changes in R_{rsSD} and FEV_1 were not related. Previously Diba et al. reported that there was no association between variability of log transformed Z_{rs} and AHR to histamine [37]. While it may be that R_{rsSD} does not relate to AHR, the lack of correlation may also be due to inherent differences between the two techniques. That is, AHR is assessed by changes in FEV_1 which is a forced maneuver, while variability of R_{rs}

is assessed during tidal breathing. As such, changes in FEV₁ and variation in R_{rs} likely have different underlying mechanisms.

Consistent with previous studies [320], we found there was a good correlation between baseline FEV₁ and PC20FEV₁. Furthermore, we found that in asthma R_{rs} was moderately correlated to PC20FEV₁, with subjects with lower FEV₁ and higher R_{rs} exhibiting smaller PC20 values. This implied that baseline obstruction was related to severity of AHR. In asthma, mechanisms that explain an increased sensitivity to methacholine include changes in intrinsic ASM function, changes in autonomic neural control of airway tone, changes in epithelial integrity and permeability, and the presence of inflammatory cells and mediators in airways [110]. Epithelial malfunction or damage resulting from these inflammatory changes disrupts its barrier function, and consequently increases responsiveness to constricting stimuli by increasing accessibility of the stimuli to the ASM. Association between epithelial permeability and AHR has been previously reported [333]. Furthermore, it has been also suggested that an increased number of inflammatory cells and the mediators released by the inflammatory cells may account for the enhanced airway sensitivity leading to narrowing. Indeed some studies have reported an inverse relationship between inflammatory mediators and the PC20 dose of methacholine [334, 335]. While we did not assess airway inflammation in our patients, it is strongly associated with asthma. The moderate correlation between R_{rs} and AHR that we observed in our patients is likely related to the inflammatory changes in their airways, associated both with narrower airways at baseline and susceptibility to induced narrowing.

X_{rs} and associated measures

In asthmatics, we found that X_{rs} was smaller (more negative) than in controls, and was decreased further following methacholine. This was in agreement with previous reports [28, 153, 167] and indicative of increased stiffness of the respiratory system. Furthermore, we found no difference in baseline E_{rs} derived from X_{rs} between controls and asthmatics, likely due to small sample size and large variability in E_{rs} among the asthmatics. However, the increases in E_{rs} were significantly larger in asthmatics than in controls. E_{rs} reflects stiffness of the respiratory system including airway wall and chest

wall stiffness, parenchymal tissue stiffness as well as contains a contribution from thoracic gas compression. E_{rs} may be increased with an increase in tissue stiffness as in pulmonary fibrosis [336], with chronic inflammation and remodeling due to an increase in airway stiffness as in asthma [337], and also with an increase in the intrinsic tissue stiffness resulting from distortion of the parenchymal tissue by narrowing of airways [232], although the latter perhaps occurs under maximal airway narrowing [210]. However, E_{rs} also varies with the amount of available compliant air spaces. Indeed, any pathological condition that blocks the lung regions from receiving ventilation increases E_{rs} by an amount inversely proportional to the lost volume of the lungs [279]. For example, de-recruitment of ventilating lung regions in asthma [19, 26, 267] and in acute lung injury [338, 339] due to small-airway closure results in increases E_{rs} [25]. Indeed a recent study [25] using an animal model of acute lung injury found that C_{rs} (inverse of E_{rs}) derived from the X_{rs} at 5 Hz was decreased by atelectasis, and inversely related to area of non-aerated regions. In line with these observations, the increases in E_{rs} in our patients suggest peripheral airway narrowing and closure.

Changes in dynamic expiratory flows also have been related to small-airway closure. A decrease in FVC is considered to be an indirect measure of airway closure and trapping which is based on the assumption that FVC declines due to an increase in the residual lung volume. The lack of association between E_{rs} and FVC observed in this study may be due to the methodological differences in FVC and E_{rs} measurement techniques. Measurement of FVC requires forced exhalation, and reduction in FVC may largely result from the dynamic compression of airways during the forced exhalation maneuver. On the other hand, since FOT is performed during normal breathing, higher E_{rs} is more likely reflective of small-airway narrowing and/or closure under normal breathing condition.

When we assessed variability of X_{rs} ($X_{rs}SD$), we found that similar to $R_{rs}SD$, $X_{rs}SD$ was higher in asthmatics than in controls, and increased similarly in both groups. The origin of temporal variation in X_{rs} is not clearly understood. However X_{rs} may vary during tidal breathing due to either tidal expiratory flow limitation (EFL) or changes in airway diameters. Indeed Dellaca et al. demonstrated the association between tidal variation in X_{rs} and lung function in chronic obstructive pulmonary disease (COPD)

[143]. They showed that in COPD patients experiencing EFL during tidal breathing, X_{rs} during expiration was significantly lower (more negative) than during inspiration, and this large difference in within-breath X_{rs} could reliably and accurately detect the presence of tidal EFL. Tidal EFL has not been found in stable asthma [340], but could conceivably occur in some airways leading to local differences in inspiratory and expiratory X_{rs} . X_{rs} may vary during breathing without flow limitation. This may possibly occur when airways close during expiration and reopen during inspirations, thereby altering airway diameters and changing the time-constants in a breathing cycle. It is not known if this occurs, but if true, this may result in variation in open air space observed by the forced oscillations. Another way to describe this is that variation in X_{rs} would also arise from heterogeneity in the variation in airway diameters during breathing (differences in the real part of impedance of small airways affecting the imaginary complex impedance of the lung) as Otis demonstrated for the static case when time constants are distributed [140]. Since low frequency X_{rs} is sensitive to airspace closure and heterogeneity in small airways, we suspect that variation in low frequency X_{rs} may imply temporal variations in spatial heterogeneity in the distal lung regions. Accordingly, the increases in $X_{rs}SD$ following methacholine suggest increased spatial heterogeneity following methacholine due to small-airway narrowing and closures or near closures.

Asthma control

We found that there was no association between $R_{rs}SD$ and patients' level of asthma control measured by their respiratory symptoms and need of a rescue inhaler. One of the possible reasons for this may be that the majority of the patients had very good ACQ scores. Also, the symptom scores in the uncontrolled asthmatics ranged from 1.17 to 2.5 (median 1.5) meaning we explored only a small portion of the available ACQ score range that spans from 0 (controlled asthma) to 6 (severely uncontrolled asthma). In the Que et al. study [38], which reported higher variability of Z_{rs} in asthmatics than in control subjects, 7 of 10 asthmatics had clinically worsened asthma stability, and had been admitted to the hospital for respiratory complications (personal communication between Geoff Maksym and Peter Macklem, Meakins-Christie Laboratories). Moreover, the Que et al. study saw much higher Z_{rs} in asthmatics than in control subjects (5.01 ± 0.9 SE

versus $1.88 \pm 0.1 \text{ cmH}_2\text{O.s.L}^{-1}$) meaning that the patients had poor baseline lung function. Furthermore, in the Lall et al. study [39], many of the children underwent changes in their therapy at their initial presentation, and required a step-up in their therapy (personal communication between Geoff Maksym and Paul Pianosi, Mayo Clinic). Unfortunately, none of these studies measured patients' asthma control; nevertheless collectively these findings suggest that increased variability of $R_{rs}SD$ may be associated with lack of asthma control although this study was unable to find any association between asthma control and variability of R_{rs} .

Limitations

As discussed above, most of our subjects had well controlled and clinically stable asthma as indicated by their ACQ scores. It may be that large alterations in $R_{rs}SD$ are associated with worsened asthma. However, it may not be feasible to perform methacholine challenge in poorly controlled or worsened asthma, but one can investigate the bronchodilator response of $R_{rs}SD$ in poorly controlled asthma.

Another limitation of the study was that our methacholine concentration was limited to the PC20 point or 16mg/ml (maximum dose recommended by ATS), whereas larger concentrations have been used in other studies [227, 306] in healthy subjects, but usually not in asthmatics. It is possible that a PC20 dose of methacholine was not enough to produce larger increases in $R_{rs}SD$. However it may be unwise to administer a methacholine dose larger than their PC20 to asthmatics with poorly controlled or severe asthma, and we chose not to attempt this.

Also, while the subjects with asthma had physician diagnosed asthma, it is possible that some of the subjects did not have asthma. Indeed, 5 subjects did not have AHR, which is strongly associated with asthma. If true, this may mean that the difference in response to methacholine between health and asthma may in fact be greater than we report.

6.5 Conclusions

In conclusion, our findings suggest that variation in R_{rs} (R_{rsSD}) asthma are likely related to breathing and lung-volume dependent changes in airway diameters. However in poorly controlled asthma, while R_{rsSD} may arise due to variation in airway diameters arising from excessive shortening of the airway smooth muscle, but this would require an investigation with sufficient patients with a broad range of uncontrolled or poorly controlled asthma.

Chapter 7: Variability of Impedance in Response to Bronchodilator

In Chapter 3, we quantified the bronchodilator (BD) response of the respiratory resistance (R_{rs}) and reactance (X_{rs}) in healthy subjects and subjects with asthma. In the same study, we also assessed variations in R_{rs} and X_{rs} , and their response to BD, which we present in this chapter. Methods for the study have been presented in Chapter 3, but they are briefly reproduced here for completeness of the chapter.

7.1 Introduction

In Chapter 3, we investigated the hypothesis that in asthma R_{rsSD} increases with activation of the airway smooth muscle (ASM) by methacholine relating to airway hyperresponsiveness (AHR). If so, R_{rsSD} should decrease by relaxing the ASM with bronchodilator (BD). This has been previously demonstrated in children with asthma. As discussed in the preceding chapter, Lall et al. found that R_{rsSD} was higher in asthmatic than in healthy children at baseline, and decreased significantly more in asthmatics than healthy children following a BD [39]. Moreover, the authors found that in asthmatics, decreases in R_{rsSD} were larger than those in R_{rs} . This suggested that R_{rsSD} may have a clinical value as an indicator of response to BD therapy in asthma. However these findings were only examined in asthmatic children. In the present study, we sought to extend the findings by Lall et al. to adult subjects with asthma. We analyzed the changes in R_{rsSD} in response to BD in the healthy and asthmatic subjects from the study in Chapter 3, and investigated the hypothesis that given a BD, R_{rsSD} decreases in asthmatics, and that this change is greater than in healthy subjects.

Lall et al. also found that R_{rsSD} and its response to BD varied amongst children with different degrees of asthma severity-based therapy. They found that children on inhaled corticosteroids, classified as mild persistent asthmatics had higher R_{rsSD} and the greatest decrease in R_{rsSD} with BD while those receiving a combination of LABA and

corticosteroids, classified moderate persistent asthmatics had the lowest baseline R_{rsSD} and the smallest decreases in R_{rsSD} with BD. This suggested that BD response of R_{rsSD} may be associated with patients' level of asthma control. Accordingly, in this study, we also investigated if R_{rsSD} and its BD response are related to asthma control. We hypothesized that, with BD, subjects with uncontrolled or poorly controlled asthma will exhibit larger decreases in R_{rsSD} than subjects with controlled asthma.

7.2 Methods

7.2.1 Subjects

Eighteen healthy subjects (11 females) and 18 subjects with asthma (10 females) were enrolled in the study (Table 3.1). Details on inclusion criteria for study participants and asthma patients' medications are provided in Section 3.2.1. All subjects provided written informed consent. The study protocol was approved by the Capital Health Research Ethics Board, Nova Scotia.

7.2.2 Measurements

The FOT and spirometry measurements are described in details in Section 3.2.2.

7.2.3 Protocol

Three one minute FOT measurements separated by 15-20 s and spirometry were performed at baseline and 12-15 min following inhalation of a BD (Salbutamol 200 mcg).

We also measured the level of dyspnea in all subjects at baseline and following BD using the modified Borg scale [327] and a 7-item pictorial scale. Furthermore, in asthmatics, each patient's level of asthma control was assessed by the 6-item asthma control questionnaire (ACQ-6) as described in Chapter 6 [65]. As in Chapter 6, the asthmatic subjects were pooled into two groups based on their ACQ score: controlled (ACQ score ≤ 1.0 , $n=9$) and uncontrolled (ACQ score > 1.0 , $n=8$). One patient did not answer the ACQ, and was excluded from the asthma control related comparisons.

7.2.4 Data Analyses

The data analyses is described in Chapters 3, 5 & 6, and is provided here in brief. The three FOT recordings were concatenated, and digitally filtered to remove breathing components up to 1 Hz. The filtered signals were then divided into 1 s data blocks with 50 % overlap while each block was multiplied by a Hamming window function to minimize the effects of non-stationarity and any remaining edge artifacts. Impedance Z_{meas} at each oscillation frequency was estimated from the ratio of Fourier transforms of the pressure to the flow signal. Z_{meas} was compensated for the impedance of the bias tubes and the bacterial filter [281, 341]. We obtained Z_{rs} , R_{rs} and X_{rs} , and variations in R_{rs} and X_{rs} as described in Section 6.2.4. Outlying Z_{rs} values resulting from coughs, swallows, and glottal closures were discarded based on statistical properties of Z_{rs} , coherence between the pressure and flow, and signal to noise ratio between the pressure and flow as described in Section 3.2.4.

7.2.5 Statistical Analyses

Data are presented as mean \pm standard error of mean (SE) unless otherwise specified. Normality and equal variance of the data were determined using Shapiro-Wilk and Levene's test respectively. For normally distributed data, we compared values between two group using two tailed unpaired t-tests, and values within a group using one tailed and two tailed paired t-tests wherever appropriate. For non-normally distributed data, between-group comparisons were performed using Mann Whitney rank sum test and within-group comparisons were performed using Wilcoxon signed rank test. For all tests, statistical significance was accepted at $p < 0.05$. All analyses were performed with SigmaPlot 12 version 12.3 (Systat Software, Inc. Chicago, Illinois, USA).

7.3 Results

Demographics

Subject demographics and lung function are presented in Table 3.1. As described in Section 3.3, healthy and asthmatic subjects were matched for age and height but not for weight; asthmatics were slightly heavier than healthy controls ($p=0.043$).

Pre and post bronchodilator lung function and mechanics

Lung function results are presented in Table 3.1 and described in Section 3.3. Briefly, FEV₁ and FVC were not different between healthy and asthmatic subjects at baseline. Following BD, FEV₁ increased in both groups with the increases being significantly larger in asthmatics than in controls. FEV₁ / FVC also increased in both groups, though not significantly differently, while FVC remained unaltered in both groups.

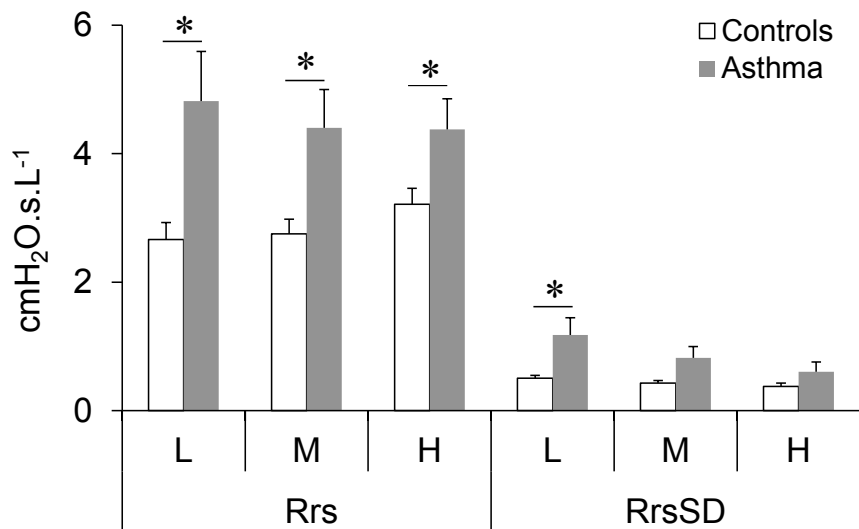


Figure 7.1: Baseline R_{rs} and R_{rsSD} in the controls subjects (n=18) and subjects with asthma (n=18). * denotes significantly different than control subjects, $p < 0.05$, L: low, M: mid, H: high frequencies

In asthmatics, R_{rsSD} was approximately one-fifth of R_{rs} at baseline, and was higher than in controls at low frequencies (Mann-Whitney rank sum test, $p=0.03$, Fig. 7.1). Like the decreases in R_{rs} in asthmatics reported in Chapter 3, there were decreases in R_{rsSD} with BD, but only at low frequencies (Wilcoxon signed rank test, $p=0.038$, Fig.

7.2). Although $R_{rs}SD$ appeared to increase in controls after BD, this was not significant. Also the changes in $R_{rs}SD$ with BD in both groups were not different.

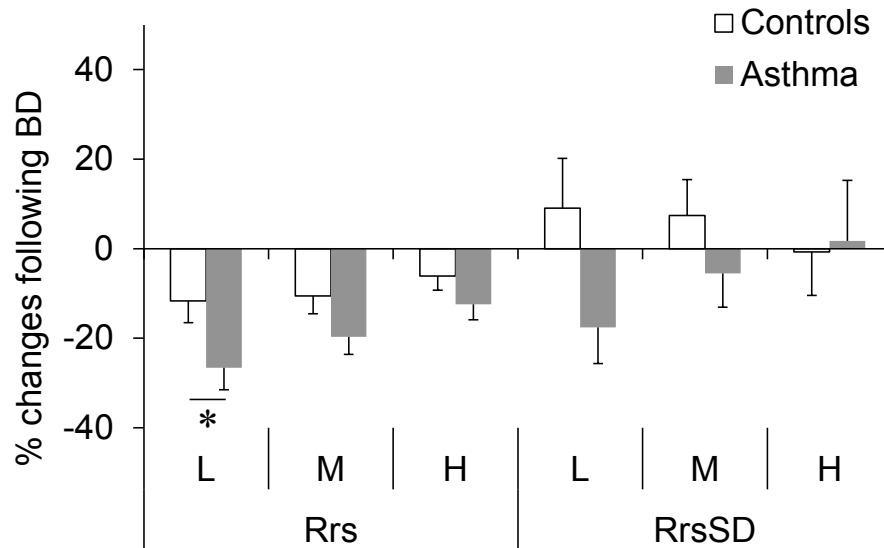


Figure 7.2: Percent changes in R_{rs} and $R_{rs}SD$ post BD. * denotes significantly different than control subjects, $p < 0.05$, L: low, M: mid, H: high frequencies

As reported in Chapter 3, there was no difference in baseline X_{rs} between the two groups, and following BD, X_{rs} increased only in asthmatics (Fig. 3.2). The results for $X_{rs}SD$ were similar to those for X_{rs} . We found that $X_{rs}SD$ was higher in asthmatics than in controls at low oscillation frequencies (Mann-Whitney rank sum test, $p=0.035$, Fig. 7.3), and decreased following BD but only in asthmatics and at low and mid frequencies (Wilcoxon signed rank test, $p < 0.001$ and $p=0.021$ respectively). Furthermore, the decreases in $X_{rs}SD$ were larger in asthmatics than that in controls at low oscillation frequencies (Man-Whitney rank sum test, $p=0.017$).

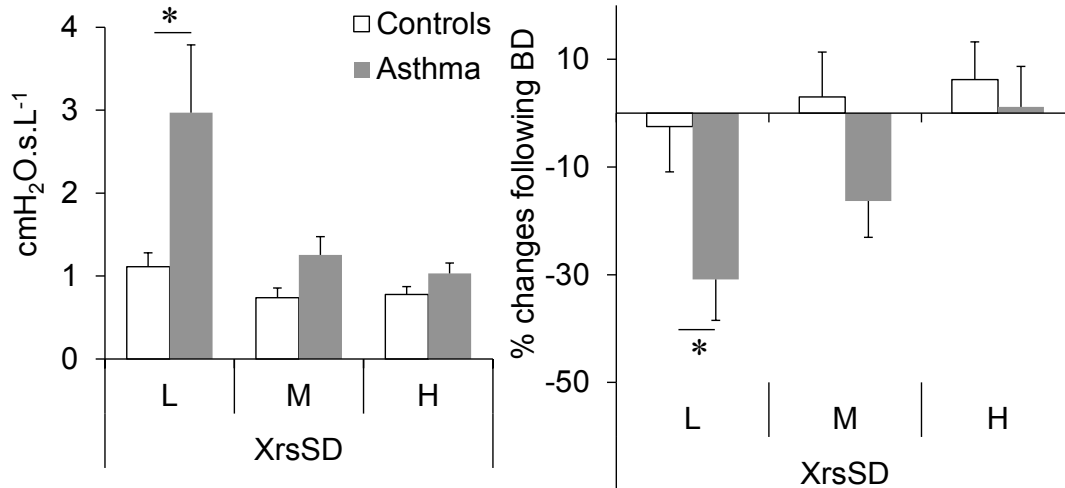


Figure 7.3: XrsSD and changes in XrsSD post BD. * denotes significantly different than control subjects, $p < 0.05$, L: low, M: mid, H: high frequencies

Correlations between FOT outcomes and FEV₁

We examined if there were correlations between changes in FEV₁ and lung mechanics. In asthmatics, FEV₁ weakly correlated to R_{rs} at low and mid frequencies at baseline and following BD with r^2 values all below 0.45, $p < 0.05$, but did not correlate at high frequencies (figures not shown here). However, FEV₁ moderately correlated to X_{rs} at all oscillation frequencies (r^2 values, low: 0.61, mid: 0.65, high: 0.62, $p < 0.001$).

Correlations between R_{rs} and R_{rs}SD

The correlations between low frequency (4 and 5 Hz) R_{rs} and R_{rs}SD at baseline and following BD are shown in Fig 7.4.

Control: In control subjects, there was a strong correlation between R_{rs} and R_{rs}SD at baseline and following BD at low frequencies (pre: slope=0.15, $r^2=0.73$, post: slope=0.26, $r^2=0.78$) and at mid frequencies (pre: slope=0.13, $r^2=0.61$, post: slope=0.18, $r^2=0.7$), and a weak correlation at high frequencies (pre: slope=0.13, $r^2=0.37$, post: slope=0.18, $r^2=0.38$). The slope of the regression line fit to R_{rs}SD versus R_{rs} increased following BD at low frequencies, but remained unchanged at mid and high frequencies.

Asthma: Similar correlations were observed in asthmatic subjects. $R_{rs}SD$ showed a strong correlation to R_{rs} before and following BD at all frequencies as shown in Fig. 7.5 (baseline, slopes=0.34, 0.27, 0.27 with $r^2=0.95, 0.84, 0.73$ and post BD, slopes=0.23, 0.19, 0.22 with $r^2=0.8, 0.78, 0.8$ at low, mid and high frequencies respectively). Furthermore, the slopes of the regression line fit to $R_{rs}SD$ versus R_{rs} decreased following BD at low and mid frequencies.

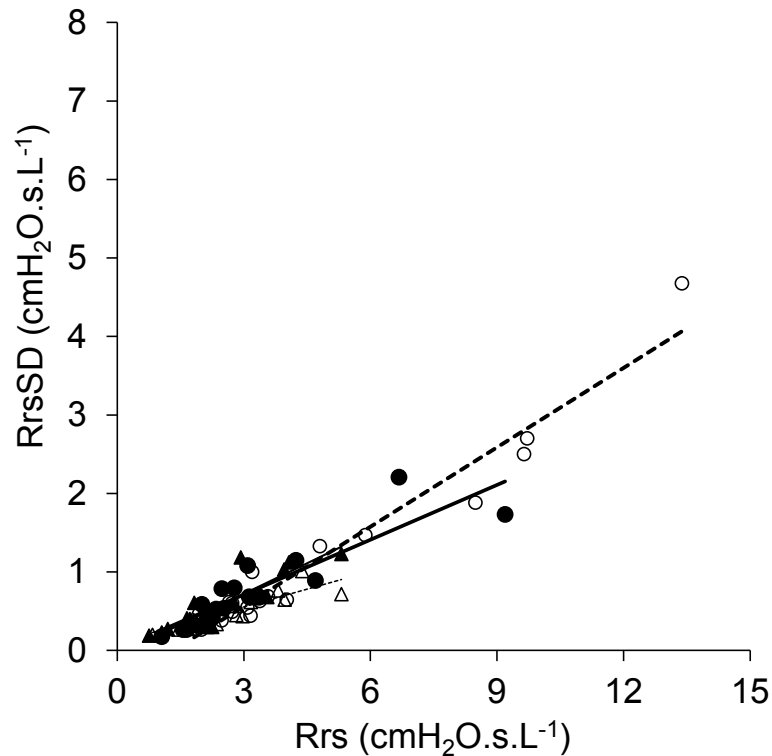


Figure 7.4: Correlations between $R_{rs}SD$ and R_{rs} pre- and post- BD in the control and asthmatic subjects at low frequencies. Circles indicate data in the asthmatics and triangles indicate data in the controls. Open symbols represent baseline data and closed symbols represent post-BD data. See text for details.

Controlled and uncontrolled asthma

Correlations in uncontrolled asthma: There was no correlation between ACQ scores and FEV_1 , R_{rs} , $R_{rs}SD$ (figures not shown here) in subjects with uncontrolled asthma.

Furthermore X_{rs} at low frequencies was not correlated to ACQ score ($r^2=0.44, p=0.07$);

however we found that E_{rs} was moderately correlated to ACQ score ($r^2=0.51$, $p=0.045$, Fig. 7.5).

Comparisons between controlled and uncontrolled asthma: Subjects in the controlled ($n=9$, 4 males) and uncontrolled ($n=8$, 2 males) groups were matched for age, height, and weight. The mean ACQ score was $0.61 \pm 0.35SD$ in the controlled group and 1.9 ± 0.7 in the uncontrolled group.

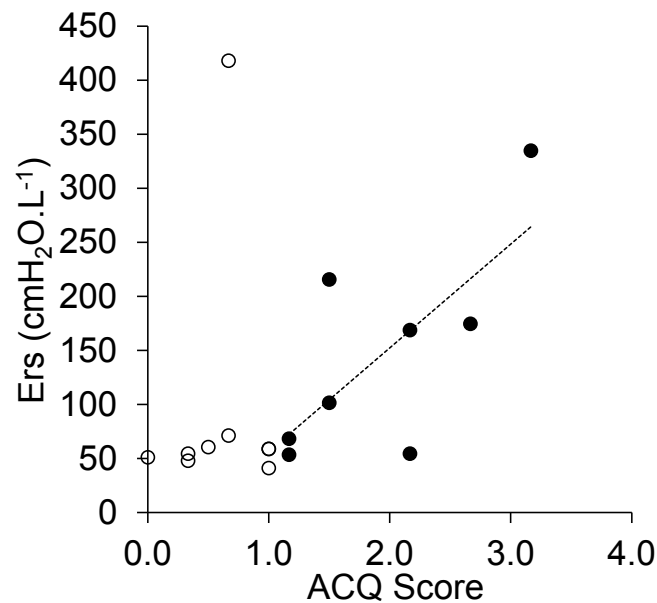


Figure 7.5: Correlation between E_{rs} and ACQ score in the subjects with asthma. Closed symbols: uncontrolled asthma, open symbols: controlled asthma. Straight line indicates regression for closed symbols (uncontrolled asthma), $r^2=0.51$, $p=0.045$

There was no significant difference in FEV_1 between controlled (mean \pm SE, 93 ± 7.4 % predicted) and uncontrolled (75 ± 9.4 % predicted) subjects. Interestingly, following BD, FEV_1 increased in both groups, though not significantly differently (Mann-Whitney rank sum test, $p=0.74$).

When we compared baseline R_{rs} and $R_{rs}SD$ between controlled and uncontrolled subjects, we found no difference between these groups ($p > 0.05$). Following BD, R_{rs} decreased in controlled subjects at all frequencies (low and mid frequencies, one tailed t-test, $p = 0.002$ and 0.003 respectively; high frequencies, Wilcoxon signed rank test,

$p=0.03$), but only decreased in uncontrolled subjects at low frequencies ($p=0.01$). However, the decreases in R_{rs} were not significantly different between the two groups. Interestingly, following BD, $R_{rs}SD$ decreased in uncontrolled subjects at low frequencies ($p=0.045$) but not in controlled subjects. Nevertheless, the changes in $R_{rs}SD$ were not different between the two groups. Furthermore there was also no difference in X_{rs} between controlled and uncontrolled subjects, and while X_{rs} increased significantly in both groups following BD, the increases were not different ($p > 0.05$).

7.4 Discussion

In this study, we investigated $R_{rs}SD$ and $X_{rs}SD$ in response to BD in healthy and asthmatic subjects, and the relationship between $R_{rs}SD$ and lack of asthma control. Our main findings are as follows. Overall, $R_{rs}SD$ and $X_{rs}SD$ both decreased in asthmatics, but not in control subjects, suggesting that variation in these parameters may be a useful measure of BD response that distinguishes asthma from health. However the responses to BD of the variations of R_{rs} were highly correlated to the mean changes in R_{rs} . Two possibilities exist, first the changes in $R_{rs}SD$ and $X_{rs}SD$ are distinguishing features of asthma, since they did not significantly change with BD in healthy subjects, whereas R_{rs} and X_{rs} did. Alternatively, it is possible that with more subjects, $R_{rs}SD$ and $X_{rs}SD$ might change in healthy subjects as well, although the changes would be smaller. In this second circumstance, the measurement of $R_{rs}SD$ and $X_{rs}SD$ would have no more physiological or clinical value than R_{rs} and X_{rs} . The implications of these findings are discussed further below.

$R_{rs}SD$ response to BD and correlations with $R_{rs}SD$

Our findings that R_{rs} and $R_{rs}SD$ are higher in subjects with asthma than in control subjects are consistent with previous reports [306] and with our findings with different subjects in Chapter 6. While $R_{rs}SD$ decreased following BD in asthma, the decreases were not different than those in R_{rs} . Thus, $R_{rs}SD$ did not provide any more clinically useful information than what could be inferred from R_{rs} alone as previously reported [37]. This suggested that short-term variation in R_{rs} may not be any more useful than R_{rs} for

monitoring response to therapy in asthma. Moreover, in agreement with previous reports [37, 38] and our data in Chapter 6, $R_{rs}SD$ showed a strong linear correlation to mean R_{rs} at baseline and following BD in asthmatics. Also, the slope of the $R_{rs}SD$ versus R_{rs} relationship at low frequencies was comparable to that in Que et al. [38] and Diba et al. [37]. These results suggest that factors which influence the relationship between R_{rs} and $R_{rs}SD$ likely do not vary across individuals, nor do they vary with airway dilation. As discussed in Chapter 6, the strong correlation between R_{rs} and $R_{rs}SD$ suggests that although their origin is uncertain, the variations in R_{rs} must be tied to factors that regulate airway diameter such as tidal breathing and lung volume.

X_{rs} and associated measures

As reported in Chapter 3, in this group of subjects we found that X_{rs} was no different in asthmatic than in control subjects, but this may be due to the fewer number of subjects and greater variability of X_{rs} in asthmatics. However with BD, as reported in Chapter 3, X_{rs} increased only in asthmatics, with the changes in X_{rs} being larger in asthmatic than in control subjects. Again, the increases in X_{rs} with BD in asthmatics were in agreement with previous publications [28, 29], and as we modeled in Chapter 3, are suggestive of recruitment of airspaces via the opening and dilation of small airways. This again clearly suggests that the BD response of X_{rs} may be a useful indicator of small-airway dysfunction in asthma.

When we examined the variation of X_{rs} ($X_{rs}SD$) we found that similar to the variation in R_{rs} , $X_{rs}SD$ at low frequencies was higher in asthmatic than in healthy subjects, and decreased with BD only in asthmatics. In line with the discussion on variability of X_{rs} in Chapter 6, variation in X_{rs} may imply temporal variations in spatial heterogeneity in the distal lung regions. Accordingly, decreases in $X_{rs}SD$ with BD suggest reduced spatial heterogeneity following opening and dilation of small airways.

$R_{rs}SD$ and asthma control

We found that $R_{rs}SD$ and its BD response was not related to patients' level of asthma control. One of the reasons behind this might be that we had a small number of subjects in the uncontrolled group, and their ACQ scores ranged from 1.17 to 3.17 with

one subject having the highest score value of 3.17, while the remaining subjects had a score ≤ 2.17 . As stated before, the ACQ score ranges from 0 (totally controlled) to 6 (severely uncontrolled). This shows that the uncontrolled group covered a limited range of ACQ scores with the scores being close to our ACQ score cut off of 1.0.

7.5 Conclusion

In conclusion, our results suggest that short-term temporal variation in R_{rs} and X_{rs} may distinguish asthma from health at baseline, but may not be clinically useful indicators of BD response in asthma. The strong linear association of variations of R_{rs} to its mean suggest that variability of R_{rs} may be tied to breathing and lung volume dependent changes in airway diameter. Furthermore, we were unable to demonstrate if variability of R_{rs} is related to patients' symptoms due to an insufficient sample size in the uncontrolled asthma group. This requires further investigation in patients with a wide range of asthma control.

Chapter 8: Variability of Impedance as a Function of Lung Volume

8.1 Introduction

Previous studies [37-39] and our studies presented in the preceding chapters found that short-term variation of respiratory resistance, R_{rs} (R_{rsSD}), is higher in asthma than in healthy subjects, but that it was highly correlated to R_{rs} . Indeed, previous studies [37-39, 230] and ours (Fig. 6.8) have found a strong linear correlation between R_{rs} and R_{rsSD} across all individuals. The correlation between R_{rs} and R_{rsSD} , and the well-known inverse relationship between R_{rs} and lung volume [342] together suggest that similar to R_{rs} , R_{rsSD} may also be dependent on lung volume. This has not been established, likely because the lung volume dependence of R_{rs} overshadows any variation in R_{rs} indicative of the ASM activity. While the lung volume dependence of R_{rsSD} has not been investigated systematically, it has been speculated from the measurements in multiple subjects breathing at their resting lung volume [37-39].

Previously Que et al. [38] and Diba et al. [37] measured R_{rsSD} in upright and supine in healthy subjects. Que et al. [38] found that in healthy subjects, R_{rsSD} increased with a decrease in lung volume in the supine position, however Diba et al. [37] were unable reproduce these findings. The reasons for these differences are not clear, but the differences may be due to factors other than lung volume contributing to R_{rsSD} . However, Que et al. [38] and Diba et al. [37] did not assess end-expiratory lung volume (EELV) and R_{rsSD} versus lung volume relationship within individual subjects. This knowledge gap formed the motivation for the present study.

Since R_{rs} varies inversely with EELV, and relates linearly to R_{rsSD} , we aimed to investigate how changes in EELV modify R_{rsSD} in healthy and asthmatic subjects. We assessed R_{rsSD} using the forced oscillation technique (FOT), at the subjects' functional residual capacity (FRC) and at two EELVs above and below FRC. Subjects' FRC was measured by body plethysmography, and changes in FRC were estimated from the

differences in end-expiratory tidal volume estimated using respiratory inductive plethysmography (RIP). We hypothesized that $R_{rs}SD$ correlates to R_{rs} with changes in lung volume, and shows a functional dependence on the lung volume similar to R_{rs} . Additionally, with increased baseline tone in asthma which further increases at lower lung volume, the lung volume dependence of $R_{rs}SD$ at lower lung volumes might be different in asthma, with greater variation at lower lung volumes than in healthy subjects.

8.2 Methods

8.2.1 Subjects

Eleven healthy subjects and 7 subjects with asthma were enrolled from Halifax Infirmary and the local community in a written informed consent process. The study protocol was approved by Capital Health Research Ethics Board, Halifax, Nova Scotia. Inclusion criteria for the study participants are provided in Section 3.2.1.

In the asthma group, 3 subjects were on short-acting beta-2 agonist (SABA), 1 subject rarely required SABA, 1 subject was on SABA when needed, inhaled corticosteroid (ICS), leukotriene receptor antagonist and intranasal steroid, and 1 subject was on ICS while one subject was on no medications.

Four healthy subjects (one male and three females) were eliminated from the data analyses. Three of these subjects had difficulty in holding the target EELVs during FOT. In the case of the fourth subject, baseline FOT measurements were substantially higher than the rest of the controls, and comparable to those in asthma. This subject participated in the study presented in Chapter 5, and her R_{rs} in the previous study was nearly 2 fold smaller than that in the present study. Furthermore, there were no differences in her past and present FEV_1 values, but her present FRC (2.6 L) was nearly 400ml larger than her FRC in the previous study. The reasons behind these observations are not clear, although other subjects that participated in both studies were not substantially different. However, FOT devices used in these two studies were different, thus it is possible that the subject perhaps breathed differently on the two devices. Due to her abnormally high R_{rs} and X_{rs}

values in this study, we chose to exclude her from our analysis. In the following section, we present data from 7 healthy subjects and 7 subjects with asthma (Table 8.1).

8.2.2 Measurements

Impedance of the respiratory system (Z_{rs}) was measured using the forced oscillation device (tremoFlo™ OS-Beta, Thorasys Thoracic Medical Equipment Inc., Montreal, Canada at 6 Hz (Fig 8.1). The device consists of a handheld unit connected to a base unit or controller (NetBurner MOD5234 NetBurner Inc, San Diego, CA) that contains electronics responsible for controlling the hand held unit. The oscillating airflow is generated by a self-actuated piston which comprises two semi-circular hollow magnets between plastic plates designed to allow air flow through a screen mesh pneumotach (PT) at its center.

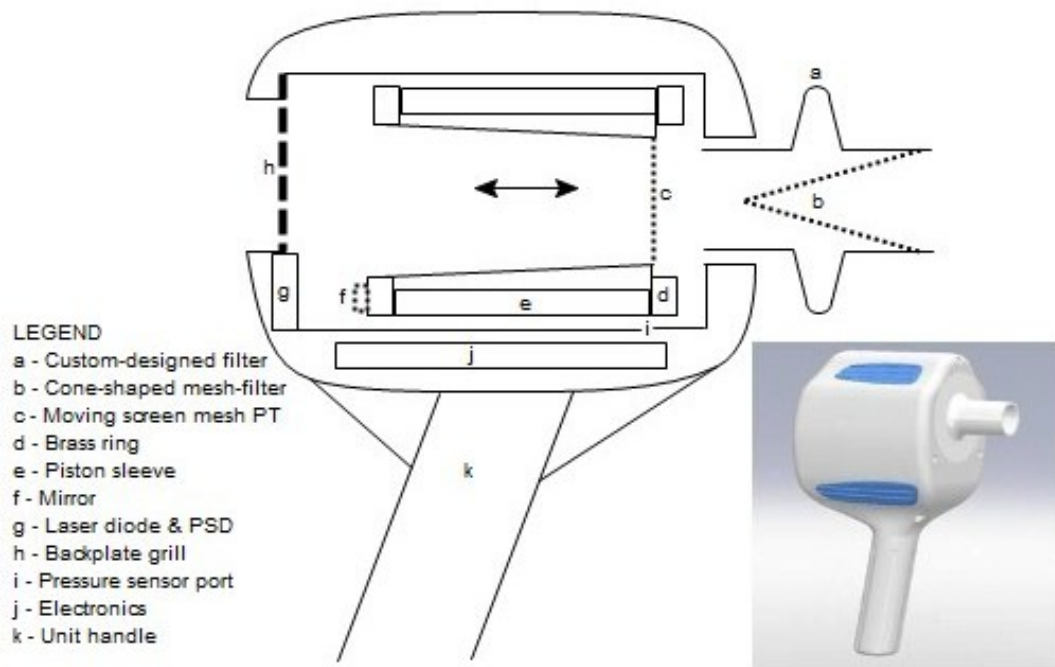


Figure 8.1: Schematic and 3D model of tremoFlo™ OS-Beta actuator unit.

The piston is surrounded by a cylindrical steel core which completes the magnetic circuit, imparting electromagnetic force to the piston when current is passed through the copper

windings. The cylinder pressure is measured by a piezoresistive pressure transducer (All Sensors Corp, Morgan Hill, CA). The flow signal is not measured directly; the device functions similarly to the *flexiVent* small animal ventilator system (SCIREQ Inc., Montreal Canada) which records volume delivered by oscillations due to the piston displacement. Flow for computation of the impedance is determined by differentiating the volume signal which depends on the accuracy of actuator position, and an accurate and constant mesh resistance.

Tidal volumes were measured using a respiratory inductive plethysmograph (Respirace, Ambulatory Monitoring Inc, NY, USA), a non-invasive respiratory monitoring device. The detail description of the RIP technique can be found elsewhere [343, 344]. Briefly, RIP consists of two transducers in the form of zigzag coils of Teflon-insulated wire sewn into elastic bands. The coils encircle the rib cage and the abdomen, and are connected to variable frequency oscillators. The rib cage and abdominal movements during respiration produce changes in the cross sectional area of the coils, altering their self-inductance, and resonant frequency of the oscillators. The changes in resonant frequencies are demodulated to produce output signals proportional to volumetric changes of the two body compartments. The sum of these two signals can be calibrated to the tidal volume measured by a spirometer or a PT.

We calibrated Respirace for each individual subject in the seated position via a recorded respiratory flow signal as follows. Subject breathed through a Fleisch pneumotach (Fleisch No. 2, Lausanne, Switzerland) connected to a differential pressure transducer (TD-05-AS, SCIREQ) for 20-25 s while wearing the Respirace bands around their chest and abdomen. The measurements were done with nose clips affixed and the cheeks supported by both palms. Although nose clips and cheek support were not necessary during RIP calibration, they were used to maintain similarity between the RIP calibration and FOT measurements. The volume at the airway opening was determined by integrating flow measured by the pneumotach. The rib cage and abdominal volume motion coefficients were obtained by fitting the Respirace signals to the tidal volume obtained by the pneumotach using multiple linear regression. The pneumotach was calibrated by the flow-integral method using a calibrated 3L syringe prior to the Respirace calibration.

The oscillator unit of RespiTrace is sensitive to temperature changes which can introduce drift to the volume signal. To keep this drift error to a minimum, the study measurements were performed over a duration of less than half an hour. Furthermore, the RespiTrace signal conditioning unit was stabilized at room temperature half an hour before all measurements, and calibrated at the start and again midway through measurements on each individual.

Spirometry and functional residual capacity (FRC) were measured in a constant volume body plethysmograph (VE20-VE62J, SensorMedics, USA). Results were accepted according to American Thoracic Society (ATS) criteria for adults and were expressed as a percentage of predicted values according to Morris et al. [289]. The body plethysmograph was calibrated before each subject assessment.

8.2.3 Protocol

The impedance of the respiratory system, Z_{rs} was measured at FRC and at different EELVs as described below. Each measurement was performed for 135 sec. Subjects breathed at FRC for 60 sec, at an EELV approximately 1 tidal volume (TV) above FRC for 1 min and resumed breathing back to their FRC over the last 15 sec. This was repeated for other EELVs: approximately 2 TV above FRC and 1 TV below FRC. Breathing at each lung volume was achieved using biofeedback of lung volume from RespiTrace; its output was displayed on a monitor during FOT measurements. FEV₁ and absolute lung volumes were measured following FOT. In asthma, patients' level of asthma control was assessed by the 6-item Asthma Control Questionnaire (ACQ) [65].

8.2.4 Data Analyses

The Fleish pneumotach and RespiTrace outputs were sampled at 500Hz (DAQ 6036E, National Instruments, Austin, TX), and acquired and processed using Labview (National Instruments, Austin, TX, USA) and Matlab (The Mathworks Inc., Natick, MA). Tidal volume signal measured by the RespiTrace was low-pass filtered using a frequency-domain filter with 1 Hz cut-off frequency as described in Section 3.2.4, and tidal volume, respiratory frequency and minute ventilation were determined for each measurement.

The pressure and the flow signals from tremoFlo™ were sampled at 256 Hz after 6 pole Bessel low-pass filtering, and processed in Matlab as follows. The signals were processed with a 4 Hz digital band-pass filter centered around the oscillation frequency of 6 Hz. The signals were divided into 0.5 s data blocks with 75% overlap, and each block was multiplied by a Hamming window function. Impedance, Z_{meas} , at the oscillation frequency was estimated from the ratio of Fourier transforms of the pressure and the flow signals. Impedance of the respiratory system, Z_{rs} , was determined after compensating Z_{meas} for impedance of the bacterial filter [281, 282] as described in Section 3.2.4. This compensation accounts for the effects of gas compression and resistive and inertive effects within the device. R_{rs} , X_{rs} , and their variations were obtained, and elastance of the respiratory system, E_{rs} , was obtained as $-2\pi f X_{\text{rs}}$, where f was the oscillation frequency, 6Hz. Changes in FRC were calculated from differences in end-expiratory tidal volumes on the RespiTrace recording.

8.2.5 Statistical Analyses

Data are presented as mean \pm standard error of mean (SE) unless otherwise specified. Normality and equal variance of the data were determined using Shapiro-Wilk and Levene's test respectively. For normally distributed data, comparisons between two groups were performed using two tailed unpaired t-tests and within-group comparisons were performed using two tailed paired Student t-test. For non-normally distributed data, the comparisons were performed using Wilcoxon signed rank test and Mann-Whitney rank sum test. Relationship between two variables was assessed using linear regression. For all tests, statistical significance was accepted at $p < 0.05$. All analyses were performed using SigmaPlot 12 version 12.3 (Systat software, Inc. Chicago, Illinois, USA).

8.3 Results

Demographics

Subject demographics and lung function are given in Table 8.1. Healthy and asthmatic subjects were matched for age, height, and weight. We found that there were no differences in spirometry and functional residual capacity (FRC) between healthy and asthmatic subjects. Based on ACQ scores, asthmatics (n=7) were classified as well controlled (ACQ score: $0.74 \pm 0.33SD$)

Baseline comparisons

At baseline, compared with controls, asthmatics had higher R_{rs} (Mann-Whitney rank sum test, $p < 0.001$), more negative X_{rs} ($p=0.004$). Furthermore, we found that there was no difference in $R_{rs}SD$, however, $X_{rs}SD$ was higher among asthmatics than in controls (Mann-Whitney rank sum test, $p=0.004$, Fig. 8.2).

Changes in end-expiratory lung volume

The lung volume protocol included 4 different changes in lung volume from FRC (2 above FRC and 2 below FRC), which are indicated in Tables 8.2 (control) and 8.3 (asthma). Accordingly control subjects were grouped into 4 subgroups (CH1, CH2, CL1, and CL2) and asthmatic subjects were grouped into 3 subgroups (AH1, AH2, and AL1). Because of small changes in FRC, and because not all subjects performed every lung volume, there were slight differences in the average FRC.

Table 8.1: Subject demographics and lung function

	Groups		p value
	Control (n=7)	Asthma (n=7)	
Sex, male / female	4 / 3	4 / 3	
Age, years	30.3 ± 2.3	27.7 ± 1.8	0.32
Height, cm	173.5 ± 3.7	167.4 ± 1.7	0.17
Weight, kg	70.5 ± 5.1	71.9 ± 5.3	0.85
BMI, kg/m ²	23.4 ± 1.6	25.6 ± 1.7	0.36
FEV ₁ , % predicted	104.4 ± 4.4	95.9 ± 3.9	0.17
FEV ₁ /FVC %	100 ± 3.2	93.9 ± 4.7	0.31
FRC, L	3.1 ± 0.3	2.87 ± 0.3	0.24
FRC, % predicted	92 ± 3.4	92.4 ± 5.4	0.94
TLC, % predicted	94.7 ± 3.3	97.5 ± 2.4	0.50

Data are presented as mean ± SE. n, number of subjects, BMI, body mass index, FEV₁, forced expiratory volume in one second as percent of predicted [289], FVC, forced vital capacity as percent of predicted [290], FRC, functional residual capacity as percent of predicted [324], TLC, total lung capacity as percent of predicted [324]

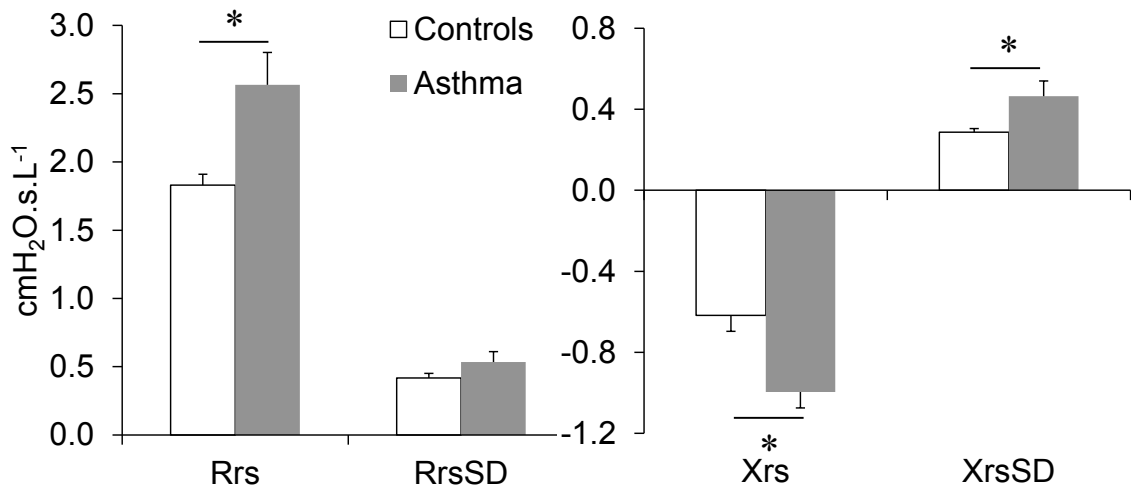


Figure 8.2: Baseline R_{rs}, X_{rs}, and variations of R_{rs} and X_{rs} in the control subjects (n=7) and subjects with asthma (n=7). * denotes significantly different than controls, p < 0.05

Table 8.2: FRC and changes in EELV in controls subjects

Group (n)	FRC, L	Changes in EELV, mL	New EELV, L
CH1 (5)	3.0 ± 0.9	630 ± 128.3	3.7 ± 0.9
CH2 (4)	3.4 ± 0.9	1440 ± 78.5	4.8 ± 0.9
CL1 (5)	2.8 ± 0.5	-601 ± 136.7	2.2 ± 0.5
CL2 (4)	3.5 ± 0.7	-1206 ± 140	2.3 ± 0.6

Data are presented as mean ± standard deviation (SD). n, number of subjects, EELV, end-expiratory lung volume; increases and decreases in EELV from FRC are indicated by positive and negative signs respectively.

Table 8.3: FRC and changes in EELV in subjects with asthma

Group (n)	FRC, L	Changes in EELV, mL	New EELV, L
AH1 (6)	2.9 ± 0.8	539 ± 120.8	3.4 ± 0.7
AH2 (3)	2.7 ± 0.2	1221 ± 151.6	4.0 ± 0.3
AL1 (5)	3.0 ± 0.7	-596 ± 151.1	2.4 ± 0.7

Data are presented as mean ± standard deviation (SD). n, number of subjects, EELV, end-expiratory lung volume; increases and decreases in EELV from FRC are indicated by positive and negative signs respectively.

Effect of changes in end-expiratory lung volumes on FOT outcome measures

Control: R_{rs} and R_{rsSD} at FRC and altered lung volumes are presented in Table 8.4, and R_{rs} and R_{rsSD} versus lung volume relationships are shown in Fig. 8.3. R_{rs} decreased with increases in lung volumes from FRC in groups CH1 and CH2, and increased with a decrease in lung volume in group CL2 but not in group CL1. Furthermore, R_{rsSD} did not change with increases in lung volumes from FRC in groups CH1 and CH2. However, it

increased significantly with decreases in lung volumes in group CL2 and marginally in group CL1 (p=0.06).

When we assessed alterations in X_{rs} , we found that X_{rs} became more negative with increases in lung volumes from FRC in groups CH1 and CH2, and with a decrease in lung volume in group CL2 but remained unaltered in group CL1 (Mann-Whitney signed rank test, p=0.06, figures not shown here). Furthermore, variation of X_{rs} , X_{rsSD} , increased with decreases in lung volume from FRC in groups CL1 and CL2, but did not change with increases in lung volume in groups CH1 and CH2.

Table 8.4: R_{rs} and R_{rsSD} at FRC and at lung volumes above and below FRC

Group (n)	R_{rs} at FRC cmH ₂ O.s.L ⁻¹	R_{rs} at EELV above / below FRC cmH ₂ O.s.L ⁻¹	R_{rsSD} at FRC cmH ₂ O.s.L ⁻¹	R_{rsSD} at EELV above / below EELV cmH ₂ O.s.L ⁻¹
CH1 (5)	1.8 ± 0.09	1.42 ± 0.15*	0.4 ± 0.04	0.4 ± 0.03
CH2 (4)	1.8 ± 0.12	1.46 ± 0.12*	0.4 ± 0.05	0.6 ± 0.12
CL1 (5)	1.8 ± 0.06	2.11 ± 0.10	0.4 ± 0.04	0.7 ± 0.09
CL2 (4)	1.9 ± 0.13	2.85 ± 0.2*	0.4 ± 0.04	1.1 ± 0.06*
AH1 (6)	2.3 ± 0.13	2.0 ± 0.21*	0.46 ± 0.03	0.6 ± 0.03*
AH2 (3)	3.0 ± 0.46	2.2 ± 0.37*	0.64 ± 0.17	0.7 ± 0.1
AL1 (5)	2.4 ± 0.15	3.2 ± 0.53	0.46 ± 0.04	0.9 ± 0.21

Data are presented as mean ± SD. * indicates values significantly different than at FRC, p < 0.05. See Tables 8.2 and 8.3 for FRC and EELVs above and below FRC.

Asthma: R_{rs} and R_{rsSD} at FRC and altered lung volumes are presented in Table 8.4, and R_{rs} and R_{rsSD} versus lung volume plots are shown in Fig. 8.4. R_{rs} decreased with increases in lung volume in groups AH1 and AH2 groups, but increased marginally with a decrease in lung volume in group AL1 (p=0.057). Furthermore R_{rsSD} increased with an increase in lung volume in group AH1, but not in group AH2. In group AL1, R_{rsSD}

increased with a decrease in lung volume in all subjects, but did not reach statistical significance ($p=0.08$), likely due to the small number of subjects.

Furthermore, X_{rs} decreased, and X_{rsSD} increased with a decrease in lung volume from FRC in group AL1, but not with increases in lung volume in groups AH1 and AH2.

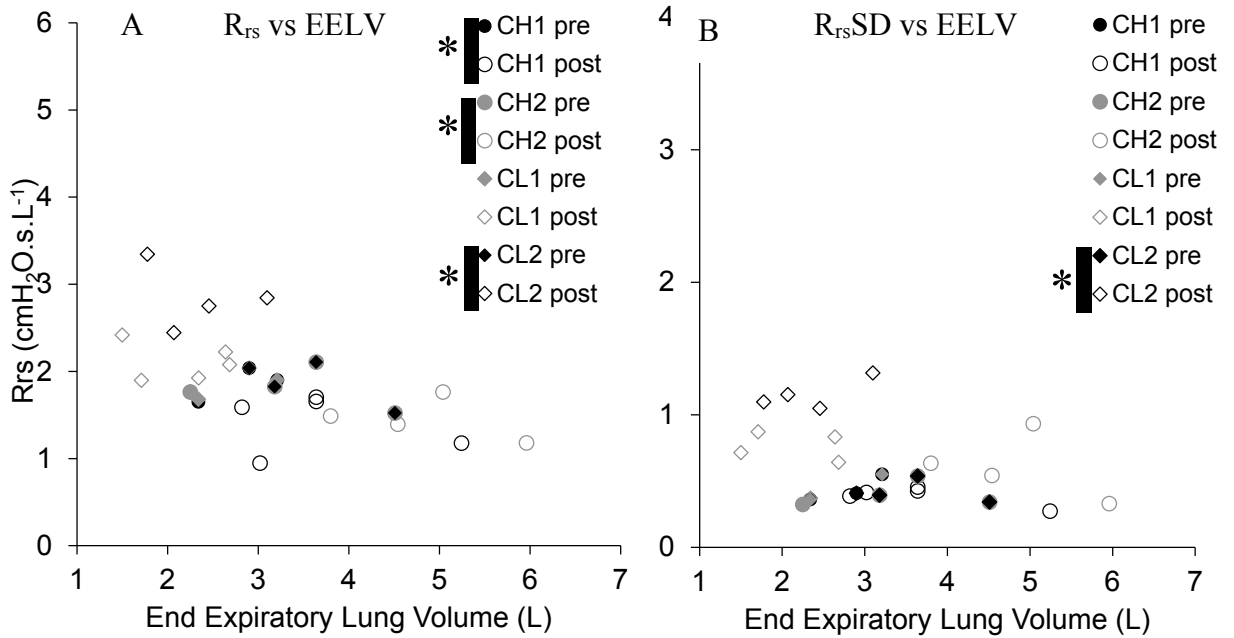


Figure 8.3: R_{rs} and R_{rsSD} versus EELV in the control subjects A) R_{rs} versus EELV B) R_{rsSD} versus EELV. The subjects were divided into 4 groups as indicated in Table 8.2. For all groups, * indicates significant difference between R_{rs} and R_{rsSD} at FRC and at an EELV from FRC, $p < 0.05$

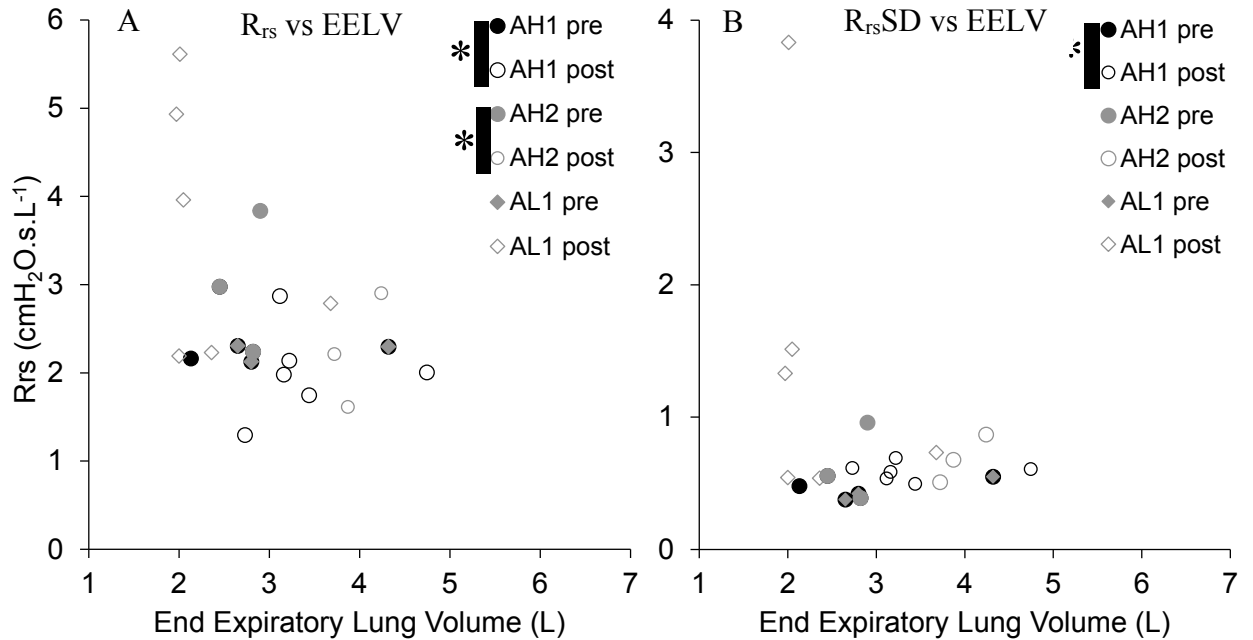


Figure 8.4: R_{rs} and R_{rsSD} versus EELV in the subjects with asthma A) R_{rs} versus EELV B) R_{rsSD} versus EELV. The subjects were divided into 4 groups as indicated in Table 8.3. * indicates significant difference between R_{rs} and R_{rsSD} at FRC and at EELV from FRC, $p < 0.05$

R_{rs} and R_{rsSD} versus lung volume: We normalized R_{rs} , R_{rsSD} , and EELVs across all subjects to their values at FRCs. Relationships between the normalized variables are presented in Fig. 8.5. Figure 8.5A shows R_{rs} plotted against EELVs while 8.5B shows R_{rsSD} plotted against EELV. Each point on the graphs represents a subject's R_{rs} (R_{rsSD}) and his/her EELV from FRC, both normalized to their FRC values as stated above. The R_{rs} and FRC for all subjects are indicated by a point with x-y coordinates (1, 1) on both graphs. The points to the left of this point represent R_{rs} or R_{rsSD} at EELVs below subjects' FRCs while the points to the right of this point represent R_{rs} (R_{rsSD}) at EELVs above their FRCs. Notice that R_{rs} was inversely dependent on lung volume, and the relationship was curvilinear. Similar to R_{rs} , R_{rsSD} was inversely related to EELV below FRC, but it increased at the lung volumes above FRC (Fig. 8.5B).

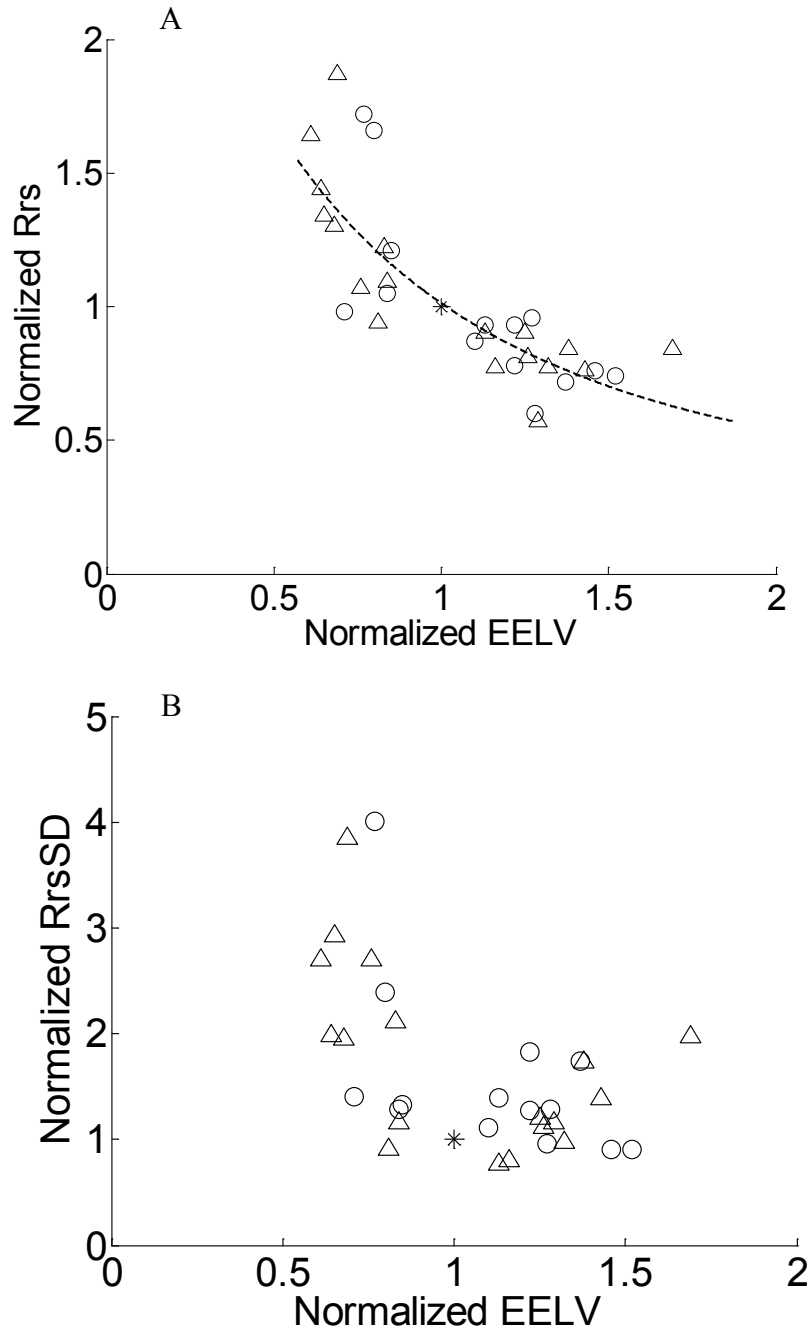


Figure 8.5: Normalized R_{rs} and $R_{rs}SD$ versus normalized EELVs in the controls (Δ) and asthmatics (\circ). All values (Table 8.2 and Table 8.3) were normalized to their respective FRC values. A) R_{rs} versus EELV B) $R_{rs}SD$ versus EELV. ‘*’ data point on both plots indicates the data point corresponding to FRC, and R_{rs} and $R_{rs}SD$ at FRC for all subjects. Normalized R_{rs} versus EELV was fit a model $y=2.44*R_{rs} (x+0.7)^{-3} + 0.5$, $r^2=0.67$
Comparison of changes in $R_{rs}SD$ between asthma and control at lower lung volumes

We hypothesized that subjects with asthma would exhibit greater variation in R_{rs} at lower lung volumes than in healthy subjects. Thus we compared FOT measures between groups CL1 (control) and AL1 (asthma) at FRC and at lung volumes decreased from FRC (Table 8.5). There were no differences in FRC and in EELVs below FRC between CL1 and AL1. Compared to subjects in group CL1, subjects in group AL1 had higher R_{rs} (Mann-Whitney rank sum test) and more negative X_{rs} at FRC (baseline), but not at lung volumes below FRC. However, there were no differences in R_{rsSD} and X_{rsSD} between the two groups at FRC and at lung volumes below FRC. Also there were no differences in the changes in these FOT outcomes with the decreases in lung volumes from FRC between CL1 and AL1.

Table 8.5: Comparisons between control (CL1) and asthma (AL1) groups at FRC and at EELVs below FRC

	Groups		p value
	CL1 (n, 5)	AL1 (n, 5)	
FRC, L	2.8 ± 0.2	3.0 ± 0.3	0.7
change	0.6 ± 0.06	0.6 ± 0.07	0.95
R_{rs} , cmH ₂ O.s.L ⁻¹	1.84 ± 0.06	2.4 ± 0.15	0.008*
change %	15.9 ± 8.7	32.2 ± 15.4	0.38
R_{rsSD} , cmH ₂ O.s.L ⁻¹	0.4 ± 0.04	0.46 (0.04)	0.37
change %	77 ± 32.6	108 (52.3)	0.63
X_{rs} , cmH ₂ O.s.L ⁻¹	-0.63 ± 0.05	-1.0 ± 0.11	0.012*
change	-0.54 ± 0.22	-0.65 ± 0.24	1
X_{rsSD} , cmH ₂ O.s.L ⁻¹	0.28 ± 0.03	0.38 ± 0.04	0.95
change %	131.6 ± 29	125.4 ± 46	0.91

Data are presented as mean ± SE. n, number of subjects; R_{rs} , respiratory resistance; X_{rs} , respiratory reactance; R_{rsSD} , standard deviation of R_{rs} ; X_{rsSD} , standard deviation of X_{rs} ; p < 0.05 indicates significant difference between asthmatic and control subjects.

Variability in end-expiratory lung volumes

We hypothesized that $R_{rs}SD$ would decrease with increases in lung volume from FRC. On the contrary, we found that $R_{rs}SD$ increased with increases in lung volume. We suspected that this might have occurred due to breath-to-breath variation in EELVs when subjects breathed above and below their FRCs on the FOT device. Thus, we quantified breath-to-breath variation in lung volumes at FRC and other EELVs (summarized in Table 8.6) in each individual from the standard deviation of the minima of the tidal volume excursions measured by Resptrace as illustrated in Fig. 8.6. It can be noticed that there was variability in lung volume at FRC, and the variability increased largely at lung volumes above FRC (groups CH1, CH2, AH2) although the increases were not statistically significant.

Table 8.6: Breath-to-breath variation in FRC and EELVs above and below FRC in control and asthmatic subjects

Group (n)	FRC (L)	Mean variation in EELV at FRC (ml)	EELV (L)	Mean variation in altered EELV (ml)
CH1 (5)	3.0 ± 0.91	78.8 ± 16.2	3.67 ± 0.95	100.6 ± 41.4
CH2 (4)	3.4 ± 0.94	89.3 ± 61.7	4.8 ± 0.91	142.5 ± 71.2
CL1 (5)	2.8 ± 0.5	61.8 ± 28.6	2.2 ± 0.54	84.1 ± 38.3
CL2 (4)	3.5 ± 0.7	86.9 ± 52.2	2.35 ± 0.57	86.5 ± 22.6
AH1 (6)	2.9 ± 0.76	74.9 ± 39.4	3.4 ± 0.7	82.1 ± 33.3
AH2 (3)	2.7 ± 0.24	68.7 ± 15.3	4.0 ± 0.27	135.9 ± 100.9
AL1 (5)	3.0 ± 0.75	63.2 ± 27	2.4 ± 0.72	69.4 ± 15.7

Data are presented as mean ± SD. n, number of subjects, FRCs and EELVs from Tables 8.2 and 8.3 are reproduced for completeness.

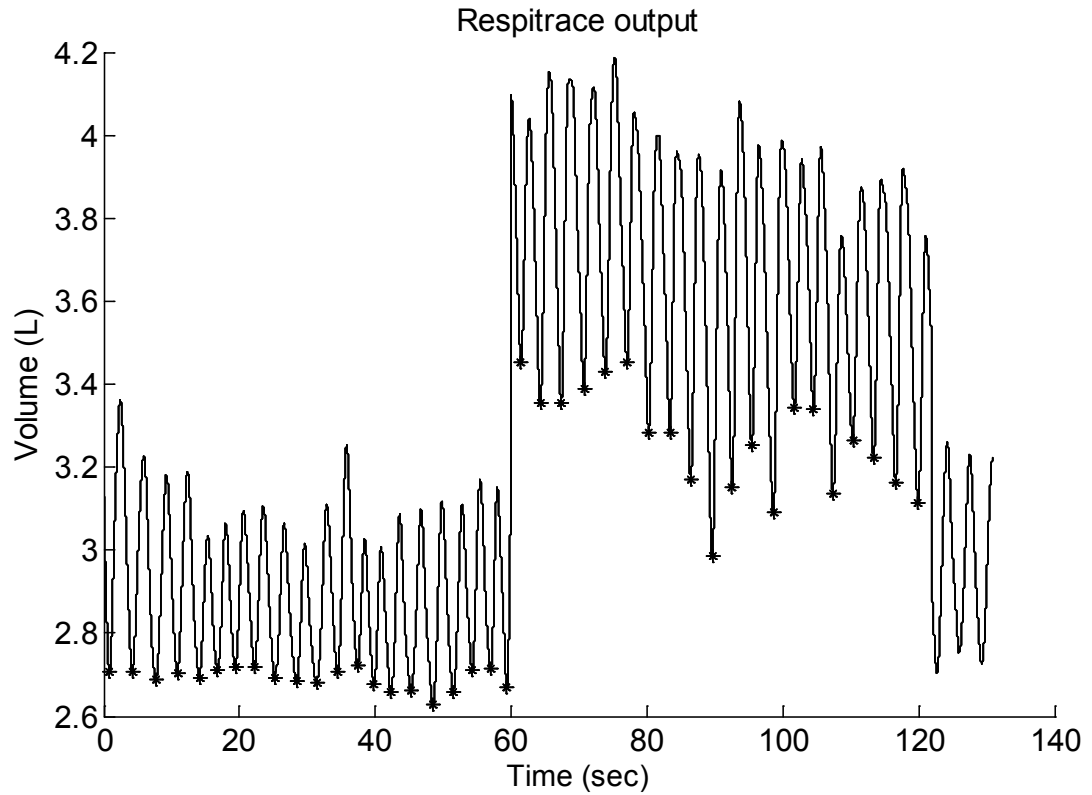


Figure 8.6: Respirace output in a representative asthmatic subject. Breath-to-breath variations in the FRC and the lung above FRC were obtained from the standard deviation of tidal volume minima indicated by stars on the tidal volume versus time recording.

Correlations between R_{rs} and R_{rsSD}

When we assessed the relationship between R_{rs} and R_{rsSD} at FRC, we found that R_{rs} strongly correlated to R_{rsSD} across all subjects with the slope of regression line of R_{rs} versus R_{rsSD} equal to 0.24 ($p < 0.001$) (Fig. 8.7).

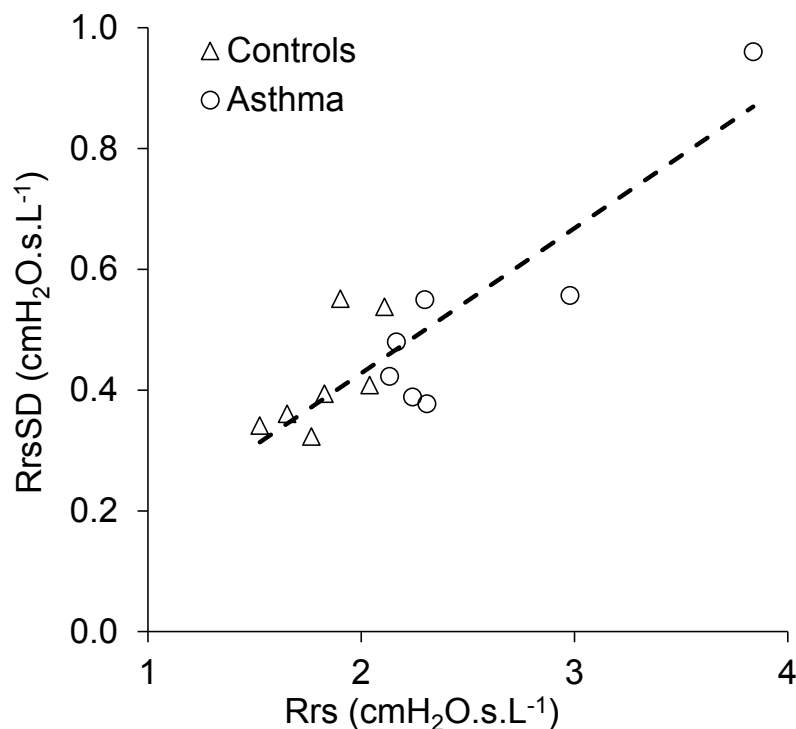


Figure 8.7: Baseline $R_{rs}SD$ versus R_{rs} in the controls ($n=7$) and subjects with asthma ($n=7$). $R_{rs}SD$ was linearly correlated to R_{rs} with slope of the relationship=0.24, $r^2=0.76$, $p < 0.001$.

8.4 Discussion

In this study, we investigated changes in $R_{rs}SD$ with changes in EELV from FRC in health and asthma, and hypothesized that in either health or asthma, $R_{rs}SD$ would increase with a reduction in lung volume and vice versa exhibiting dependence on lung volume similar to R_{rs} . While the well-known inverse lung volume dependence of R_{rs} was observed, we were unable to demonstrate the lung volume dependence of $R_{rs}SD$. In healthy subjects, $R_{rs}SD$ did not change with increasing EELV from FRC, but increased with a decrease of 1.2 L in EELV from FRC in 4 subjects (group CL2). On the other hand, in subjects with asthma, $R_{rs}SD$ increased with the increase of 540 ml in EELV from FRC (group AH1), and appeared to decrease with the decreases in lung volume from FRC (group AL1), although did not reach significance. The increases in $R_{rs}SD$ with EELV were likely due to difficulties in breathing normally at the altered lung volumes

using biofeedback. The subjects were unable to hold the altered EELV steady over the duration of measurements. Thus, while $R_{rs}SD$ was associated with R_{rs} with decreases in lung volume, because of the increased variability at higher lung volumes, we cannot discount that there might also be higher variability at the low lung volumes.

Interestingly, we found that variation of X_{rs} increased with decreases in lung volume in both healthy and asthmatic subjects. While this could simply be due to the unsteadiness in maintaining lung volume, it is also possible that it could have been due to increased temporal variability of heterogeneity of airway opening in peripheral regions with the decreases in lung volume from FRC. Small airways could limit airflow with narrowed diameters and thus would appear closed at the FOT oscillation frequencies, as the time constants for these paths became large relative to the oscillation period.

Baseline comparisons

While we were unable to investigate the relationship between $R_{rs}SD$ and R_{rs} at different end-expiratory lung volumes, we did find that the relationship between R_{rs} and $R_{rs}SD$ at baseline was consistent with our other studies in this thesis. Also consistent with previous reports [27, 153, 330], we found that R_{rs} was higher, and X_{rs} was more negative in asthmatics than in controls at baseline. Furthermore, variation of X_{rs} was also higher in asthmatics than in controls, however variation of R_{rs} did not differ between the two groups.

Changes in variation of R_{rs} and X_{rs} with lung volume

As expected, R_{rs} decreased when lung volume increased and vice versa, but, in majority of subjects $R_{rs}SD$ increased regardless of this lung volume dependence of R_{rs} . These findings were unexpected; indeed we predicted that at higher lung volumes, $R_{rs}SD$ would decrease, associated with the decreases in R_{rs} . The mostly likely explanation for this unpredicted behavior is that despite airway dilation at higher lung volumes, variation in R_{rs} increased due to additional noise, swamping any underlying correlation between $R_{rs}SD$ and R_{rs} . Even though the subjects raised their EELVs above FRC, they had difficulty in holding the new lung volume fairly steady for one minute. In fact there was variation in the lung volumes above FRC in the majority of the subjects. This was also

evidenced in the change in their breathing pattern at the increased EELV. This might have led to the slight increases in $R_{rs}SD$. Like at EELVs above FRC, $R_{rs}SD$ also increased with decreases in EELVs from FRC. Although this agreed with our hypothesis that decreases in airway diameter would increase variation in resistance, the increases in $R_{rs}SD$ may also have been due to increased variability in EELV when breathing below FRC.

We also hypothesized that in asthma, there would be a larger decrease in $R_{rs}SD$ at lower EELV than in controls. This would be because increased baseline ASM tone in asthma would reduce airway diameter further relative to control, thus at reduced lung volumes, R_{rs} may vary more in asthmatics than in controls due to the inverse quadratic dependence of resistance on airway diameter. While in groups CL1 and AL1, $R_{rs}SD$ increased with the decrease in EELVs, we did not find any significant difference. It may be that any difference were too small relative to contributions due to the variation in EELV. Therefore comparing increases in $R_{rs}SD$ between the two groups was not meaningful.

We also found that $X_{rs}SD$ was not different between healthy and asthmatic subjects, but it increased at EELVs below FRC in both groups without significant differences similar to $R_{rs}SD$. Two possibilities exist, either the increases in $X_{rs}SD$ were due to increases in noise as discussed above or it is possible that they resulted from increased temporal variation in spatial heterogeneity at reduced lung volume. Previously Gobbi et al. [230] found that variation in inspiratory X_{rs} increased with reduction in lung volume in health and asthma, but lung volume was reduced by chest wall strapping. The chest wall strapping might have restricted variation in EELV, thus implying that variation in X_{rs} is more related to a decrease in volume than increased variability in breathing pattern.

Correlations between R_{rs} and $R_{rs}SD$

The inverse relationship between R_{rs} and lung volume has been previously shown [342]. Theoretically an isotropic change in lung volume would lead to an inverse cubic dependence on linear dimension such as diameter, since resistance of a tube decreases proportional to length but increases to the 4th power of diameter. Due to this non-linear

transformation between changes in airway diameters and R_{rs} , even small decreases in airway diameters result in large increases in R_{rs} , and $R_{rs}SD$ may be linearly related to R_{rs} for purely geometric reasons. The linear association between R_{rs} and $R_{rs}SD$ has been consistently reported in previous studies in both adults [37, 38, 230] and children [39], and have also been found in our studies in Chapters 6 and 7 (Figures 6.8 and 7.4). The strong association between R_{rs} and $R_{rs}SD$ at FRC found in this study was in agreement with the literature and our results presented in Chapter 6 and 7.

Effect of lung volume changes on R_{rs}

Since we measured resistance and reactance of the total respiratory system, our measurements also contained contribution from the chest wall. Changes in R_{rs} with lung volume in both controls and asthmatics were consistent with the inverse volume dependence of R_{rs} found in the literature [124, 129, 342, 345]. At EELVs above FRC, changes in R_{rs} and X_{rs} can largely be accounted for by the changes in the lung resistance and reactance alone since the chest wall resistance and reactance are smaller at higher lung volumes [129]. However the chest wall resistance increases at lower lung volumes and would contribute a small increases to R_{rs} at reduced EELV [129].

When lung volume decreases due to derecruitment, airway closure, elastance of the lung increases. Therefore elastance increasingly dominates the reactance as lung volume decreases below FRC.

Effect of lung volume changes on X_{rs}

As anticipated, X_{rs} decreased with decreases in lung volume in both healthy and asthmatic subjects [129], indicating increased stiffness of the respiratory system at volumes below FRC. As lung volume decreases, it is known that derecruitment occurs with air space closure leading to an increase in elastance because of the reduced amount of communicating lung volume. Thus decreases in X_{rs} at volumes below FRC were likely reflective of lung volume de-recruitment [25] caused by, airway closure or near closure [24]. Furthermore, we found that in healthy subjects, X_{rs} decreased with increases in lung volume as well. This was likely reflective of stiffened lungs due to increases in

parenchymal tissue stiffness with alveolar stretching, increase in surface tension [346, 347] or increase in airway inertance with airway lengthening [134]. Studies in humans have shown that in accord with the shape of the quasi-static pressure-volume (P-V) curve, respiratory compliance decreases near TLC [348, 349]. Our increase in the negative X_{rs} in healthy subjects may mean that at lung volumes above FRC, the subjects were perhaps closer on the P-V curve where its slope starts decreasing with an increase in lung volume, and the lungs start becoming stiffer.

In asthmatics, X_{rs} did not alter with the increases in lung volume. This might have occurred because of increased variability and small sample size. However, the decreases in X_{rs} with lung volume in asthmatics suggest small-airway narrowing or closure. Small-airway narrowing or closure is known to be an important functional abnormality in asthma that can be found at FRC in both seated and supine postures [350]. Most convincing evidence of small-airway narrowing or closure is provided by imaging studies which have shown the occurrence of patchy areas of poor or non-existent ventilation in asthmatic lungs, called ventilation defects [19, 26, 351]. Heterogeneity and airspace closure are likely to be amplified with reduction in lung volume leading to further decreases in X_{rs} , and increases in E_{rs} observed in the asthmatic subjects in this study. Note that with the loss of communicating airspace with peripheral airway closure, some of the oscillations would be shunted to the airway wall, which would lead to the measured change in E_{rs} being less than due to the effects occurring in the lung periphery.

Limitations

This study had important methodological limitations which we address here. In order to assess the relationship between lung volume and short term variation of R_{rs} , we measured R_{rs} at FRC and at EELVs above and below FRC in individual subjects, using biofeedback to control lung volume. However, the majority of our subjects had difficulty holding their altered lung volumes as well as FRC. Moreover there was also large variability in end-expiratory lung volumes. In future, if anyone were to proceed to actually verify the lung volume dependence of $R_{rs}SD$, we would suggest perhaps doing it in animal models where animals could be mechanically ventilated to eliminate noise, and lung volumes could be regulated by adjusting peak end-expiratory pressure. It could also

be done in humans, but it is challenging for ethical reasons, and more importantly, scientific value of such an investigation is not warranted.

8.5 Conclusion

In conclusion, in this study we were unable to find if $R_{rs}SD$ exhibits dependence on end-expiratory lung volume. This was due to additional noise introduced in the data by difficulty in holding EELV. Variability of R_{rs} may be dependent on lung volume, however investigating this in wakeful humans is challenging. Nonetheless variation in R_{rs} may be probed in experimental animal models.

Chapter 9: Discussion

In this chapter, I summarize the work presented in this thesis, and discuss key findings. I also discuss physiological significance and implications of the findings. This is followed by the summary of original contributions made by this thesis. Lastly directions for future work are proposed.

9.1 Summary

9.1.1 Small-airway function and Lung mechanics

Chapter 3 used FOT and a computational model of the human lung to quantify the relative contributions of small and large airways to BD response in asthma. Using FOT, we found that following BD, E_{rs} decreased only in asthma, and with a magnitude similar to the decrease in R_{rs} . Importantly, we found that healthy subjects also responded to BD, but with a decrease in R_{rs} only, and no change in E_{rs} . We were able to explain these results using a multi-branch airway model that included small-airway occlusion and central-airway narrowing to account for *in vivo* mechanics in health and asthma. Using the model, we showed that in the asthmatics, BD caused the decrease in R_{rs} from both dilation of central airways and opening of small airways, whereas the decrease in E_{rs} following BD must have occurred nearly entirely from the opening of small airways. On the other hand, in the healthy subjects, the decrease in R_{rs} with BD was almost entirely due to the dilation of central airways. Together these results suggested that in their contribution to changes in respiratory mechanics i) the central airways were responsive to BD in both health and asthma in a remarkably similar degree, whereas the small airways were responsive only in asthma, and ii) low frequency X_{rs} and E_{rs} predicted from X_{rs} describe the behavior of the small airways better than R_{rs} , and are sensitive measures of airway function in asthma at the level of the small airways.

Continuing my modeling studies one step further, in Chapter 4 i) we investigated the effect of small-airway heterogeneity on E_{rs} and frequency dependence of R_{rs} over 0.2-

5 Hz and 5-20 Hz, and ii) computationally quantified the effect of upper airway shunt impedance on the impedance of respiratory system in asthma. In particular, using a relatively simple model, we reproduced much of the mechanics in 3 groups of subjects with either mild, moderate, or severe airway obstruction as previously published [27]. Here, although the models were multi-branched and composed of thousands of airways, I am using the term simple to describe the limited range of obstruction patterns I employed. This was done by closing the 10th generation airways to 10% of their initial diameters to account for the *in vivo* X_{rs} at 5 Hz, and narrowing remaining airways to account for the *in vivo* R_{rs} at 18 Hz. We chose this simple model of airway occlusion to easily enumerate the number of airways that needed to be occluded as a simple measure of airway heterogeneity, and by doing this, we found some interesting results. While we were able to produce frequency dependence of R_{rs} in the model which increased with small-airway heterogeneity, this frequency dependence was shifted a few Hz upward and leftward relative to *in vivo*. This difference is likely due to other factors not included in my model, and I suggest these are most likely either a more distributed pattern of airway narrowing, or a finite central-airway wall compliance, or both in combination. These factors could correct the frequency dependence to higher frequencies by broadening or altering the distribution of time constants of obstructed pathways in the model to slightly shorter time-scales than produced by 90% airway narrowing, or alternatively, by distributing the narrowing of the central airways to shift their effective time constants to slightly longer time scales. The frequency dependence of R_{rs} calculated as a difference in R_{rs} at two frequencies depended of course strongly on the frequency range used to compute the frequency dependence. By comparison, while E_{rs} increased with the imposed heterogeneity, accounting for the altered mechanics from mild to severe, the changes in E_{rs} were consistent, independent of the frequency range I simulated. The sensitivity of E_{rs} to small airways, and the specificity of its changes with BD to asthma, and its consistency indicated that E_{rs} may be more useful measure of airway heterogeneity, and a more distinguishing measure of the differences between health and asthma compared with either R_{rs} alone or the frequency dependence of R_{rs} in the FOT frequency range. This last point is especially true in mild or moderate asthma, where frequency dependence in the FOT range is very modest. Interestingly, this study also showed that the principle features

of lung mechanics, excepting the proper frequency range for frequency dependence of R_{rs} in asthma were reproduced in the airway tree model using a simple bimodal distribution of small-airway closure.

Examining the effect of upper airway shunt on the model impedance, we found that upper airway shunt led to a substantial decrease in R_{rs} in moderate and severe asthma at all frequencies. However and perhaps somewhat surprisingly, it did not have a major effect on the frequency dependence of R_{rs} . This was largely due to the greater impedance of the shunt pathway, and likely to the similarity in frequency dependence of the shunt to the measured R_{rs} in asthma leading to a largely parallel shift in R_{rs} .

In Chapters 3 and 4, for the first time we computationally quantified small-airway heterogeneity observed in asthmatic subjects using a simplified bimodal model of airway narrowing which provided a functional index as the number of airways occluded. An important and surprising finding of these studies is that reproducing the mechanics in asthma required occluding a substantial fraction of the small airways of the lung; 40-47% in mild, 67% in moderate, and 81% in severe asthma. This is much larger than that would be predicted from examining the ventilation defect volume in asthma reported in imaging studies [293, 294]. However as discussed in Section 2.10, others have been able to match the defect volumes prescribed by imaging, and predict the mechanics *in vivo* [23, 274] This was possible because they occluded the airspaces to match the imaging data restricting the defect volume to be the same, and then the important difference with my approach may be that they allowed the airways in the non-defective volume to be narrowed according to a distribution function, which would broaden the time-constant distribution, and may shift the frequency dependence of R_{rs} to match *in vivo* data. However it is important to note that FOT and imaging assesses the lung with different characteristic times. For example, ventilation imaging is usually done during a breath hold of 15-20 s, while the FOT frequency range is from 0.3 Hz and above using the optimal ventilator waveform or greater than 4 Hz for typical FOT implying time constants of less than 3 s or less than 0.25 s are probed with FOT. The long recording time in imaging allows the inhaled gas tracer to ventilate more of the lung regions with increasingly much longer time constants as the image is acquired. These regions would appear ventilated depending on the thresholds utilized, and thus could underestimate the

defect volume, relative to the mechanics interpreted from FOT frequencies. Since FOT operates at much shorter characteristic times, it should therefore be more sensitive to airway occlusions and likely predicts a larger defect volume, as we appear to indicate in our studies. To match the *in vivo* E_{rs} asthma, we applied 90% narrowing to the selected airways in a specific airway generation meaning that the closed regions had very long time constants, and the remaining regions had very short time constants. This also likely explains why our frequency dependence was shifted to lower frequencies relative to the *in vivo* data. This could be examined by distributing the central-airway narrowing permitting wider time-constant distributions. It is also worth mentioning here that since we restricted airway occlusions to a specific generation, the defect volumes should be closely related to the fraction of small airways occluded.

In Chapter 7, we found that E_{rs} was moderately correlated to asthma symptoms as measured by ACQ, whereas FEV_1 and ACQ score were not related. This suggests that small-airway dysfunction in asthma likely contributed to the expression of asthma symptoms, and lack of asthma control. How abnormalities in small airways lead to asthma symptoms is unclear. One possible explanation is that decreases in small-airway caliber increase the work of breathing due to an increase in resistive load [352]. In addition, the presence of even minimal peripheral airway heterogeneity leads to large heterogeneity when bronchoconstriction occurs [20]. Perhaps, the resultant increased stiffness of the respiratory system is perceived by patients as dyspnea and difficulty in breathing, which, which we directly measured by E_{rs} . Indeed increased stiffness is strongly associated with breathlessness during bronchoconstriction in asthma [353].

Together, this thesis showed that E_{rs} is a more useful indicator of the changes occurring in asthma, and reflects airway occlusion in asthma. It is likely also useful to note that while E_{rs} is determined by the elasticity of the parenchyma, its changes are not likely due to changes in any intrinsic tissue stiffness, but due to changes in E_{rs} from loss of communicating airspaces. This thesis reinforces the findings of other studies that X_{rs} is an important measure of airway function in asthma.

9.1.2 Variability of respiratory resistance and reactance

Chapter 6 and 7 studied temporal variability of R_{rs} (R_{rsSD}) and X_{rs} (X_{rsSD}) in healthy and asthmatic subjects following BD or methacholine. Like our lab and others have previously shown [38, 39], we found that R_{rsSD} was higher in asthmatic than in healthy subjects at low frequencies 4-5 Hz. Furthermore R_{rsSD} was altered with methacholine and BD only in asthmatics but not differently than R_{rs} . However, we also found that R_{rsSD} and R_{rs} followed a robust relationship that linearly scaled with bronchoconstriction and bronchodilation. This suggested that variability of R_{rs} was related to changes in airway diameters during breathing and to changes in lung volume. Our results indicated that because R_{rsSD} was well correlated with R_{rs} , R_{rsSD} did not provide any new information on airway calibre than R_{rs} in this study but we extend this result for the first time to include bronchodilator behaviour in adults.

Similar results were obtained for temporal variability in X_{rs} (X_{rsSD}), and its changes with methacholine and BD are reported here for the first time. We found that X_{rsSD} was higher in asthmatics than in healthy subjects, and was altered in response to methacholine and BD, but only in asthmatics. One of the possible mechanisms of temporal variation of X_{rs} in asthma may be variations in small-airway occlusions during inspiration and expiration. Note that this does not necessarily mean full airway collapse and closure, since all that is required is that the airways narrow sufficiently such that the effective time constant of a particular path to the distal parenchyma becomes too long and the airway is effectively closed to FOT oscillations. In our model in Chapters 4 and 5, we narrowed the airways to 90% which was more than sufficient to alter E_{rs} . Accordingly changes in X_{rsSD} with methacholine and BD are suggestive of temporal variations in spatial heterogeneity as peripheral airways narrow and dilate altering the observed mechanical stiffness of the lung, as the variations in small airways alter the effective time-constant distribution of the lung. While the clinical utility of X_{rsSD} is unknown, our findings do imply that X_{rsSD} is a characteristic feature of asthma.

A number of previous studies investigating the short term variation of impedance or resistance in healthy and asthmatic subjects reported inconsistent results. Some studies found that variation of R_{rs} or Z_{rs} was significantly higher in asthmatics than in normal

subjects [37-39] while others found no differences in the variation between the two groups [251]. On similar lines, our findings were also inconsistent. Chapter 6 found significantly higher $R_{rs}SD$ in asthmatics ($n=19$) than in healthy subjects ($n=19$) (asthma versus control, FEV_1 : 91.6 ± 3.5 SE % predicted versus 98.6 ± 3.1 % predicted, R_{rs} : 4.2 ± 0.65 versus 2.2 ± 0.16 $cmH_2O.s.L^{-1}$, $R_{rs}SD$: 0.99 ± 0.02 versus 0.46 ± 0.05 $cmH_2O.s.L^{-1}$ each respectively) whereas in a similar study with different subjects, Chapter 8 (control: $n=7$, asthma: $n=7$, of these subjects, 3 control and 6 asthmatic subjects were common to Chapter 6 and 8 studies), found no difference in variability between healthy and asthmatic subjects (asthma versus control, FEV_1 : 95.87 ± 3.9 versus 101.4 ± 4.4 % predicted, R_{rs} : 2.6 ± 0.24 versus 1.8 ± 0.08 $cmH_2O.s.L^{-1}$, $R_{rs}SD$: 0.53 ± 0.08 versus 0.42 ± 0.03 $cmH_2O.s.L^{-1}$). This was likely due to differences in subjects and number of subjects. The difference between the studies is also likely related to the differences in the degree of asthma control. In Chapter 6, 5 of 19 patients were uncontrolled while in Chapter 8, all patients ($n=7$) were well-controlled. This suggested that $R_{rs}SD$ may be a distinguishing feature of poorly controlled asthma. However, when we examined this hypothesis in the study presented in Chapter 6, we found that there was no correlation between asthma symptom score and $R_{rs}SD$. This might have occurred because of insufficient sample size, as we only had a few uncontrolled subjects. Future studies are warranted taking care to enrol subjects with a wide range of asthma control.

In summary, our studies report that while R_{rs} and X_{rs} were altered with methacholine and BD in both healthy and asthmatic subjects, variations in R_{rs} and X_{rs} were altered only in asthmatics. This suggests that variations in R_{rs} and X_{rs} , and their response to methacholine and BD may be distinguishing features of asthma. However, the changes in the variations were not different than the changes in mean R_{rs} and X_{rs} values. This suggests that while variability is a feature that is higher in asthma, and is altered with BD or methacholine, because it behaves similarly to R_{rs} and X_{rs} , the measurement of short term variability may not have any clinical value more than R_{rs} .

9.1.3 Removing artifacts using Wavelet Transforms

Chapter 6 presented a novel technique based on discrete wavelet transforms to eliminate FOT artifacts such as coughs, momentary glottis closures, swallows, and vocalizations. We found that artifacts could be removed using Daubechies wavelets by applying thresholds to squared detail coefficients of both pressure and flow signals. Cough artifacts were identified by thresholding 1st level wavelet coefficients and swallows could be identified using 2nd level wavelet coefficients of pressure signal with greater than 90% sensitivity and specificity. Furthermore, male vocalizations could be identified using 1st level wavelet coefficients of pressure with 88% sensitivity and 100% specificity. Lastly, airflow leaks at the mouth piece could be identified using 3rd level coefficients of flow signal with greater than 95% sensitivity and specificity.

This study showed that the artifacts could be removed using the wavelet transform based technique automatically with high sensitivity and specificity. It is recommended in commercial FOT devices which use sophisticated filtering and signal analyses algorithms to improve quality of data.

9.1.4 Variability of resistance with changes in lung volume

Chapter 8 attempted to assess the relationship between R_{rsSD} and lung volume by tracking variations in R_{rs} during breathing at lung volumes above and below FRC in health and asthma. In this study we found that R_{rsSD} was increased regardless of the sign of the changes in lung volume from FRC. This occurred likely due to variation in EELV which masked any suspected changes in R_{rsSD} with changes in lung volume from FRC. We also found that very few subjects were able to alter their lung volume from FRC and breathe steadily reproducibly keeping variation in EELV small from breath to breath. To avoid the noise introduced by variations in EELV during FOT measurements, it may be more appropriate to test this question in mechanically ventilated and anesthetized patients, although that has its limitations as well. While this study could be performed in asthma patients who are on mechanical ventilation for other reasons, this would be challenging. However it could be performed in animal models of asthma.

9.2 Significance and Implications

Reactance and airway dysfunction in asthma (Chapters 3, 4, and 6)

Chapter 3 and 6 studied E_{rs} derived from X_{rs} in response to BD and methacholine in asthma respectively, while Chapter 4 compared the sensitivity of FOT outcomes, E_{rs} and the frequency dependence of R_{rs} to small-airway heterogeneity in asthma. The sensitivity of X_{rs} and E_{rs} to changes in small airways has been previously demonstrated in animal models [25] and with computational modelling [24]. In the FOT studies (Chapters 3 and 6), we found that E_{rs} was significantly altered with methacholine and BD in asthma. This means that X_{rs} is a potentially clinically useful measure of airway function in asthma at the level of small airways.

Modeling the *in vivo* mechanics and its BD response in health and asthma (Chapter 3) revealed that the R_{rs} responded significantly to BD in both health and asthma, while the E_{rs} response to BD occurred only in asthma. Additionally the changes in R_{rs} that were attributable to central airways were nearly the same in health and in asthma. This is an important result as it revealed that in terms of their contribution to respiratory mechanics, central airways respond to BD perhaps indicating little change in the airway smooth muscle and its shortening ability in these airways in both health and asthma while small airways in asthma have a dysfunctional response. This finding emphasizes the importance for monitoring the effectiveness of treatments aimed at preventing and improving small-airway dysfunction in asthma. Furthermore, modeling changes in mechanics with increasing levels of airway obstruction (Chapter 4) revealed that small-airway heterogeneity was better associated with E_{rs} than frequency dependence of R_{rs} over 5-20 Hz. Together these interesting findings imply that tracking origins of airway dysfunction in asthma may be better performed using X_{rs} and associated measures than R_{rs} and associated measures.

Correlation between E_{rs} and asthma symptoms score (Chapter 7) suggests that heterogeneous narrowing and closure of small airways contributes to lack of asthma control. This implies that treatment in asthma should be aimed at improving small-airway function. Improvement in small-airway function may alleviate asthma symptoms, and improve asthma control. The association between E_{rs} and asthma symptoms also implies

E_{rs} is a potentially useful measure for monitoring patient's response to treatment and effectiveness of treatment.

Quantifying small-airway closure as a simple measure of heterogeneity in asthma (Chapters 3 and 4), we found that a significant fraction of lung was required to be essentially closed to model mechanics in patients with mild, moderate, or severe airway obstruction, and this volume was also much larger than that predicted by magnetic resonant imaging and computed tomography studies. This finding may be due in part to the different characteristic times of each measurement which may have implications for studies employing image guided modeling approaches to evaluate relationship between ventilation defects and dynamic lung function.

Overall these studies underscore the potential for FOT as a clinically useful tool for evaluating early small-airway obstruction and response to therapy in asthma. Importantly, these studies also suggest that asthma therapy should target small airways to prevent and reduce small-airway narrowing and closure.

Wavelet based Artifact Removal (Chapter 5)

In Chapter 5, we developed a novel technique based on discrete wavelet transform to remove artifacts in FOT recordings with high sensitivity and specificity. Application of this algorithm in a commercial device would likely be easy, and could yield fast and automatic removal of transient artifacts in impedance data.

Short term variability of R_{rs} and X_{rs} (Chapters 6 and 7)

While $R_{rs}SD$ was higher in asthma than in health, was responsive to methacholine and BD only in asthma, and also moderately correlated to AHR, there was a very strong association between R_{rs} and $R_{rs}SD$. Also changes in $R_{rs}SD$ were not different than those in R_{rs} . This implies that $R_{rs}SD$ may not convey any additional information than provided by R_{rs} . Although origins of $R_{rs}SD$ are not clearly understood, the strong linear association of variability of R_{rs} to mean R_{rs} suggest that fluctuations in R_{rs} during breathing may have a geometric origin, and both R_{rs} and its variation are related to airway diameter. It is possible that some of the increased variation in airway diameters in asthma may result from increased contractile activity of the ASM. However, this is perhaps much smaller

compared to breathing related changes in diameters, and any baseline level of variation in ASM activity and variation in R_{rs} with asthma is increased simply because airway diameters are reduced. This also implies that FOT performed during spontaneous breathing may not be a sensitive tool to assess changes in ASM activity that contributes to variability of airway function in asthma.

9.3 Original Contributions Made

This listing gives the novel contributions made by this dissertation including the novel data collected, models developed and the novel findings of studies in this dissertation.

- 1) I measured R_{rs} and X_{rs} pre and post BD in health and asthma, and modeled the *in vivo* mechanics using a three dimensional multi-branch airway tree model originally developed by Del Leary of our lab.
- 2) I modeled small-airway heterogeneity in asthmatic subjects by occluding selected airways in a single generation to 10% of their initial diameters. This matched the model X_{rs} to X_{rs} in asthma at low frequencies. I then matched the model R_{rs} to *in vivo* R_{rs} at low frequencies by narrowing remaining airways. This model could account for most of the changes in mechanics, and enabled the quantification of small-airway heterogeneity by enumerating the number of small airways occluded.
- 3) Comparing the model's response to simulated bronchodilation to the *in vivo* response, I found that the central airways were similarly responsive to BD in both health and asthma, while the small airways were responsive only in asthma, indicating that it was the BD response of the small airways that better distinguished asthma from health.

- 4) I showed E_{rs} was a sensitive measure of small-airway disease in asthma. This is an important finding as it implies a potential for X_{rs} in clinical settings to assess airway function and response to therapy in asthma.
- 5) Using the airway tree model, I modeled the respiratory mechanics in 3 groups of asthmatic subjects, those with either mild, moderate, or severe airway obstruction reported previously by Cavalcanti et al. [27] by imposing small-airway heterogeneity and central-airway narrowing in the model. I found that E_{rs} increased consistently when estimated at either 0.2 Hz or 5 Hz. On the other hand, while R_{rs} exhibited pronounced frequency dependence at very low frequencies, the frequency dependence was less in magnitude in the FOT range, than the changes in E_{rs} . Together, this indicates that E_{rs} was a more robust and sensitive measure of small-airway heterogeneity relative to the frequency dependence of R_{rs} in the FOT frequency range of 5-20 Hz.
- 6) Using the model, I enumerated number of airways required to be occluded to model small-airway heterogeneity in mild to severely obstructed patients with asthma. With this approach, I showed that occlusion of 40%, 67%, and 81% of the lung respectively accounted for the heterogeneity in mild, moderate, and severe asthma, and this was substantially larger than that reported by imaging studies.
- 7) Using the model, I quantified the effect of upper airway shunt impedance on respiratory impedance in mild, moderate, and severe asthma. I showed that shunt impedance did not affect frequency dependence of R_{rs} over both low frequency range of 0.2-5 Hz and FOT range of 5-20 Hz. Moreover the shunt also had no substantial effect on X_{rs} at 5 Hz, but it did lead to modest underestimation of X_{rs} at the lowest frequency, 0.2 Hz and its overestimating at the highest frequency, 20 Hz.
- 8) I found that E_{rs} was moderately associated with patient's asthma control assessed by ACQ score. While this was found in a small group of subjects, it may mean that lack of asthma control is related to small-airway disease in asthma.

- 9) I measured respiratory impedance in healthy adults wherein artifact causing events such as light coughs, swallows, momentary glottal narrowing caused by vocalizations, and airflow leaks were introduced in the measurement in a controlled manner.
- 10) I developed a discrete wavelet transform based algorithm to eliminate above said artifacts. I showed that the algorithm eliminated the controlled artifacts with high sensitivity and specificity. It could also satisfactorily eliminate spontaneous artifacts in healthy and asthmatic subjects, and may be useful in a commercial device.
- 11) I imaged the momentary glottis movement produced by short, lightly audible 'hee' sound during FOT in one healthy subject, and confirmed that vocalizations affect respiratory impedance values.
- 12) Previously Que et al. assessed the temporal variation in Z_{rs} in healthy subjects before and after a single dose of methacholine [38], and Diba et al. assessed variation in Z_{rs} during methacholine challenge also in healthy subjects only [37]. In this thesis, I assessed the short term temporal variation in R_{rs} and X_{rs} in both healthy and asthmatic subjects during methacholine challenge.
- 13) I presented the methacholine response of variation of R_{rs} in a dose-response curve showing variability versus increasing methacholine concentrations.
- 14) Previously Lall et al. [39] measured changes in variability of R_{rs} with BD in children with asthma, while this thesis measured changes in variability with BD in adult subjects with asthma.
- 15) I found that short term temporal variability in X_{rs} was higher in asthma than in healthy subjects, and increased with methacholine, and decreased with BD only in asthma.

16) I found that R_{rs} and X_{rs} were responsive to methacholine and BD in both health and asthma, but variability of R_{rs} and X_{rs} was responsive only in asthma. This suggested that temporal variations of R_{rs} and X_{rs} may be distinguishing features of methacholine and BD response of asthma.

9.4 Future Directions

This dissertation raised a number of interesting research questions. In this section, I briefly discuss these questions and suggest directions for future work.

- 1) Chapter 3 evaluated elastance derived from X_{rs} as a measure of small-airway obstruction in asthma highlighting the importance of small airways in the bronchodilator response in asthma. Since small airways are also locale of the early disease in chronic obstructive pulmonary disease (COPD), a similar investigation could be done in patients with COPD. Indeed BD is effective in COPD, and is administered as therapy. While altered X_{rs} in COPD is attributed to loss of elastic recoil, it also has a contribution from airflow limitation during normal breathing in some subjects [143]. The approach developed in this thesis may be able to estimate a component of the change in X_{rs} that can be ascribed to loss of parenchymal units, and contribute to the reduced elastic recoil. It may also be useful to assess changes in E_{rs} in COPD in response to a BD, to assess the effect of BD therapy on small-airway closure.
- 2) While we assessed the BD response of R_{rs} and E_{rs} in adult subjects with asthma, and noted that it was peripheral behavior that largely distinguished asthma from health, the same may not be true in children, who have less peripheral airspaces, and narrower central airways. Thus an interesting continuation could be to similarly apply this approach in children with asthma.

- 3) As discussed in Chapter 4, recent imaging studies demonstrate that obstructive diseases such as asthma and COPD are characterized by ventilation defects which are the regions receiving inadequate or no ventilation. These ventilation defects are known to be formed largely by obstruction, closure or near closure of small airways. Our results predicted greater degree of airway closure although required to account for the altered mechanics in asthma than reported generally using imaging methods. Our hypothesis for the difference is that the defect volume found in imaging approaches is smaller since images are taken over a long time, and areas with time constants from seconds to 15 or 20 s (the typical duration for acquisition) become ventilated during measurement. Thus, it would be interesting to assess if possible the role of breath hold duration on defect volume in imaging studies, and relate this to the changes in E_{rs} as determined from X_{rs} in FOT, and in particular employ FOT to lower frequencies representative of the characteristic time used for image acquisition. It would also be useful to correlate if the predicted changes in defect volume with BD from imaging then match the changes in E_{rs} from FOT.
- 4) One additional interesting future work would be to assess E_{rs} in poorly controlled asthma at baseline and following 2-3 months after changes in therapy to evaluate effect of changes in therapy on small-airway function and its relationship with lack of asthma control. If E_{rs} response to BD were positively associated with changes in therapy, then this would strongly indicate E_{rs} response to BD could be useful in improving asthma control, and should be tested in a prospective trial. This would be to test if E_{rs} response to BD can be used to guide a step-up in therapy. For example, if the BD response in E_{rs} is larger than a given threshold, the trial would increase therapy. This study would be designed similar to the study of Sont et al. who in their seminal study adjusted patients treatment based on their degree of AHR [354].
- 5) Chapter 4 imposed small-airway heterogeneity using a fairly simple approach that involved narrowing selected airways in a single generation to 10% of their initial diameters. This essentially led to a bimodal distribution of relative airway closure, and perhaps produced a somewhat bimodal and limited time-constant heterogeneity

than that exists *in vivo*. A further step would be to distribute closure using a wider distribution of narrowing and over multiple generations similar to Tgavalekos et al., Kaczka et al., and Campana et al. [23, 215, 274]. This will broaden the distribution of time constants, and may better account for frequency dependence of resistance. However, to address a useful index regarding the number of airways occluded, such as achievable when using the bimodal distribution, one would need to introduce a threshold for which airways would be considered narrowed. While this may fit the data better, it could lose something in its utility as an easily interpreted measure of small-airway disease. Also, we assumed rigid airway walls in the model. Including airway wall compliance will introduce more time constants in the pathways of the lung also broadening the time-constant distribution, and if this affected the frequency dependence in the proper frequency range, could allow a better fit to the impedance data.

- 6) In Chapter 5, a novel technique based on discrete wavelet transform was developed to automatically eliminate the most common FOT artifacts. A range of discrete wavelet coefficients thresholds were identified for the artifacts. However, this was done only in healthy adult subjects with and without asthma. It is possible that the coefficients may need to be adjusted based on much higher impedance values that are found in children. Thus a next step would be to identify thresholds for children, and verify if they are the same as those found in adults. Similarly it is possible that the threshold may vary among individuals with severe or uncontrolled asthma, or COPD. Thus another future direction for continuation of this work would be to determine wavelet thresholds for the artifacts according to patients' asthma severity or COPD.
- 7) Chapter 6 and 7 focused on determining R_{rsSD} to evaluate AHR, asthma control status, and response to BD in adult subjects with asthma. This study was performed in awake subjects. While some of the variation in R_{rs} in asthma is thought to originate from fluctuations in airway diameter due to excessive contraction of the airway smooth muscle, it is also known to be influenced by other factors such as body position, changes in glottal aperture and flow and volume changes. Variations in

airway diameters that occur during spontaneous breathing regulate variations in R_{rs} . It may be possible to assess the variability of R_{rs} in anesthetized and mechanically ventilated animals. This would eliminate breathing noise and other factors.

- 8) In our study examining variability in R_{rs} and X_{rs} in asthma, we also examined if there were differences between controlled and uncontrolled asthma. However, there were only a few subjects that were uncontrolled. It is possible that variability in uncontrolled asthma was higher, but the study was insufficiently powered to assess this. Thus although the difference may not be large, this may be a possible future study to evaluate $R_{rs}SD$ and its changes in naïve symptomatic or very poorly controlled subjects.
- 9) This dissertation assessed the relationship between asthma symptoms and variation in R_{rs} at a single visit (baseline). An interesting future step would be a longitudinal study that would assess variability in patients undergoing changes in asthma therapy. Thus, in addition to an initial measurement, a follow up measurement around 2 to 3 months following the initial measurement could be performed. This would help determine whether the adjustments in a patient's therapy have led to changes in variation in R_{rs} , and if these changes actually correlate with the patient's asthma control status.
- 10) Chapter 7 focussed on determining the relationship between variability of R_{rs} and end-expiratory lung volume. The study protocol required subjects to breathe on the FOT device at predetermined end-expiratory lung volumes above and below their FRC for one minute. Unfortunately, despite the large differences in the predetermined volumes, the variation in end-expiratory lung volume likely overshadowed any suspected dependence in variation in R_{rs} versus lung volume we sought to confirm. Very few subjects could achieve all target volumes and hold these volumes steady to test our hypothesis. Thus if the origin of variation in R_{rs} is unconsciously determined, it would be better to test this question in anesthetized and mechanically ventilated subjects while their lung volume is controlled by adjusting peak end-expiratory pressure. This would eliminate noise due to changes in end-expiratory lung volume

and, also the end-expiratory lung volume would be precisely set. However this would require a complex experimental set up including a mechanical ventilator. Also while some subjects with asthma have mechanical ventilation for elective surgeries, and this study may be feasible over time, the scientific value of this study may not be warranted in humans.

REFERENCES

- [1] Brown R H 2004 Marching to the beat of different drummers: individual airway response diversity *Eur Respir J* **24** 193-4
- [2] Sporik R, Holgate S T, Platts-Mills T A and Cogswell J J 1990 Exposure to house-dust mite allergen (Der p I) and the development of asthma in childhood. A prospective study *N Engl J Med* **323** 502-7
- [3] Bahadori K, Doyle-Waters M M, Marra C, Lynd L, Alasaly K, Swiston J and FitzGerald J M 2009 Economic burden of asthma: a systematic review *BMC Pulm Med* **9** 24
- [4] 1998 Worldwide variation in prevalence of symptoms of asthma, allergic rhinoconjunctivitis, and atopic eczema: ISAAC. The International Study of Asthma and Allergies in Childhood (ISAAC) Steering Committee *Lancet* **351** 1225-32
- [5] 1996 Variations in the prevalence of respiratory symptoms, self-reported asthma attacks, and use of asthma medication in the European Community Respiratory Health Survey (ECRHS) *Eur Respir J* **9** 687-95
- [6] Masoli M, Fabian D, Holt S, Beasley R and Program G I f A G 2004 The global burden of asthma: executive summary of the GINA Dissemination Committee report *Allergy* **59** 469-78
- [7] 2012 Asthma, 2012. (Canada: Statistics Canada)
- [8] Barnett S B and Nurmagambetov T A 2011 Costs of asthma in the United States: 2002-2007 *J Allergy Clin Immunol* **127** 145-52
- [9] 2012 Lung Disease Imposes Major Costs on Canada's Economy
- [10] Yanai M, Sekizawa K, Ohru T, Sasaki H and Takishima T 1992 Site of airway obstruction in pulmonary disease: direct measurement of intrabronchial pressure *J Appl Physiol* **72** 1016-23
- [11] Hamid Q, Song Y, Kotsimbos T C, Minshall E, Bai T R, Hegele R G and Hogg J C 1997 Inflammation of small airways in asthma *J Allergy Clin Immunol* **100** 44-51
- [12] Wagner E M, Bleecker E R, Permutt S and Liu M C 1998 Direct assessment of small airways reactivity in human subjects *Am J Respir Crit Care Med* **157** 447-52
- [13] Kaminsky D A, Irvin C G, Gurka D A, Feldsien D C, Wagner E M, Liu M C and Wenzel S E 1995 Peripheral airways responsiveness to cool, dry air in normal and asthmatic individuals *Am J Respir Crit Care Med* **152** 1784-90
- [14] Kaminsky D A, Irvin C G, Lundblad L, Moriya H T, Lang S, Allen J, Viola T, Lynn M and Bates J H 2004 Oscillation mechanics of the human lung periphery in asthma *J Appl Physiol* **97** 1849-58
- [15] Despas P J, Leroux M and Macklem P T 1972 Site of airway obstruction in asthma as determined by measuring maximal expiratory flow breathing air and a helium-oxygen mixture *J Clin Invest* **51** 3235-43
- [16] Tgavalekos N T, Musch G, Harris R S, Vidal Melo M F, Winkler T, Schroeder T, Callahan R, Lutchen K R and Venegas J G 2007 Relationship between airway

- narrowing, patchy ventilation and lung mechanics in asthmatics. *Eur Respir J* **29** 1174-81
- [17] in 't Veen J C, Beekman A J, Bel E H and Sterk P J 2000 Recurrent exacerbations in severe asthma are associated with enhanced airway closure during stable episodes *Am J Respir Crit Care Med* **161** 1902-6
- [18] King G G, Downie S R, Verbanck S, Thorpe C W, Berend N, Salome C M and Thompson B 2005 Effects of methacholine on small airway function measured by forced oscillation technique and multiple breath nitrogen washout in normal subjects *Respir Physiol Neurobiol* **148** 165-77
- [19] King G G, Eberl S, Salome C M, Young I H and Woolcock A J 1998 Differences in airway closure between normal and asthmatic subjects measured with single-photon emission computed tomography and technegas. *Am J Respir Crit Care Med* **158** 1900-6
- [20] Venegas J G, Winkler T, Musch G, Vidal Melo M F, Layfield D, Tgavalekos N, Fischman A J, Callahan R J, Bellani G and Harris R S 2005 Self-organized patchiness in asthma as a prelude to catastrophic shifts *Nature* **434** 777-82
- [21] King G G, Carroll J D, Muller N L, Whittall K P, Gao M, Nakano Y and Pare P D 2004 Heterogeneity of narrowing in normal and asthmatic airways measured by HRCT *Eur Respir J* **24** 211-8
- [22] Zeidler M R, Klerup E C, Goldin J G, Kim H J, Truong D A, Simmons M D, Sayre J W, Liu W, Elashoff R and Tashkin D P 2006 Montelukast improves regional air-trapping due to small airways obstruction in asthma *Eur Respir J* **27** 307-15
- [23] Tgavalekos N T, Tawhai M, Harris R S, Musch G, Mush G, Vidal-Melo M, Venegas J G and Lutchen K R 2005 Identifying airways responsible for heterogeneous ventilation and mechanical dysfunction in asthma: an image functional modeling approach. *J Appl Physiol* **99** 2388-97
- [24] Lutchen K R and Gillis H 1997 Relationship between heterogeneous changes in airway morphometry and lung resistance and elastance *J Appl Physiol* **83** 1192-201
- [25] Dellaca R L, Andersson Olerud M, Zannin E, Kostic P, Pompilio P P, Hedenstierna G, Pedotti A and Frykholm P 2009 Lung recruitment assessed by total respiratory system input reactance *Intensive Care Med* **35** 2164-72
- [26] Samee S, Altes T, Powers P, de Lange E E, Knight-Scott J, Rakes G, Mugler J P, Ciambotti J M, Alford B A, Brookeman J R and Platts-Mills T A 2003 Imaging the lungs in asthmatic patients by using hyperpolarized helium-3 magnetic resonance: assessment of response to methacholine and exercise challenge *J Allergy Clin Immunol* **111** 1205-11
- [27] Cavalcanti J V, Lopes A J, Jansen J M and Melo P L 2006 Detection of changes in respiratory mechanics due to increasing degrees of airway obstruction in asthma by the forced oscillation technique *Respir Med* **100** 2207-19
- [28] Cavalcanti J V, Lopes A J, Jansen J M and de Melo P L 2006 Using the forced oscillation technique to evaluate bronchodilator response in healthy volunteers and in asthma patients presenting a verified positive response *J Bras Pneumol* **32** 91-8

- [29] Van Noord J A, Smeets J, Clément J, Van de Woestijne K P and Demedts M 1994 Assessment of reversibility of airflow obstruction. *Am J Respir Crit Care Med* **150** 551-4
- [30] Van Noord J A, Clément J, Van de Woestijne K P and Demedts M 1991 Total respiratory resistance and reactance in patients with asthma, chronic bronchitis, and emphysema *Am Rev Respir Dis* **143** 922-7
- [31] Peslin R, Duvivier C, Gallina C and Cervantes P 1985 Upper airway artifact in respiratory impedance measurements *Am Rev Respir Dis* **132** 712-4
- [32] Thorpe C W and Bates J H 1997 Effect of stochastic heterogeneity on lung impedance during acute bronchoconstriction: a model analysis *J Appl Physiol* **82** 1616-25
- [33] Suki B and Frey U 2003 Temporal dynamics of recurrent airway symptoms and cellular random walk *J Appl Physiol (1985)* **95** 2122-7
- [34] Frey U, Maksym G and Suki B 2011 Temporal complexity in clinical manifestations of lung disease *J Appl Physiol* **110** 1723-31
- [35] Bellia V, Cibella F, Coppola P, Greco V, Insalaco G, Milone F, Oddo S and Peralta G 1984 Variability of peak expiratory flow rate as a prognostic index in asymptomatic asthma *Respiration* **46** 328-33
- [36] Troyanov S, Ghezzi H, Cartier A and Malo J L 1994 Comparison of circadian variations using FEV1 and peak expiratory flow rates among normal and asthmatic subjects *Thorax* **49** 775-80
- [37] Diba C, Salome C M, Reddel H K, Thorpe C W, Toelle B and King G G 2007 Short-term variability of airway caliber-a marker of asthma? *J Appl Physiol* **103** 296-304
- [38] Que C L, Kenyon C M, Olivenstein R, Macklem P T and Maksym G N 2001 Homeokinesis and short-term variability of human airway caliber *J Appl Physiol (1985)* **91** 1131-41
- [39] Lall C A, Cheng N, Hernandez P, Pianosi P T, Dali Z, Abouzied A and Maksym G N 2007 Airway resistance variability and response to bronchodilator in children with asthma *Eur Respir J* **30** 260-8
- [40] Teeter J G and Bleecker E R 1998 Relationship between airway obstruction and respiratory symptoms in adult asthmatics *Chest* **113** 272-7
- [41] Shingo S, Zhang J and Reiss T F 2001 Correlation of airway obstruction and patient-reported endpoints in clinical studies *Eur Respir J* **17** 220-4
- [42] Cowie R L, Underwood M F and Field S K 2007 Asthma symptoms do not predict spirometry *Can Respir J* **14** 339-42
- [43] Weibel E R 1984 *The Pathways for Oxygen: Structure and Function in the Mammalian Respiratory System*. (Cambridge, Mass.: Harvard University Press)
- [44] West J B 2008 *Respiratory Physiology The Essentials*: Lippincott Williams & Wilkins)
- [45] WEIBEL E R and GOMEZ D M 1962 Architecture of the human lung. Use of quantitative methods establishes fundamental relations between size and number of lung structures *Science* **137** 577-85
- [46] Weibel E R 1963 *Morphometry of the Human Lung* (New York: Academic Press)

- [47] Tawhai M H, Hunter P, Tschirren J, Reinhardt J, McLennan G and Hoffman E A 2004 CT-based geometry analysis and finite element models of the human and ovine bronchial tree *J Appl Physiol* **97** 2310-21
- [48] Bateman E D, Hurd S S, Barnes P J, Bousquet J, Drazen J M, FitzGerald M, Gibson P, Ohta K, O'Byrne P, Pedersen S E, Pizzichini E, Sullivan S D, Wenzel S E and Zar H J 2008 Global strategy for asthma management and prevention: GINA executive summary *Eur Respir J* **31** 143-78
- [49] Wagner E M, Liu M C, Weinmann G G, Permutt S and Bleecker E R 1990 Peripheral lung resistance in normal and asthmatic subjects *Am Rev Respir Dis* **141** 584-8
- [50] Holgate S T and Polosa R 2006 The mechanisms, diagnosis, and management of severe asthma in adults *Lancet* **368** 780-93
- [51] Vignola A M, Gagliardo R, Siena A, Chiappara G, Bonsignore M R, Bousquet J and Bonsignore G 2001 Airway remodeling in the pathogenesis of asthma *Curr Allergy Asthma Rep* **1** 108-15
- [52] Moreno R H, Hogg J C and Paré P D 1986 Mechanics of airway narrowing *Am Rev Respir Dis* **133** 1171-80
- [53] Macklem P T 1989 Mechanical factors determining maximum bronchoconstriction *Eur Respir J Suppl* **6** 516s-9s
- [54] Woolcock A J, Salome C M and Yan K 1984 The shape of the dose-response curve to histamine in asthmatic and normal subjects *Am Rev Respir Dis* **130** 71-5
- [55] Jubber A S, Foster R W, Hassan N A, Carpenter J R and Small R C 1993 Airway response to inhaled methacholine in normal human subjects *Pulm Pharmacol* **6** 177-84
- [56] Clough J B and Holgate S T 1989 The natural history of bronchial hyperresponsiveness *Clin Rev Allergy* **7** 257-78
- [57] Boulet L P 2003 Asymptomatic airway hyperresponsiveness: a curiosity or an opportunity to prevent asthma? *Am J Respir Crit Care Med* **167** 371-8
- [58] Taylor D R, Bateman E D, Boulet L P, Boushey H A, Busse W W, Casale T B, Chanez P, Enright P L, Gibson P G, de Jongste J C, Kerstjens H A, Lazarus S C, Levy M L, O'Byrne P M, Partridge M R, Pavord I D, Sears M R, Sterk P J, Stoloff S W, Szeffler S J, Sullivan S D, Thomas M D, Wenzel S E and Reddel H K 2008 A new perspective on concepts of asthma severity and control *Eur Respir J* **32** 545-54
- [59] Cockcroft D W and Swystun V A 1996 Asthma control versus asthma severity *J Allergy Clin Immunol* **98** 1016-8
- [60] *From the Global Strategy for Asthma Management and Prevention*, Global Initiative for Asthma (GINA) 2014. Available from: <http://www.ginasthma.org/>.
- [61] Hanania N A 2007 Revisiting asthma control: how should it best be defined? *Pulm Pharmacol Ther* **20** 483-92
- [62] Program N A E a P 2007 Expert Panel Report 3 (EPR-3): Guidelines for the Diagnosis and Management of Asthma-Summary Report 2007 *J Allergy Clin Immunol* **120** S94-138
- [63] Thomas M, Kay S, Pike J, Williams A, Rosenzweig J R, Hillyer E V and Price D 2009 The Asthma Control Test (ACT) as a predictor of GINA guideline-defined

- asthma control: analysis of a multinational cross-sectional survey *Prim Care Respir J* **18** 41-9
- [64] Stempel D A, McLaughlin T P, Stanford R H and Fuhlbrigge A L 2005 Patterns of asthma control: a 3-year analysis of patient claims *J Allergy Clin Immunol* **115** 935-9
- [65] Juniper E F, O'Byrne P M, Guyatt G H, Ferrie P J and King D R 1999 Development and validation of a questionnaire to measure asthma control *Eur Respir J* **14** 902-7
- [66] Juniper E F, Svensson K, Mörk A C and Ståhl E 2005 Measurement properties and interpretation of three shortened versions of the asthma control questionnaire *Respir Med* **99** 553-8
- [67] Nathan R A, Sorkness C A, Kosinski M, Schatz M, Li J T, Marcus P, Murray J J and Pendergraft T B 2004 Development of the asthma control test: a survey for assessing asthma control *J Allergy Clin Immunol* **113** 59-65
- [68] Liu A H, Zeiger R, Sorkness C, Mahr T, Ostrom N, Burgess S, Rosenzweig J C and Manjunath R 2007 Development and cross-sectional validation of the Childhood Asthma Control Test *J Allergy Clin Immunol* **119** 817-25
- [69] Juniper E F, Gruffydd-Jones K, Ward S and Svensson K 2010 Asthma Control Questionnaire in children: validation, measurement properties, interpretation *Eur Respir J* **36** 1410-6
- [70] Robertson C F, Rubinfeld A R and Bowes G 1992 Pediatric asthma deaths in Victoria: the mild are at risk *Pediatr Pulmonol* **13** 95-100
- [71] Ayres J G, Jyothish D and Ninan T 2004 Brittle asthma *Paediatr Respir Rev* **5** 40-4
- [72] Frey U and Suki B 2008 Complexity of chronic asthma and chronic obstructive pulmonary disease: implications for risk assessment, and disease progression and control *Lancet* **372** 1088-99
- [73] Busse W W 2011 Asthma diagnosis and treatment: filling in the information gaps *J Allergy Clin Immunol* **128** 740-50
- [74] 1987 Standards for the diagnosis and care of patients with chronic obstructive pulmonary disease (COPD) and asthma. This official statement of the American Thoracic Society was adopted by the ATS Board of Directors, November 1986 *Am Rev Respir Dis* **136** 225-44
- [75] Boulet L P, Becker A, Berube D, Beveridge R and Ernst P 1999 Canadian Asthma Consensus Report, 1999. Canadian Asthma Consensus Group *Cmaj* **161** S1-61
- [76] 2008 British Guideline on the Management of Asthma *Thorax* **63 Suppl 4** iv1-121
- [77] Goldstein M F, Veza B A, Dunsky E H, Dvorin D J, Belecanech G A and Haralabatos I C 2001 Comparisons of peak diurnal expiratory flow variation, postbronchodilator FEV(1) responses, and methacholine inhalation challenges in the evaluation of suspected asthma *Chest* **119** 1001-10
- [78] Crapo R O, Casaburi R, Coates A L, Enright P L, Hankinson J L, Irvin C G, MacIntyre N R, McKay R T, Wanger J S, Anderson S D, Cockcroft D W, Fish J E and Sterk P J 2000 Guidelines for methacholine and exercise challenge testing-

1999. This official statement of the American Thoracic Society was adopted by the ATS Board of Directors, July 1999 *Am J Respir Crit Care Med* **161** 309-29
- [79] Sears M R, Taylor D R, Print C G, Lake D C, Li Q Q, Flannery E M, Yates D M, Lucas M K and Herbison G P 1990 Regular inhaled beta-agonist treatment in bronchial asthma *Lancet* **336** 1391-6
- [80] Woolcock A J 1987 Epidemiologic methods for measuring prevalence of asthma *Chest* **91** 89S-92S
- [81] Sly P D and Robertson C F 1990 A review of pulmonary function testing in children *J Asthma* **27** 137-47
- [82] Fischl M A, Pitchenik A and Gardner L B 1981 An index predicting relapse and need for hospitalization in patients with acute bronchial asthma *N Engl J Med* **305** 783-9
- [83] B. W J 1995 *Pulmonary Pathophysiology The Essentials*: Williams & Wilkins)
- [84] Pellegrino R, Viegi G, Brusasco V, Crapo R O, Burgos F, Casaburi R, Coates A, van der Grinten C P, Gustafsson P, Hankinson J, Jensen R, Johnson D C, MacIntyre N, McKay R, Miller M R, Navajas D, Pedersen O F and Wanger J 2005 Interpretative strategies for lung function tests *Eur Respir J* **26** 948-68
- [85] Coates A L, Desmond K J, Demizio D and Allen P D 1994 Sources of variation in FEV1 *Am J Respir Crit Care Med* **149** 439-43
- [86] Enright P L, Lebowitz M D and Cockcroft D W 1994 Physiologic measures: pulmonary function tests. Asthma outcome *Am J Respir Crit Care Med* **149** S9-18
- [87] Mead J 1979 *The lung in transition between health and disease*, ed P Macklem and S Permutt (New York: Marcel Dekker Inc.) pp 43-51
- [88] Orehek J, Nicoli M M, Delpierre S and Beaupre A 1981 Influence of the previous deep inspiration on the spirometric measurement of provoked bronchoconstriction in asthma *Am Rev Respir Dis* **123** 269-72
- [89] Oostveen E, MacLeod D, Lorino H, Farré R, Hantos Z, Desager K, Marchal F and Measurements E T F o R I 2003 The forced oscillation technique in clinical practice: methodology, recommendations and future developments *Eur Respir J* **22** 1026-41
- [90] Parham W M, Shepard R H, Norman P S and Fish J E 1983 Analysis of time course and magnitude of lung inflation effects on airway tone: relation to airway reactivity *Am Rev Respir Dis* **128** 240-5
- [91] Malmberg P, Larsson K, Sundblad B M and Zhiping W 1993 Importance of the time interval between FEV1 measurements in a methacholine provocation test *Eur Respir J* **6** 680-6
- [92] Pellegrino R, Sterk P J, Sont J K and Brusasco V 1998 Assessing the effect of deep inhalation on airway calibre: a novel approach to lung function in bronchial asthma and COPD *Eur Respir J* **12** 1219-27
- [93] Skloot G, Permutt S and Togias A 1995 Airway hyperresponsiveness in asthma: a problem of limited smooth muscle relaxation with inspiration *J Clin Invest* **96** 2393-403
- [94] Delacourt C, Lorino H, Herve-Guillot M, Reinert P, Harf A and Housset B 2000 Use of the forced oscillation technique to assess airway obstruction and reversibility in children *Am J Respir Crit Care Med* **161** 730-6

- [95] Li J T 1995 Home peak expiratory flow rate monitoring in patients with asthma *Mayo Clin Proc* **70** 649-56
- [96] Reddel H K, Salome C M, Peat J K and Woolcock A J 1995 Which index of peak expiratory flow is most useful in the management of stable asthma? *Am J Respir Crit Care Med* **151** 1320-5
- [97] Apter A J, Affleck G, Reisine S T, Tennen H A, Barrows E, Wells M, Willard A and ZuWallack R L 1997 Perception of airway obstruction in asthma: sequential daily analyses of symptoms, peak expiratory flow rate, and mood *J Allergy Clin Immunol* **99** 605-12
- [98] Frey U, Brodbeck T, Majumdar A, Taylor D R, Town G I, Silverman M and Suki B 2005 Risk of severe asthma episodes predicted from fluctuation analysis of airway function *Nature* **438** 667-70
- [99] Lapp N L and Hyatt R E 1967 Some factors affecting the relationship of maximal expiratory flow to lung volume in health and disease *Dis Chest* **51** 475-81
- [100] McFadden E R and Linden D A 1972 A reduction in maximum mid-expiratory flow rate. A spirographic manifestation of small airway disease *Am J Med* **52** 725-37
- [101] Currie G P, Fardon T C and Lee D K 2005 The role of measuring airway hyperresponsiveness and inflammatory biomarkers in asthma *Ther Clin Risk Manag* **1** 83-92
- [102] Burgel P R, de Blic J, Chanez P, Delacourt C, Devillier P, Didier A, Dubus J C, Frachon I, Garcia G, Humbert M, Laurent F, Louis R, Magnan A, Mahut B, Perez T, Roche N, Tillie-Leblond I, Tunon de Lara M and Dusser D 2009 Update on the roles of distal airways in asthma *Eur Respir Rev* **18** 80-95
- [103] Sorkness R L, Bleecker E R, Busse W W, Calhoun W J, Castro M, Chung K F, Curran-Everett D, Erzurum S C, Gaston B M, Israel E, Jarjour N N, Moore W C, Peters S P, Teague W G, Wenzel S E and National Heart L n, and Blood Institute Severe Asthma Research Program 2008 Lung function in adults with stable but severe asthma: air trapping and incomplete reversal of obstruction with bronchodilation *J Appl Physiol* **104** 394-403
- [104] Quanjer P H, Weiner D J, Pretto J J, Brazzale D J and Boros P W 2013 Measurement of FEF_{25-75%} and FEF_{75%} does not contribute to clinical decision making *Eur Respir J*
- [105] Cockcroft D W, Killian D N, Mellon J J and Hargreave F E 1977 Bronchial reactivity to inhaled histamine: a method and clinical survey *Clin Allergy* **7** 235-43
- [106] Sterk P J, Fabbri L M, Quanjer P H, Cockcroft D W, O'Byrne P M, Anderson S D, Juniper E F and Malo J L 1993 Airway responsiveness. Standardized challenge testing with pharmacological, physical and sensitizing stimuli in adults. Report Working Party Standardization of Lung Function Tests, European Community for Steel and Coal. Official Statement of the European Respiratory Society *Eur Respir J Suppl* **16** 53-83
- [107] Chai H, Farr R S, Froehlich L A, Mathison D A, McLean J A, Rosenthal R R, Sheffer A L, Spector S L and Townley R G 1975 Standardization of bronchial inhalation challenge procedures *J Allergy Clin Immunol* **56** 323-7

- [108] Orehek J 1983 The concept of airway "sensitivity" and "reactivity" *Eur J Respir Dis Suppl* **131** 27-48
- [109] Sterk P J, Daniel E E, Zamel N and Hargreave F E 1985 Limited bronchoconstriction to methacholine using partial flow-volume curves in nonasthmatic subjects *Am Rev Respir Dis* **132** 272-7
- [110] Sterk P J and Bel E H 1989 Bronchial hyperresponsiveness: the need for a distinction between hypersensitivity and excessive airway narrowing *Eur Respir J* **2** 267-74
- [111] Enright P L, Lebowitz M D and Cockcroft D W 1994 Physiologic measures: pulmonary function tests. Asthma outcome *Am J Respir Crit Care Med* **149** S9-18; discussion S9-20
- [112] Cockcroft D W, Murdock K Y, Berscheid B A and Gore B P 1992 Sensitivity and specificity of histamine PC20 determination in a random selection of young college students *J Allergy Clin Immunol* **89** 23-30
- [113] Woolcock A J and King G 1995 Is there a specific phenotype for asthma? *Clin Exp Allergy* **25 Suppl 2** 3-7
- [114] Ramsdale E H, Morris M M, Roberts R S and Hargreave F E 1985 Asymptomatic bronchial hyperresponsiveness in rhinitis *J Allergy Clin Immunol* **75** 573-7
- [115] van Haren E H, Lammers J W, Festen J, Heijerman H G, Groot C A and van Herwaarden C L 1995 The effects of the inhaled corticosteroid budesonide on lung function and bronchial hyperresponsiveness in adult patients with cystic fibrosis *Respir Med* **89** 209-14
- [116] Ramsdale E H, Morris M M, Roberts R S and Hargreave F E 1984 Bronchial responsiveness to methacholine in chronic bronchitis: relationship to airflow obstruction and cold air responsiveness *Thorax* **39** 912-8
- [117] Tashkin D P, Altose M D, Connett J E, Kanner R E, Lee W W and Wise R A 1996 Methacholine reactivity predicts changes in lung function over time in smokers with early chronic obstructive pulmonary disease. The Lung Health Study Research Group *Am J Respir Crit Care Med* **153** 1802-11
- [118] Cockcroft D W, Marciniuk D D, Hurst T S, Cotton D J, Laframboise K F, McNab B D and Skomro R P 2001 Methacholine challenge: test-shortening procedures *Chest* **120** 1857-60
- [119] Cockcroft D W and Davis B E 2009 Diagnostic and therapeutic value of airway challenges in asthma *Curr Allergy Asthma Rep* **9** 247-53
- [120] Dubois A B, Brody A W, Lewis D H and Burgess B F, Jr. 1956 Oscillation mechanics of lungs and chest in man *J Appl Physiol* **8** 587-94
- [121] Daróczy B and Hantos Z 1982 An improved forced oscillatory estimation of respiratory impedance *Int J Biomed Comput* **13** 221-35
- [122] Delavault E, Saumon G and Georges R 1980 Characterization and validation of forced input method for respiratory impedance measurement *Respir Physiol* **40** 119-36
- [123] Lándsér F J, Nagles J, Demedts M, Billiet L and van de Woestijne K P 1976 A new method to determine frequency characteristics of the respiratory system *J Appl Physiol* **41** 101-6
- [124] Michaelson E D, Grassman E D and Peters W R 1975 Pulmonary mechanics by spectral analysis of forced random noise *J Clin Invest* **56** 1210-30

- [125] R F and D N 1991 Mechanical impedance of the forced excitation generator in respiratory impedance measurements *Eur Respir Rev.* **1** 132–8
- [126] Ducharme F M, Davis G M and Ducharme G R 1998 Pediatric reference values for respiratory resistance measured by forced oscillation *Chest* **113** 1322-8
- [127] Brown N J, Xuan W, Salome C M, Berend N, Hunter M L, Musk A W, James A L and King G G 2010 Reference equations for respiratory system resistance and reactance in adults. *Respir Physiol Neurobiol* **172** 162-8
- [128] Oostveen E, Boda K, van der Grinten C P, James A L, Young S, Nieland H and Hantos Z 2013 Respiratory impedance in healthy subjects: baseline values and bronchodilator response *Eur Respir J* **42** 1513-23
- [129] Nagels J, Lãndsér F J, van der Linden L, Clément J and Van de Woestijne K P 1980 Mechanical properties of lungs and chest wall during spontaneous breathing *J Appl Physiol* **49** 408-16
- [130] Navajas D, Farre R, Rotger M M, Milic-Emili J and Sanchis J 1988 Effect of body posture on respiratory impedance *J Appl Physiol* **64** 194-9
- [131] Duggan C J, Watson R A and Pride N B 2004 Postural changes in nasal and pulmonary resistance in subjects with asthma *J Asthma* **41** 701-7
- [132] Grimby G, Takishima T, Graham W, Macklem P and Mead J 1968 Frequency dependence of flow resistance in patients with obstructive lung disease *J Clin Invest* **47** 1455-65
- [133] Daroczy B and Hantos Z 1990 Generation of optimum pseudorandom signals for respiratory impedance measurements *Int J Biomed Comput* **25** 21-31
- [134] Peslin R, and J. J. Fredberg ed 1986 *Oscillation mechanics of the respiratory system* vol III (Bethesda: American Physiological Society)
- [135] Beydon N, Davis S D, Lombardi E, Allen J L, Arets H G, Aurora P, Bisgaard H, Davis G M, Ducharme F M, Eigen H, Gappa M, Gaultier C, Gustafsson P M, Hall G L, Hantos Z, Healy M J, Jones M H, Klug B, Lodrup Carlsen K C, McKenzie S A, Marchal F, Mayer O H, Merkus P J, Morris M G, Oostveen E, Pillow J J, Seddon P C, Silverman M, Sly P D, Stocks J, Tepper R S, Viložni D and Wilson N M 2007 An official American Thoracic Society/European Respiratory Society statement: pulmonary function testing in preschool children *Am J Respir Crit Care Med* **175** 1304-45
- [136] Lãndsér F J, Clément J and Van de Woestijne K P 1982 Normal values of total respiratory resistance and reactance determined by forced oscillations: influence of smoking. *Chest* **81** 586-91
- [137] Finucane K E, Dawson S V, Phelan P D and Mead J 1975 Resistance of intrathoracic airways of healthy subjects during periodic flow *J Appl Physiol* **38** 517-30
- [138] Clément J, Dumoulin B, Gubbelmans R, Hendriks S and van de Woestijne K P 1987 Reference values of total respiratory resistance and reactance between 4 and 26 Hz in children and adolescents aged 4-20 years *Bull Eur Physiopathol Respir* **23** 441-8
- [139] Cuijpers C E, Wesseling G, Swaen G M and Wouters E F 1993 Frequency dependence of oscillatory resistance in healthy primary school children *Respiration* **60** 149-54

- [140] Otis A B, McKerrow C B, Bartlett R A, Mead J, McIlroy M B, Selver-Stone N J and Radford E P, Jr. 1956 Mechanical factors in distribution of pulmonary ventilation *J Appl Physiol* **8** 427-43
- [141] Mead J 1969 Contribution of compliance of airways to frequency-dependent behavior of lungs *J Appl Physiol* **26** 670-3
- [142] Mount L E 1955 The ventilation flow-resistance and compliance of rat lungs *J Physiol* **127** 157-67
- [143] Dellacà R L, Santus P, Aliverti A, Stevenson N, Centanni S, Macklem P T, Pedotti A and Calverley P M 2004 Detection of expiratory flow limitation in COPD using the forced oscillation technique. *Eur Respir J* **23** 232-40
- [144] Macklem P T 1971 Airway obstruction and collateral ventilation *Physiol Rev* **51** 368-436
- [145] Hantos Z, Daróczy B, Suki B, Galgóczy G and Csendes T 1986 Forced oscillatory impedance of the respiratory system at low frequencies *J Appl Physiol* **60** 123-32
- [146] Navajas D, Farré R, Canet J, Rotger M and Sanchis J 1990 Respiratory input impedance in anesthetized paralyzed patients *J Appl Physiol* **69** 1372-9
- [147] Lutchen K R, Yang K, Kaczka D W and Suki B 1993 Optimal ventilation waveforms for estimating low-frequency respiratory impedance *J Appl Physiol* **75** 478-88
- [148] Kaczka D W, Ingenito E P, Suki B and Lutchen K R 1997 Partitioning airway and lung tissue resistances in humans: effects of bronchoconstriction. *J Appl Physiol* **82** 1531-41
- [149] Kaczka D W, Ingenito E P, Israel E and Lutchen K R 1999 Airway and lung tissue mechanics in asthma. Effects of albuterol. *Am J Respir Crit Care Med* **159** 169-78
- [150] Kaczka D W, Ingenito E P and Lutchen K R 1999 Technique to determine inspiratory impedance during mechanical ventilation: implications for flow limited patients *Ann Biomed Eng* **27** 340-55
- [151] Fredberg J J, Keefe D H, Glass G M, Castile R G and Frantz I D 1984 Alveolar pressure nonhomogeneity during small-amplitude high-frequency oscillation *J Appl Physiol* **57** 788-800
- [152] Fredberg J J, Ingram R H, Castile R G, Glass G M and Drazen J M 1985 Nonhomogeneity of lung response to inhaled histamine assessed with alveolar capsules *J Appl Physiol* **58** 1914-22
- [153] Clément J, Ländsér F J and Van de Woestijne K P 1983 Total resistance and reactance in patients with respiratory complaints with and without airways obstruction. *Chest* **83** 215-20
- [154] Di Mango A M, Lopes A J, Jansen J M and Melo P L 2006 Changes in respiratory mechanics with increasing degrees of airway obstruction in COPD: detection by forced oscillation technique *Respir Med* **100** 399-410
- [155] Hayden M J, Petak F, Hantos Z, Hall G and Sly P D 1998 Using low-frequency oscillation to detect bronchodilator responsiveness in infants *Am J Respir Crit Care Med* **157** 574-9
- [156] Zerah F, Lorino A M, Lorino H, Harf A and Macquin-Mavier I 1995 Forced oscillation technique vs spirometry to assess bronchodilatation in patients with asthma and COPD *Chest* **108** 41-7

- [157] Wouters E F, Verschoof A C, Polko A H and Visser B F 1989 Impedance measurements of the respiratory system before and after salbutamol in COPD patients *Respir Med* **83** 309-13
- [158] Park J W, Lee Y W, Jung Y H, Park S E and Hong C S 2007 Impulse oscillometry for estimation of airway obstruction and bronchodilation in adults with mild obstructive asthma *Ann Allergy Asthma Immunol* **98** 546-52
- [159] Yaegashi M, Yalamanchili V A, Kaza V, Weedon J, Heurich A E and Akerman M J 2007 The utility of the forced oscillation technique in assessing bronchodilator responsiveness in patients with asthma *Respir Med* **101** 995-1000
- [160] Nair A, Ward J and Lipworth B J 2011 Comparison of bronchodilator response in patients with asthma and healthy subjects using spirometry and oscillometry *Ann Allergy Asthma Immunol* **107** 317-22
- [161] Lutchen K R, Hantos Z, Peták F, Adamicza A and Suki B 1996 Airway inhomogeneities contribute to apparent lung tissue mechanics during constriction *J Appl Physiol* **80** 1841-9
- [162] Lundblad L K, Thompson-Figueroa J, Allen G B, Rinaldi L, Norton R J, Irvin C G and Bates J H 2007 Airway hyperresponsiveness in allergically inflamed mice: the role of airway closure *Am J Respir Crit Care Med* **175** 768-74
- [163] Walker P P, Hadcroft J, Costello R W and Calverley P M 2009 Lung function changes following methacholine inhalation in COPD *Respir Med* **103** 535-41
- [164] Larsen G L, Morgan W, Heldt G P, Mauger D T, Boehmer S J, Chinchilli V M, Lemanske R F, Martinez F, Strunk R C, Szeffler S J, Zeiger R S, Taussig L M, Bacharier L B, Guilbert T W, Radford S, Sorkness C A and Childhood Asthma Research and Education Network of the National Heart L n, and Blood Institute 2009 Impulse oscillometry versus spirometry in a long-term study of controller therapy for pediatric asthma *J Allergy Clin Immunol* **123** 861-7.e1
- [165] Kelly V J, Brown N J, Sands S A, Borg B M, King G G and Thompson B R 2012 Effect of airway smooth muscle tone on airway distensibility measured by the forced oscillation technique in adults with asthma *J Appl Physiol* **112** 1494-503
- [166] Duiverman E J, Neijens H J, Van der Snee-van Smaalen M and Kerrebijn K F 1986 Comparison of forced oscillometry and forced expirations for measuring dose-related responses to inhaled methacholine in asthmatic children. *Bull Eur Physiopathol Respir* **22** 433-6
- [167] van Noord J A, Clement J, van de Woestijne K P and Demedts M 1989 Total respiratory resistance and reactance as a measurement of response to bronchial challenge with histamine. *Am Rev Respir Dis* **139** 921-6
- [168] Marchal F, Schweitzer C and Khallouf S 2003 Respiratory conductance response to a deep inhalation in children with exercise-induced bronchoconstriction *Respir Med* **97** 921-7
- [169] Bhagat R G and Grunstein M M 1984 Comparison of responsiveness to methacholine, histamine, and exercise in subgroups of asthmatic children *Am Rev Respir Dis* **129** 221-4
- [170] Wesseling G J, Vanderhoven-Augustin I M and Wouters E F 1993 Forced oscillation technique and spirometry in cold air provocation tests *Thorax* **48** 254-9

- [171] Pennings H J and Wouters E F 1997 Effect of inhaled beclomethasone dipropionate on isocapnic hyperventilation with cold air in asthmatics, measured with forced oscillation technique *Eur Respir J* **10** 665-71
- [172] Snashall P D, Parker S, Ten Haave P, Simmons D and Noble M I 1991 Use of an impedance meter for measuring airways responsiveness to histamine *Chest* **99** 1183-5
- [173] Pairon J C, Iwatsubo Y, Hubert C, Lorino H, Nouaigui H, Gharbi R and Brochard P 1994 Measurement of bronchial responsiveness by forced oscillation technique in occupational epidemiology *Eur Respir J* **7** 484-9
- [174] Weersink E J, vd Elshout F J, van Herwaarden C V and Folgering H 1995 Bronchial responsiveness to histamine and methacholine measured with forced expirations and with the forced oscillation technique *Respir Med* **89** 351-6
- [175] Mansur A H, Manney S and Ayres J G 2008 Methacholine-induced asthma symptoms correlate with impulse oscillometry but not spirometry *Respir Med* **102** 42-9
- [176] Desager K N, Buhr W, Willemen M, van Bever H P, de Backer W, Vermeire P A and Lándsér F J 1991 Measurement of total respiratory impedance in infants by the forced oscillation technique *J Appl Physiol* **71** 770-6
- [177] Srikasibhandha S 1983 [Measurement of respiratory resistance in newborn infants with the oscillation method] *Anaesthetist* **32** 214-8
- [178] Badia J R, Farré R, Montserrat J M, Ballester E, Hernandez L, Rotger M, Rodriguez-Roisin R and Navajas D 1998 Forced oscillation technique for the evaluation of severe sleep apnoea/hypopnoea syndrome: a pilot study *Eur Respir J* **11** 1128-34
- [179] Navajas D, Farré R, Rotger M, Badia R, Puig-de-Morales M and Montserrat J M 1998 Assessment of airflow obstruction during CPAP by means of forced oscillation in patients with sleep apnea. *Am J Respir Crit Care Med* **157** 1526-30
- [180] Van de Woestijne K P 1993 The forced oscillation technique in intubated, mechanically-ventilated patients *Eur Respir J* **6** 767-9
- [181] Peslin R, Felicio da Silva J, Duvivier C and Chabot F 1993 Respiratory mechanics studied by forced oscillations during artificial ventilation. *Eur Respir J* **6** 772-84
- [182] Farre R, Rotger M and Navajas D 1991 Time-domain digital filter to improve signal-to-noise ratio in respiratory impedance measurements *Med Biol Eng Comput* **29** 18-24
- [183] Cauberghs M and Van de Woestijne K P 1989 Effect of upper airway shunt and series properties on respiratory impedance measurements *J Appl Physiol* **66** 2274-9
- [184] Peslin R, Duvivier C, Didelon J and Gallina C 1985 Respiratory impedance measured with head generator to minimize upper airway shunt *J Appl Physiol* **59** 1790-5
- [185] Uchida A, Ito S, Suki B, Matsubara H and Hasegawa Y 2013 Influence of cheek support on respiratory impedance measured by forced oscillation technique *Springerplus* **2** 342
- [186] Wheatley J R and Amis T C 1998 Mechanical properties of the upper airway *Curr Opin Pulm Med* **4** 363-9

- [187] Peslin R, Duvivier C and Jardin P 1984 Upper airway walls impedance measured with head plethysmograph *J Appl Physiol Respir Environ Exerc Physiol* **57** 596-600
- [188] Engel L A ed 1986 *Dynamic Distribution of Gas Flow* vol III (Bethesda, MD: American Physiological Society)
- [189] Scott R and L.J. G 1994 The assessment of cardiogenic interference on respiratory input impedance measurements and attempts to minimize effects using adaptive filtering *Eur. Respir. Review* **4** 126-9
- [190] Suki B, Peslin R, Duvivier C and Farré R 1989 Lung impedance in healthy humans measured by forced oscillations from 0.01 to 0.1 Hz *J Appl Physiol (1985)* **67** 1623-9
- [191] Hall G L, Hantos Z, Peták F, Wildhaber J H, Tiller K, Burton P R and Sly P D 2000 Airway and respiratory tissue mechanics in normal infants *Am J Respir Crit Care Med* **162** 1397-402
- [192] Lutchen K R, Suki B, Zhang Q, Petak F, Daroczy B and Hantos Z 1994 Airway and tissue mechanics during physiological breathing and bronchoconstriction in dogs *J Appl Physiol* **77** 373-85
- [193] Downie S R, Salome C M, Verbanck S, Thompson B R, Berend N and King G G 2013 Effect of methacholine on peripheral lung mechanics and ventilation heterogeneity in asthma *J Appl Physiol (1985)* **114** 770-7
- [194] Kjeldgaard J M, Hyde R W, Speers D M and Reichert W W 1976 Frequency dependence of total respiratory resistance in early airway disease *Am Rev Respir Dis* **114** 501-8
- [195] Hantos Z, Daróczy B, Suki B and Nagy S 1987 Low-frequency respiratory mechanical impedance in the rat. p 36
- [196] Gillis H L and Lutchen K R 1999 How heterogeneous bronchoconstriction affects ventilation distribution in human lungs: a morphometric model *Ann Biomed Eng* **27** 14-22
- [197] Lutchen K R, Greenstein J L and Suki B 1996 How inhomogeneities and airway walls affect frequency dependence and separation of airway and tissue properties *J Appl Physiol (1985)* **80** 1696-707
- [198] Bates J H, Decramer M, Zin W A, Harf A, Milic-Emili J and Chang H K 1986 Respiratory resistance with histamine challenge by single-breath and forced oscillation methods *J Appl Physiol* **61** 873-80
- [199] Bates J H, Ludwig M S, Sly P D, Brown K, Martin J G and Fredberg J J 1988 Interrupter resistance elucidated by alveolar pressure measurement in open-chest normal dogs *J Appl Physiol* **65** 408-14
- [200] Bates J H, Abe T, Romero P V and Sato J 1989 Measurement of alveolar pressure in closed-chest dogs during flow interruption *J Appl Physiol* **67** 488-92
- [201] Tomioka S, Bates J H and Irvin C G 2002 Airway and tissue mechanics in a murine model of asthma: alveolar capsule vs. forced oscillations *J Appl Physiol* **93** 263-70
- [202] Hirai T, McKeown K A, Gomes R F and Bates J H 1999 Effects of lung volume on lung and chest wall mechanics in rats *J Appl Physiol* **86** 16-21

- [203] Similowski T and Bates J H 1991 Two-compartment modelling of respiratory system mechanics at low frequencies: gas redistribution or tissue rheology? *Eur Respir J* **4** 353-8
- [204] Ludwig M S, Dreshaj I, Solway J, Munoz A and Ingram R H 1987 Partitioning of pulmonary resistance during constriction in the dog: effects of volume history *J Appl Physiol* **62** 807-15
- [205] Hantos Z, Daróczy B, Suki B, Nagy S and Fredberg J J 1992 Input impedance and peripheral inhomogeneity of dog lungs *J Appl Physiol* **72** 168-78
- [206] Fredberg J J and Stamenovic D 1989 On the imperfect elasticity of lung tissue *J Appl Physiol* **67** 2408-19
- [207] Kapsali T, Permutt S, Laube B, Scichilone N and Togias A 2000 Potent bronchoprotective effect of deep inspiration and its absence in asthma *J Appl Physiol* **89** 711-20
- [208] Hantos Z, Adamicza A, Govaerts E and Daróczy B 1992 Mechanical impedances of lungs and chest wall in the cat *J Appl Physiol* **73** 427-33
- [209] Gomes R F, Shen X, Ramchandani R, Tepper R S and Bates J H 2000 Comparative respiratory system mechanics in rodents *J Appl Physiol* **89** 908-16
- [210] Wagers S, Lundblad L K, Ekman M, Irvin C G and Bates J H 2004 The allergic mouse model of asthma: normal smooth muscle in an abnormal lung? *J Appl Physiol* **96** 2019-27
- [211] Allen G and Bates J H 2004 Dynamic mechanical consequences of deep inflation in mice depend on type and degree of lung injury *J Appl Physiol* **96** 293-300
- [212] Takubo Y, Guerassimov A, Ghezzi H, Triantafillopoulos A, Bates J H, Hoidal J R and Cosio M G 2002 Alpha1-antitrypsin determines the pattern of emphysema and function in tobacco smoke-exposed mice: parallels with human disease *Am J Respir Crit Care Med* **166** 1596-603
- [213] Suki B, Yuan H, Zhang Q and Lutchen K R 1997 Partitioning of lung tissue response and inhomogeneous airway constriction at the airway opening *J Appl Physiol* **82** 1349-59
- [214] Kaczka D W, Hager D N, Hawley M L and Simon B A 2005 Quantifying mechanical heterogeneity in canine acute lung injury: impact of mean airway pressure *Anesthesiology* **103** 306-17
- [215] Kaczka D W, Brown R H and Mitzner W 2009 Assessment of heterogeneous airway constriction in dogs: a structure-function analysis *J Appl Physiol* **106** 520-30
- [216] Kaczka D W, Ingenito E P, Body S C, Duffy S E, Mentzer S J, DeCamp M M and Lutchen K R 2001 Inspiratory lung impedance in COPD: effects of PEEP and immediate impact of lung volume reduction surgery *J Appl Physiol* **90** 1833-41
- [217] Kaczka D W, Lutchen K R and Hantos Z 2011 Emergent behavior of regional heterogeneity in the lung and its effects on respiratory impedance *J Appl Physiol (1985)* **110** 1473-81
- [218] Kaczka D W, Massa C B and Simon B A 2007 Reliability of estimating stochastic lung tissue heterogeneity from pulmonary impedance spectra: a forward-inverse modeling study *Ann Biomed Eng* **35** 1722-38

- [219] Mead J, Turner J M, Macklem P T and Little J B 1967 Significance of the relationship between lung recoil and maximum expiratory flow *J Appl Physiol* **22** 95-108
- [220] Mead J, Takishima T and Leith D 1970 Stress distribution in lungs: a model of pulmonary elasticity *J Appl Physiol* **28** 596-608
- [221] James A L and Wenzel S 2007 Clinical relevance of airway remodelling in airway diseases *Eur Respir J* **30** 134-55
- [222] BUTLER J, CARO C G, ALCALA R and DUBOIS A B 1960 Physiological factors affecting airway resistance in normal subjects and in patients with obstructive respiratory disease *J Clin Invest* **39** 584-91
- [223] Vincent N J, Knudson R, Leith D E, Macklem P T and Mead J 1970 Factors influencing pulmonary resistance *J Appl Physiol* **29** 236-43
- [224] Nadel J A and Tierney D F 1961 Effect of a previous deep inspiration on airway resistance in man *J Appl Physiol* **16** 717-9
- [225] Shen X, Gunst S J and Tepper R S 1997 Effect of tidal volume and frequency on airway responsiveness in mechanically ventilated rabbits *J Appl Physiol* **83** 1202-8
- [226] Bates J H, Schuessler T F, Dolman C and Eidelman D H 1997 Temporal dynamics of acute isovolume bronchoconstriction in the rat *J Appl Physiol* **82** 55-62
- [227] Ding D J, Martin J G and Macklem P T 1987 Effects of lung volume on maximal methacholine-induced bronchoconstriction in normal humans *J Appl Physiol* **62** 1324-30
- [228] Meinero M, Coletta G, Dutto L, Milanese M, Nova G, Sciolla A, Pellegrino R and Brusasco V 2007 Mechanical response to methacholine and deep inspiration in supine men *J Appl Physiol (1985)* **102** 269-75
- [229] Torchio R, Gulotta C, Ciacco C, Perboni A, Guglielmo M, Crosa F, Zerbini M, Brusasco V, Hyatt R E and Pellegrino R 2006 Effects of chest wall strapping on mechanical response to methacholine in humans *J Appl Physiol* **101** 430-8
- [230] Gobbi A, Pellegrino R G, Gulotta C, Antonelli A, Pompilio P P, Crimi C, Torchio R, Dutto L, Parola P, Dellaca R L and Brusasco V 2013 SHORT-TERM VARIABILITY OF RESPIRATORY IMPEDANCE AND EFFECT OF DEEP BREATH IN ASTHMATIC AND HEALTHY SUBJECTS WITH AIRWAY SMOOTH MUSCLE ACTIVATION AND UNLOADING *J Appl Physiol*
- [231] Nagase T, Martin J G and Ludwig M S 1993 Comparative study of mechanical interdependence: effect of lung volume on Raw during induced constriction *J Appl Physiol* **75** 2500-5
- [232] Bates J H, Lauzon A M, Dechman G S, Maksym G N and Schuessler T F 1994 Temporal dynamics of pulmonary response to intravenous histamine in dogs: effects of dose and lung volume *J Appl Physiol* **76** 616-26
- [233] Cheung D, Schot R, Zwinderman A H, Zagers H, Dijkman J H and Sterk P J 1997 Relationship between loss in parenchymal elastic recoil pressure and maximal airway narrowing in subjects with alpha1-antitrypsin deficiency *Am J Respir Crit Care Med* **155** 135-40
- [234] Gold W M, Kaufman H S and Nadel J A 1967 Elastic recoil of the lungs in chronic asthmatic patients before and after therapy *J Appl Physiol* **23** 433-8

- [235] Woolcock A J and Read J 1968 The static elastic properties of the lungs in asthma *Am Rev Respir Dis* **98** 788-94
- [236] Finucane K E and Colebatch H J 1969 Elastic behavior of the lung in patients with airway obstruction *J Appl Physiol* **26** 330-8
- [237] McCarthy D S and Sigurdson M 1980 Lung elastic recoil and reduced airflow in clinically stable asthma *Thorax* **35** 298-302
- [238] Pellegrino R, Wilson O, Jenouri G and Rodarte J R 1996 Lung mechanics during induced bronchoconstriction *J Appl Physiol* **81** 964-75
- [239] Brusasco V, Pellegrino R, Violante B and Crimi E 1992 Relationship between quasi-static pulmonary hysteresis and maximal airway narrowing in humans *J Appl Physiol* **72** 2075-80
- [240] Moreno R H, Dahlby R, Hogg J C and Pare P D 1985 Increased airway responsiveness caused by airway cartilage softening in rabbits *Am. Rev. Respir. Dis.*)
- [241] Moreno R H, Lisboa C, Hogg J C and Paré P D 1993 Limitation of airway smooth muscle shortening by cartilage stiffness and lung elastic recoil in rabbits *J Appl Physiol* **75** 738-44
- [242] Que C L, Kolmaga C, Durand L G, Kelly S M and Macklem P T 2002 Phonspirometry for noninvasive measurement of ventilation: methodology and preliminary results *J Appl Physiol* **93** 1515-26
- [243] Kleiger R E, Miller J P, Bigger J T and Moss A J 1987 Decreased heart rate variability and its association with increased mortality after acute myocardial infarction *Am J Cardiol* **59** 256-62
- [244] Gimeno F, van der Weele L T, Koeter G H, de Monchy J G and van Altena R 1993 Variability of forced oscillation (Siemens Siregnost FD 5) measurements of total respiratory resistance in patients and healthy subjects *Ann Allergy* **71** 56-60
- [245] Timmins S C, Coatsworth N, Palnitkar G, Thamrin C, Farrow C E, Schoeffel R E, Berend N, Diba C, Salome C M and King G G 2013 Day-to-day variability of oscillatory impedance and spirometry in asthma and COPD *Respir Physiol Neurobiol* **185** 416-24
- [246] Timonen K L, Randell J T, Salonen R O and Pekkanen J 1997 Short-term variations in oscillatory and spirometric lung function indices among school children *Eur Respir J* **10** 82-7
- [247] Goldman M D, Carter R, Klein R, Fritz G, Carter B and Pachucki P 2002 Within- and between-day variability of respiratory impedance, using impulse oscillometry in adolescent asthmatics *Pediatr Pulmonol* **34** 312-9
- [248] Trubel H and Banikol W K 2005 Variability analysis of oscillatory airway resistance in children *Eur J Appl Physiol* **94** 364-70
- [249] Cauberghe M and Van de Woestijne K P 1992 Changes of respiratory input impedance during breathing in humans *J Appl Physiol* **73** 2355-62
- [250] Irvin C G 2003 Lung volume: a principle determinant of airway smooth muscle function *Eur Respir J* **22** 3-5
- [251] Muskulus M, Slats A M, Sterk P J and Verduyn-Lunel S 2010 Fluctuations and determinism of respiratory impedance in asthma and chronic obstructive pulmonary disease *J Appl Physiol* **109** 1582-91

- [252] Leary D, Bhatawadekar S A, Parraga G and Maksym G N 2012 Modeling stochastic and spatial heterogeneity in a human airway tree to determine variation in respiratory system resistance *J Appl Physiol* **112** 167-75
- [253] Reindl K, Falliers C, Halberg F, Chai H, Hillman D and Nelson W 1969 Circadian acrophase in peak expiratory flow rate and urinary electrolyte excretion of asthmatic children: phase shifting of rhythms by prednisone given in different circadian system phases *Rass Neurol Veg* **23** 5-26
- [254] Reinberg A and Gervais P 1972 Circadian rhythms in respiratory functions, with special reference to human chronophysiology and chronopharmacology *Bull Physiopathol Respir (Nancy)* **8** 663-77
- [255] Hetzel M R and Clark T J 1980 Comparison of normal and asthmatic circadian rhythms in peak expiratory flow rate *Thorax* **35** 732-8
- [256] Boezen H M, Schouten J P, Postma D S and Rijcken B 1995 Relation between respiratory symptoms, pulmonary function and peak flow variability in adults *Thorax* **50** 121-6
- [257] Thamrin C, Stern G, Strippoli M P, Kuehni C E, Suki B, Taylor D R and Frey U 2009 Fluctuation analysis of lung function as a predictor of long-term response to beta2-agonists *Eur Respir J* **33** 486-93
- [258] Suki B, Bates J H T and Frey U 2011 *Comprehensive Physiology*: John Wiley & Sons, Inc.)
- [259] Cernelc M, Suki B, Reinmann B, Hall G L and Frey U 2002 Correlation properties of tidal volume and end-tidal O₂ and CO₂ concentrations in healthy infants *J Appl Physiol (1985)* **92** 1817-27
- [260] Kotaru C, Coreno A, Skowronski M, Muswick G, Gilkeson R C and McFadden E R 2005 Morphometric changes after thermal and methacholine bronchoprovocations. *J Appl Physiol* **98** 1028-36
- [261] Brown R H, Croisille P, Mudge B, Diemer F B, Permutt S and Togias A 2000 Airway narrowing in healthy humans inhaling methacholine without deep inspirations demonstrated by HRCT *Am J Respir Crit Care Med* **161** 1256-63
- [262] Ballester E, Reyes A, Roca J, Guitart R, Wagner P D and Rodriguez-Roisin R 1989 Ventilation-perfusion mismatching in acute severe asthma: effects of salbutamol and 100% oxygen *Thorax* **44** 258-67
- [263] Murata K, Itoh H, Senda M, Todo G, Yonekura Y and Torizuka K 1986 Ventilation imaging with positron emission tomography and nitrogen 13 *Radiology* **158** 303-7
- [264] Brown R H, Georgakopoulos J and Mitzner W 1998 Individual canine airways responsiveness to aerosol histamine and methacholine in vivo *Am J Respir Crit Care Med* **157** 491-7
- [265] Downie S R, Salome C M, Verbanck S, Thompson B, Berend N and King G G 2007 Ventilation heterogeneity is a major determinant of airway hyperresponsiveness in asthma, independent of airway inflammation *Thorax* **62** 684-9
- [266] Hardaker K M, Downie S R, Kermode J A, Farah C S, Brown N J, Berend N, King G G and Salome C M 2011 Predictors of airway hyperresponsiveness differ between old and young patients with asthma *Chest* **139** 1395-401

- [267] Altes T A, Powers P L, Knight-Scott J, Rakes G, Platts-Mills T A, de Lange E E, Alford B A, Mugler J P and Brookeman J R 2001 Hyperpolarized ^3He MR lung ventilation imaging in asthmatics: preliminary findings. *J Magn Reson Imaging* **13** 378-84
- [268] Bayat S, Porra L, Suhonen H, Suortti P and Sovijärvi A R 2009 Paradoxical conducting airway responses and heterogeneous regional ventilation after histamine inhalation in rabbit studied by synchrotron radiation CT. *J Appl Physiol* **106** 1949-58
- [269] Thomas A C, Kaushik S S, Nouls J, Potts E N, Slipetz D M, Foster W M and Driehuys B 2012 Effects of corticosteroid treatment on airway inflammation, mechanics, and hyperpolarized ^3He magnetic resonance imaging in an allergic mouse model. *J Appl Physiol* **112** 1437-44
- [270] Gillis H L and Lutchen K R 1999 Airway remodeling in asthma amplifies heterogeneities in smooth muscle shortening causing hyperresponsiveness *J Appl Physiol* **86** 2001-12
- [271] Lutchen K R, Jensen A, Atileh H, Kaczka D W, Israel E, Suki B and Ingenito E P 2001 Airway constriction pattern is a central component of asthma severity: the role of deep inspirations *Am J Respir Crit Care Med* **164** 207-15
- [272] Brown R H and Mitzner W 2003 Functional imaging of airway narrowing *Respir Physiol Neurobiol* **137** 327-37
- [273] Tgavalekos N T, Venegas J G, Suki B and Lutchen K R 2003 Relation between structure, function, and imaging in a three-dimensional model of the lung *Ann Biomed Eng* **31** 363-73
- [274] Campana L, Kenyon J, Zhalehdoust-Sani S, Tzeng Y S, Sun Y, Albert M and Lutchen K R 2009 Probing airway conditions governing ventilation defects in asthma via hyperpolarized MRI image functional modeling. *J Appl Physiol* **106** 1293-300
- [275] Anafi R C and Wilson T A 2001 Airway stability and heterogeneity in the constricted lung *J Appl Physiol (1985)* **91** 1185-92
- [276] Cauberghs M and Van de Woestijne K P 1983 Mechanical properties of the upper airway *J Appl Physiol Respir Environ Exerc Physiol* **55** 335-42
- [277] Burgel P R 2011 The role of small airways in obstructive airway diseases *Eur Respir Rev* **20** 23-33
- [278] Lutchen K R, Greenstein J L and Suki B 1996 How inhomogeneities and airway walls affect frequency dependence and separation of airway and tissue properties *J Appl Physiol* **80** 1696-707
- [279] Bates J H T 2009 *Lung Mechanics: An Inverse Modeling Approach* (Cambridge, UK; New York: Cambridge University Press)
- [280] Bhatwadekar S A, Leary D, Chen Y, Ohishi J, Hernandez P, Brown T, McParland C and Maksym G N 2013 A study of artifacts and their removal during forced oscillation of the respiratory system *Ann Biomed Eng* **41** 990-1002
- [281] Davey B L and Bates J H 1993 Regional lung impedance from forced oscillations through alveolar capsules *Respir Physiol* **91** 165-82
- [282] Schuessler T F and Bates J H 1995 A computer-controlled research ventilator for small animals: design and evaluation *IEEE Trans Biomed Eng* **42** 860-6

- [283] Miller M R, Hankinson J, Brusasco V, Burgos F, Casaburi R, Coates A, Crapo R, Enright P, van der Grinten C P, Gustafsson P, Jensen R, Johnson D C, MacIntyre N, McKay R, Navajas D, Pedersen O F, Pellegrino R, Viegi G, Wanger J and Force A E T 2005 Standardisation of spirometry. *Eur Respir J* **26** 319-38
- [284] Quanjer P H, Stanojevic S, Cole T J, Baur X, Hall G L, Culver B H, Enright P L, Hankinson J L, Ip M S, Zheng J, Stocks J and Initiative E G L F 2012 Multi-ethnic reference values for spirometry for the 3-95-yr age range: the global lung function 2012 equations *Eur Respir J* **40** 1324-43
- [285] Tawhai M H, Nash M P, Lin C L and Hoffman E A 2009 Supine and prone differences in regional lung density and pleural pressure gradients in the human lung with constant shape *J Appl Physiol* **107** 912-20
- [286] Leary D, Winkler T, Braune A and Maksym G N 2014 Effects of airway tree asymmetry on the emergence and spatial persistence of ventilation defects *J Appl Physiol (1985)*
- [287] Barnas G M, Yoshino K, Stamenovic D, Kikuchi Y, Loring S H and Mead J 1989 Chest wall impedance partitioned into rib cage and diaphragm-abdominal pathways *J Appl Physiol* **66** 350-9
- [288] Barnas G M, Yoshino K, Loring S H and Mead J 1987 Impedance and relative displacements of relaxed chest wall up to 4 Hz *J Appl Physiol* **62** 71-81
- [289] Morris J F, Koski A and Johnson L C 1971 Spirometric standards for healthy nonsmoking adults. *Am Rev Respir Dis* **103** 57-67
- [290] Morris J F 1976 Spirometry in the evaluation of pulmonary function. *West J Med* **125** 110-8
- [291] Bhatawadekar S A, Leary D and Maksym G N 2015 Modelling resistance and reactance with heterogeneous airway narrowing in mild to severe asthma *Canadian Journal of Physiology and Pharmacology*
- [292] Vignola A M, Mirabella F, Costanzo G, Di Giorgi R, Gjomarkaj M, Bellia V and Bonsignore G 2003 Airway remodeling in asthma *Chest* **123** 417S-22S
- [293] Svenningsen S, Kirby M, Starr D, Leary D, Wheatley A, Maksym G N, McCormack D G and Parraga G 2013 Hyperpolarized (3) He and (129) Xe MRI: differences in asthma before bronchodilation *J Magn Reson Imaging* **38** 1521-30
- [294] Thomen R P, Sheshadri A, Quirk J D, Kozlowski J, Ellison H D, Szczesniak R D, Castro M and Woods J C 2014 Regional Ventilation Changes in Severe Asthma after Bronchial Thermoplasty with (3)He MR Imaging and CT *Radiology* 140080
- [295] B. W J 2008 *Respiratory Physiology The Essentials*: Lippincott Williams & Wilkins)
- [296] Verbanck S, Schuermans D, Van Muylem A, Paiva M, Noppen M and Vincken W 1997 Ventilation distribution during histamine provocation *J Appl Physiol (1985)* **83** 1907-16
- [297] Woolcock A J, Vincent N J and Macklem P T 1969 Frequency dependence of compliance as a test for obstruction in the small airways *J Clin Invest* **48** 1097-106
- [298] Yamaguchi M, Niimi A, Ueda T, Takemura M, Matsuoka H, Jinnai M, Otsuka K, Oguma T, Takeda T, Ito I, Matsumoto H, Hirai T, Chin K and Mishima M 2009 Effect of inhaled corticosteroids on small airways in asthma: investigation using impulse oscillometry *Pulm Pharmacol Ther* **22** 326-32

- [299] Goldman M D, Saadeh C and Ross D 2005 Clinical applications of forced oscillation to assess peripheral airway function *Respir Physiol Neurobiol* **148** 179-94
- [300] Smith H, Reinhold P and Goldman M 2005 "Forced oscillation technique and impulse oscillometry" *European Respiratory Monograph* **31** 72-105
- [301] Leary D, Winkler T, Braune A and Maksym G N 2014 Effects of airway tree asymmetry on the emergence and spatial persistence of ventilation defects *J Appl Physiol* **117** 353-62
- [302] Barnas G M, Yoshino K, Fredberg J, Kikuchi Y, Loring S H and Mead J 1990 Total and local impedances of the chest wall up to 10 Hz *J Appl Physiol (1985)* **68** 1409-14
- [303] Greenblatt E E, Butler J P, Venegas J G and Winkler T 2014 Pendelluft in the bronchial tree *J Appl Physiol (1985)* **117** 979-88
- [304] Amin S. and B. S 2014 Spatial Organization of Constriction Pattern Contributes to Apparent Airway Hyperresponsiveness And Inter-subject Variability in Response to Challenge and Dilation. In: *Biomedical Engineering Society, 2014 Annual Meeting*, (San Antonio, TX, USA: Biomedical Engineering Society) pp P-Fri-507
- [305] Maki B E 1986 Interpretation of the coherence function when using pseudorandom inputs to identify nonlinear systems *IEEE Trans Biomed Eng* **33** 775-9
- [306] Que C L, Kenyon C M, Olivenstein R, Macklem P T and Maksym G N Homeokinesis and short-term variability of human airway caliber **91** 1131-41
- [307] Schweitzer C, Chone C and Marchal F 2003 Influence of data filtering on reliability of respiratory impedance and derived parameters in children. *Pediatr Pulmonol* **36** 502-8
- [308] Addison P 2005 Wavelet transforms and the ECG: a review. *Physiol Meas* **26** R155-99
- [309] Khalil M and Duchêne J 2000 Uterine EMG analysis: a dynamic approach for change detection and classification. *IEEE Trans Biomed Eng* **47** 748-56
- [310] Petrosian A P D, Homan R, Dasheiff R, Wunsch D 2000 Recurrent neural network based prediction of epileptic seizures in intra- and extracranial EEG **30** 201-18
- [311] Kandaswamy A, Kumar C S, Ramanathan R P, Jayaraman S and Malmurugan N 2004 Neural classification of lung sounds using wavelet coefficients *Comput Biol Med* **34** 523-37
- [312] Lándsér F J, Nagels J, Clément J and Van de Woestijne K P 1976 Errors in the measurement of total respiratory resistance and reactance by forced oscillations. *Respir Physiol* **28** 289-301
- [313] Marchal F, Schweitzer C, Demoulin B, Choné C and Peslin R 2004 Filtering artefacts in measurements of forced oscillation respiratory impedance in young children. *Physiol Meas* **25** 1153-66
- [314] Robinson P D, Turner M, Brown N J, Salome C, Berend N, Marks G B and King G G 2011 Procedures to improve the repeatability of forced oscillation measurements in school-aged children. *Respir Physiol Neurobiol* **177** 199-206

- [315] Dellacà R L, Duffy N, Pompilio P P, Aliverti A, Koulouris N G, Pedotti A and Calverley P M 2007 Expiratory flow limitation detected by forced oscillation and negative expiratory pressure. *Eur Respir J* **29** 363-74
- [316] Franken H, Clément J and Van de Woestijne K P 1983 Systematic and random errors in the determination of respiratory impedance by means of the forced oscillation technique: a theoretical study *IEEE Trans Biomed Eng* **30** 642-51
- [317] Peslin R, Duvivier C and Gallina C 1985 Total respiratory input and transfer impedances in humans *J Appl Physiol* **59** 492-501
- [318] Bijaoui E, Baconnier P F and Bates J H 2001 Mechanical output impedance of the lung determined from cardiogenic oscillations *J Appl Physiol* **91** 859-65
- [319] Ståhl E 2000 Correlation between objective measures of airway calibre and clinical symptoms in asthma: a systematic review of clinical studies *Respir Med* **94** 735-41
- [320] Woolcock A J, Peat J K, Salome C M, Yan K, Anderson S D, Schoeffel R E, McCowage G and Killalea T 1987 Prevalence of bronchial hyperresponsiveness and asthma in a rural adult population *Thorax* **42** 361-8
- [321] Juniper E F, Guyatt G H, Epstein R S, Ferrie P J, Jaeschke R and Hiller T K 1992 Evaluation of impairment of health related quality of life in asthma: development of a questionnaire for use in clinical trials *Thorax* **47** 76-83
- [322] Riccioni G, D'Orazio N, Di Ilio C, Della Vecchia R, Ballone E, Menna V and Guagnano M T 2003 Bronchial hyperresponsiveness and quality of life in asthmatics *Respiration* **70** 496-9
- [323] 1995 Standardization of Spirometry, 1994 Update. American Thoracic Society. *Am J Respir Crit Care Med* **152** 1107-36
- [324] GOLDMAN H I and BECKLAKE M R 1959 Respiratory function tests; normal values at median altitudes and the prediction of normal results *Am Rev Tuberc* **79** 457-67
- [325] Juniper E F, Cockcroft D W and Hargreave F E 1994 *Histamine and Methacholine inhalation tests: Tidal breathing method. Laboratory procedure and standardization.* (Lund, Sweden: Astra Draco AB)
- [326] Hargreave F E, Ryan G, Thomson N C, O'Byrne P M, Latimer K, Juniper E F and Dolovich J 1981 Bronchial responsiveness to histamine or methacholine in asthma: measurement and clinical significance *J Allergy Clin Immunol* **68** 347-55
- [327] Wilson R C and Jones P W 1989 A comparison of the visual analogue scale and modified Borg scale for the measurement of dyspnoea during exercise *Clin Sci (Lond)* **76** 277-82
- [328] O'Connor G, Sparrow D, Taylor D, Segal M and Weiss S 1987 Analysis of dose-response curves to methacholine. An approach suitable for population studies *Am Rev Respir Dis* **136** 1412-7
- [329] Peat J K, Salome C M, Berry G and Woolcock A J 1992 Relation of dose-response slope to respiratory symptoms and lung function in a population study of adults living in Busselton, Western Australia *Am Rev Respir Dis* **146** 860-5
- [330] Pasker H G, Schepers R, Clement J and Van de Woestijne K P 1996 Total respiratory impedance measured by means of the forced oscillation technique in subjects with and without respiratory complaints *Eur Respir J* **9** 131-9

- [331] Wouters E F, Polko A H, Schouten H J and Visser B F 1988 Contribution of impedance measurement of the respiratory system to bronchial challenge tests *J Asthma* **25** 259-67
- [332] Tzeng Y S, Lutchen K R and Albert M S 2008 The Difference in Ventilation Heterogeneity between Asthmatic and Healthy Subjects Quantified using Hyperpolarized ³He MRI *J Appl Physiol*
- [333] Ilowite J S, Bennett W D, Sheetz M S, Groth M L and Nierman D M 1989 Permeability of the bronchial mucosa to ^{99m}Tc-DTPA in asthma *Am Rev Respir Dis* **139** 1139-43
- [334] Kirby J G, Hargreave F E, Gleich G J and O'Byrne P M 1987 Bronchoalveolar cell profiles of asthmatic and nonasthmatic subjects *Am Rev Respir Dis* **136** 379-83
- [335] Kelly C, Ward C, Stenton C S, Bird G, Hendrick D J and Walters E H 1988 Number and activity of inflammatory cells in bronchoalveolar lavage fluid in asthma and their relation to airway responsiveness *Thorax* **43** 684-92
- [336] Kelly S M, Bates J H and Michel R P 1994 Altered mechanical properties of lung parenchyma in postobstructive pulmonary vasculopathy *J Appl Physiol* **77** 2543-51
- [337] Brackel H J, Pedersen O F, Mulder P G, Overbeek S E, Kerrebijn K F and Bogaard J M 2000 Central airways behave more stiffly during forced expiration in patients with asthma *Am J Respir Crit Care Med* **162** 896-904
- [338] Crotti S, Mascheroni D, Caironi P, Pelosi P, Ronzoni G, Mondino M, Marini J J and Gattinoni L 2001 Recruitment and derecruitment during acute respiratory failure: a clinical study *Am J Respir Crit Care Med* **164** 131-40
- [339] Hubmayr R D 2002 Perspective on lung injury and recruitment: a skeptical look at the opening and collapse story *Am J Respir Crit Care Med* **165** 1647-53
- [340] Boczkowski J, Murciano D, Pichot M H, Ferretti A, Pariente R and Milic-Emili J 1997 Expiratory flow limitation in stable asthmatic patients during resting breathing *Am J Respir Crit Care Med* **156** 752-7
- [341] Schuessler T F and Bates J H A computer-controlled research ventilator for small animals: design and evaluation **42** 860-6
- [342] Briscoe W A and Dubois A B 1958 The relationship between airway resistance, airway conductance and lung volume in subjects of different age and body size *J Clin Invest* **37** 1279-85
- [343] Cohn M A, Watson H, Weissahaut R and Scott F, Sackner, M.A 1978 A transducer for non-invasive monitoring of respiration. In: *ISAM, Proceedings of the The Second International Symposium on Ambulatory Monitoring*, ed F D Scott, et al.: London: Academic Press) pp 119-28
- [344] Watson H 1980 The technology of respiratory inductive plethysmography. In: *ISAM, Proceedings of the Third International Symposium on Ambulatory Monitoring.*, ed F D Scott, et al.: London: Academic Press) pp 537-58
- [345] Petro W, von Nieding G, Böll W and Smidt U 1981 Determination of respiratory resistance by an oscillation method. Studies of long-term and short-term variability and dependence upon lung volume and compliance *Respiration* **42** 243-51

- [346] Smith J C and Stamenovic D 1986 Surface forces in lungs. I. Alveolar surface tension-lung volume relationships *J Appl Physiol* **60** 1341-50
- [347] Milic-Emili J and D'Angelo E 2005 *Physiological Basis of Respiratory Disease*, ed Q Hamid, *et al.* (BC, Canada: BC Decker Inc)
- [348] Oostveen E, Peslin R, Gallina C and Zwart A 1989 Flow and volume dependence of respiratory mechanical properties studied by forced oscillation *J Appl Physiol* **67** 2212-8
- [349] D'Angelo E, Calderini E, Torri G, Robatto F M, Bono D and Milic-Emili J 1989 Respiratory mechanics in anesthetized paralyzed humans: effects of flow, volume, and time *J Appl Physiol* **67** 2556-64
- [350] McCarthy D and Milic-Emili J 1973 Closing volume in asymptomatic asthma *Am Rev Respir Dis* **107** 559-70
- [351] de Lange E E, Altes T A, Patrie J T, Gaare J D, Knake J J, Mugler J P and Platts-Mills T A 2006 Evaluation of asthma with hyperpolarized helium-3 MRI: correlation with clinical severity and spirometry. *Chest* **130** 1055-62
- [352] Farah C S, King G G, Brown N J, Downie S R, Kermode J A, Hardaker K M, Peters M J, Berend N and Salome C M 2012 The role of the small airways in the clinical expression of asthma in adults *J Allergy Clin Immunol* **129** 381-7, 7.e1
- [353] Loughheed D M, Webb K A and O'Donnell D E 1995 Breathlessness during induced lung hyperinflation in asthma: the role of the inspiratory threshold load *Am J Respir Crit Care Med* **152** 911-20
- [354] Sont J K, Willems L N, Bel E H, van Krieken J H, Vandenbroucke J P and Sterk P J 1999 Clinical control and histopathologic outcome of asthma when using airway hyperresponsiveness as an additional guide to long-term treatment. The AMPUL Study Group *Am J Respir Crit Care Med* **159** 1043-51

Appendix A

Asthma Control Questionnaire used for Chapters 6, 7 and 8



Capital Health

ASTHMA CONTROL QUESTIONNAIRE ©

PATIENT ID _____

DATE _____

Page 1 of 2

Please answer questions 1 – 6.

Circle the number of the response that best describes how you have been during the past week.

- | | |
|--|---|
| 1. On average, during the past week, how often were you woken by your asthma during the night? | 0 Never
1 Hardly Ever
2 A few times
3 Several times
4 Many times
5 A great many times
6 Unable to sleep because of asthma |
| 2. On average, during the past week, how bad were your asthma symptoms when you woke up in the morning? | 0 No symptoms
1 Very Mild Symptoms
2 Mild symptoms
3 Moderate symptoms
4 Quite severe symptoms
5 Severe symptoms
6 Very severe symptoms |
| 3. In general during the past week, how limited were you in your activities because of your asthma? | 0 Not limited at all
1 Very slightly limited
2 Slightly limited
3 Moderately limited
4 Very limited
5 Extremely limited
6 Totally limited |
| 4. In general during the past week, how much shortness of breath did you experience because of your asthma? | 0 None
1 A very little
2 A little
3 A moderate amount
4 Quite a lot
5 A great deal
6 A very great deal |

- | | |
|--|---|
| <p>1. In general during the past week, how much of the time did you wheeze?</p> | <p>0 Not at all
 1 Hardly any of the time
 2 A little of the time
 3 A moderate amount of the time
 4 A lot of time
 5 Most of the time
 6 All the time</p> |
| <p>2. On average, during the past week, how many puffs/inhalations of short-acting bronchodilator (eg. Ventolin/ Bricanyl) have you used each day?

 (If you are not sure how to answer this question, please ask for help)</p> | <p>0 None
 1 1-2 puffs/ inhalations most days
 2 3-4 puffs/ inhalations most days
 3 5-8 puffs/ inhalations most days
 4 9-12 puffs/ inhalations most days
 5 13-16 puffs/ inhalations most days
 6 More than 16 puffs/ inhalations most days</p> |

To be completed by a member of the clinic staff

- | | |
|---|--|
| <p>3. FEV1 pre-bronchodilator:</p> <p>FEV1 predicted:</p> <p>FEV1 % predicted:</p> <p>(Record actual values on the dotted Lines and score the FEV₁ % predicted in the next column)</p> | <p>0 > 95% predicted
 1 95 – 90 %
 2 89 – 80 %
 3 79 – 70 %
 4 69 – 60 %
 5 59 – 50 %
 6 < 50% predicted</p> |
|---|--|

Appendix B

February 2, 2015

PERMISSION LETTER

01_03

Springer reference

Annals of Biomedical Engineering

May 2013, Volume 41, Issue 5, pp. 990-1002

Date: 08 Jan 2013

A Study of Artifacts and Their Removal During Forced Oscillation of the Respiratory System

Authors: Swati A. Bhatwadekar, Del Leary, Y. Chen, J. Ohishi, P. Hernandez, T. Brown, C. McParland, Geoff N. Maksym

© Biomedical Engineering Society 2013

DOI 10.1007/s10439-012-0735-9

Print ISSN 0090-6964

Online ISSN 1573-9686

Journal no. 10439

Your project

Requestor: Swati Bhatwadekar
SwatiB@Dal.Ca

University: Dalhousie University

Purpose: Dissertation/Thesis

With reference to your request to reuse material in which Springer Science+Business Media controls the copyright, our permission is granted free of charge under the following conditions:

Springer material

- represents original material which does not carry references to other sources (if material in question refers with a credit to another source, authorization from that source is required as well);
- requires full credit (Springer and the original publisher, book/journal title, chapter/article title, volume, year of publication, page, name(s) of author(s), original copyright notice) to the publication in which the material was originally published by adding: "With kind permission of Springer Science+Business Media";
- may not be altered in any manner. Abbreviations, additions, deletions and/or any other alterations shall be made only with prior written authorization of the author and/or Springer Science+Business Media;
- Springer does not supply original artwork or content.

This permission

- is non-exclusive;
- is valid for one-time use only for the purpose of defending your thesis and with a maximum of 100 extra copies in paper. If the thesis is going to be published, permission needs to be reobtained.

PERMISSION LETTER

01_03

- includes use in an electronic form, provided it is an author-created version of the thesis on his/her own website and his/her university's repository, including UMI (according to the definition on the Sherpa website: <http://www.sherpa.ac.uk/romeo/>);
- is subject to courtesy information to the co-author or corresponding author;
- is personal to you and may not be sublicensed, assigned, or transferred by you to any other person without Springer's written permission;
- is only valid if no personal rights, trademarks, or competitive products are infringed.

This license is valid only when the conditions noted above are met.

Permission free of charge does not prejudice any rights we might have to charge for the reproduction of our copyrighted material in the future.

Rights and Permissions
Springer Science+Business Media
Tiergartenstr. 17 69121
Heidelberg Germany

From: Springer, Permissions

To: Swati Bhatawadekar

Subject: RE: Request for copyright permission

Date: February-04-15 2:06:01 AM

Attachments: image001.png

Dear Swati Bhatawadekar,

An author may self-archive an author-created version of his/her article on his/her own website and or in his/her institutional repository. He/she may also deposit this version on his/her funder's or funder's designated repository at the funder's request or as a result of a legal obligation, provided it is not made publicly available until 12 months after official publication. He/ she may not use the publisher's PDF version, which is posted on <http://link.springer.com>, for the purpose of selfarchiving or deposit. Furthermore, the author may only post his/her version provided acknowledgement is given to the original source of publication and a link is inserted to the published article on Springer's website. The link must be accompanied by the following text: "The final publication is available on <http://link.springer.com>".

Sincerely,

Rights and Permissions

Springer Science+Business Media

Tiergartenstr. 17 69121 Heidelberg Germany

From: Swati Bhatawadekar [mailto:SwatiB@Dal.Ca]
Sent: February-16-15 1:10 PM
To: pubs@nrcresearchpress.com
Subject: Permission to reuse a recently accepted manuscript

Hi,

This is Swati Bhatawadekar from Dalhousie University. I am looking to obtain permission to reproduce my recently accepted manuscript in the Canadian Journal of Physiology and Pharmacology. However, there is no RightsLink link when I click the abstract or open the PDF of this article, likely because the article is only published on Web.

Modelling resistance and reactance with heterogeneous airway narrowing in mild to severe asthma

Swati A. Bhatawadekar, Ms., Del Leary, Geoffrey N. Maksym
Canadian Journal of Physiology and Pharmacology, Published on the web 21 January 2015, 10.1139/cjpp-2014-0436

I am attaching a letter to request permission for this article. Any help in this matter would be much appreciated.

Thanks and Best regards,
Swati Bhatawadekar

From: pubs@nrcresearchpress.com
To: Swati Bhatawadekar
Subject: FW: Permission to reuse a recently accepted manuscript
Date: February-18-15 12:08:50 PM

Dear Swati Bhatawadekar,

Please review: <http://www.nrcresearchpress.com/page/authors/information/rights>
As one of the authors of this paper, you may reuse your published material.
Permission is granted.

Thank you for checking.

Best regards,



Eileen Evans-Nantais
Client Service Representative
Canadian Science Publishing
65 Auriga Drive, Suite 203, Ottawa, ON K2E 7W6
T: 613-656-9846 ext.232 F: 613-656-9838